NASA CR-170,308

A Reproduced Copy

OF

NASA CR-170,308

Reproduced for NASA

by the

NASA Scientific and Technical Information Facility

FFNo 672 Aug 65

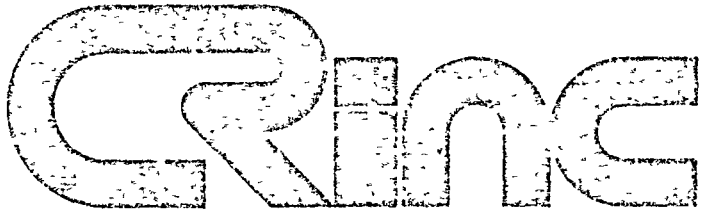

The University of Kansas Center for Research, Inc.
2291 Irving Hill Drive-Campus West
Lawrence, Kansas 66045

Progress Report for
"A Research Program to Reduce Interior Noise
in General Aviation Airplanes"
(NASA Cooperative Agreement NCCI-6)

STUDY OF NOISE REDUCTION CHARACTERISTICS OF DOUBLE-WALL PANELS

KU-FRL-417-21

Prepared by: Ramasamy Navaneethan, Project Manager
Brian Quayle
Scott Stevenson
Mike Graham

Approved by: Jan Roskam, Principal Investigator

Flight Research Laboratory
University of Kansas Center for Research, Inc.
Lawrence, Kansas 66045

May 1983

SUMMARY

In this report the work carried out to investigate the noise reduction characteristics of general aviation type, flat, double-wall structures, at the University of Kansas Flight Research Laboratory, is presented. The test specimens are typical of the double-wall structures that are currently being used in general aviation aircraft. The object of this investigation is to generate a data base of such panels. A secondary objective is to develop a simple theory that will reasonably predict the noise reduction characteristics of such panels without excessive computer memory and time.

The experimental study was carried out on 20-by-20-inch panels with an exposed area of 18 by 18 inches. The tests were performed at normal incidence and at room temperature and pressure. A frequency range from 20 to 5000 Hz was covered. The noise source was a slowly swept sine wave generator.

The experimental results, in general, follow the expected trends. At low frequencies the double-wall structures are no better than the single-wall structures. However, for depths normally used in the general aviation industry, the double-wall structure becomes effective from 300 Hz. At high frequencies, double-wall panels are very attractive. The graphite-epoxy skin panels have higher noise reduction at very low frequencies (>100 Hz) than the Kevlar skin panels. But the aluminum panels have higher noise reduction in the high-frequency region, due to their greater mass. Use of fiberglass insulation is not effective in the low-frequency region, and at times it is even negative. But the insulation is effective in the high-frequency region.

It damps out the panel-air-panel resonances as well as increases noise reduction due to viscous effects.

The interior trim panel used in the industry can be advantageously used as a noise control treatment element in double-wall structures. However, the tests indicate that most trim panels do not behave like limp panels. Certain base material and treatment combinations for the trim panels perform much better than others, even in spite of their weight penalties; and further study may be required to determine exactly their noise attenuation characteristics. In the meantime, use of measured single-panel slope for the trim panels as an additional parameter provides a reasonable approximation for theoretical predictions.

Within its limitations, the theoretical model predicts the transmission loss of these multilayered panels reasonably well.

TABLE OF CONTENTS

LIST OF SYMBOLS

Symbol	Definition	Dimension
p	Pressure	Pascal
n	Number of layers	-
α	Absorption coefficient	-
τ	Transmission coefficient	-

Subscript	
i	Incident
r	Reflected
t	Transmitted
k	Integer
n	Number of layers

LIST OF ABBREVIATIONS

Abbreviation	Definition
KU-FRL	University of Kansas Flight Research Lab
NR	Noise Reduction (dB)
TL	Transmission Loss (dB)

LIST OF FIGURES

LIST OF FIGURES (continued)

LIST OF FIGURES (continued)

LIST OF FIGURES (continued)

LIST OF FIGURES (continued)

LIST OF FIGURES (continued)

LIST OF TABLES

CHAPTER 1

INTRODUCTION

This report is a continuation of the documentation of the research accomplished under the continuing NASA Cooperative Agreement NCCI-6. The progress of the research accomplished during the period May 1, 1982, through October 31, 1982, of the current project year (May 1, 1982, through April 30, 1983) was included in the previous report, KU-FRL-417-19 (Reference 1).

The present report covers the period from November 1982 through April 1983. As explained in Reference 1, during the period June 1982 through September 1982 the progress on the experimental investigation was delayed due to the theft of the Apple computer used in the data acquisition system. An H8 computer was bought in its place and was interfaced with the real-time analyzer. The calibration of the facility with this computer and development of the required software took approximately two more months. The present data acquisition and analysis procedures are described in Appendix A.

In the present reporting period the noise reduction characteristics of double-wall panels were investigated. The double-wall panels are made up of two panels (one representative of the skin and the other of the trim) separated either by an airgap or by a fiberglass thermal insulation material. In industry this configuration is widely used. The skin panel normally is designed for the structural integrity of the airplane. The interior trim panel is used for decorative purposes. Typically, inexpensive, light-weight materials are used in commercially

oriented, general aviation airplanes; but more luxurious materials such as carpet, leather, etc., are used in business and executive type aircraft. In pressurized aircraft and in aircraft flying at high altitudes, fiberglass insulation is used to provide thermal insulation. The objective of the present investigation is to study the sound attenuation characteristics of such panels and to use them as a part of the treatment to reduce externally generated noise. In this investigation both aluminum and fiber-reinforced materials were used as the skin materials. The trim panels investigated are the ones used in the industry. Beech Aircraft Corporation and Cessna Aircraft Company (Wallace Division) provided the test specimens. The panel details and the configurations tested are described in Chapter 2. The results of the experimental investigation are presented in Chapter 3.

The computer program described in References 1 and 2 was used to calculate the noise reduction characteristics of the double-wall panel configurations. In Chapter 4 the theoretical values calculated using this program are compared with the experimental results obtained. The conclusions and recommendations conclude this report.

CHAPTER 2

DESCRIPTION OF TEST FACILITY AND TEST PANELS

2.1 DESCRIPTION OF THE ACOUSTIC TEST FACILITY

The KU-FRL acoustic test facility was used in this investigation. A detailed description of this test facility and its characteristics is given in References 3 and 4. Salient features are excerpted from these reports and presented in Appendix A. In the same appendix the limitations of the facility are also described. All the panels tested were 20 inches by 20 inches with 18-inch-by-18-inch exposed area. The tests were conducted under normal incidence at room temperature. The only modifications to the test facility were the three adapter tubes added to accommodate the three panel depths tested. A diagram of the facility with the adapters is shown in Figure 2.1. The output from the test facility is in the form of noise reduction curves plotted as a function of frequency. The noise reduction across a structure is defined as

$$NR = 10 \text{ Log} |p_s/p_r|^2 \qquad (2.1)$$

where NR = Noise reduction (dB)

p_s = Measured pressure on the source side (Pa)

p_r = Pressure on the receiver side (Pa).

2.2 DESCRIPTION OF THE TEST PANELS

The double-wall test specimens were made of skin, airgap or fiberglass insulation, and a trim panel. Figure 2.2 shows a typical double-wall configuration tested. Three types of skin panels were used in the investigation. The first type was .032" aluminum panel. This panel

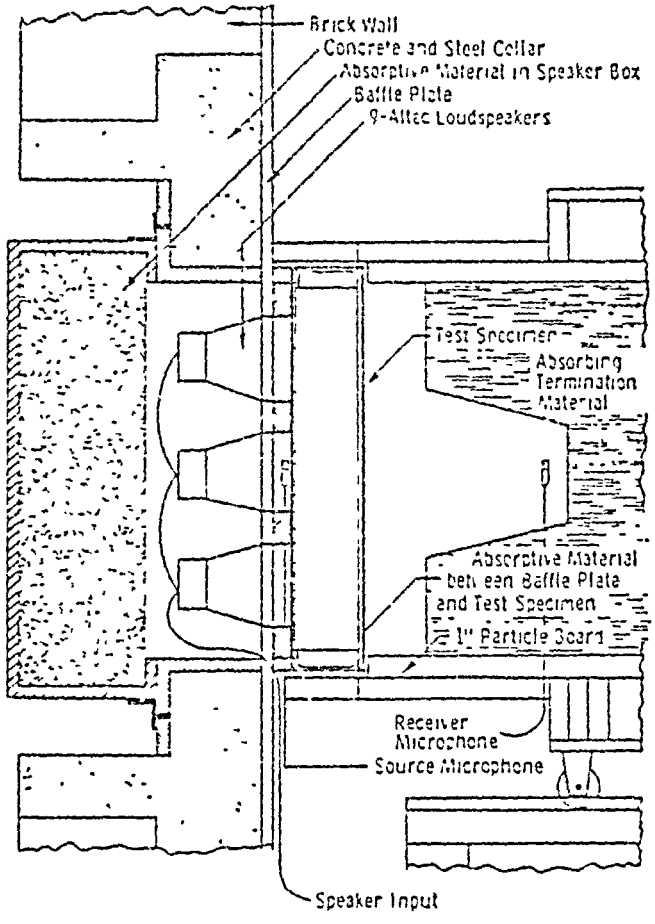

Figure 2.1: Schematic Diagram of the Test Facility with the Adapter to Test Double-Wall Panel

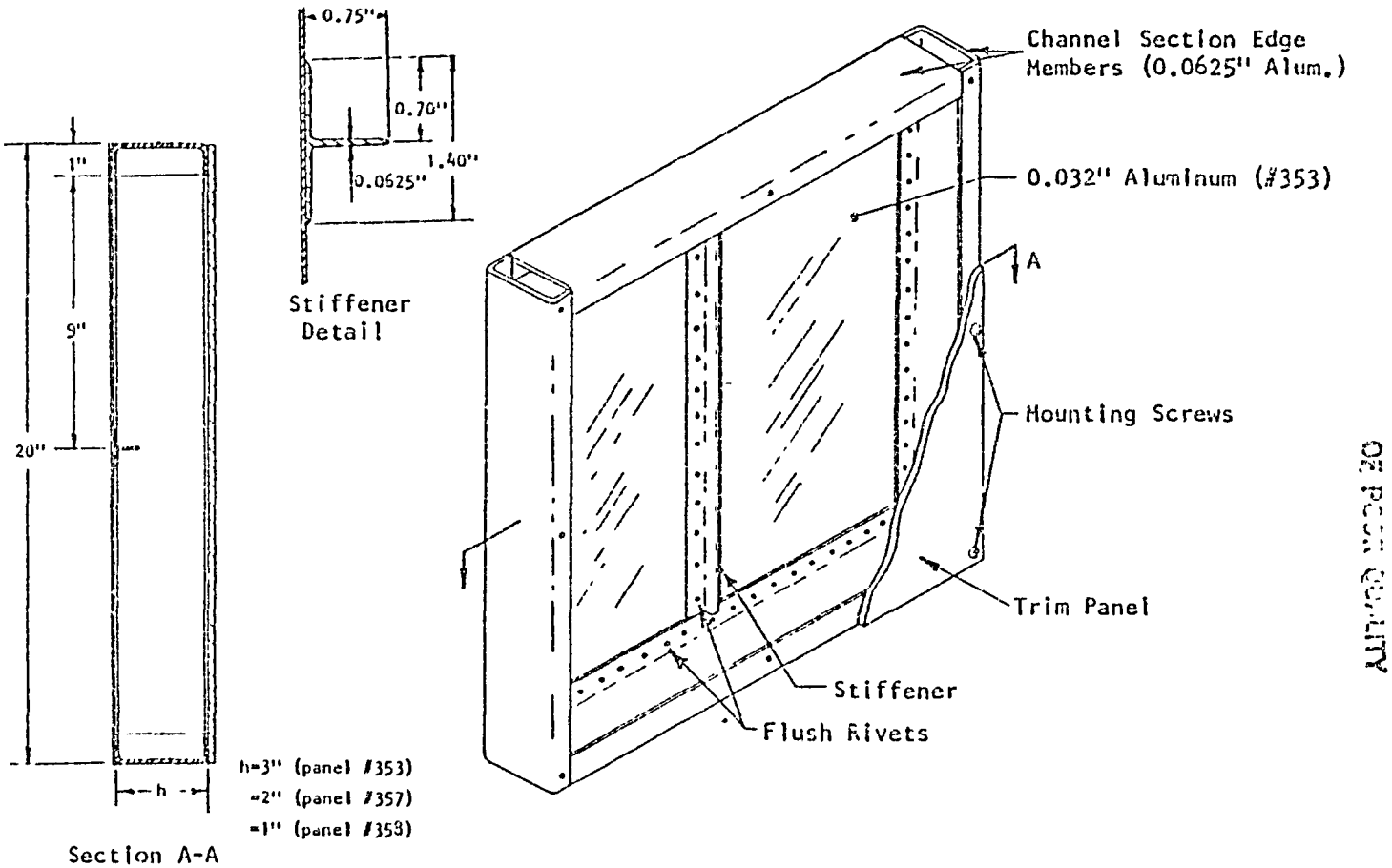

Figure 2.2a: Details of Typical Skin Panels Tested: Group 1, Aluminum, with 1 Stiffener

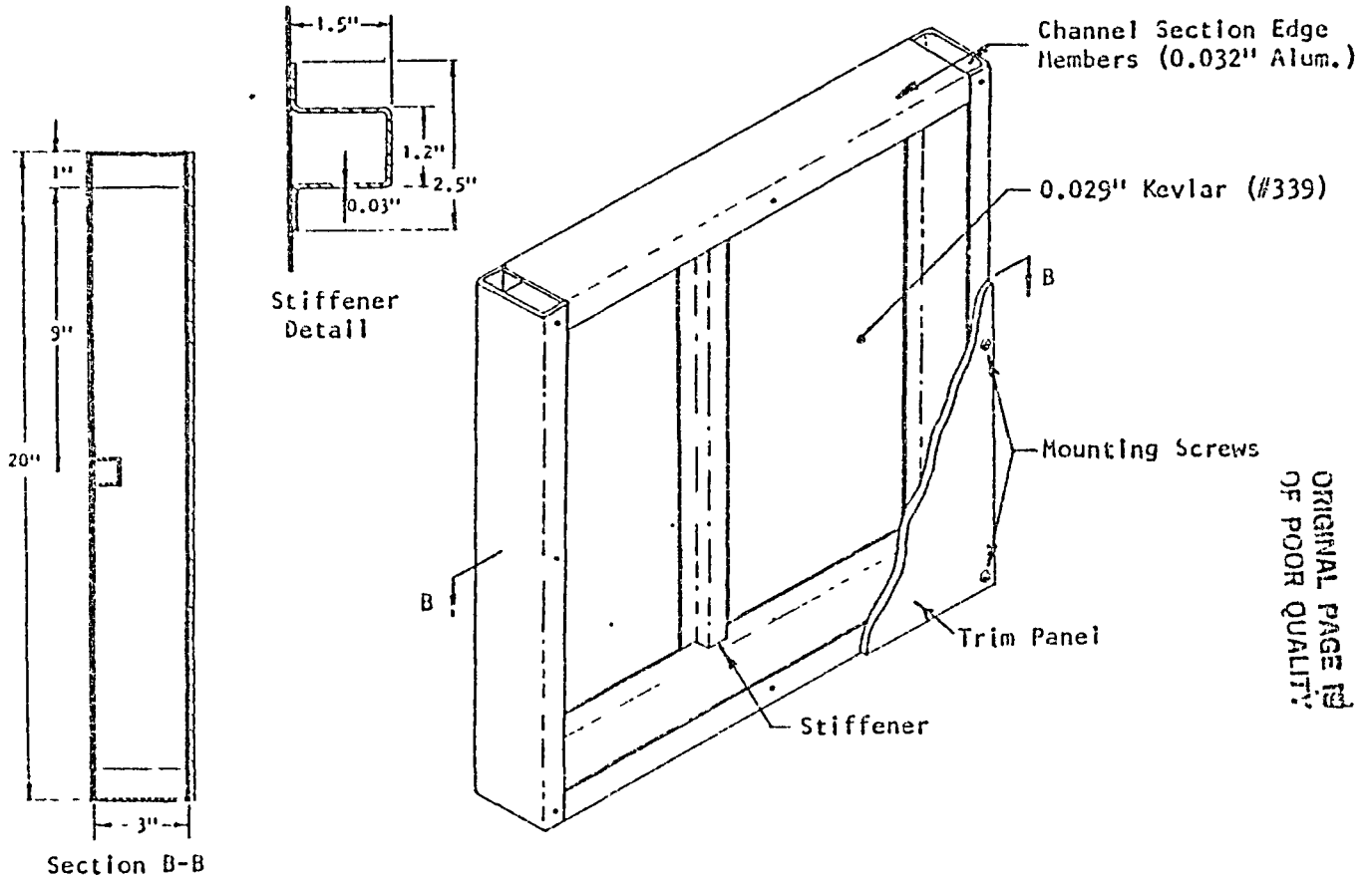

Figure 2.2b: Details of Typical Skin Panels Tested: Group 2, Kevlar, with 1 Stiffener

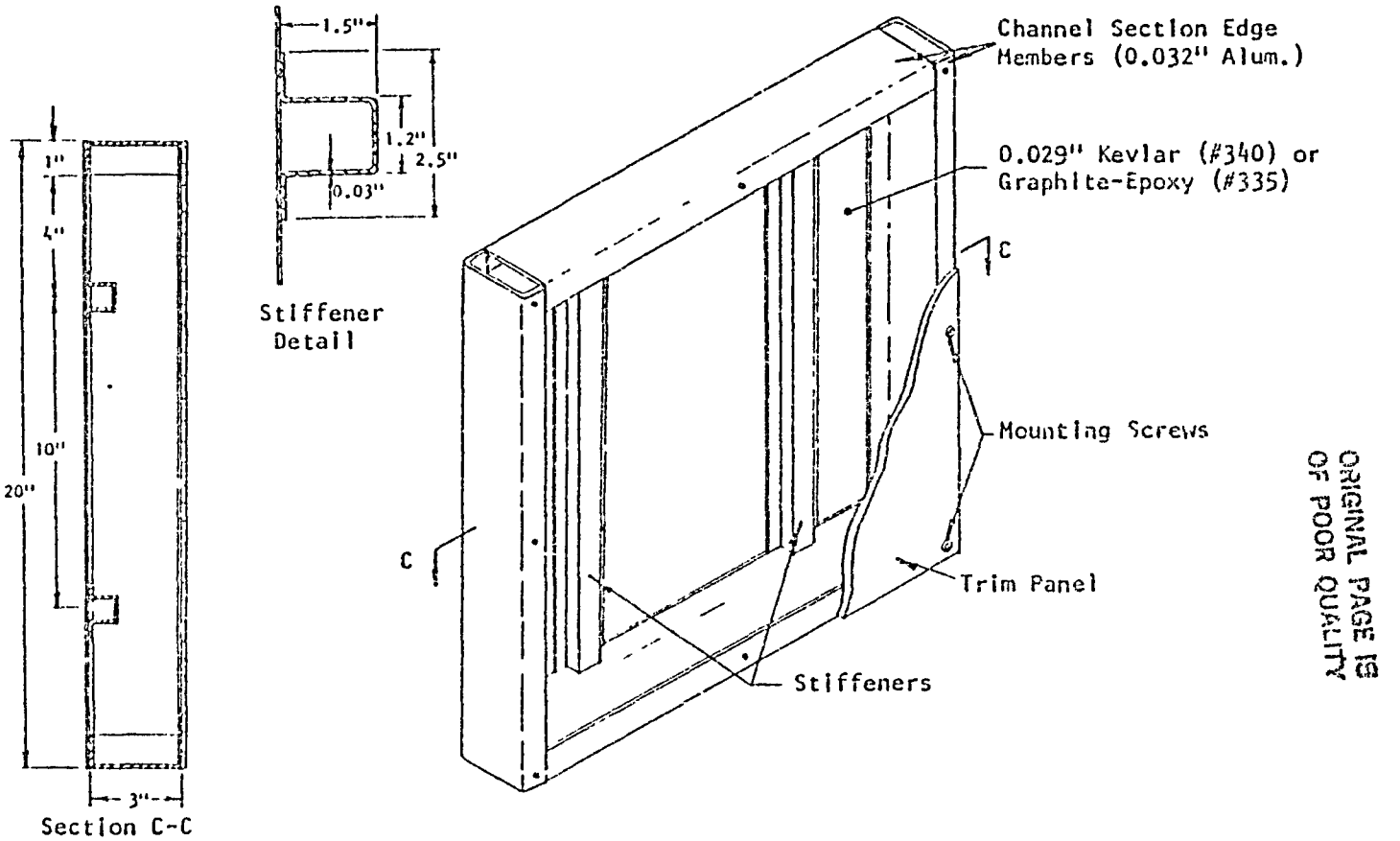

Figure 2.2c: Details of Typical Skin Panels Tested: Group 3, with 2 Stiffeners

was stiffened with a single extruded "T" section stiffener, riveted down the center. This stiffener divided the panel into two equal-area bays (see Figure 2.2a). Three test panels of this type were used. These three panels vary only in the depth of the edge members riveted to the edge of the skin panel. This variance allows for the depths of one, two, and three inches used in this investigation. The second type of skin panel was made of .029" thick graphite-epoxy. Each of the three layers of the panel was made of a woven cloth material with the two main directions of the fibers perpendicular to each other. The ply orientation for the three layers is 45°-0°-45°. Only one panel of this type was used in the present investigation. This particular panel had two "hat" stiffeners (see Figure 2.2c). The mechanical properties of this panel are given in Reference 5. The third type of skin panel used was made of .029" thick Kevlar* material. Once again it had three layers of equal thickness with ply orientation 45°-0°-45°. Two panels of this type were used: one with one "hat" stiffener, and the other with two "hat" stiffeners. Refer to Table 2.1 for further information. The effects of the material and stiffeners were studied using these panels.

The insulation material used was loose fiberglass material with density .07 lb/cubic inch. This material came enclosed in very thin vinyl bags and thicknesses of 3, 2, and 1 inch.

The trim panels tested were the typical trim panels being used or being proposed to be used in the general aviation aircraft. The trim panels were constructed of lightweight base materials such as closed-cell polyvinyl chloride foam, aluminum, and fiberglass. The

---

*Made by DuPont Corporation

Table 2.1: Skin Panels Tested at the KU-FRL Acoustic Test Facility

Panel	Material	Depth (in)	Number of Stiffeners	Thickness (in)	Weight* (lb)
		Group 1			
353	2024-T3 Aluminum	3	1	0.032	1.53
357	2024-T3 Aluminum	2	1	0.032	1.53
358	2024-T3 Aluminum	1	1	0.032	1.53
		Group 2**			
339	Kevlar	3	1	0.029	0.70
340	Kevlar	3	2	0.029	0.85
335	Graphite-Epoxy	3	2	0.029	0.90

*Skin and stiffener weight only

**All composite panels have three layers of the same thickness. Ply orientation is 45°-0°-45°.

foam panels were usually coated with a protective sheathing to give the foam damage tolerance. Over the base material some type of decorative material (called trim panel treatment hereafter) such as simulated leather, upholstery fabric, carpet, etc., is usually applied. The trim panels tested have been divided into three groups, depending on their base material. Group 1 trim panels have a Klegecell base, while Group 2 have a Rohacell base. The panels in these groups vary in the thickness of their base material and in their trim panel treatment. Group 3 panels have miscellaneous base materials such as compressed fiberglass, 45% open-pore aluminum, and Lexan. These panels and their relevant characteristics are described in Table 2.2.

The skin panel and the trim panel were attached by means of the channel section members (see Figure 2.2). The channel section was riveted along the edges to the aluminum skin. In the case of composite skin panels, they were epoxied. Two types of attachment of the trim panel to this channel section were investigated. In the first case, the trim panel was screwed to the flange by means of eight screws. Most of the tests were carried out in this configuration. The effect of "floating" the trim panel was investigated by using a pressure-sensitive, double-sided adhesive tape. The flange of the channel section was 1" all around; hence, it was not exposed to the direct sound pressure field.

Table 2.2: Trim Panels Tested at the KU-FRL Acoustic Test Facility

Panel	Material and Treatment	Trim Panel Area Density (lb/ft^2)
	Group 1	
317	0.125" Klege-Cell type 75 with 1 layer of type A fiberglass both sides	0.128
315	0.25" Klege-Cell type 75 with 1 layer of type A fiberglass both sides	0.168
318	Same as (317) but with 0.020" Royalite covering	0.258
	Group 2	
341	0.125" Rohacell grade 51 with 1 layer of 120 phenolic pre-preg skin both sides	0.134
323	0.25" Rohacell grade 51 with 1 layer of 120 phenolic pre-preg skin both sides	0.180
347	Same as (323) but with 2 layers of 120 phenolic pre-preg skin both sides	0.301
342	Same as (341) but with 0.020" Royalite covering	0.279
343	Same as (341) but with 0.5" carpet	0.674
344	Same as (341) but with 0.25" neoprene + leather covering	0.432
325	Same as (323) but with 0.125" neoprene + wool covering	0.428
	Group 3	
312	45% open 0.025" Aluminum with 0.5" foam + leather covering	0.472
314	0.090" Lexan	0.596
352	0.187" compressed fiberglass with 0.2" carpet	0.450

CHAPTER 3

EXPERIMENTAL INVESTIGATION

3.1 INTRODUCTION

The noise reduction tests of the double-wall structures were conducted at the KU-FRL acoustic test facility. Various trim and skin panel combinations were investigated. For each skin and trim panel configuration, the effect of the fiberglass insulation was also tested. The noise reduction curve as a function of frequency was obtained by slowly sweeping the frequency, measuring the source and the receiver microphone levels, and subtracting the receiver microphone level from the source microphone level at each frequency. This was done in two stages: first from 20 Hz to 500 Hz, and then from 500 Hz to 5000 Hz. In the first case the analysis bandwidth was 2 Hz, and in the second case it was 10 Hz. This was done to get narrow bandwidth at low frequencies as well as to cover a broader frequency range. This also permitted change of gains between these two frequency ranges. All tests were performed at normal angle of incidence and at room temperature and pressure. There was no pressure differential between the source and the receiver side.

Most of the tests were done at least twice to ensure repeatability. The repeatability of the tests was generally good, the results agreeing within 1-2 dB in the low-frequency region. In the high-frequency region the least square lines agreed within 2-4 dB. The noise reduction curves for all the tests are presented in Appendix B. Figures B.1 through B.13 show the results of double-wall structures with aluminum skin and 3"

depth. The results of 1-inch- and 2-inch-thick, double-wall structures with aluminum skin are given in Figure B.14 through B.17 and B.18 through B.21, respectively. The results of the double-wall structures with composite skins (335, 339, and 340) are presented in Figures B.22 through B.34, B.35 through B.47, and B.48 through B.60, respectively. The results of tests with "free-free" trim panels are given in Figures B.61 through B.66. As described in Chapter 2, the free-free edge condition for the trim panel is achieved by using a pressure-sensitive, thick (1/8") adhesive tape.

A typical noise reduction curve of a double-wall structure is shown in Figure 3.1. It can be divided into three parts. In the very low frequency the noise reduction is a function of the stiffness of the skin and the trim panel. This region can be called the stiffness-controlled region. In the second frequency region, varying anywhere from 50 to 600 Hz, two resonance dips dominate the noise reduction. The first one normally corresponds to either the skin or the trim panel fundamental resonance frequency. For the panels tested, resonance frequencies of trim and skin panels are so close that it is not possible to separate them. The second major resonance corresponds to the panel-air-panel described in Reference 6. In the high frequency region (above 600 Hz) the narrow-band analysis (analysis bandwidth 10 Hz) indicates a multitude of resonances, resulting in dips and peaks in the noise reduction curve. These resonances are due to the higher order skin and trim panel modes, double-wall modes, and the cavity modes of the test facility itself. In order to study the trends in this frequency region, a least-square line approximation is used. Previous studies

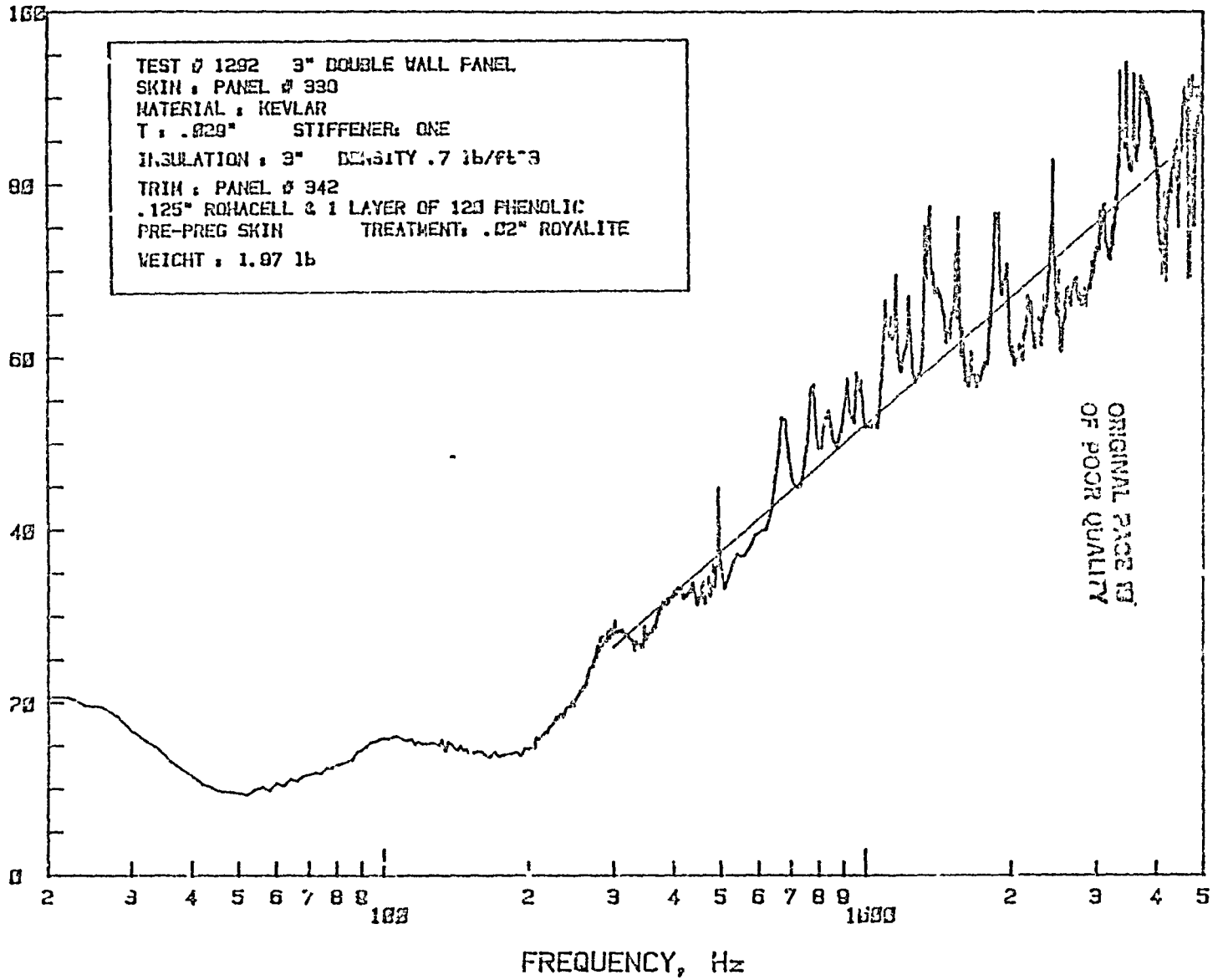

Figure 3.1: Typical Noise Reduction Characteristics of a Double-Wall Panel

at this facility have indicated that the slope of the least-square lines of simple panels corresponds to the calculated mass law slope (i.e., 6 dB/octave). In general, for the double-wall structure, the slope of the least mean-square line lies anywhere between 6 dB/octave (predicted by mass law for single panels) and 12 dB/octave (predicted by classical transmission theory for double-wall structures; see Reference 6). The effects of various parameters on the noise reduction values will now be studied at selected frequencies. These frequencies cover the three frequency regions described above. In the high-frequency region only the least-square line will be used. The choice of these frequencies is rather arbitrary and at times can be misleading because of the wide variations in the characteristics of the panels tested. For a complete review, the original noise reduction curves in Appendix B should be consulted.

Some of these double-wall panels tested showed very high noise reduction values in the high frequency region. This posed some problems in the measurement of the receiver microphone sound pressure levels. At the KU-FRL acoustic test facility the panels could be excited either by a random noise signal or by a slowly-swept sine wave signal. Previous measurements at this facility have shown that the differences in the noise reduction characteristics due to either type of excitation were small, when analyzed through a narrow band analyzer. The latter type of excitation was chosen for this series of tests to improve the accuracy in the measurement of receiver microphone signals. With slowly swept sine waves it is possible to concentrate the sound energy over a very small frequency range. This produced a source sound pres-

sure level of 110-120 dB at these frequencies. Hence the receiver microphone signal was correspondingly higher. Even with this type of excitation the problem was not completely solved. The signal to (ambient) noise ratio was still low in many cases. In addition, during many tests the change in the signal strength within a frequency sweep exceeded the dynamic range of the instrumentation used. As described above, the noise reduction characteristics were investigated by dividing the analysis in two frequency ranges: a) 20-500 Hz with 2 Hz bandwidth, and b) 500-5000 Hz with 10 Hz bandwidth. The dynamic range of the spectrum analyzer used (SD 335) was 60 dB. Hence the maximum change in the receiver microphone level that could be measured in either of the two passes was only 60 dB. This did not pose any problem either during the low-frequency sweep or with panels exhibiting lower high-frequency noise reduction. However, this was not enough for panels with noise reduction higher than 80 dB in the high-frequency region. In such cases the receiver microphone level was near maximum at 500 Hz and was below the minimum level above 3000 Hz. Hence true signal level could not be found at some frequencies above 3000 Hz. The only way this problem could have been overcome was to further subdivide the frequency range. But as mentioned above, the signal levels were so low that further amplification did not improve the results very much, due to deteriorating signal-to-noise ratio. This dynamic range limitation produced scatter in the data when the noise reduction values were higher than 80 dB. Even though this appears to be a serious limitation, it is not so. This phenomenon also occurs in aircraft interior noise measurements. At very high transmission loss values of the fuse-

lage sidewall, the ambient noise level inside the aircraft may be higher than the level transmitted from the sidewall. Under these conditions it may not be worthwhile to have higher noise reduction for the fuselage sidewall. Also more importantly, the noise level inside the aircraft is normally dominated by the low frequency noise. Hence, the overall level inside the aircraft is determined by the low-frequency noise level. The contribution of the sound pressure level at these frequencies to the overall noise level will be negligible. In practice, if the sound pressure level at any frequency range is below 20 dB of the highest band level, then it may safely be neglected without affecting the overall sound pressure level. Hence a dynamic range of 60 dB is more than adequate to predict the interior levels accurately. Hence no further attempt was made to increase the dynamic range of the instrumentation used in the test facility.

3.2 EFFECT OF SKIN PANEL

The effect of skin panels was investigated using four different skin panels. They were the following:

a. .032" aluminum panel with one "T" stiffener (panel 353)

b. .029" thick, 3-ply (45°-0°-45°) graphite-epoxy laminate with two hat stiffeners (panel 335)

c. .029" thick, 3-ply (45°-0°-45°) Kevlar panel with one hat stiffener (panel 339)

d. .029" thick, 3-ply (45°-0°-45°) Kevlar panel with two hat stiffeners (panel 340).

The parameters investigated with these panels are the effects of the panel material and stiffeners. The noise reduction values of these four panels are compared under similar configurations in Figures 3.2 through 3.9. These figures show the noise reduction values at four selected frequencies: two in the low-frequency region (40 and 100 Hz) and two in the high-frequency region (1000 and 3000 Hz). The noise reduction values at 300 and 500 Hz are not plotted, as they fall in the resonance frequency region. Because the panels are so different in their characteristics, the X-axes in these figures are panel numbers and do not represent any continuously varying parameters. Hence these figures are essentially bar charts with values at four frequencies. The influence of the skin panels is plotted for trim panels 312, 314, 315, 318, 425, 342, 344, and 352. For each trim panel two figures are given: one with the fiberglass insulation between the skin and the trim panel, and the other without (i.e., airgap). In all cases the depth of the double wall was maintained at three inches.

The effect of the skin panel material can be studied by comparing the noise reduction values of panels 335 (graphite-epoxy), 340 (Kevlar), and 353 (aluminum). There is a slight difference in their thickness: both Kevlar and graphite-epoxy panels are .029" thick, and the aluminum panel is .032" thick. The mass and the stiffness are the major variables. The weights of these individual panels are .9 lb (graphite-epoxy panel 3350), .85 lb (Kevlar panel 340), and 1.35 lb (aluminum panel 353). Kevlar panel 339, which has one stiffener, weighs .7 lb. At low frequencies the noise reduction of double-wall panels is a function of the stiffness of the skin and the trim panel. In these

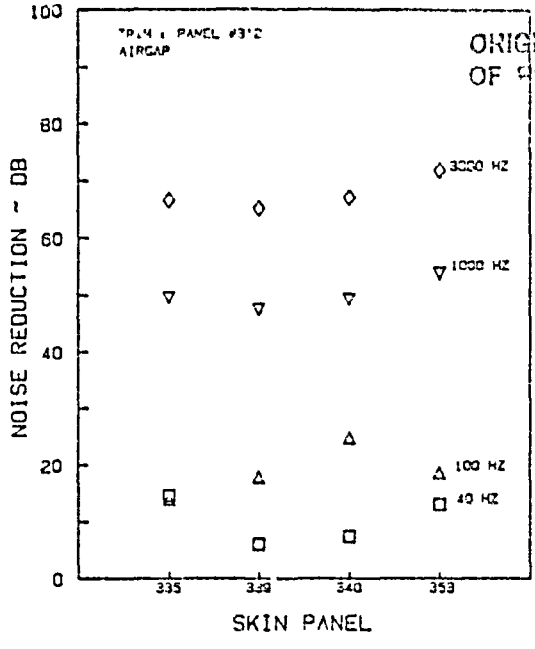

a. Airgap

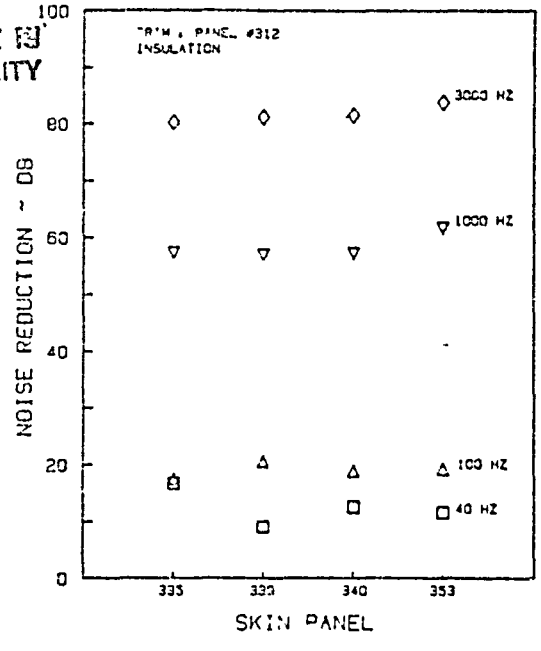

b. Fiberglass Insulation

Figure 3.2: Effect of Skin Panel on the Noise Reduction Characteristics of Double-Wall Panel with Trim Panel 312

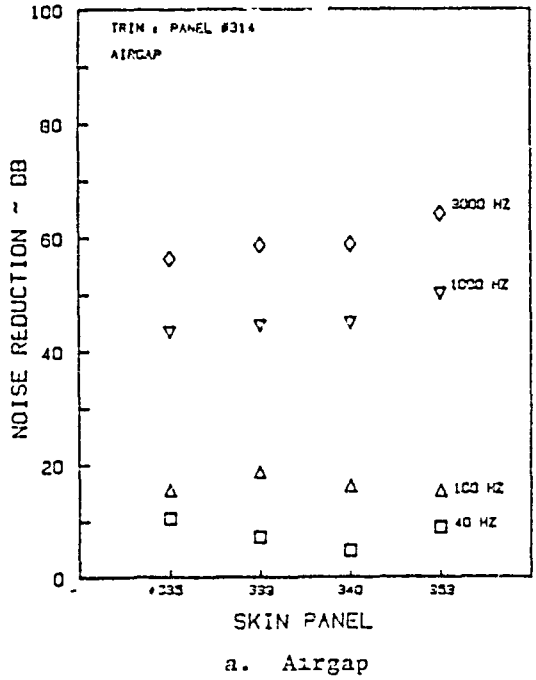

a. Airgap

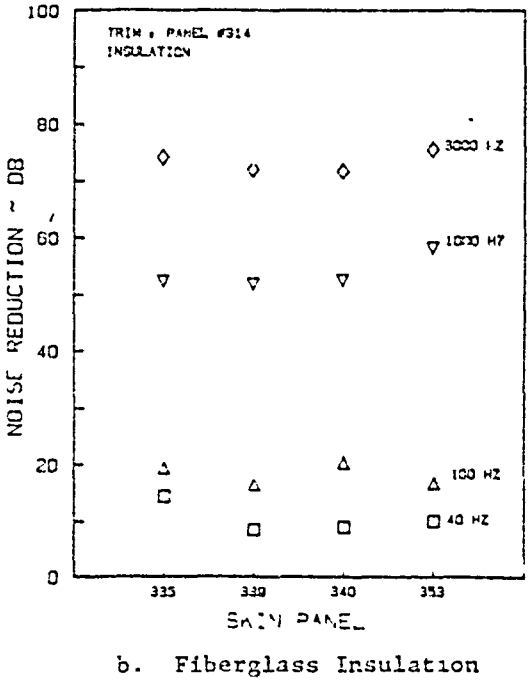

b. Fiberglass Insulation

Figure 3.3: Effect of Skin Panel on the Noise Reduction Characteristics of Double-Wall Panel with Trim Panel 314

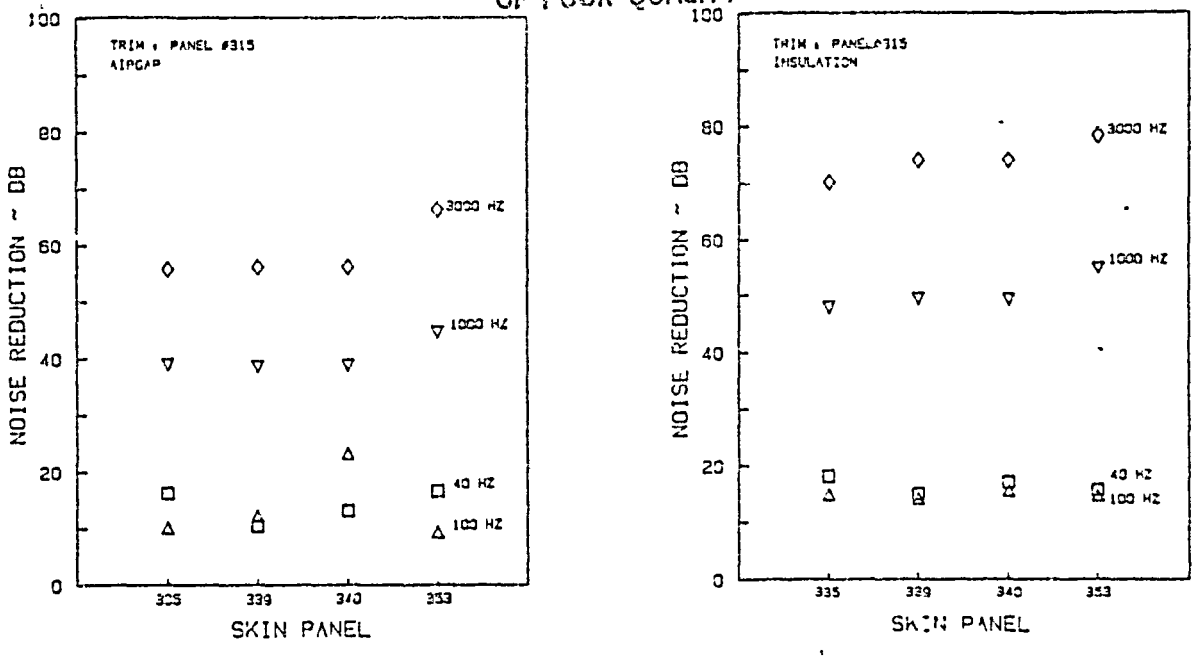

a. Airgap

b. Fiberglass Insulation

Figure 3.4: Effect of Skin Panel on the Noise Reduction Characteristics of Double-Wall Panel with Trim Panel 315

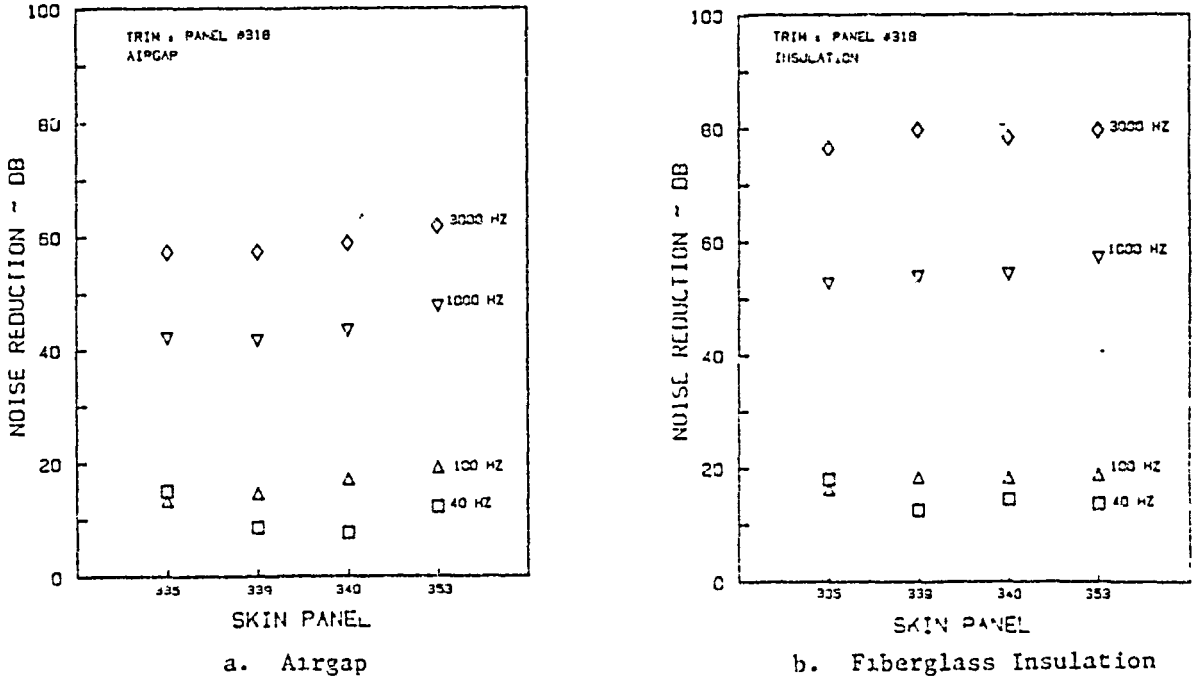

a. Airgap

b. Fiberglass Insulation

Figure 3.5: Effect of Skin Panel on the Noise Reduction Characteristics of Double-Wall Panel with Trim Panel 318

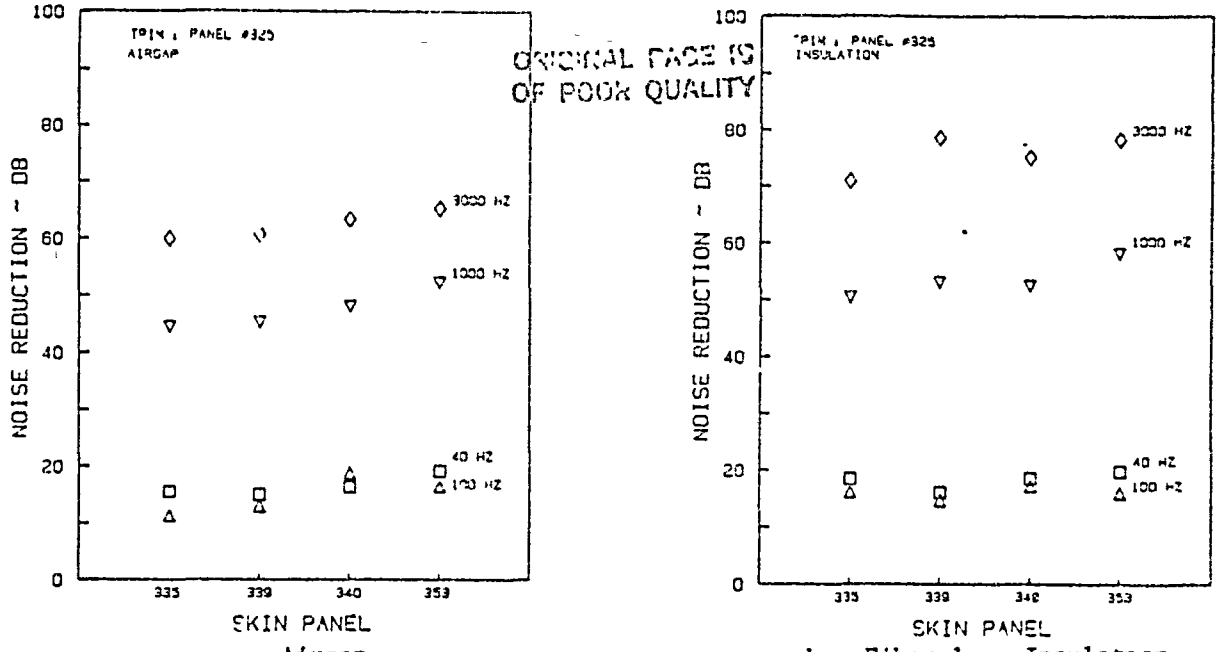

a. Airgap b. Fiberglass Insulation

Figure 3.6: Effect of Skin Panel on the Noise Reduction Characteristics of Double-Wall Panel with Trim Panel 325

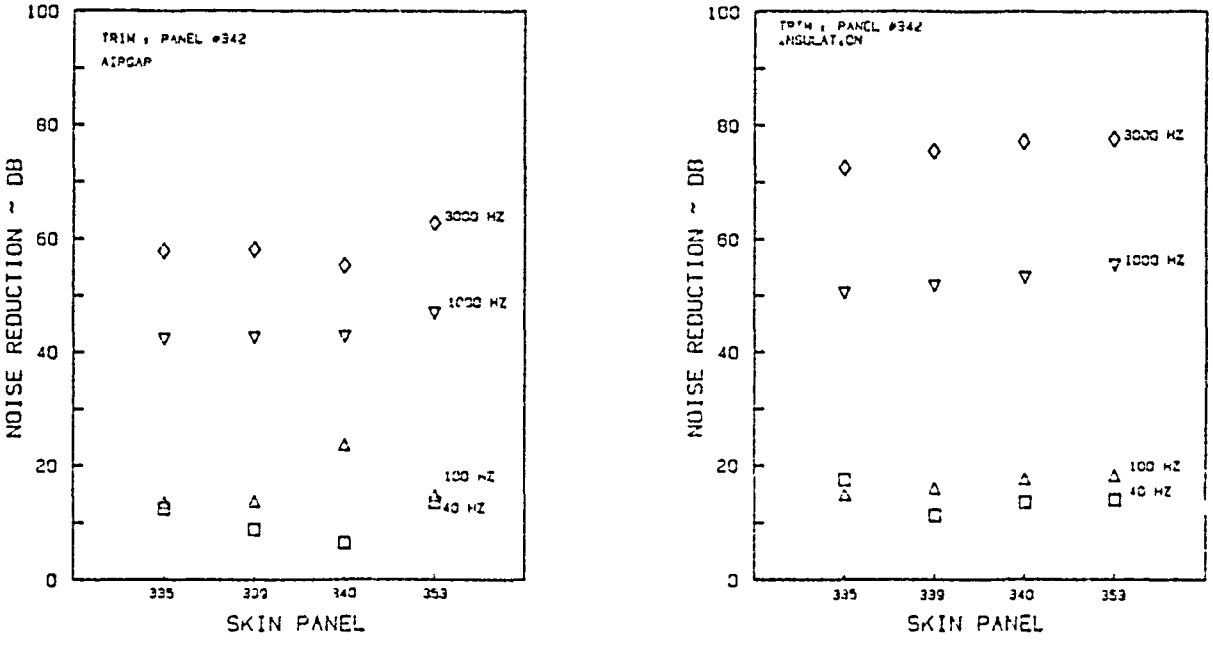

a. Airgap b. Fiberglass Insulation

Figure 3.7: Effect of Skin Panel on the Noise Reduction Characteristics of Double-Wall Panel with Trim Panel 342

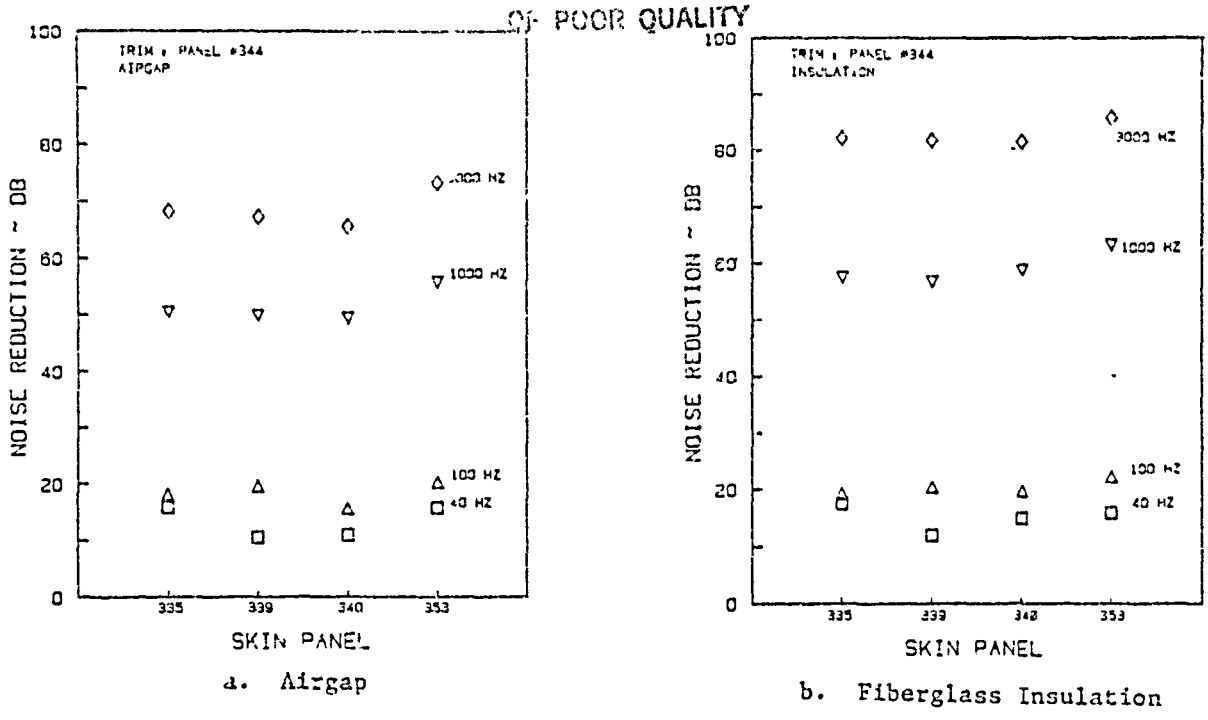

a. Airgap

b. Fiberglass Insulation

Figure 3.8: Effect of Skin Panel on the Noise Reduction Characteristics of Double-Wall Panel with Trim Panel 344

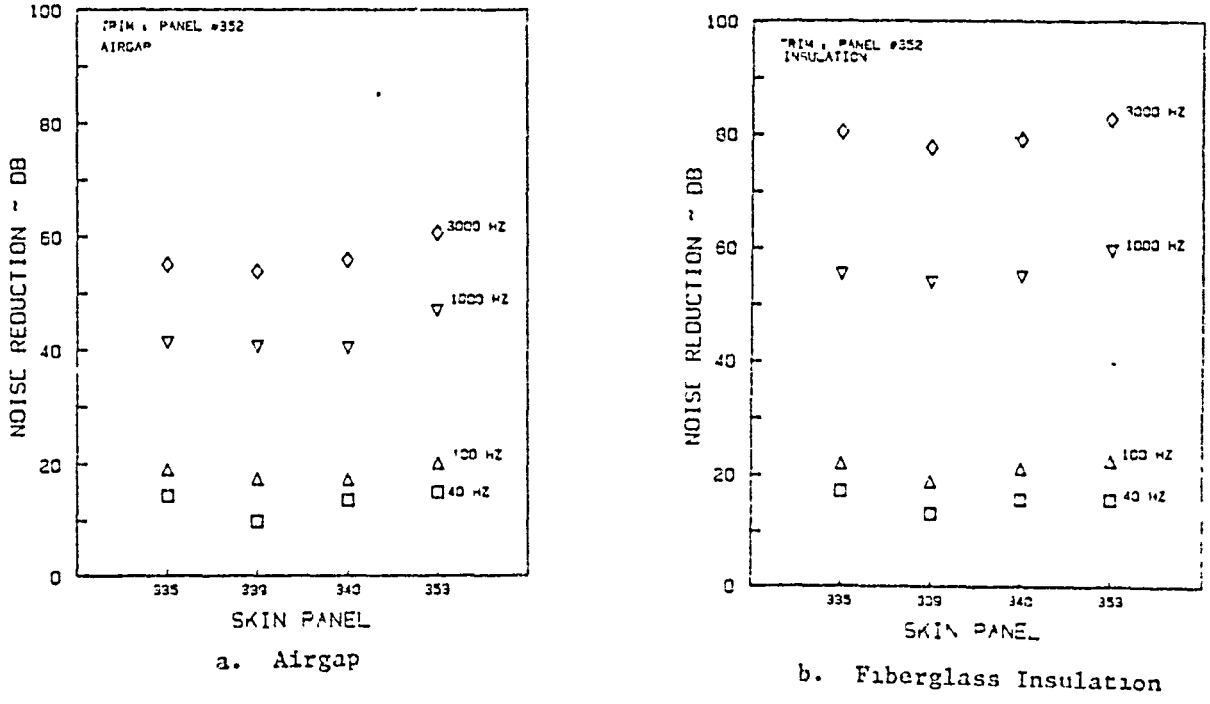

a. Airgap

b. Fiberglass Insulation

Figure 3.9: Effect of Skin Panel on the Noise Reduction Characteristics of Double-Wall Panel with Trim Panel 352

figures, the trim panel has been kept the same for each plot. Hence the noise reduction at 40 Hz in each plot is a function only of the stiffness of the skin panel being studied. However, the stiffness of the skin panel is a function not only of the material properties but also of the number and the type of the stiffeners used. The aluminum and the composite panels had different types of stiffeners. In the case of aluminum it was an extruded "T" section. For composite panels it was a hat section. This precludes any conclusions about the relative stiffness effects of the various skin materials. In general, for the skin panels tested, the graphite-epoxy skin panel and the aluminum skin panel have the same noise reduction at 40 Hz, while the Kevlar skin panel has up to 7 dB less noise reduction. This is consistent with the single panel tests reported in Reference 5. The noise reduction values at 100 Hz vary very widely because they are very close to either the skin or the trim panel fundamental resonance frequency.

At frequencies of 1000 Hz and 3000 Hz the noise reduction is mainly a function of the surface density of the double-wall panel. All other parameters being constant, it is a function of the skin panel surface density. Since the surface densities of the graphite-epoxy panel (panel 335) and the Kevlar panel (panel 340) are nearly equal, they have nearly the same noise reduction. The aluminum skin panel (panel 353) is considerably heavier and hence has higher noise reduction. For double-wall panels with an airgap, the increase in noise reduction values closely match theoretically predicted 3-4 dB at 1000 Hz. At 3000 Hz two phenomena occur. First, the first harmonic of the double-wall resonance falls in this frequency region. The dips in the noise re-

duction introduced by this resonance are strong enough to mask the increased noise reduction due to higher surface density of the aluminum skin panel. Second, this is the frequency region with very high noise reduction. Hence, as explained in Section 3.1, the variations in the noise reduction values are not truly reflected in the results, due to dynamic range limitations. Hence the effect of the increased mass of the aluminum skin panel is not seen in the experimental results. This is especially true with fiberglass insulation. Panels with insulation show very high noise reduction (>80 dB) above 3000 Hz.

The effect of the stiffener can be studied by comparing the results of the Kevlar panel with one stiffener (panel 339) and with two stiffeners (panel 340). In this case other parameters of the double-wall panels are the same. At very low frequency of 40 Hz, the effect of the stiffener is to increase the noise reduction by the increase in the stiffness of the skin panel. This trend is confirmed in all but three cases tested (see Figures 3.2 through 3.9). The exception occurred in two cases with airgap. These exceptions are considered to be due to experimental scatter. The increase in noise reduction at 40 Hz due to increased stiffness is less than 3 dB. Once again at 100 Hz, near the fundamental resonance frequency of the skin/trim panel, there is a wide fluctuation in the test results. The results show a very small increase in noise reduction at 1000 and 3000 Hz due to the two stiffeners. However, this increase is so small that it is within the scatter of the experimental results.

3.3 EFFECT OF PANEL DEPTH

In general aviation aircraft the space available for the installation of double-wall type structures for interior noise control is very limited, due to already small interior dimensions. A quick survey among the manufacturers indicated that 2-3" is about the maximum depth that can be allowed. Hence the effect of the double-wall depth was investigated for only three cases: 1 inch, 2 inches, and 3 inches. For this investigation, aluminum skin panel and four trim panels were used. The trim panels tested were one from each group of the base materials described in Chapter 2. These panels were 312, 318, 325, and 352. The tests were performed both with and without the fiberglass insulation in the space between skin and trim panels. The results from the tests have been cross plotted in Figures 3.10 through 3.13 for the cases investigated. For each test condition six frequencies are shown.

At 40 Hz, which is below the fundamental resonance frequency of the skin or trim panels, the experimental results show a very small decrease with increase in panel depth. The decrease was less than 3 dB in all cases. This trend was not predicted by the simple theory described in Chapter 4. It is believed to be due to the trim panel attachment procedure used in the investigation. The trim panel was attached to the edge channel members by means of screws. The depth of these channel sections determines the panel thickness (see Figure 2.2). It is possible that with higher panel depth, the stiffness of this member decreases, decreasing the double-wall panel stiffness.

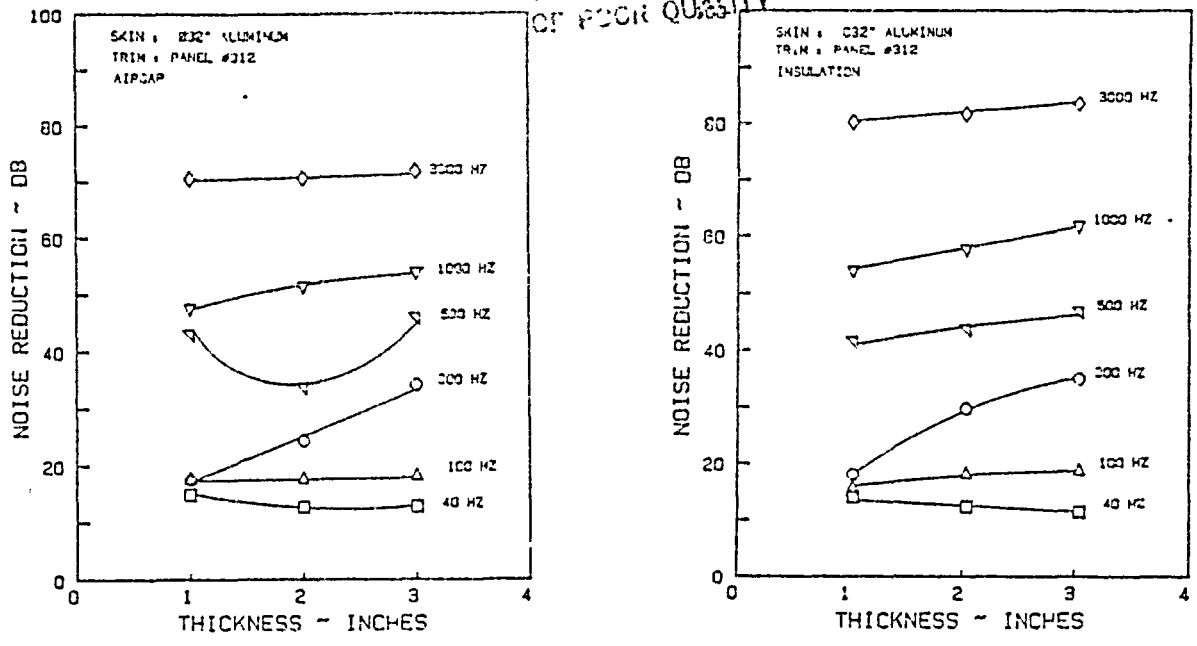

a. Airgap b. Fiberglass Insulation

Figure 3.10: Effect of Panel Depth on the Noise Reduction Characteristics of Double-Wall Panel with Aluminum Skin and Trim Panel 312

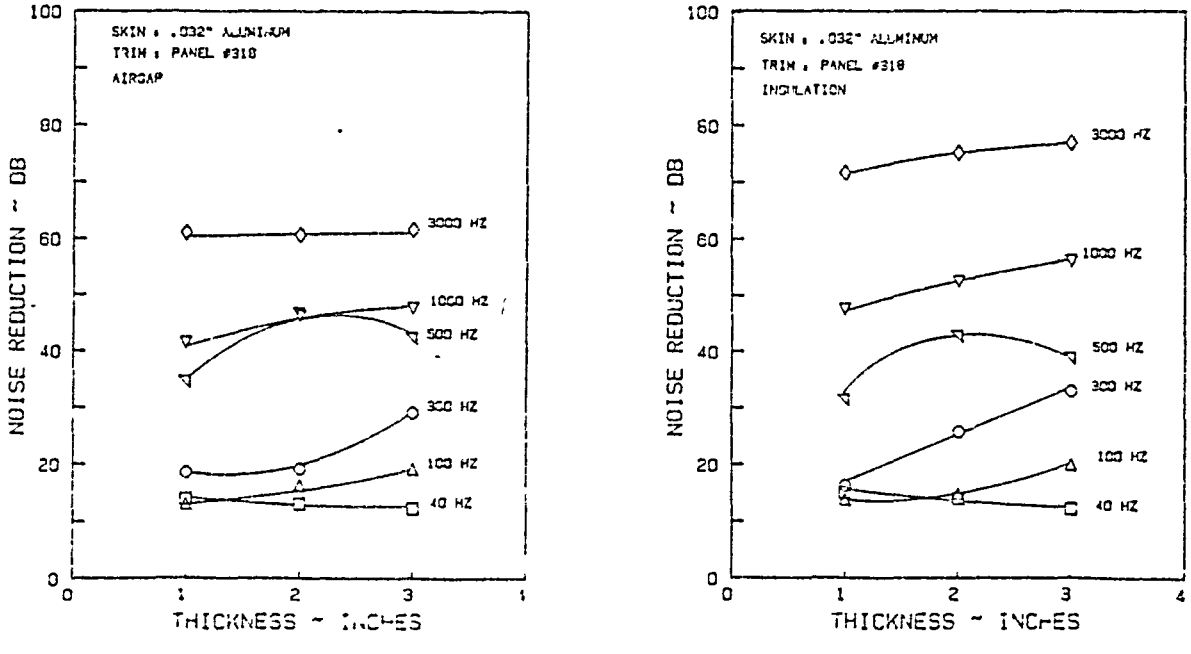

a. Airgap b. Fiberglass Insulation

Figure 3.11: Effect of Panel Depth on the Noise Reduction Characteristics of Double-Wall Panel with Aluminum Skin and Trim Panel 318

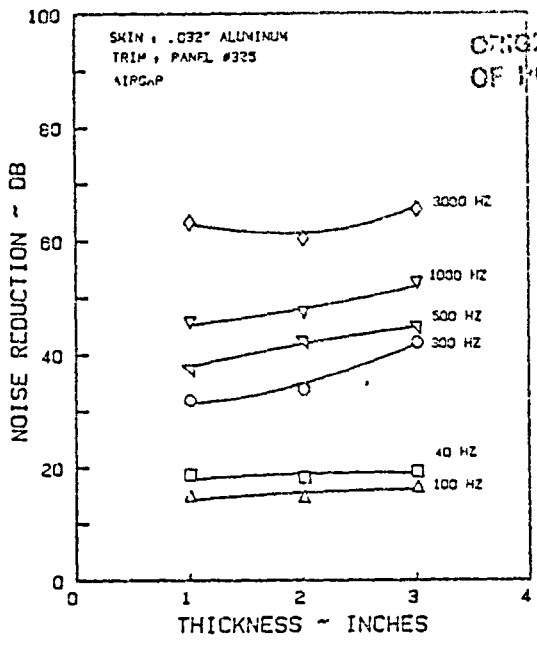

a. Airgap

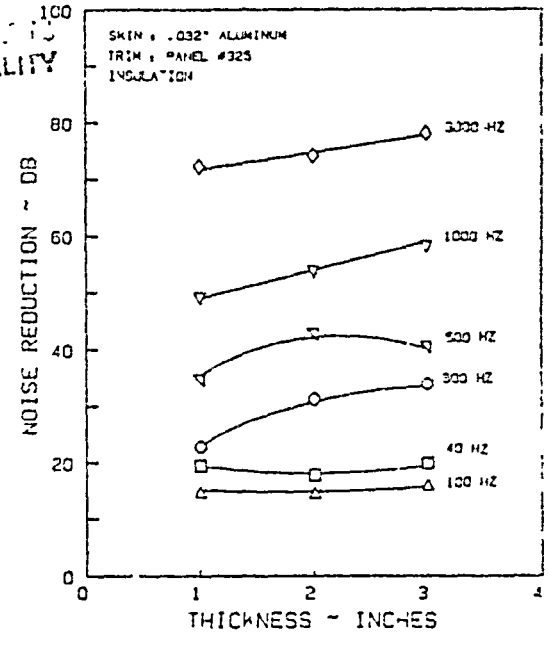

b. Fiberglass Insulation

Figure 3.12: Effect of Panel Depth on the Noise Reduction Characteristics of Double-Wall Panel with Aluminum Skin and Trim Panel 325

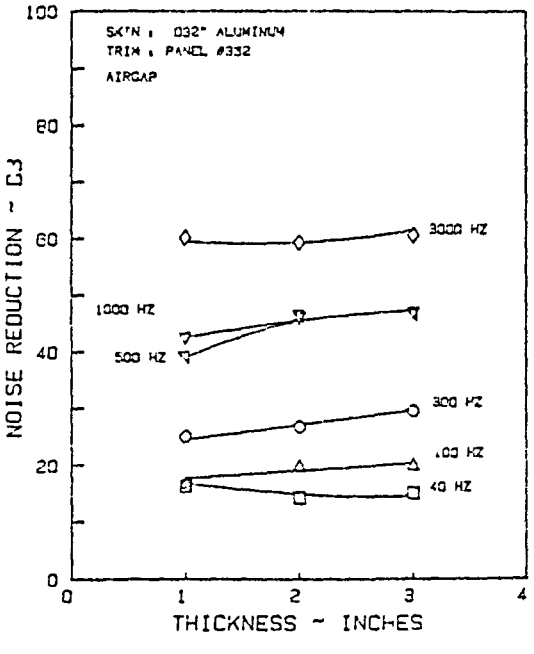

a. Airgap

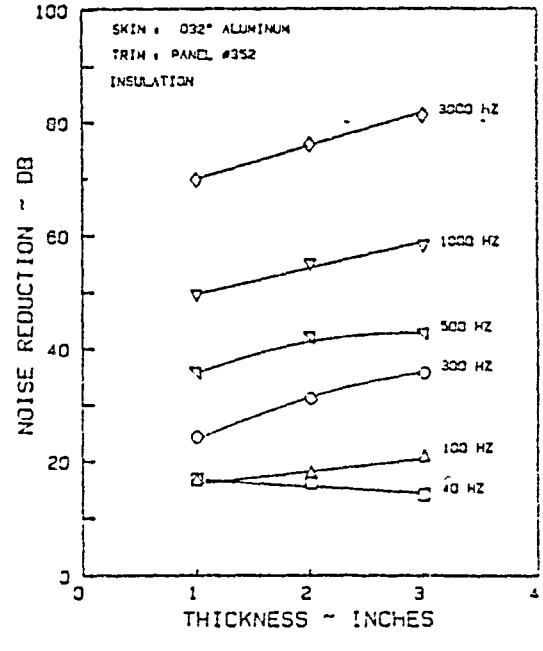

b. Fiberglass Insulation

Figure 3.13: Effect of Panel Depth on the Noise Reduction Characteristics of Double-Wall Panel with Aluminum Skin and Trim Panel 352

This decrease in stiffness may cause the reduction experienced in the test results. This effect is present even with the insulation. An opposite phenomenon occurs at 100 Hz. This frequency is on the other side of the fundamental resonance frequency for most of the panels, and hence a slight increase is expected with increase in panel depth. The increase was 3-5 dB. The decrease in stiffness as described above can cause such a trend.

The noise reduction values at 300 and 500 Hz are also plotted in Figures 3.10 through 3.13. This frequency region is the most important region for the interior noise control of the general aviation aircraft. The noise reduction values at 300 Hz show an increase, with the increase in panel depth. The shape of the curves, however, is different for different trim panels. This is because the experimental double-wall resonance frequency occurs in this region. The noise reduction values depend very much on the value of the double-wall resonance frequency. The simple theory used in the theoretical analysis overpredicts the double-wall resonance frequency (see Chapter 4). Hence comparisons of the trend of the noise reduction values at 300 Hz could not be made. The trend of the frequency values themselves is the same--only shifted by 75-100 Hz depending on the panel configuration. Similarly, at 500 Hz the variations in noise reduction could not be explained in terms of the simple theory. Except for trim panel 312 with airgap, the experimental results show either a steady increase or a slight peaking at 2" depth. The double-wall panel with trim panel 312 has a definite dip at 500 Hz at 2" panel depth. It is believed that the porous aluminum base material may contribute to this phenomenon.

At 1000 Hz, for all cases tested the noise reduction shows a steady increase with increase in panel depth. As the panel depth is increased, the first harmonic of the double-wall resonance frequency decreases. On either side of this frequency, the slope of the noise reduction curve will be high. At 1000 Hz we are in this region for all three depths tested. This slope is higher if the resonance frequency is closer to 1000 Hz. Because of this the noise reduction of the 3" depth panel is higher than that of the 2" panel. The increase is smaller for the airgap (6 dB max.) than for the insulation (11 dB max.). Some of the increase in noise reduction of the panels with insulation is due to the viscous shear in the insulation. This shear loss manifests itself as the real part of the complex propagation constant (see Reference 6). The effect of the harmonic of the double-wall resonance frequency is more apparent at 3000 Hz with airgap. The resonance in this case is so strong that it lowers the overall noise reduction of the double-wall panels with 2" depth at this frequency. Hence the cross plot of noise reduction vs thickness shows a dip at two inches at this frequency. These results are consistent with the theoretical predictions and also with the results of the dual pane window tests (Reference 7) carried out at this test facility. The addition of the insulation damps out this dip. In addition, viscous shear losses in the insulation increase the noise reduction beyond 80 dB for three (panels 312, 318, and 325) out of the four trim panels tested. As described in Section 3.1, any increase in the noise reduction over this value does not get truly reflected in the test results. In the case of trim panel 352, which has a lower noise reduction at

1-inch panel depth (70 dB), the effect of increase in depth is more prominent.

3.4 EFFECT OF FIBERGLASS INSULATION

Even though all double-wall tests have been done with and without airgaps, aluminum skin panel and four trim panels (312, 318, 325, and 352) were chosen for comparative study. The cross plots at 40, 100, 1000, and 3000 Hz are given in Figures 3.14 through 3.17. The Y axis of these figures is the change in noise reduction due to the fiberglass insulation of density .17 lb/cubic ft. These values were obtained by subtracting the noise reduction values of the panels with insulation, from those without the insulation (shown in Figures 3.10 through 3.13). At 40 and 100 Hz the effect of the fiberglass is negligible. In fact, in some cases it is even negative. At high frequencies the fiberglass has two effects, as described in the previous section. First, it eliminates the dip in the noise reduction curve observed due to the harmonics of the double-wall resonance frequencies. Secondly, the sound level is also attenuated by the viscous shear losses when it travels through the porous media (Reference 6). At any given frequency the attenuation due to this effect is linearly proportional to the thickness of the insulation. The experimental results tend to confirm this trend in those cases, where the noise reduction measurements are not affected by the limitation of the dynamic range of the instruments. At 3000 Hz the increase due to the insulation varies from 3 dB (for trim panel 312) to 11 dB (for trim panel 352) for 2 inch variation in the panel depth.

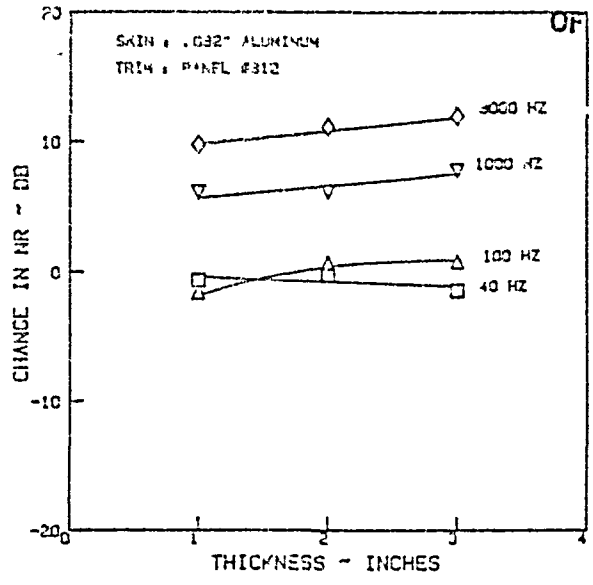

Figure 3.14: Effect of Fiberglass Insulation on the Noise Reduction Characteristics of Double-Wall Panel with Aluminum Skin and Trim Panel 312

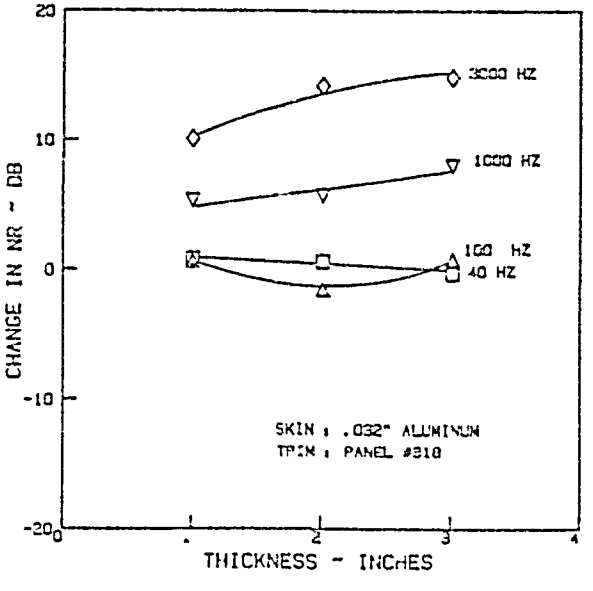

Figure 3.15: Effect of Fiberglass Insulation on the Noise Reduction Characteristics of Double-Wall Panel with Aluminum Skin and Trim Panel 310

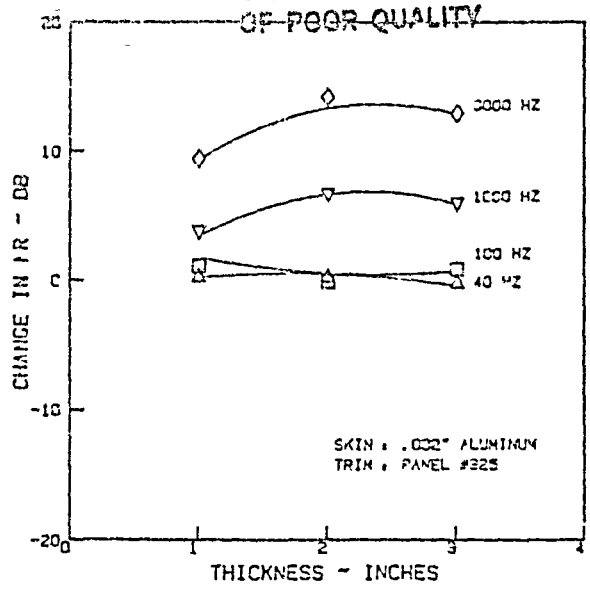

Figure 3.16: Effect of Fiberglass Insulation on the Noise Reduction Characteristics of Double-Wall Panel with Aluminum Skin and Trim Panel 325

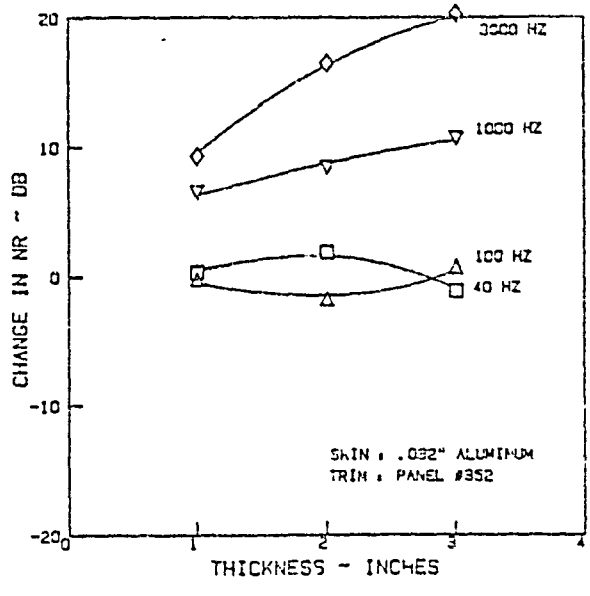

Figure 3.17: Effect of Fiberglass Insulation on the Noise Reduction Characteristics of Double-Wall Panel with Aluminum Skin and Trim Panel 352

3.5 EFFECT OF TRIM PANELS

The interior trim panels are used in the general aviation industry for decorative purposes. They also form a part of the interior noise control treatment. But it is the decorative purpose which determines the type of material and treatment that will be used. Normally a trim panel has a base material, which provides the stiffness and also makes it easier to install. The treatment such as simulated leather, upholstery, etc., is applied solely for decorative purposes. Theoretically, these panels are treated as limp panels having mass-law impedance. Tests at this facility of various materials have shown that such an assumption may not be valid (References 1 and 2). During the present series of tests, the effect of these panels was investigated when used as a part of a double-wall structure. As described in Chapter 2, the trim panels were divided into three groups, based on their base material. Tables 3.1 and 3.2 give the noise reduction values at 40 and 3000 Hz for four skin panels. As expected, there is considerable scatter in the data. Figures 3.18 through 3.25 show this effect as a function of the total panel surface density. For each skin panel the noise reduction obtained is plotted as a function of the suface density of the panel. Since the other panel parameters have been held constant for each plot, the variation of the surface density in each figure is due to the variation of the surface (area) density of the trim panels. These cross plots must be interpreted with care because the noise reduction due to the trim panel at any frequency is not a function solely of the mass of the panel, which explains the considerable scatter seen

Table 3.1: Effect of Trim Panels on Noise Reduction Characteristics of Double-Wall Panel; 40 Hz

Trim Panel	Airgap				Insulation			
	Skin Panel				Skin Panel			
	353	335	339	340	353	335	339	340
312	13	15	6	7	12	17	9	13
314	9	11	7	7	10	15	9	9
315	17	16	11	13	16	18	15	15
317	13	12	7	8	13	16	12	15
318	12	15	9	8	13	17	11	13
323	19	17	16	15	19	21	15	17
325	18	15	15	15	20	19	16	18
341	14	14	7	8	15	16	13	15
342	14	12	9	8	14	18	12	14
343	9	12	7	6	13	13	11	11
344	14	15	9	9	14	16	10	13
* 347	24	25	19	20	23	24	19	22
352	15	16	10	13	14	16	12	13

* Has the highest noise reduction at 40 Hz

Table 3.2: Effect of Trim Panels on Noise Reduction Characteristics of Double-Wall Panel; 3000 Hz

Trim Panel	Airgap				Insulation			
	Skin Panel				Skin Panel			
	353	335	339	340	353	335	339	340
* 312	72	66	65	67	84	80	80	80
314	64	58	59	59	76	75	73	73
315	66	56	56	56	78	70	73	74
317	61	57	57	55	71	69	71	70
318	62	57	57	59	78	75	77	78
323	58	54	52	58	74	69	76	74
325	65	60	61	63	78	71	78	77
341	59	56	57	55	75	69	75	73
342	63	58	55	58	78	73	76	77
343	68	65	67	66	77	74	75	74
* 344	72	67	66	64	84	80	80	80
347	60	54	54	54	73	69	74	72
352	61	55	54	56	80	78	76	77

* Have the highest noise reduction at 3000 Hz

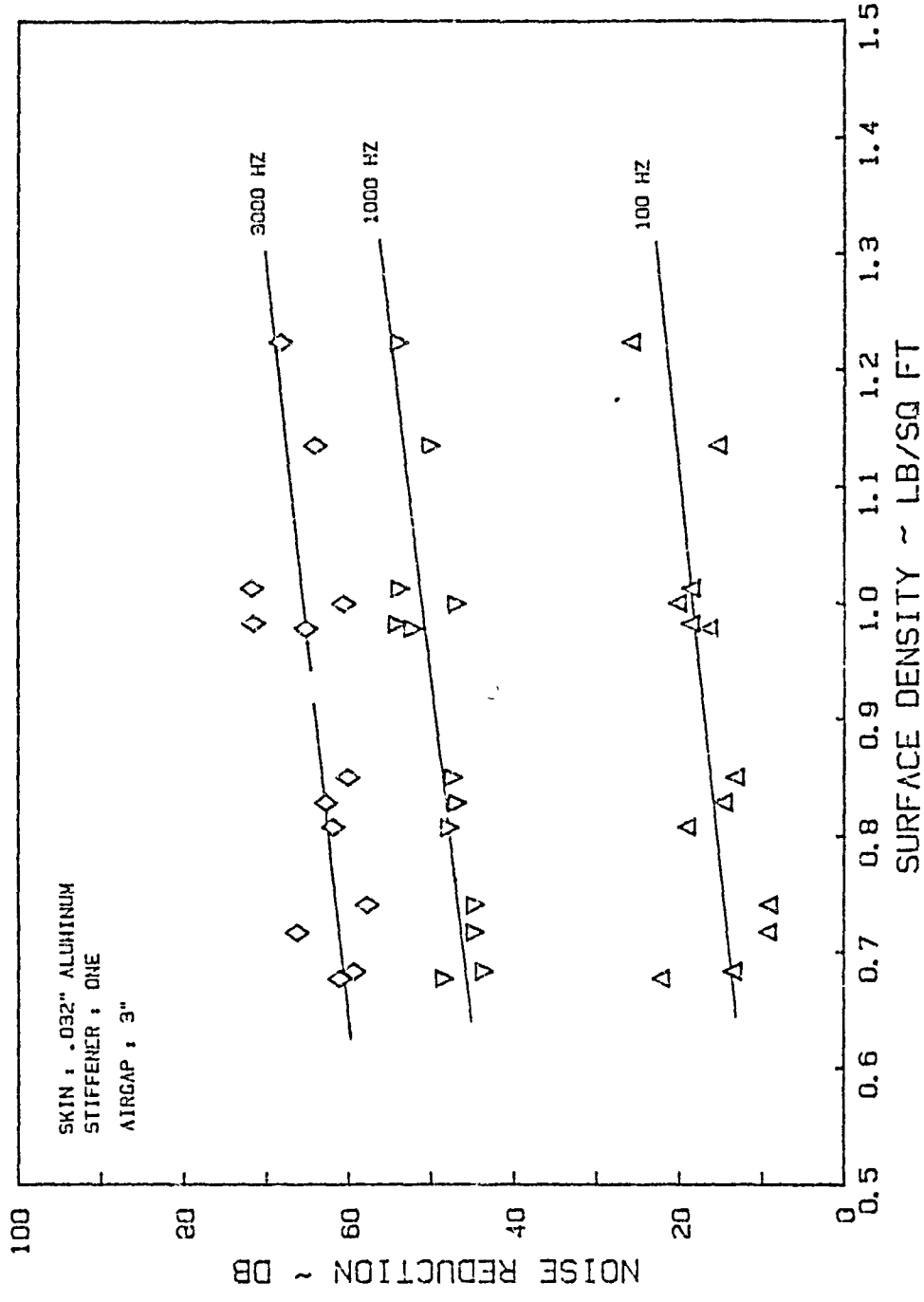

Figure 3.18: Effect of Total Panel Area Density on the Noise Reduction Characteristics of Double-Wall Panel with Aluminum Skin (Panel 353) and Airgap

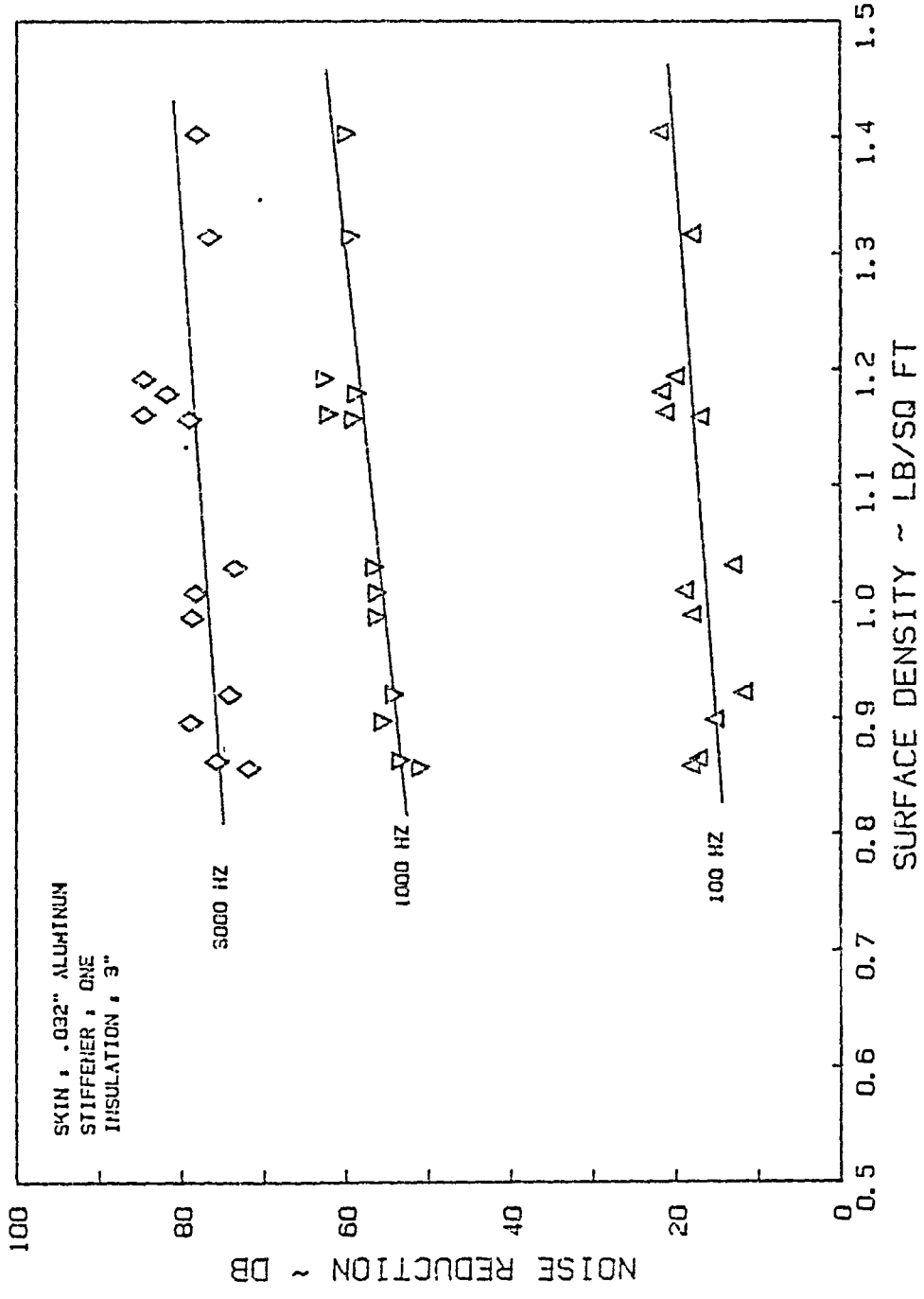

Figure 3.19: Effect of Total Panel Area Density on the Noise Reduction Characteristics of Double-Wall Panel with Aluminum Skin (Panel 353) and Insulation

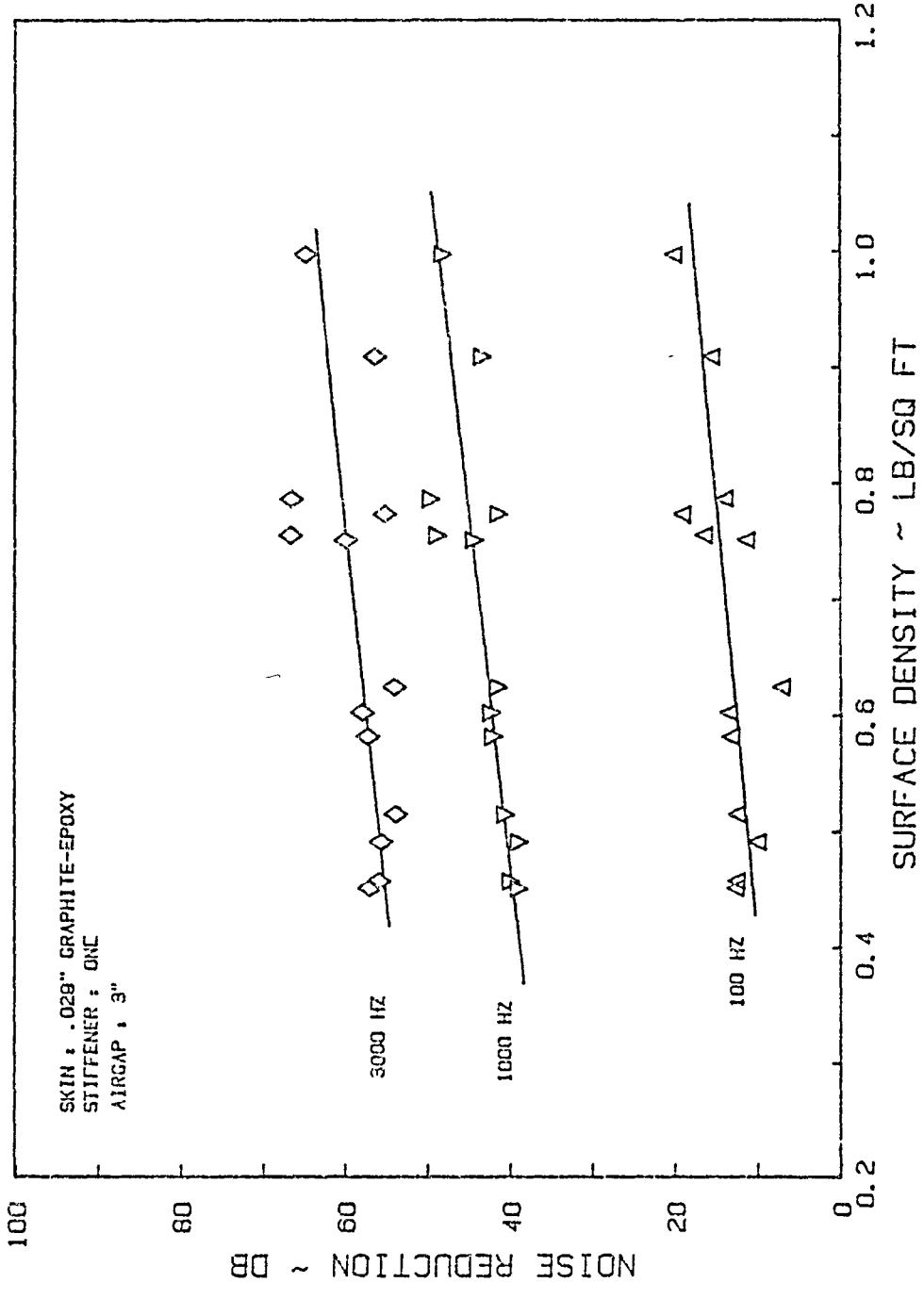

Figure 3.20: Effect of Total Panel Area Density on the Noise Reduction Characteristics of Double-Wall Panel with Graphite-Epoxy Skin (Panel 335) and Airgap

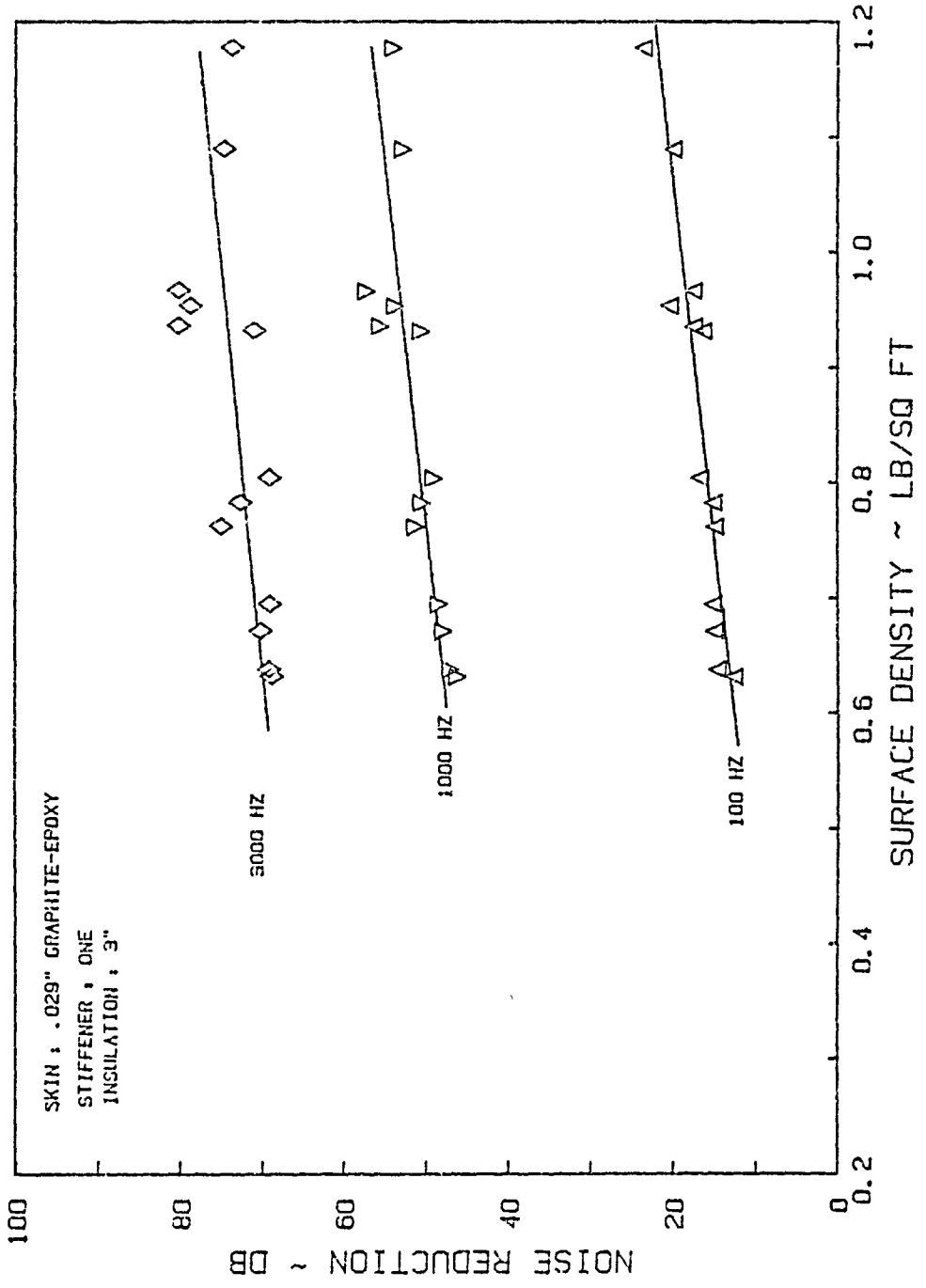

Figure 3.21: Effect of Total Panel Area Density on the Noise Reduction Characteristics of Double-Wall Panel with Graphite-Epoxy Skin (Panel 335) and Insulation

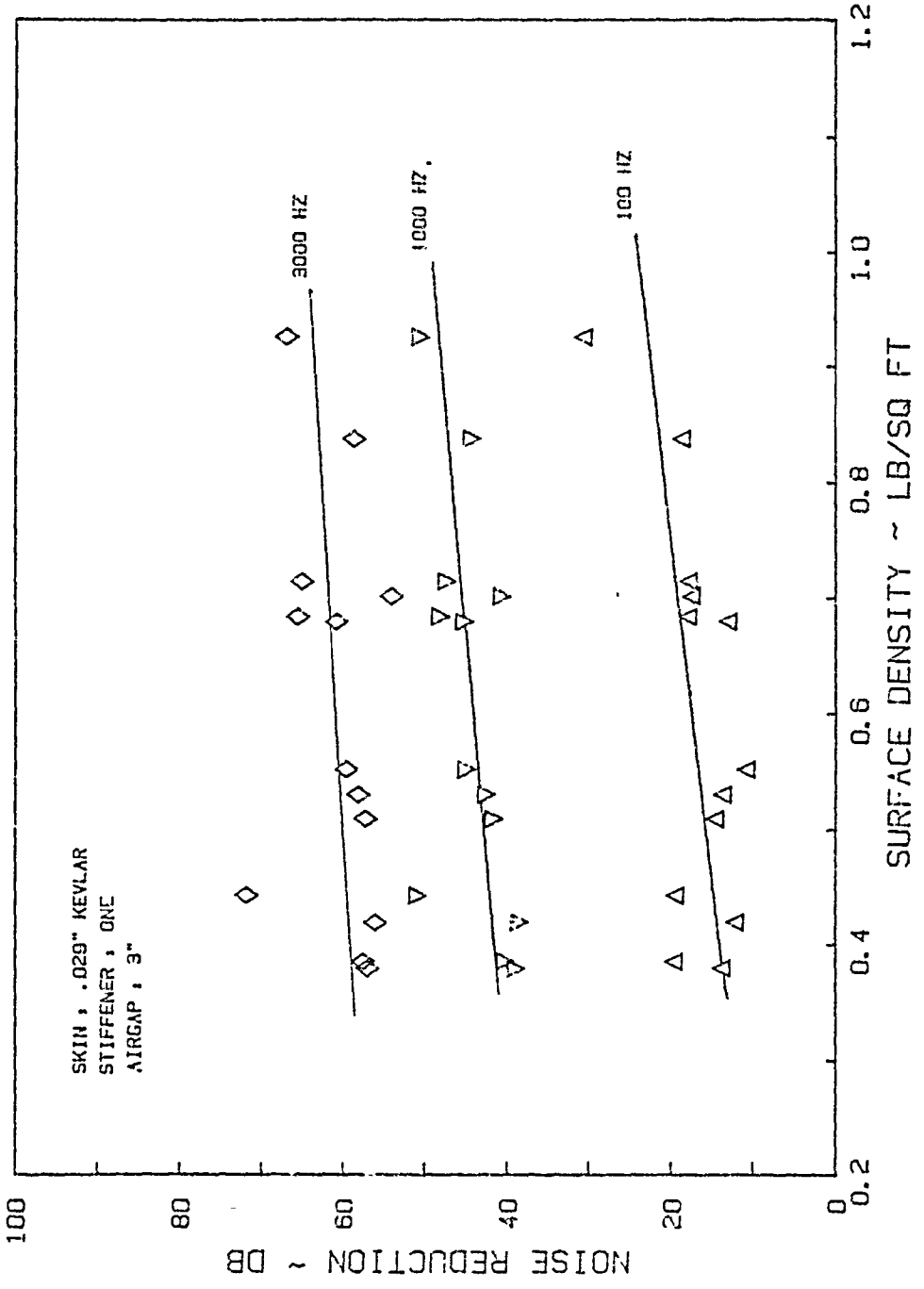

Figure 3.22: Effect of Total Panel Area Density on the Noise Reduction Characteristics of Double-Wall Panel with Kevlar Skin (Panel 339) and Airgap

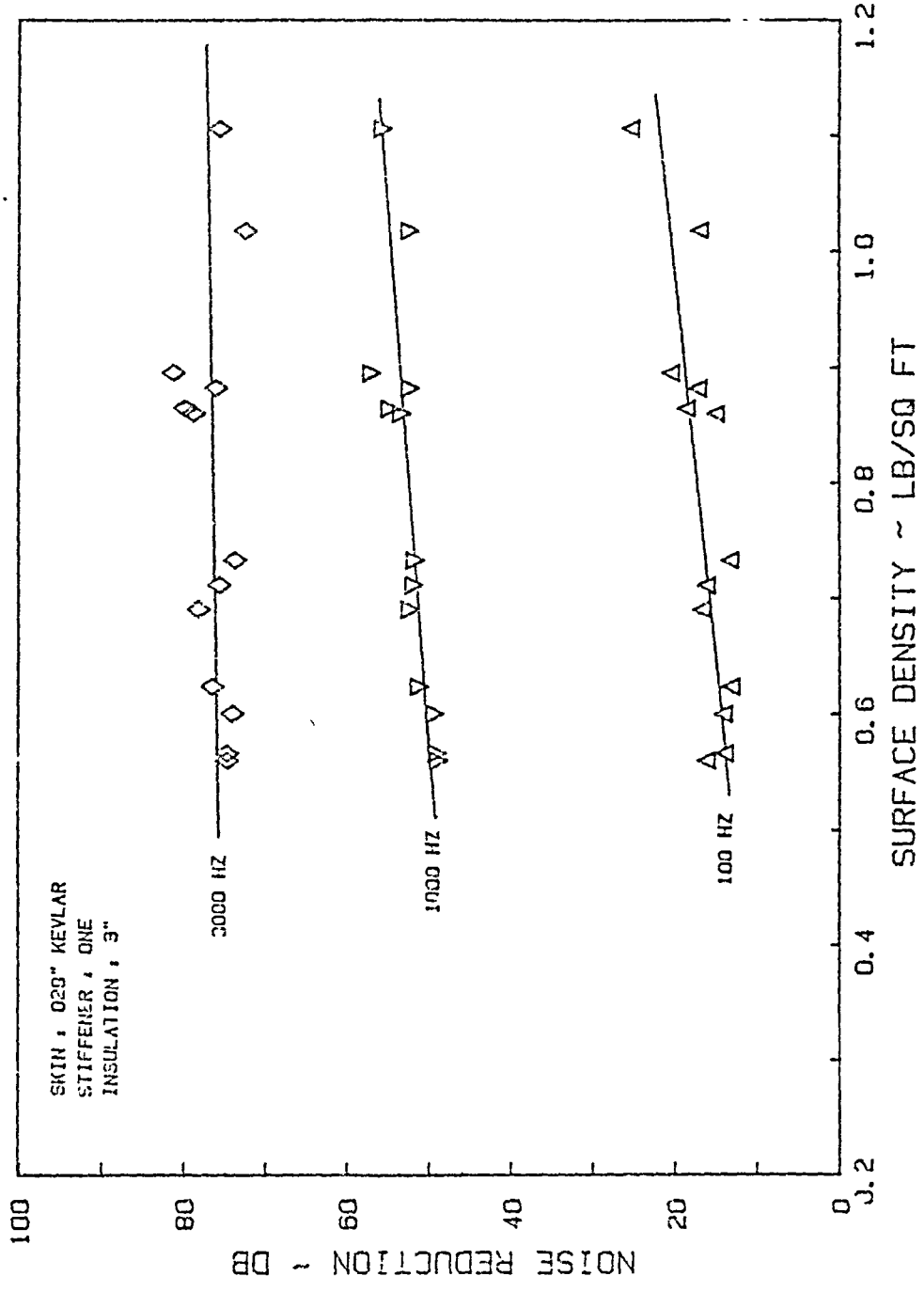

Figure 3.23: Effect of Total Panel Area Density on the Noise Reduction Characteristics of Double-Wall Panel with Kevlar Skin (Panel 339) and Insulation

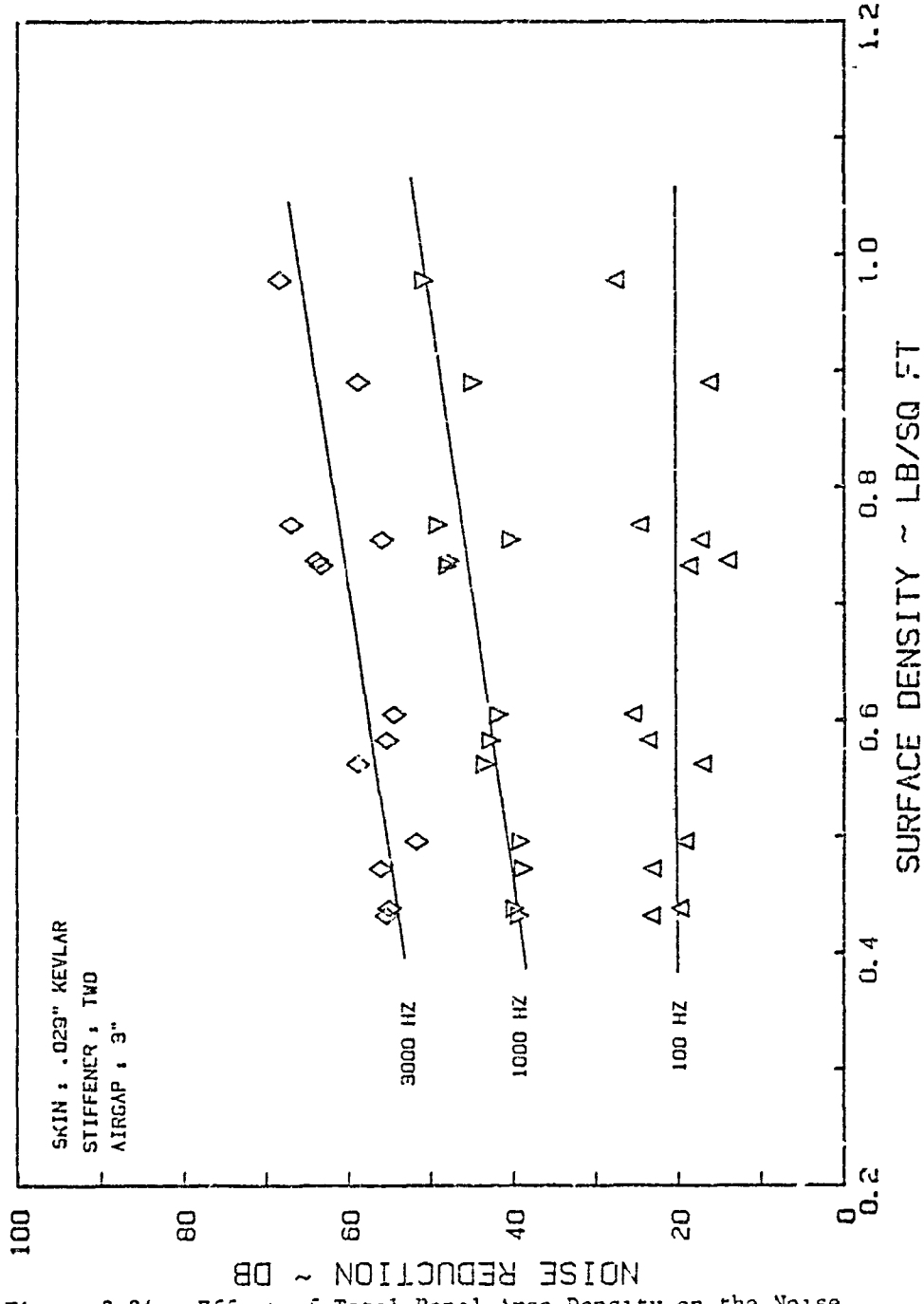

Figure 3.24: Effect of Total Panel Area Density on the Noise Reduction Characteristics of Double-Wall Panel with Kevlar Skin (Panel 340) and Airgap

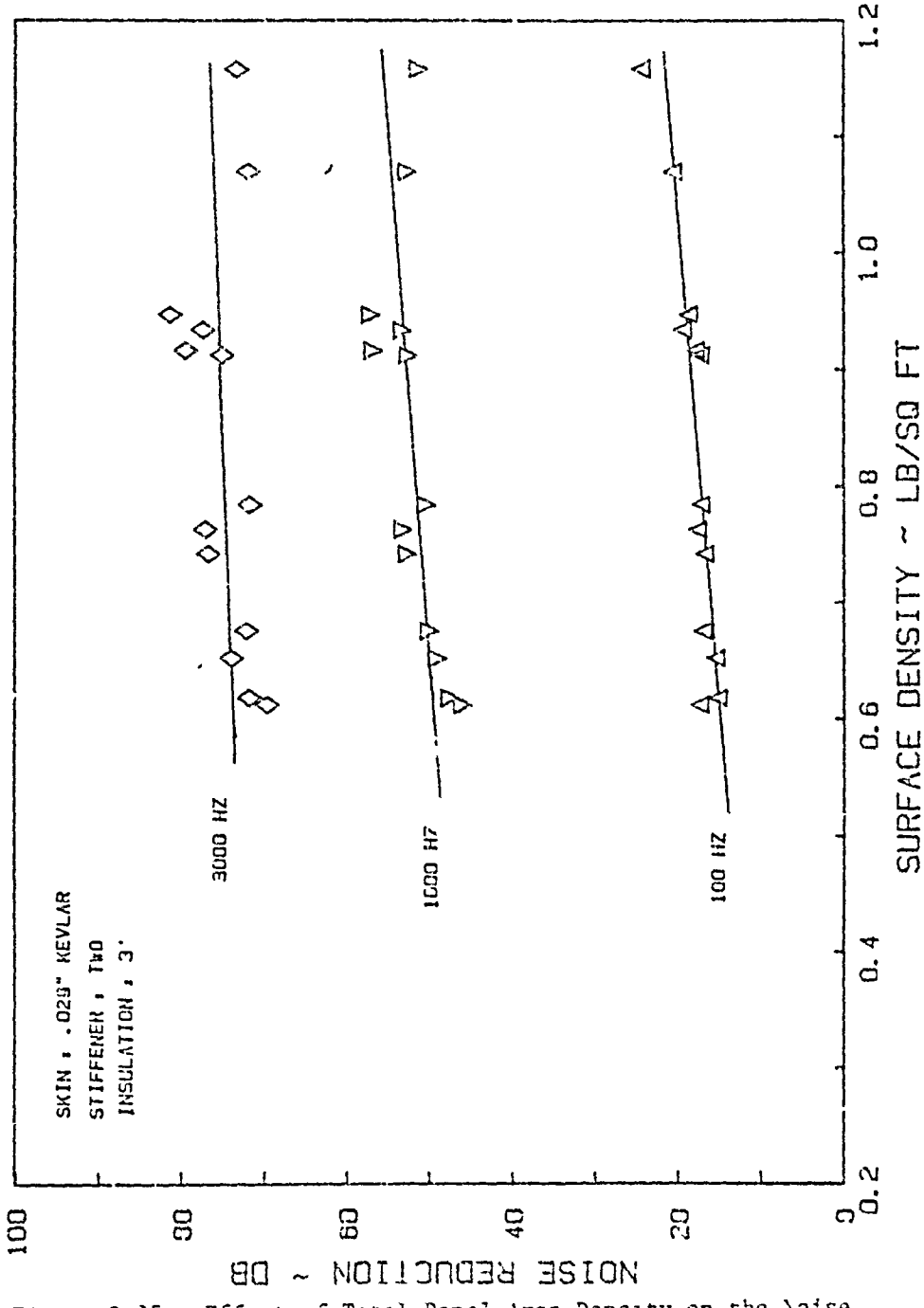

Figure 3.25: Effect of Total Panel Area Density on the Noise Reduction Characteristics of Double-Wall Panel with Kevlar Skin (Panel 340) and Insulation

in these plots. However, the mass of the trim panel is still (at least in the high frequency region) a major factor and represents the trade-off parameter that most often decides what material will be selected for use. Because of the scatter, mean square lines are shown, which indicate, as expected, increasing noise reduction with increase in mass. From Tables 3.1 and 3.2 it can be seen that trim panels 312 and 344 perform consistently better than the other panels, even after consideration of their higher area density. Both these panels are treated with flexible 1/2" foam material, over which is applied a (simulated) leather covering. The thickness of the foam may be one of the reasons for the better performance of these panels.

Four trim panels--312, 318, 325, and 352 (one each from groups 1 and 2, and two from group 3)--were selected for further investigation. Each of these panels has a different base material: 312 has 45% open pore aluminum, 318 has Rohacell core, 325 has Klege-cell base, and 352 has compressed fiberglass core. These trim panels are representative of the trim panels being used in the general aviation industry. Single panel noise reduction tests were performed, and the results are given in Figures 3.26 through 3.29. These results confirm that the limp panel assumption may not be valid for these panels. At this test facility, the noise reduction curve of a standard .032" aluminum panel shows a slope of 6 dB/octave, which corresponed to mass-law value. However, three of the four trim panels tested had less than 6 dB/octave slope. These values are tabulated in the next chapter. Only panel 312 had a slope of 8 dB/octave, far higher than mass-law slope. Panel 352 had a near zero slope, as can be seen from Figure 3.29. Both these

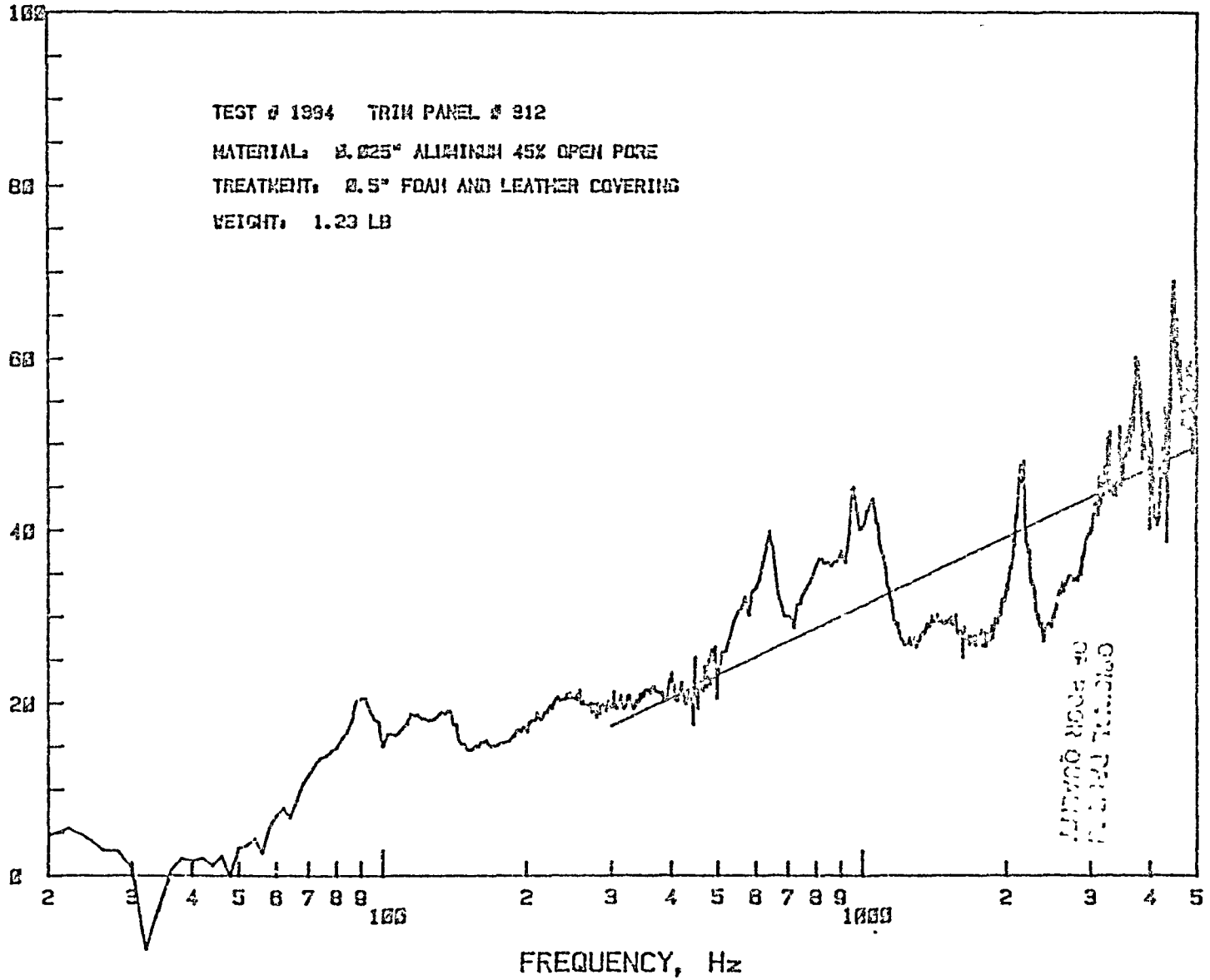

Figure 3.26: Noise Reduction Characteristics of Trim Panel 312

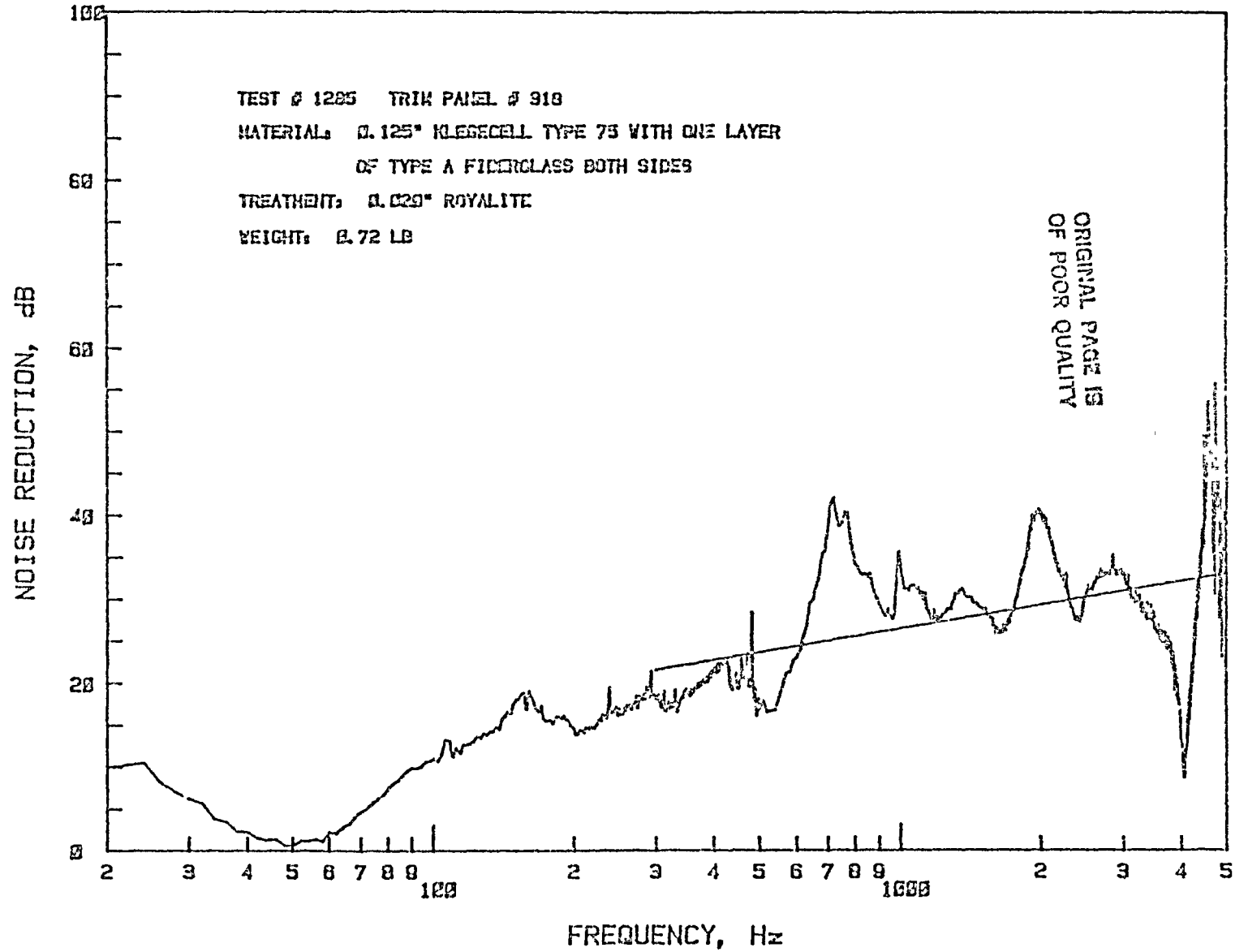

Figure 3.27: Noise Reduction Characteristics of Trim Panel 318

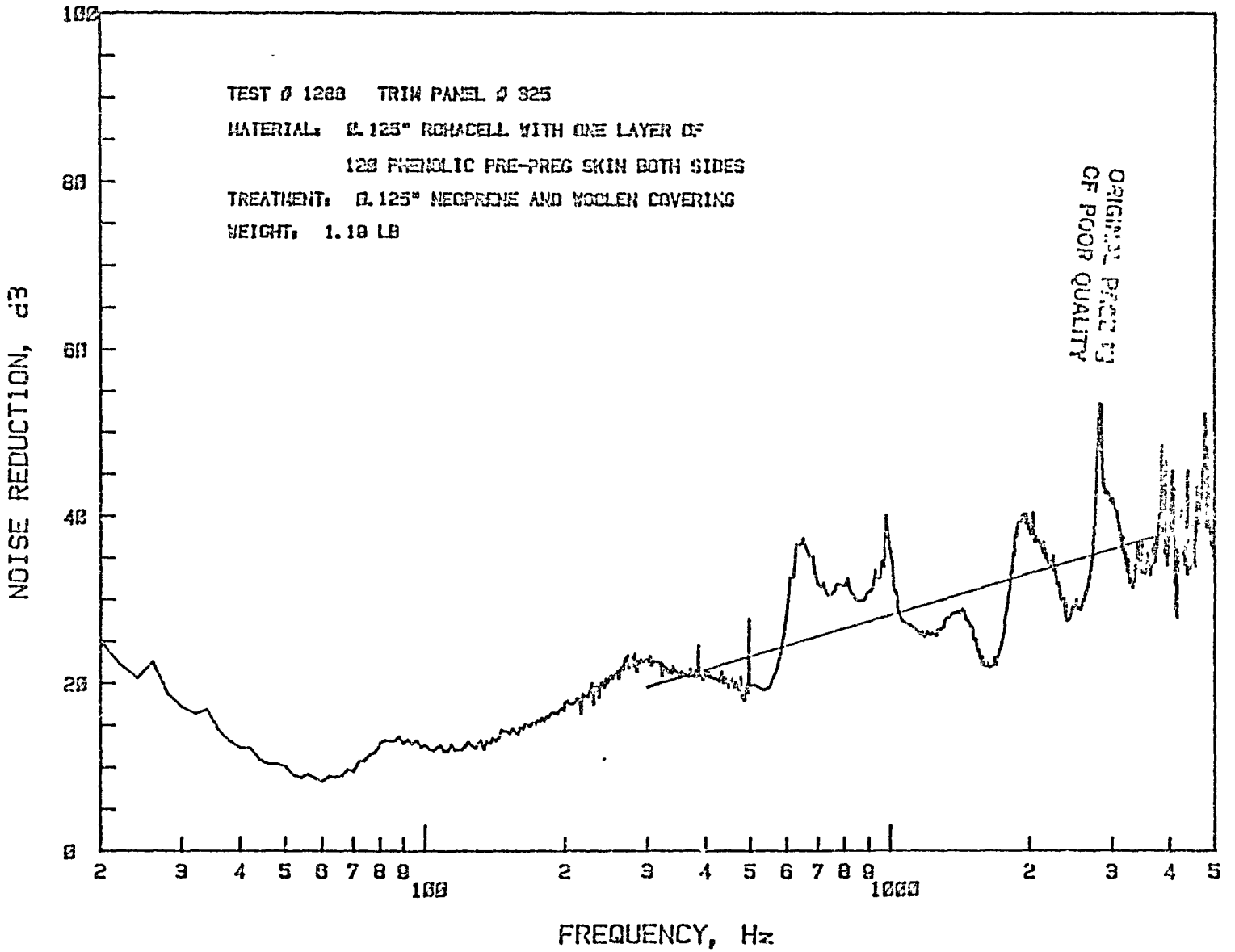

Figure 3.28: Noise Reduction Characteristics of Trim Panel 327

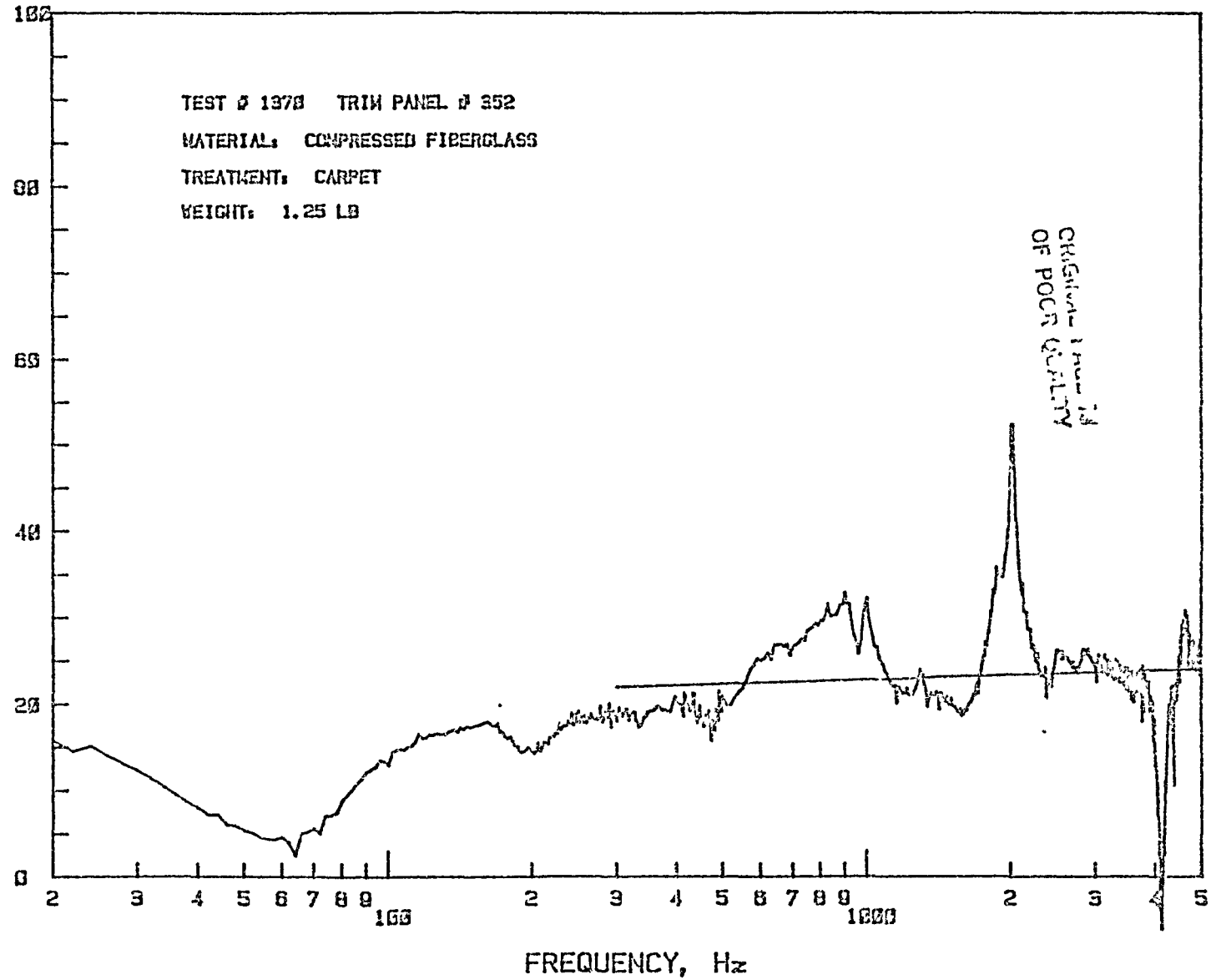

Figure 3.29: Noise Reduction Characteristics of Trim Panel 352

panels have nearly the same area density. While double-wall tests confirmed these trends, they also indicated that the effectiveness of panel 312 decreased and that of panel 352 increased, thus evening out the difference. This aspect is further discussed in the next chapter.

In the low frequency region of 40-100 Hz, panel 347 was superior to all other panels tested. Panel 347 was the thickest panel in group 2 and has two layers of 120 phenolic skin applied to both sides to stiffen the base material. Also it is made of light Rohacell material. This property of high stiffness and low mass increases its fundamental resonance frequency. This makes panel 347 superior to other panels in the low-frequency, stiffness-controlled region.

The effect of attachment of the trim panel to the channel section was also investigated. Two types of attachment procedures were tried. In one case the trim panel was screwed to the channel section by means of eight screws as shown in Figure 2.2. The second attachment was to simulate free-free edge conditions for the trim panel. This was done by using 1/8" thick pressure-sensitive adhesive tape. The results are compared in Tables 3.3 through 3.5. The results indicate that the effect of the attachment is felt only in the very low frequency region. An increase of 0-2 dB is observed with the free-free edge condition. This might be due to the better isolation of the trim panel at very low frequencies. At 100 Hz the results were inconclusive. It is possible that the vibration isolation of this tape is not effective at and above 100 Hz. At very high frequencies the panels with tape attachment indicate a gain of 0-3 dB. The results are within the experimental scatter observed in this frequency region. Increased mass of the 1/8" tape all around might have caused some of the increase.

Table 3.3: Effect of Trim Panel Attachment on the Noise Reduction Characteristics of Double-Wall Panels with Aluminum Skin; Depth 3"

a. Trim Panel 318

Frequency (Hz)	Airgap		Insulation	
	Screw	Tape	Screw	Tape
40	12	14	13	16
100	18	18	17	17
300	29	32	30	31
500	42	41	39	46
1000	48	50	56	59
3000	62	63	78	80

b. Trim Panel 325

Frequency (Hz)	Airgap		Insulation	
	Screw	Tape	Screw	Tape
40	18	18	20	20
100	16	16	16	16
300	42	43	34	35
500	45	46	41	46
1000	53	53	59	59
3000	65	65	78	78

Table 3.4: Effect of Trim Panel Attachment on the Noise Reduction Characteristics of Double-Wall Panels with Aluminum Skin; Depth 2"

a. Trim Panel 318

Frequency (Hz)	Airgap		Insulation	
	Screw	Tape	Screw	Tape
40	13	14	14	16
100	16	15	14	15
300	19	26	26	26
500	45	42	43	42
1000	47	50	53	57
3000	61	63	78	80

b. Trim Panel 325

Frequency (Hz)	Airgap		Insulation	
	Screw	Tape	Screw	Tape
40	16	16	18	20
100	14	14	15	14
300	34	35	32	35
500	42	45	43	41
1000	47	49	54	56
3000	61	63	74	76

Table 3.5: Effect of Trim Panel Attachment on the Noise Reduction Characteristics of Double-Wall Panels with Aluminum Skin; Panel Depth 1"

a. Trim Panel 318

Frequency (Hz)	Airgap		Insulation	
	Screw	Tape	Screw	Tape
40	14	15	15	16
100	13	13	13	14
300	19	21	16	17
500	35	32	32	36
1000	42	43	48	51
3000	61	62	72	75

b. Trim Panel 325

Frequency (Hz)	Airgap		Insulation	
	Screw	Tape	Screw	Tape
40	17	18	20	20
100	15	12	15	15
300	32	30	23	24
500	37	41	35	35
1000	46	46	50	51
3000	63	64	73	73

CHAPTER 4

THEORETICAL ANALYSIS

4.1 INTRODUCTION

The prediction of aircraft interior noise levels has attracted considerable attention during recent years. One of the important parts of this investigation is the accurate determination of sound transmission loss across a fuselage sidewall throughout the frequency range of interest. A typical fuselage sidewall consists of skin, trim, septa, fiberglass insularion, and airgap. A computer program was developed at the KU-FRL to calculate the transmission loss across the double-wall structures whose noise reduction characteristics were being investigated experimentally. The main objective of the program was to compare the computer-calculated results with the results obtained from experimental investigations. The program is described in detail in References 1 and 2.

The program follows the classical acoustic transmission loss theory used in References 8 and 9. In this program the sound transmission loss of a multilayered panel is calculated from the pressure losses across individual layers. The pressure loss across each layer is a function of its own impedance as well as the terminating impedance for that layer. The transmission loss of a multilayered panel is obtained from the following equation:

$$TL = 10 \log|p_i/p_t|^2$$

where TL = Transmission loss across the panel (dB)

p_i = Blocked pressure on the incident side (Pa)

p_t = Pressure on the receiver side (Pa)

p_i/p_t = Pressure ratio across the panel of n layers

n = Total number of layers in the panel.

The pressure ratio across the entire panel is calculated from the pressure ratios across each layer as

$$\{p_i/p_t\}^2 = \{p_i/p_2 \cdot p_2/p_3 \cdots p_k/p_{k+1} \cdots p_n/p_t\}^2$$

where p_k/p_{k+1} = the pressure ratio across kth layer.

The pressure ratio across each layer is calculated from the impedance model of that layer. Reference 2 details the types of impedance models available in the KU-FRL program. This program has been checked out using the inputs from Reference 9. A few of the impedance models have been modified to facilitate comparison with the test results. Important modifications are

a. Actual transmission loss should measure only the incident pressure on the source side. But at the KU-FRL acoustic test facility the source microphone measures the blocked sound pressure, which consists of both incident and reflected pressures. This effect has been taken into account in the program.

b. The receiver microphone measures both the transmitted sound pressure and the reflected pressure from the receiver cavity. As explained in Appendix A, the receiver cavity absorbs most of the transmitted energy. Hence the contribution of the reflected pressure is assumed to be negligible. In other words, the absorption coefficient of the cavity has been assumed to be equal to 1.

c. At low frequency the receiving cavity stiffens the panel due to Helmholtz effect. This effect increases the measured fundamental resonance frequency of the single panel. Hence the measured resonance frequency is greater than the calculated resonance frequency. This effect can also be expected for the double-wall panels. Since the purpose of the program is only to calculate the double-wall transmission loss values, no modifications have been done to account for this effect. This effect is taken into account by inputting the measured single panel resonance frequency of the trim and the skin panel, instead of calculating their resonance frequencies within the program.

d. In practice the trim panel is modelled as a limp panel. In classical sound transmission loss theory, limp panel impedance is directly proportional to the surface density and the frequency. The transmission loss resulting from this impedance is known as mass-law transmission loss. Under these assumptions the transmission loss increases by 6 dB for doubling of either the mass or the frequency. In a transmission loss vs frequency plot, this produces 6 dB/ octave slope. However, as can be seen from the test results (Figures 3.26 through 3.29), the slope of the least mean-square line of the trim panels varies considerably. Hence a simple mass-law assumption seems to be invalid for such trim panels. Three out of the four panels tested had slopes less than the theoretical values. Hence the use of mass-law

approximation produces a higher transmission loss for a double panel. In order to overcome this problem, an additional option for the trim panel was introduced for the trim panel impedance. In this option the measured slope is used. The model uses mass law impedance for low frequency and impedance corresponding to the measured slope at high frequency. The experimental slope is input as a ratio of the measured slope to theoretical slope (6 dB/octave), and this ratio is called the slope factor. Values of these factors for various trim panels are given in Reference 2. For this study these values were measured from Figures 3.26 through 3.29.

At this point it is pertinent to explain the difference in the terminology used to describe the experimental and the theoretical results. The experimental results are called "noise reduction," and the theoretical results are called "transmission loss." The reason for this is the following. The sound energy attenuation measured in this test facility is made up of two parts. Reference 6 defines the noise reduction at any frequency as

$$NR = 10 \log(1 + \tau/\alpha)$$

where τ = Panel transmission loss coefficient at that frequency

α = Absorption coefficient of the receiver cavity at that frequency.

The panel transmission loss coefficient is related to the panel pressure ratio by

$$1/\tau = (p_i/p_t)^2$$

where p_i = Blocked incident pressure (Pa)

p_t = Transmitted pressure (Pa).

The absorption coefficient is normally less than one. When the cavity is nearly fully absorptive, as in the case of the KU-FRL acoustic test facility, the noise reduction and transmission loss will be nearly the same. In case the cavity is not fully absorptive, noise reduction values in general will be less than transmission loss. At cavity resonance frequencies such simplifications will not be valid. At the KU-FRL experimental test facility the receiver microphone measures both the transmitted pressure and the very weak reflections from the cavity walls. Hence the sound attenuation characteristics measured from this facility are noise reduction. The theoretical values calculated from the program do not contain any corrections and hence are transmission loss values.

4.2 DETAILS OF THE INPUT DATA

For the theoretical investigation the parameters chosen to vary were

a. Panel depth

b. Effect of sound insulation

c. Effect of skin structure

d. Effect of trim panel material and treatment.

Four skin panels and four trim panels were used for the comparison of the theoretical and the calculated values. The skin panels tested are given in Table 2.1. Trim panels used were 312, 318, 325, and 352. The details of these panels are presented in Table 2.2. The impedance

model used for the skin and trim panels was the single mode approximation. This approximation, described in detail in Reference 2, requires single panel resonance frequencies of the skin panel and its damping ratio around that frequency region. The single panel test results from Reference 5 were used for the resonance frequencies. The damping values of these panels had been measured and were reported in Reference 1. These values were used in the calculation of the impedance. These values are tabulated in Table 4.1

The mechanical properties of the fiberglass insulation were unknown. This insulation material was very similar to PF 105 fiberglass insulation discussed in Reference 6. Also the minor variations in porosity and resistivity of the insulation did not significantly change the transmission loss values. Hence the porosity and the resistivity of PF 105 material was used. However, actual fiberglass density was input.

The input data required for the trim panels were fundamental resonance frequency, damping ratio, and the experimental slope of the noise reduction and damping tests of the trim panels alone. These values are tabulated in Table 4.2.

4.3 RESULTS AND DISCUSSION

The outputs from the computer runs are plotted in Figures 4.1 through 4.24 for the 48 combinations considered. These calculated values are plotted as dotted lines over the experimental values. Each figure contains two plots: one with the fiberglass insulation between the skin and the trim panel and the other without the insulation.

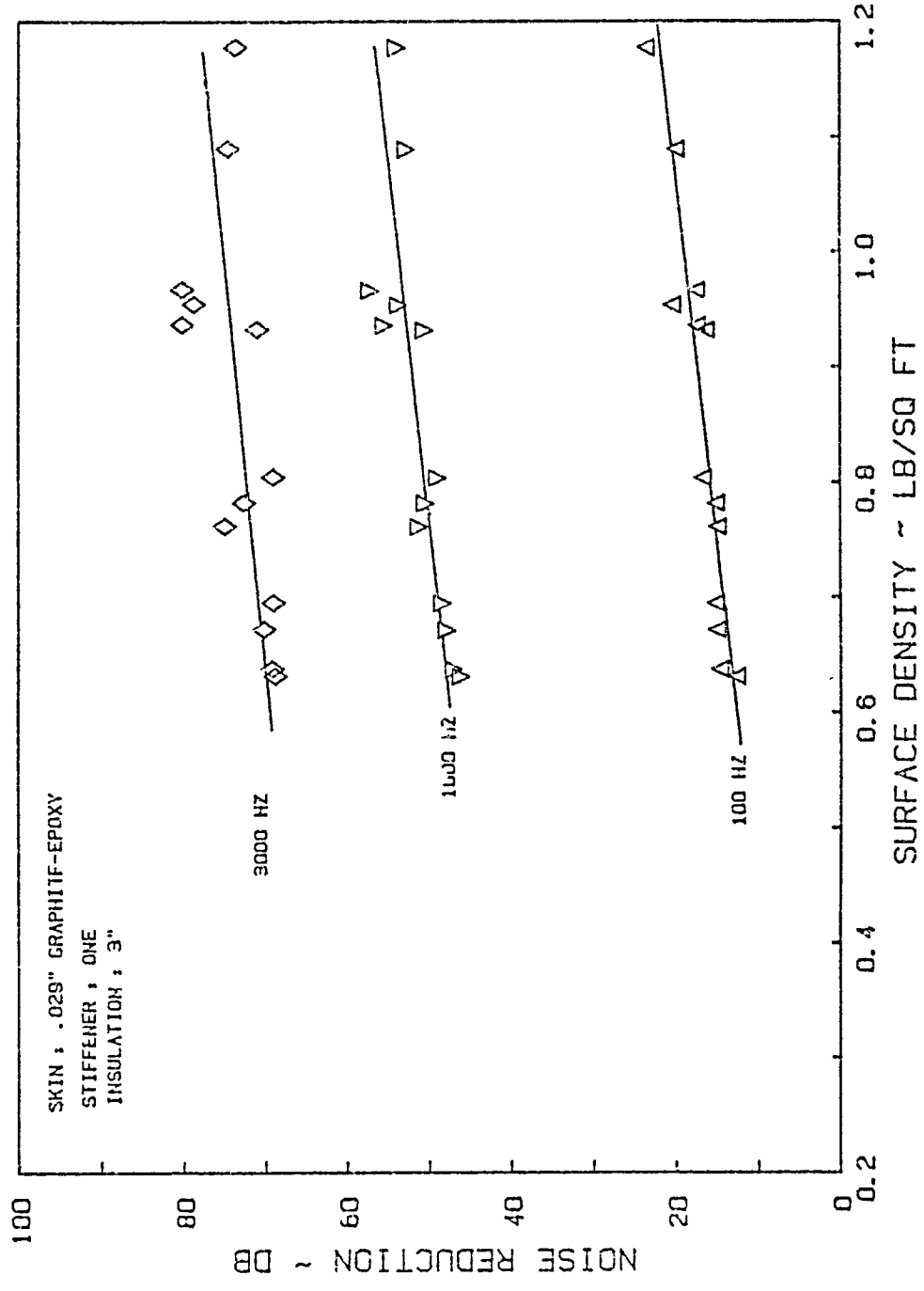

Figure 3.21: Effect of Total Panel Area Density on the Noise Reduction Characteristics of Double-Wall Panel with Graphite-Epoxy Skin (Panel 335) and Insulation

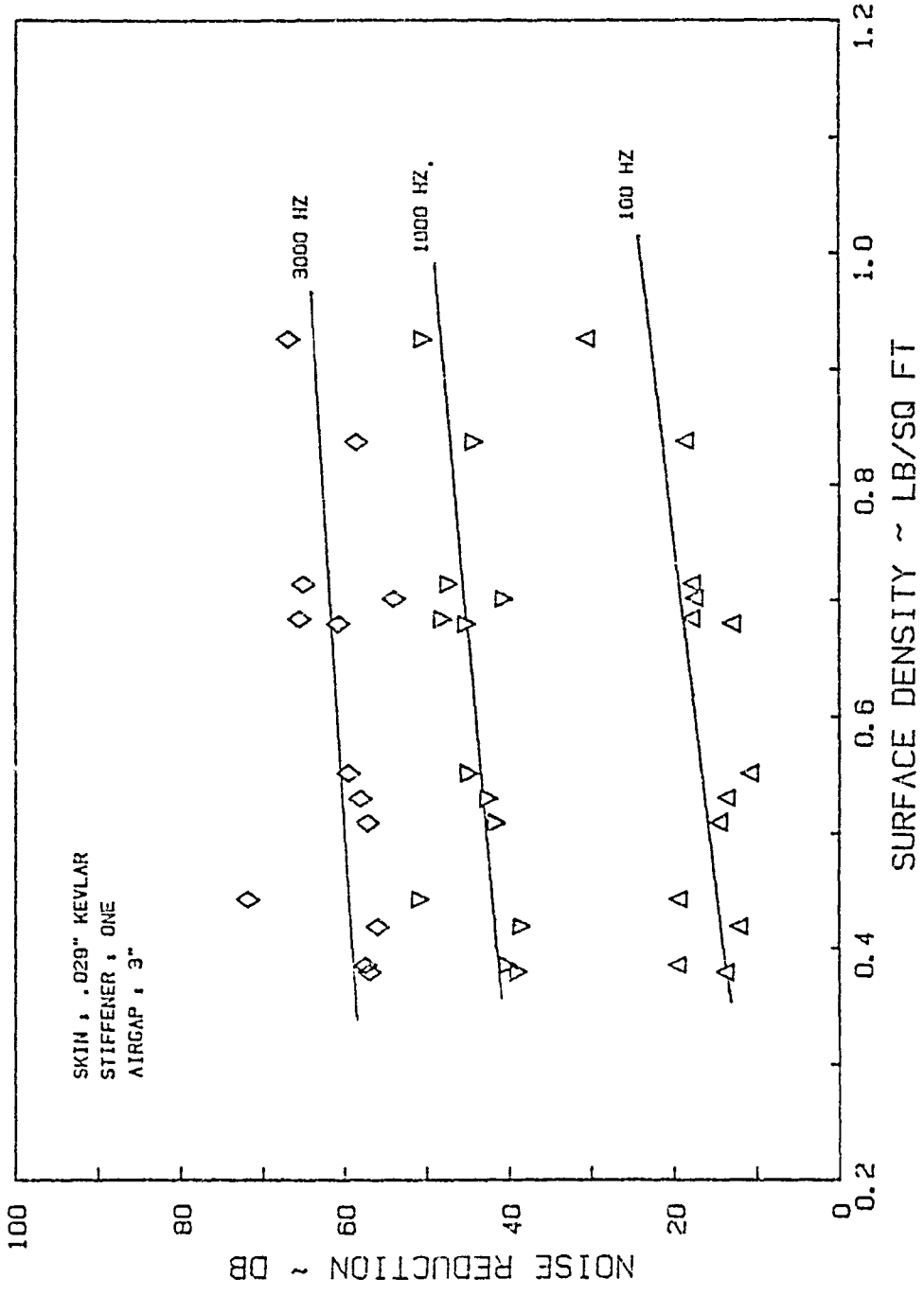

Figure 3.22: Effect of Total Panel Area Density on the Noise Reduction Characteristics of Double-Wall Panel with Kevlar Skin (Panel 339) and Airgap

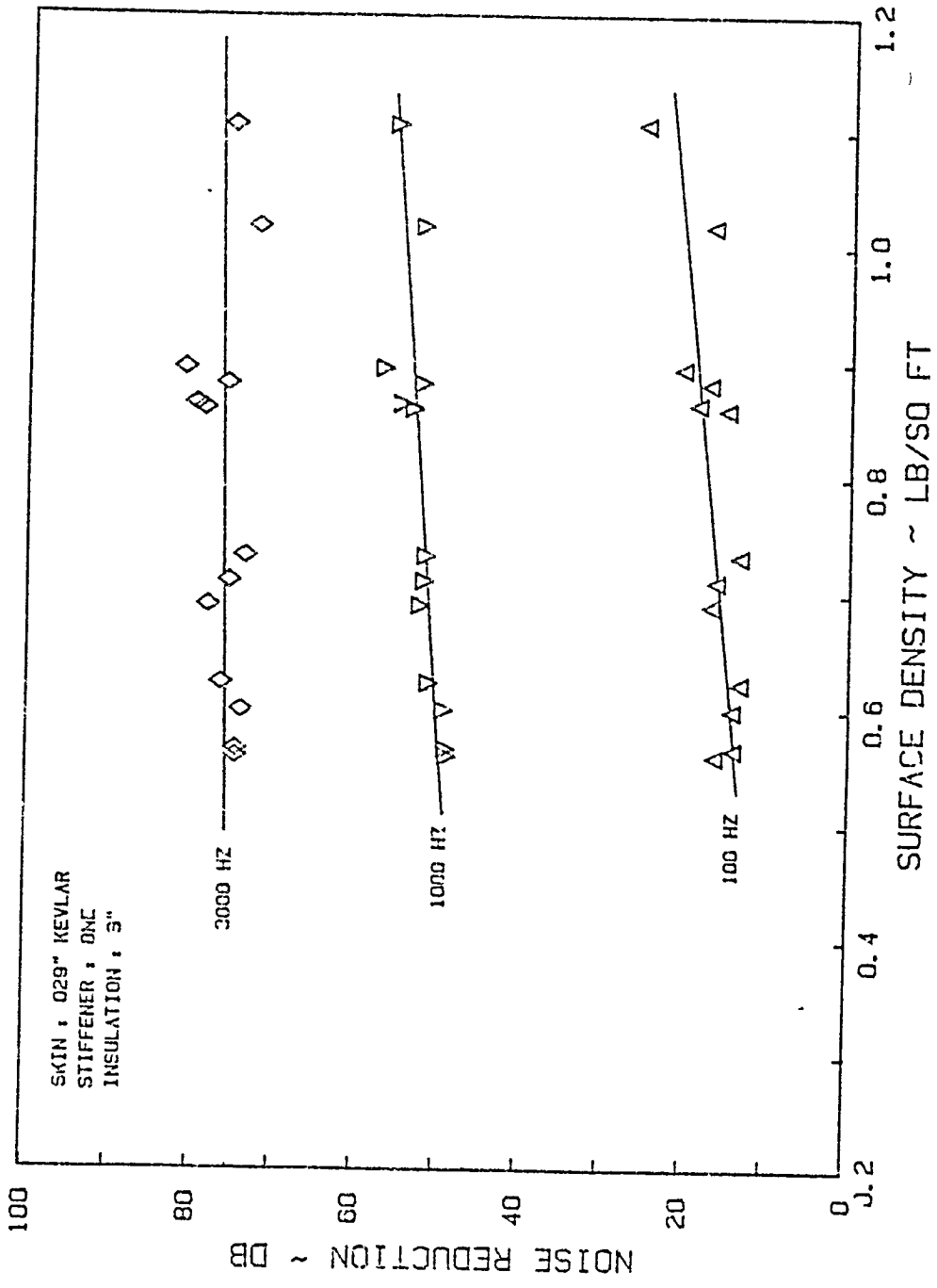

Figure 3.23: Effect of Total Panel Area Density on the Noise Reduction Characteristics of Double-Wall Panel with Kevlar Skin (Panel 339) and Insulation

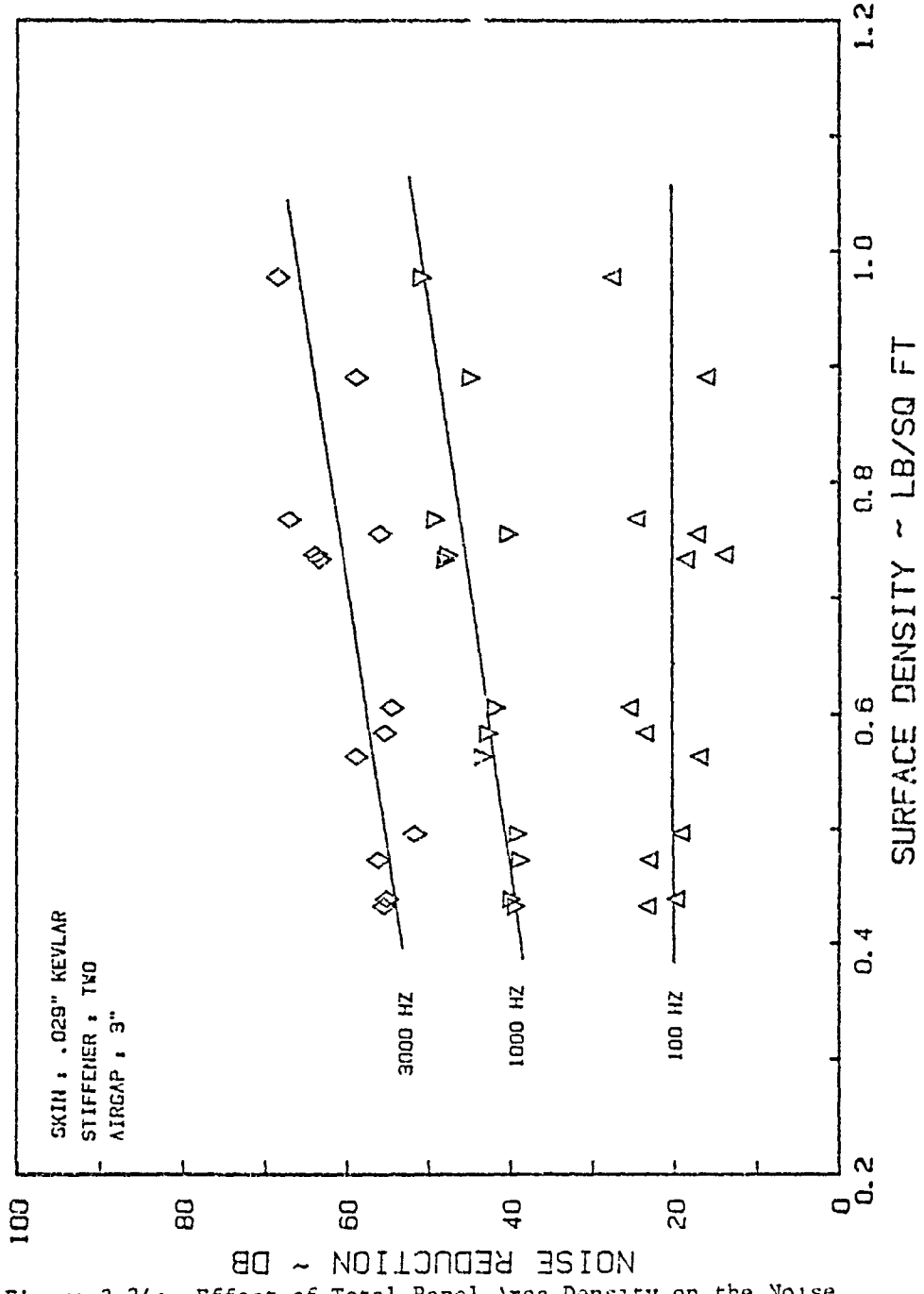

Figure 3.24: Effect of Total Panel Area Density on the Noise Reduction Characteristics of Double-Wall Panel with Kevlar Skin (Panel 340) and Airgap

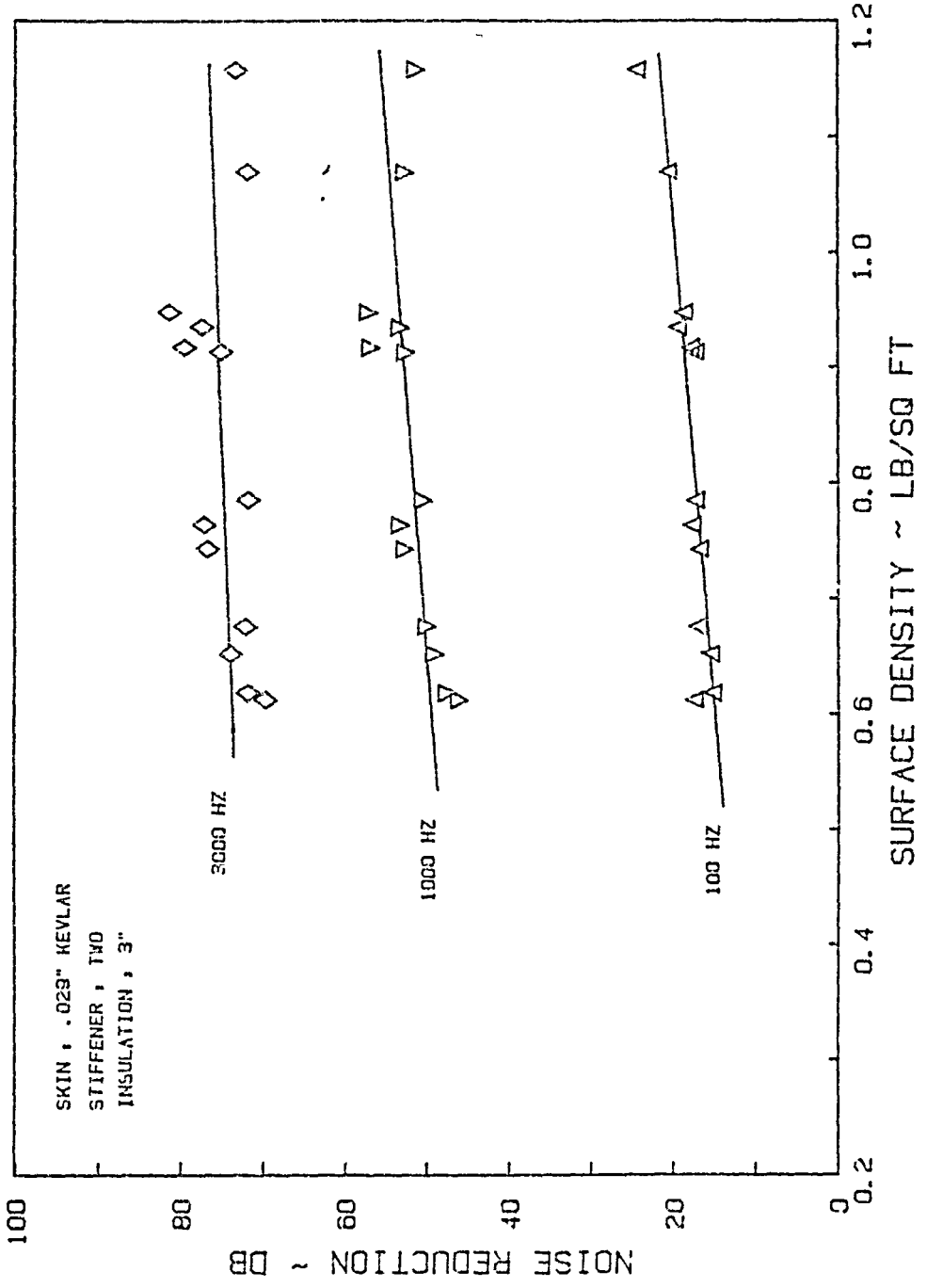

Figure 3.25: Effect of Total Panel Area Density on the Noise Reduction Characteristics of Double-Wall Panel with Kevlar Skin (Panel 340) and Insulation

in these plots. However, the mass of the trim panel is still (at least in the high frequency region) a major factor and represents the trade-off parameter that most often decides what material will be selected for use. Because of the scatter, mean square lines are shown, which indicate, as expected, increasing noise reduction with increase in mass. From Tables 3.1 and 3.2 it can be seen that trim panels 312 and 344 perform consistently better than the other panels, even after consideration of their higher area density. Both these panels are treated with flexible 1/2" foam material, over which is applied a (simulated) leather covering. The thickness of the foam may be one of the reasons for the better performance of these panels.

Four trim panels--312, 318, 325, and 352 (one each from groups 1 and 2, and two from group 3)--were selected for further investigation. Each of these panels has a different base material: 312 has 45% open pore aluminum, 318 has Rohacell core, 325 has Klege-cell base, and 352 has compressed fiberglass core. These trim panels are representative of the trim panels being used in the general aviation industry. Single panel noise reduction tests were performed, and the results are given in Figures 3.26 through 3.29. These results confirm that the limp panel assumption may not be valid for these panels. At this test facility, the noise reduction curve of a standard .032" aluminum panel shows a slope of 6 dB/octave, which corresponed to mass-law value. However, three of the four trim panels tested had less than 6 dB/octave slope. These values are tabulated in the next chapter. Only panel 312 had a slope of 9 dB/octave, far higher than mass-law slope. Panel 352 had a near zero slope, as can be seen from Figure 3.29. Both these

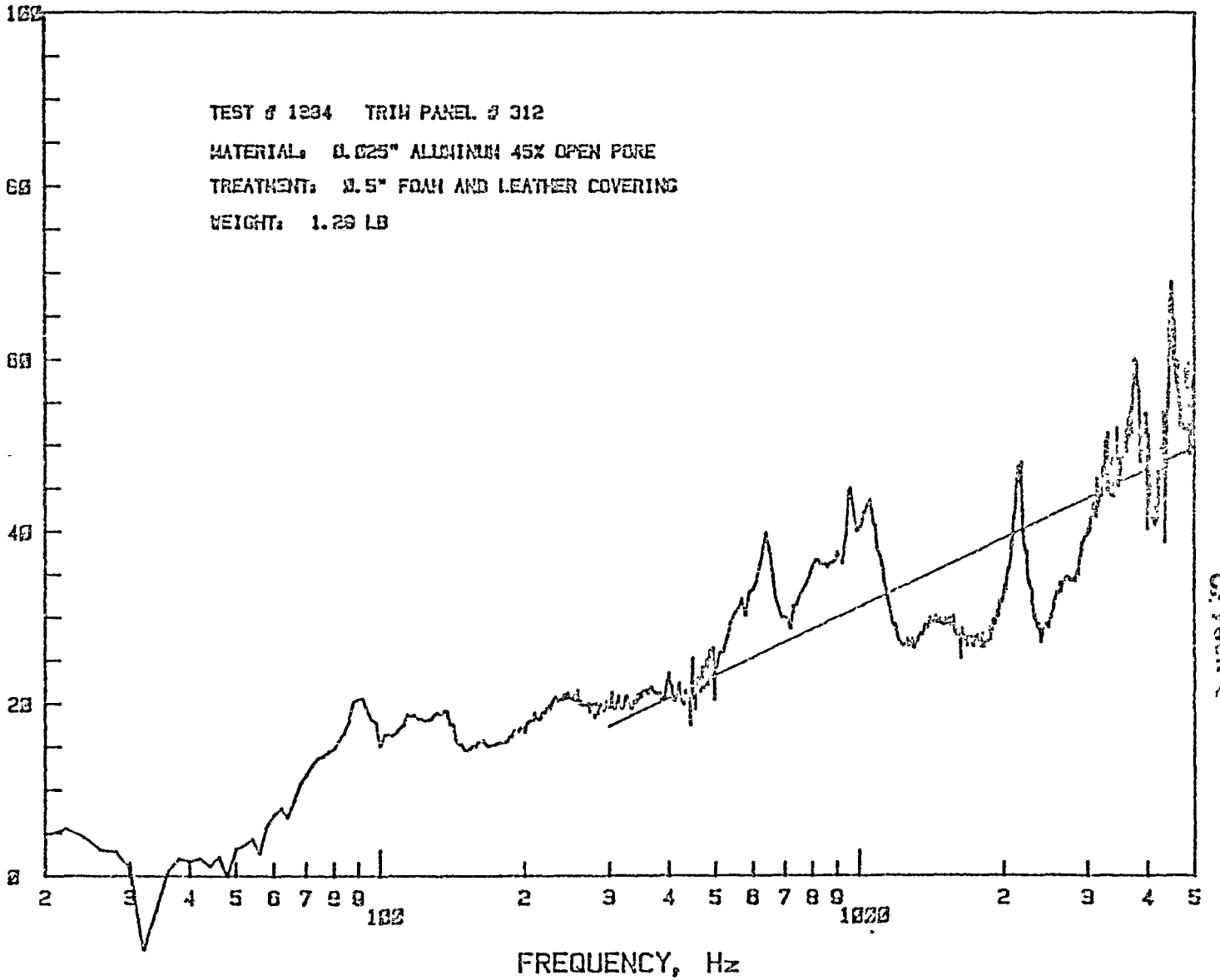

Figure 3.26: Noise Reduction Characteristics of Trim Panel 312

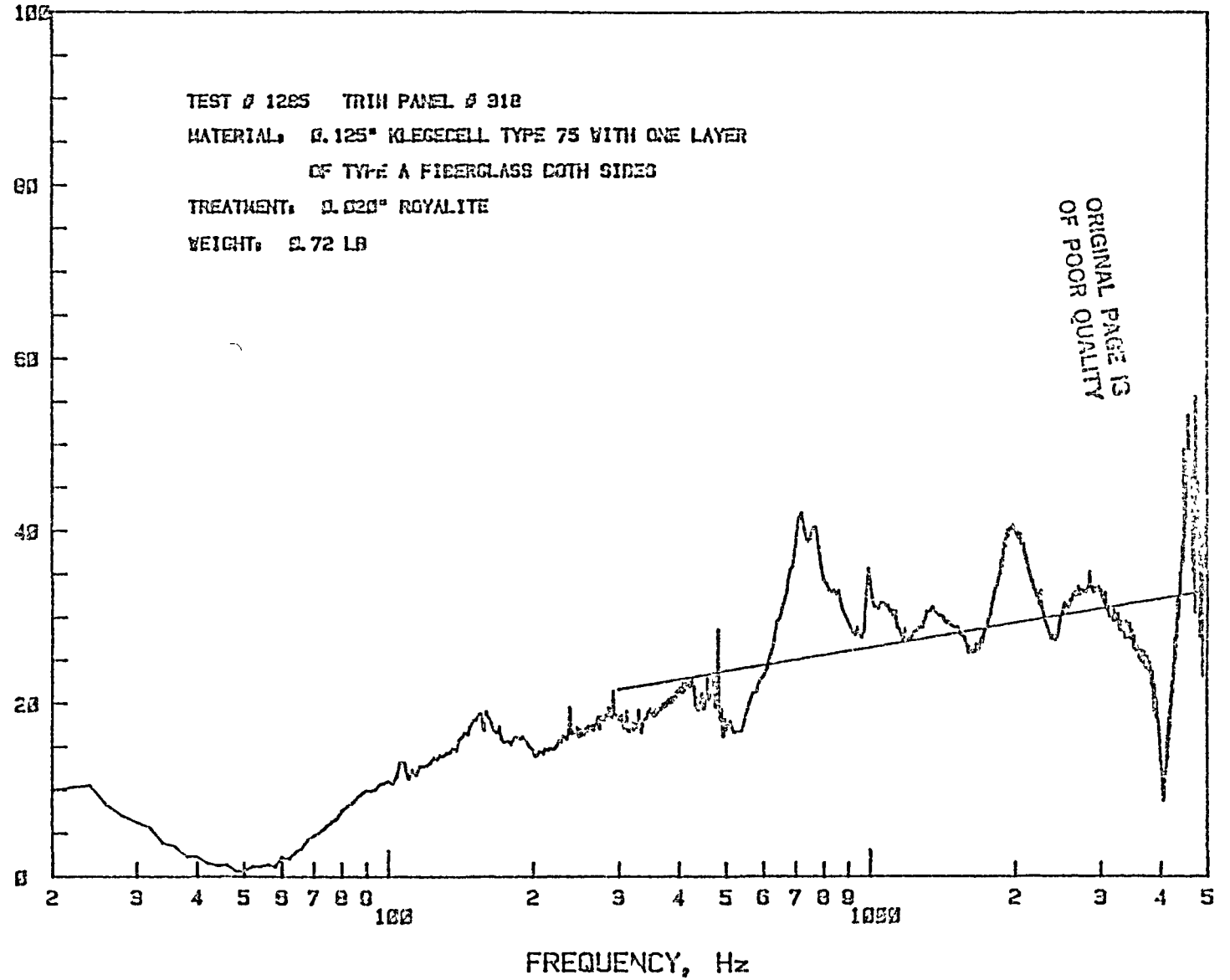

Figure 3.27: Noise Reduction Characteristics of Trim Panel 318

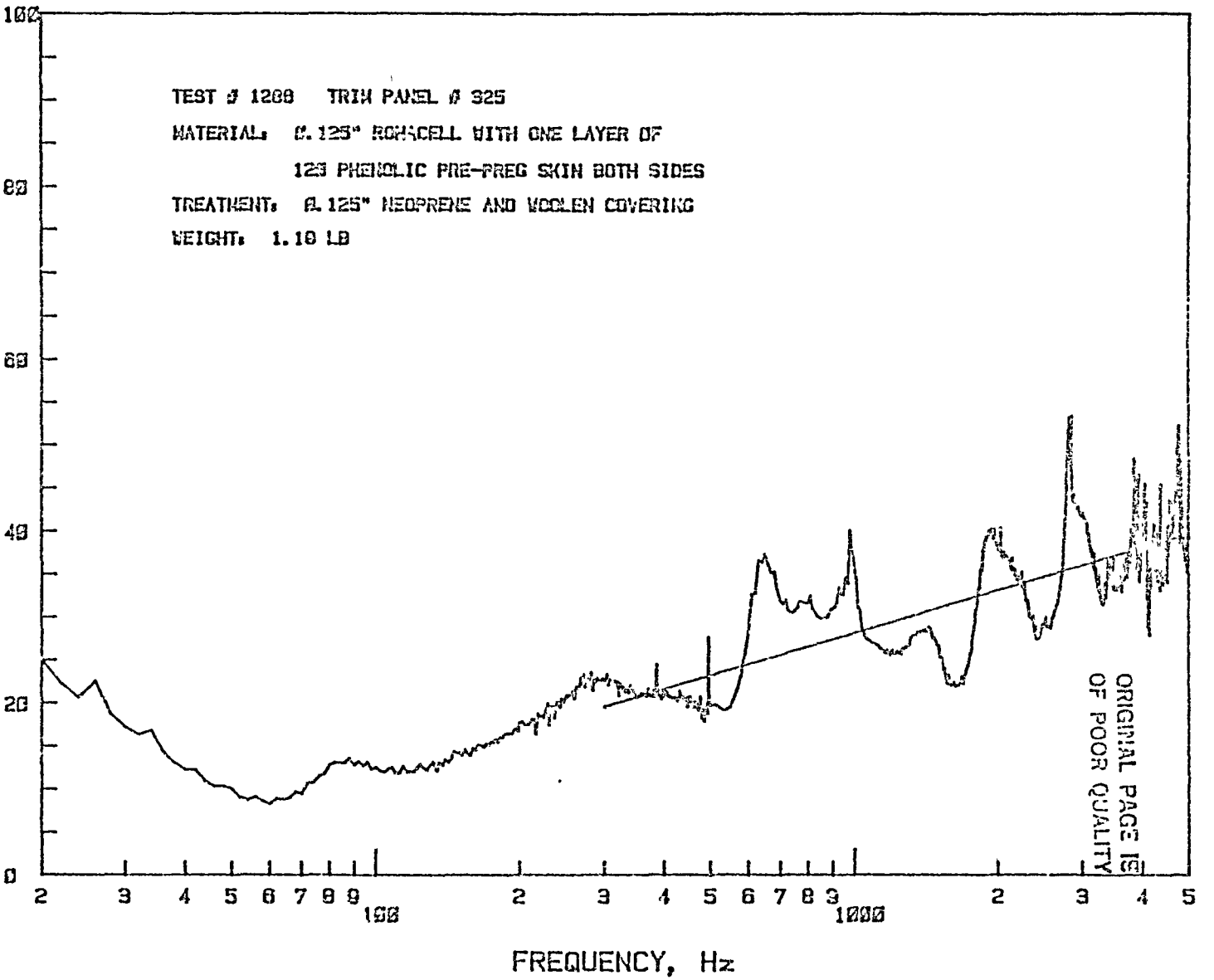

Figure 3.28: Noise Reduction Characteristics of Trim Panel 325

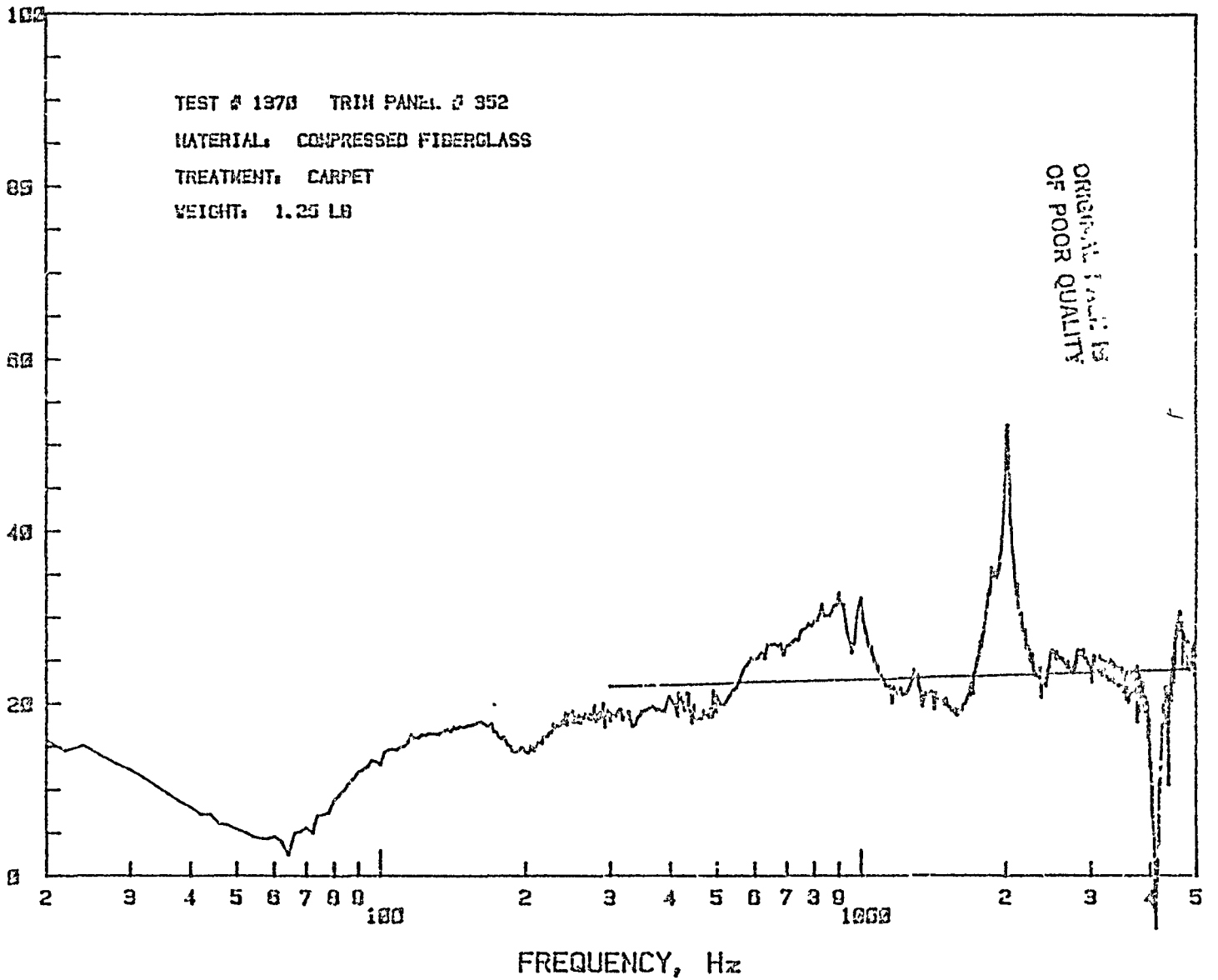

Figure 3.29: Noise Reduction Characteristics of Trim Panel 352

panels have nearly the same area density. While double-wall tests confirmed these trends, they also indicated that the effectiveness of panel 312 decreased and that of panel 352 increased, thus evening out the difference. This aspect is further discussed in the next chapter.

In the low frequency region of 40-100 Hz, panel 347 was superior to all other panels tested. Panel 347 was the thickest panel in group 2 and has two layers of 120 phenolic skin applied to both sides to stiffen the base material. Also it is made of light Rohacell material. This property of high stiffness and low mass increases its fundamental resonance frequency. This makes panel 347 superior to other panels in the low-frequency, stiffness-controlled region.

The effect of attachment of the trim panel to the channel section was also investigated. Two types of attachment procedures were tried. In one case the trim panel was screwed to the channel section by means of eight screws as shown in Figure 2.2. The second attachment was to simulate free-free edge conditions for the trim panel. This was done by using 1/8" thick pressure-sensitive adhesive tape. The results are compared in Tables 3.3 through 3.5. The results indicate that the effect of the attachment is felt only in the very low frequency region. An increase of 0-2 dB is observed with the free-free edge condition. This might be due to the better isolation of the trim panel at very low frequencies. At 100 Hz the results were inconclusive. It is possible that the vibration isolation of this tape is not effective at and above 100 Hz. At very high frequencies the panels with tape attachment indicate a gain of 0-3 dB. The results are within the experimental scatter observed in this frequency region. Increased mass of the 1/8" tape all around might have caused some of the increase.

Table 3.3: Effect of Trim Panel Attachment on the Noise Reduction Characteristics of Double-Wall Panels with Aluminum [illegible]; Depth 3"

a. Trim Panel 318

Frequency (Hz)	Airgap		Insulation	
	Screw	Tape	Screw	Tape
40	12	14	13	16
100	18	18	17	17
300	29	32	30	31
500	42	41	39	46
1000	48	50	56	59
3000	62	63	78	80

b. Trim Panel 325

Frequency (Hz)	Airgap		Insulation	
	Screw	Tape	Screw	Tape
40	18	18	20	20
100	16	16	16	16
300	42	43	34	35
500	45	46	41	46
1000	53	53	59	59
3000	65	65	78	78

Table 3.4: Effect of Trim Panel Attachment on the Noise Reduction Characteristics of Double-Wall Panels with Aluminum Skin; Depth 2"

a. Trim Panel 318

Frequency (Hz)	Airgap		Insulation	
	Screw	Tape	Screw	Tape
40	13	14	14	16
100	16	15	14	13
300	19	26	26	26
500	45	42	43	42
1000	47	50	53	57
3000	61	63	78	80

b. Trim Panel 325

Frequency (Hz)	Airgap		Insulation	
	Screw	Tape	Screw	Tape
40	16	1(	18	20
100	14	14	15	14
300	34	35	32	35
500	42	45	43	41
1000	47	49	54	56
3000	61	63	74	76

Table 3.3: Effect of Trim Panel Attachment on the Noise Reduction Characteristics of Double-Wall Panels with Aluminum Skin; Panel Depth 1"

a. Trim Panel 318

Frequency (Hz)	Airgap		Insulation	
	Screw	Tape	Screw	Tape
40	14	15	15	16
100	13	13	13	14
300	19	21	16	17
500	35	32	32	36
1000	42	43	48	51
3000	61	62	72	75

b. Trim Panel 325

Frequency (Hz)	Airgap		Insulation	
	Screw	Tape	Screw	Tape
40	17	18	20	20
100	15	12	15	15
300	32	30	23	24
500	37	41	35	35
1000	46	46	50	51
3000	63	64	73	73

CHAPTER 4

THEORETICAL ANALYSIS

4.1 INTRODUCTION

The prediction of aircraft interior noise levels has attracted considerable attention during recent years. One of the important parts of this investigation is the accurate determination of sound transmission loss across a fuselage sidewall throughout the frequency range of interest. A typical fuselage sidewall consists of skin, trim, septa, fiberglass insulation, and airgap. A computer program was developed at the KU-FRL to calculate the transmission loss across the double-wall structures whose noise reduction characteristics were being investigated experimentally. The main objective of the program was to compare the computer-calculated results with the results obtained from experimental investigations. The program is described in detail in References 1 and 2.

The program follows the classical acoustic transmission loss theory used in References 8 and 9. In this program the sound transmission loss of a multilayered panel is calculated from the pressure losses across individual layers. The pressure loss across each layer is a function of its own impedance as well as the terminating impedance for that layer. The transmission loss of a multilayered panel is obtained from the following equation:

$$TL = 10 \log|p_i/p_t|^2$$

where TL = Transmission loss across the panel (dB)

p_i = Blocked pressure on the incident side (Pa)

p_t = Pressure on the receiver side (Pa)

p_1/p_t = Pressure ratio across the panel of n layers

n = Total number of layers in the panel.

The pressure ratio across the entire panel is calculated from the pressure ratios across each layer as

$$\{p_1/p_t\}^2 = \{p_1/p_2 \cdot p_2/p_3 \cdots p_k/p_{k+1} \cdots p_n/p_t\}^2$$

where p_k/p_{k+1} = the pressure ratio across ktn layer.

The pressure ratio across each layer is calculated from the impedance model of that layer. Reference 2 details the types of impedance models available in the KU-FRL program. This program has been checked out using the inputs from Reference 9. A few of the impedance models have been modified to facilitate comparison with the test results. Important modifications are

a. Actual transmission loss should measure only the incident pressure on the source side. But at the KU-FRL acoustic test facility the source microphone measures the blocked sound pressure, which consists of both incident and reflected pressures. This effect has been taken into account in the program.

b. The receiver microphone measures both the transmitted sound pressure and the reflected pressure from the receiver cavity. As explained in Appendix A, the receiver cavity absorbs most of the transmitted energy. Hence the contribution of the reflected pressure is assumed to be negligible. In other words, the absorption coefficient of the cavity has been assumed to be equal to 1.

c. At low frequency the receiving cavity stiffens the panel due to Helmholtz effect. This effect increases the measured fundamental resonance frequency of the single panel. Hence the measured resonance frequency is greater than the calculated resonance frequency. This effect can also be expected for the double-wall panels. Since the purpose of the program is only to calculate the double-wall transmission loss values, no modifications have been done to account for this effect. This effect is taken into account by inputting the measured single panel resonance frequency of the trim and the skin panel, instead of calculating their resonance frequencies within the program.

d. In practice the trim panel is modelled as a limp panel. In classical sound transmission loss theory, limp panel impedance is directly proportional to the surface density and the frequency. The transmission loss resulting from this impedance is known as mass-law transmission loss. Under these assumptions the transmission loss increases by 6 dB for doubling of either the mass or the frequency. In a transmission loss vs frequency plot, this produces 6 dB/octave slope. However, as can be seen from the test results (Figures 3.26 through 3.29), the slope of the least mean-square line of the trim panels varies considerably. Hence a simple mass-law assumption seems to be invalid for such trim panels. Three out of the four panels tested had slopes less than the theoretical values. Hence the use of mass-law

approximation produces a higher transmission loss for a double panel. In order to overcome this problem, an additional option for the trim panel was introduced for the trim panel impedance. In this option the measured slope is used. The model uses mass law impedance for low frequency and impedance corresponding to the measured slope at high frequency. The experimental slope is input as a ratio of the measured slope to theoretical slope (6 dB/octave), and this ratio is called the slope factor. Values of these factors for various trim panels are given in Reference 2. For this study these values were measured from Figures 3.26 through 3.29.

At this point it is pertinent to explain the difference in the terminology used to describe the experimental and the theoretical results. The experimental results are called "noise reduction," and the theoretical results are called "transmission loss." The reason for this is the following. The sound energy attenuation measured in this test facility is made up of two parts. Reference 6 defines the noise reduction at any frequency as

$$NR = 10 \log(1 + \tau/\alpha)$$

where τ = Panel transmission loss coefficient at that frequency

α = Absorption coefficient of the receiver cavity at that frequency.

The panel transmission loss coefficient is related to the panel pressure ratio by

$$1/\tau = (p_i/p_t)^2$$

where p_i = Blocked incident pressure (Pa)

p_t = Transmitted pressure (Pa).

The absorption coefficient is normally less than one. When the cavity is nearly fully absorptive, as in the case of the KU-FRL acoustic test facility, the noise reduction and transmission loss will be nearly the same. In case the cavity is not fully absorptive, noise reduction values in general will be less than transmission loss. At cavity resonance frequencies such simplifications will not be valid. At the KU-FRL experimental test facility the receiver microphone measures both the transmitted pressure and the very weak reflections from the cavity walls. Hence the sound attenuation characteristics measured from this facility are noise reduction. The theoretical values calculated from the program do not contain any corrections and hence are transmission loss values.

4.2 DETAILS OF THE INPUT DATA

For the theoretical investigation the parameters chosen to vary were

a. Panel depth

b. Effect of sound insulation

c. Effect of skin structure

d. Effect of trim panel material and treatment.

Four skin panels and four trim panels were used for the comparison of the theoretical and the calculated values. The skin panels tested are given in Table 2.1. Trim panels used were 312, 318, 325, and 352. The details of these panels are presented in Table 2.2. The impedance

model used for the skin and trim panels was the single mode approximation. This approximation, described in detail in Reference 2, requires single panel resonance frequencies of the skin panel and its damping ratio around that frequency region. The single panel test results from Reference 5 were used for the resonance frequencies. The damping values of these panels had been measured and were reported in Reference 1. These values were used in the calculation of the impedance. These values are tabulated in Table 4.1

The mechanical properties of the fiberglass insulation were unknown. This insulation material was very similar to PF 105 fiberglass insulation discussed in Reference 6. Also the minor variations in porosity and resistivity of the insulation did not significantly change the transmission loss values. Hence the porosity and the resistivity of PF 105 material was used. However, actual fiberglass density was input.

The input data required for the trim panels were fundamental resonance frequency, damping ratio, and the experimental slope of the noise reduction and damping tests of the trim panels alone. These values are tabulated in Table 4.2.

4.3 RESULTS AND DISCUSSION

The outputs from the computer runs are plotted in Figures 4.1 through 4.24 for the 48 combinations considered. These calculated values are plotted as dotted lines over the experimental values. Each figure contains two plots: one with the fiberglass insulation between the skin and the trim panel and the other without the insulation.

Table 4.1: Input Data for Skin Panels

Skin Panel	Resonance Frequency	Damping Ratio	Mass/unit area kg/m^2
353, 357, 358	50	.015	2.24
335	70	.03	1.58
339	40	.02	1.23
340	55	.02	1.48

Table 4.2: Input Data for Trim Panels

Trim Panel	Resonance Frequency Hz	Damping Ratio	Mass per unit area	Slope Factor
312	0	.042	2.26	1.33
318	50	.060	1.26	0.58
325	60	.074	2.04	0.83
352	62	.063	2.20	0.05

$$\text{Slope Factor} = \frac{\text{Measured Slope}}{6}$$

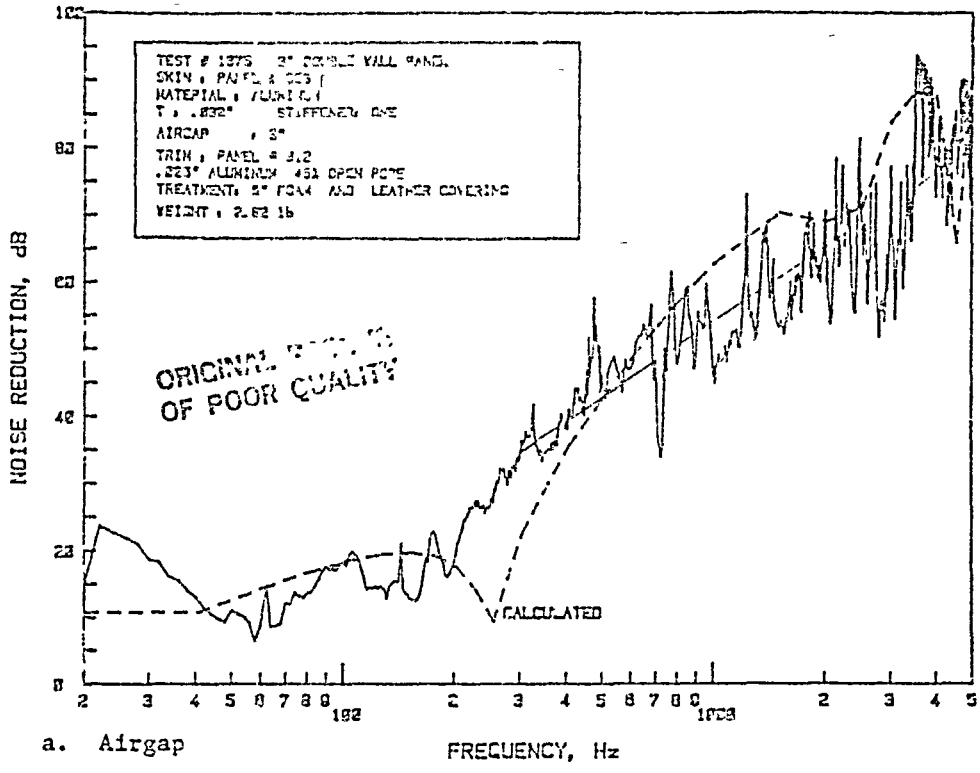

a. Airgap

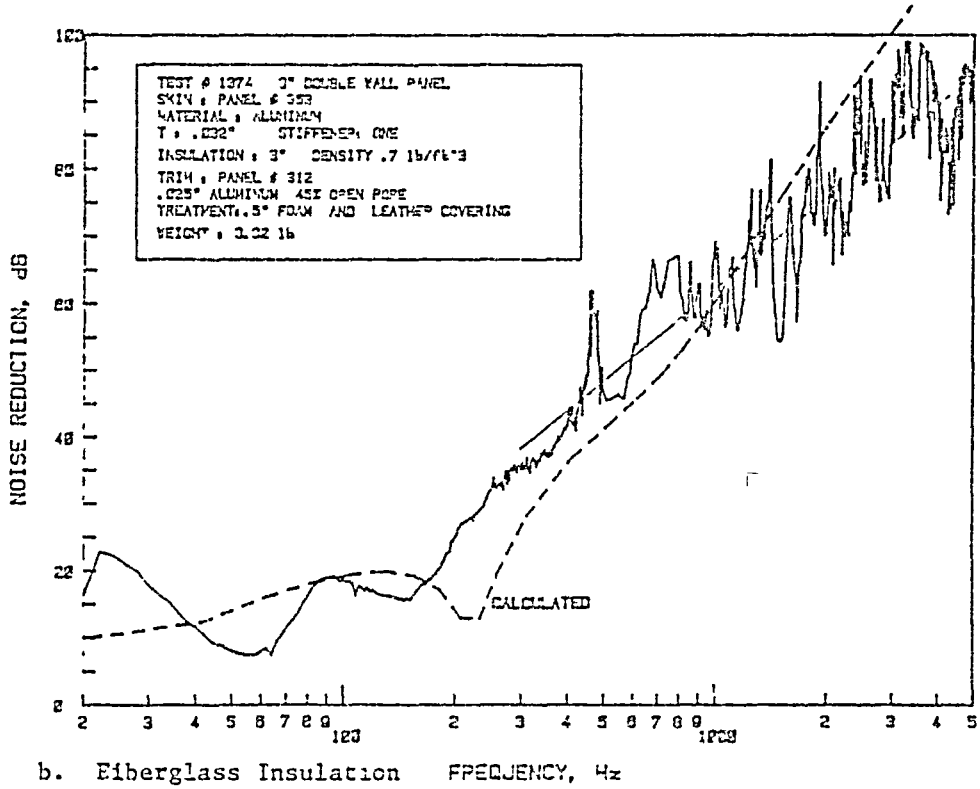

b. Eiberglass Insulation

Figure 4.1: Comparison of Experimental and Theoretical Noise Reduction Characteristics of Double-Wall Panel Made of Aluminum Skin (Panel 353) and Trim Panel 312; Panel Depth 3"

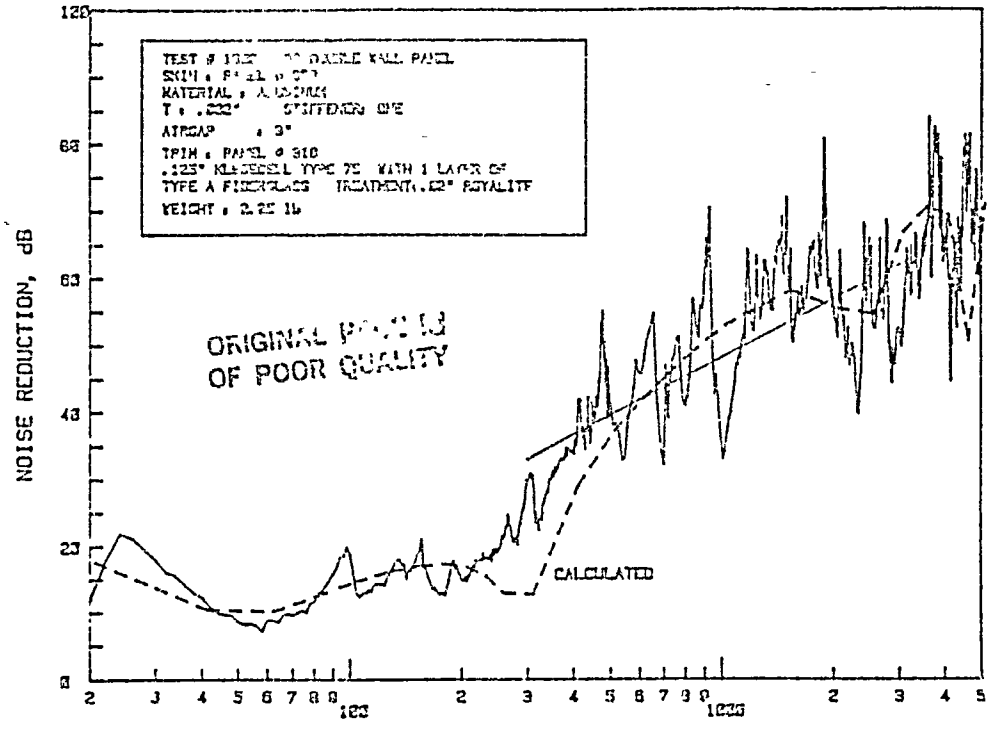

a. Airgap

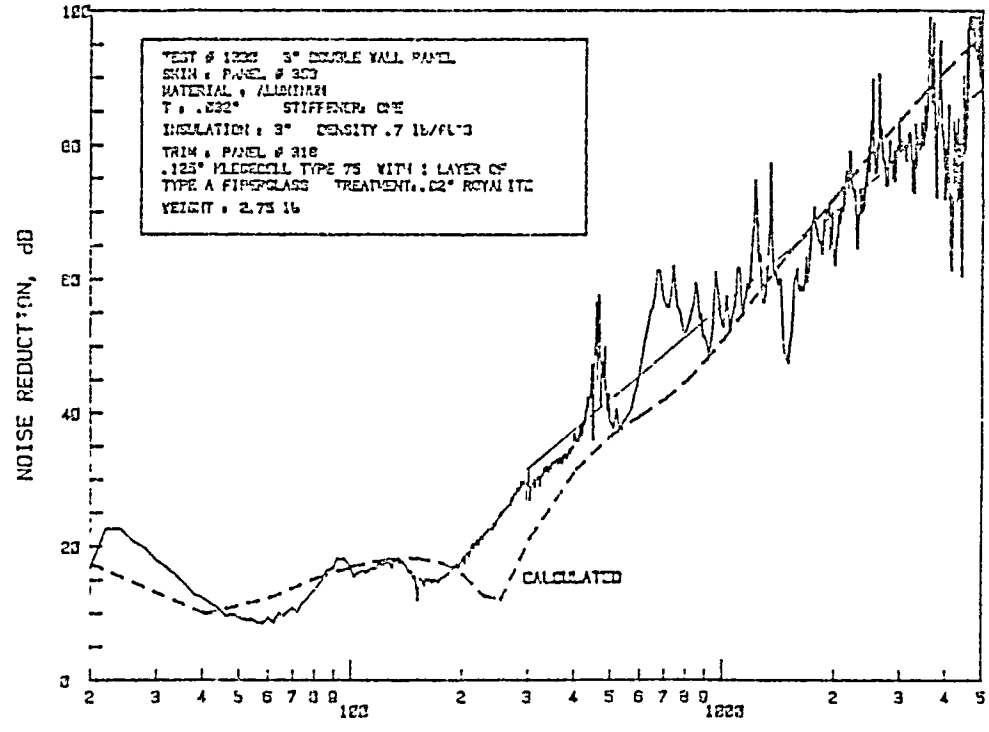

b. Fiberglass Insulation

Figure 4.2: Comparison of Experimental and Theoretical Noise Reduction Characteristics of Double-Wall Panel Made of Aluminum Skin (Panel 353) and Trim Panel 318; Panel Depth 3"

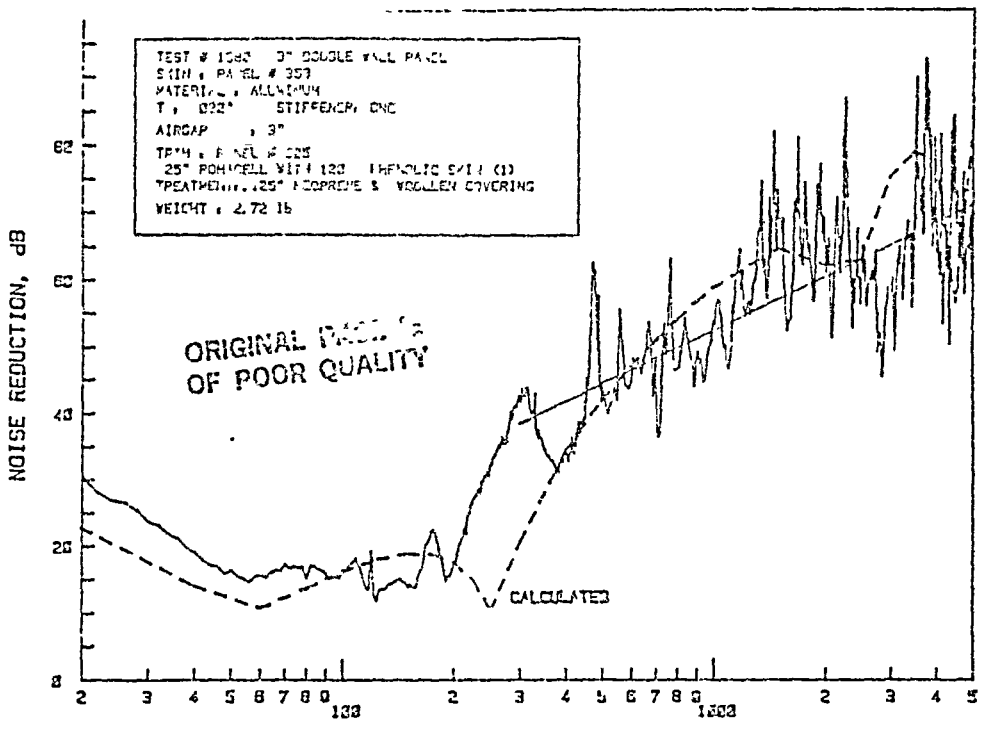

a. Airgap

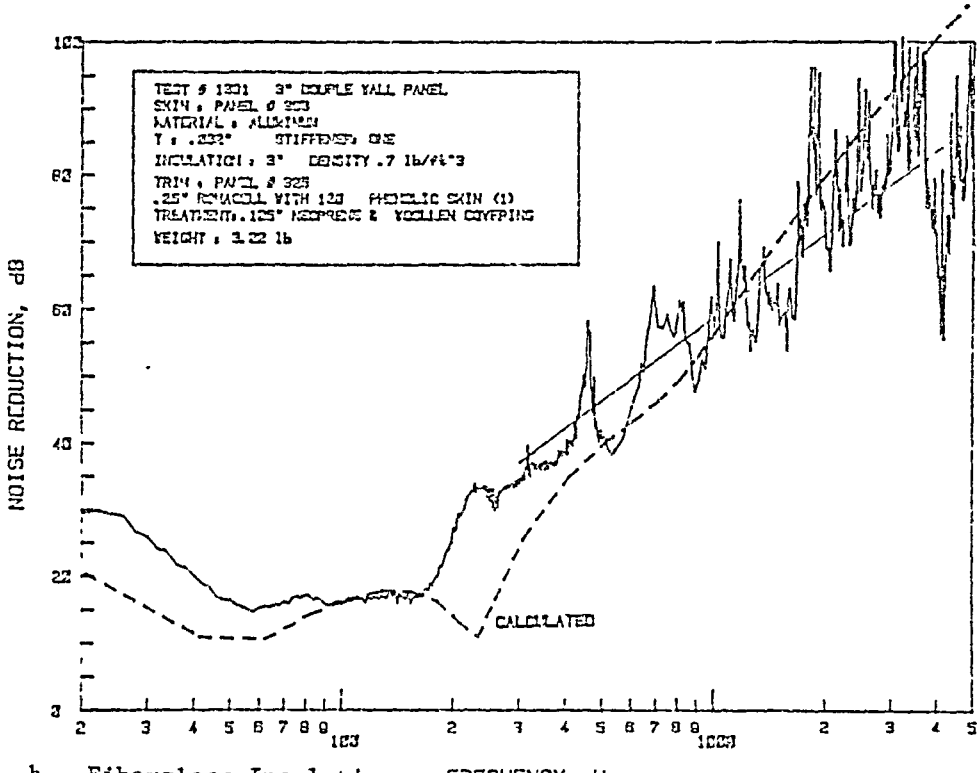

b. Fiberglass Insulation

Figure 4.3: Comparison of Experimental and Theoretical Noise Reduction Characteristics of Double-Wall Panel Made of Aluminum Skin (Panel 353) and Trim Panel 325; Panel Depth 3"

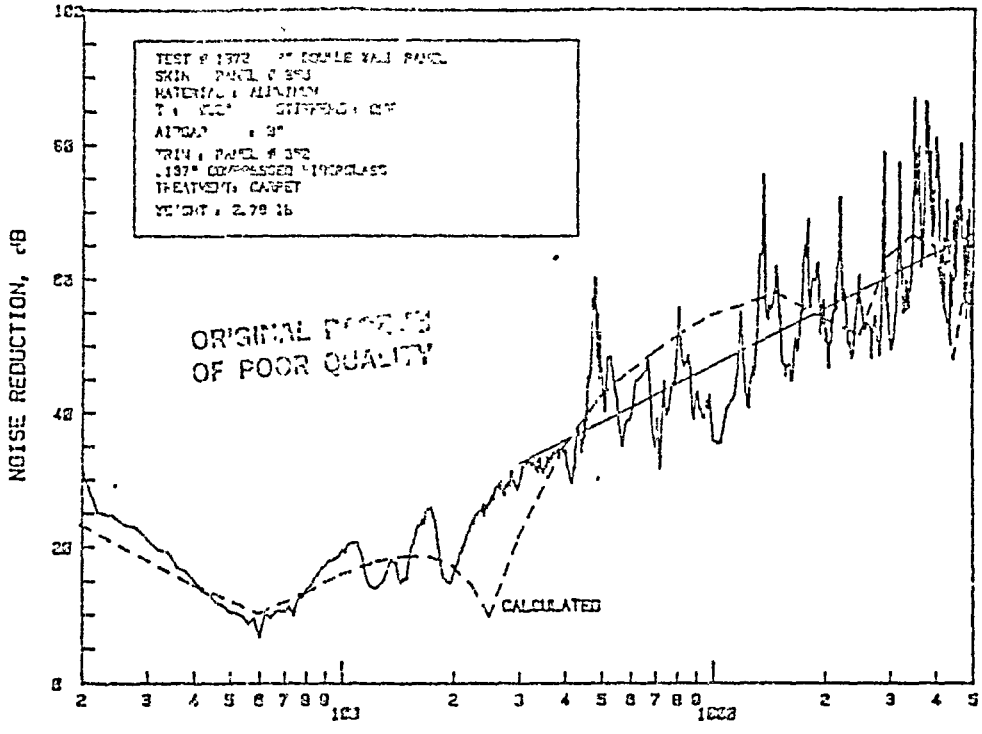

a. Airgap

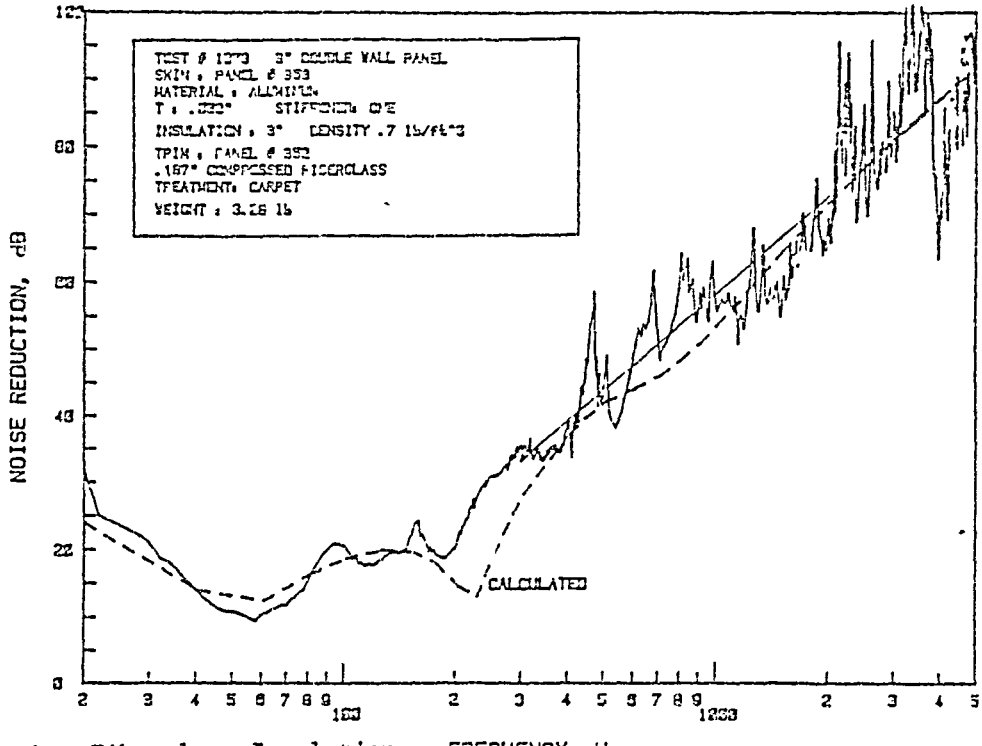

b. Fiberglass Insulation

Figure 4.4: Comparison of Experimental and Theoretical Noise Reduction Characteristics of Double-Wall Panel Made of Aluminum Skin (Panel 353) and Trim Panel 352; Panel Depth 3"

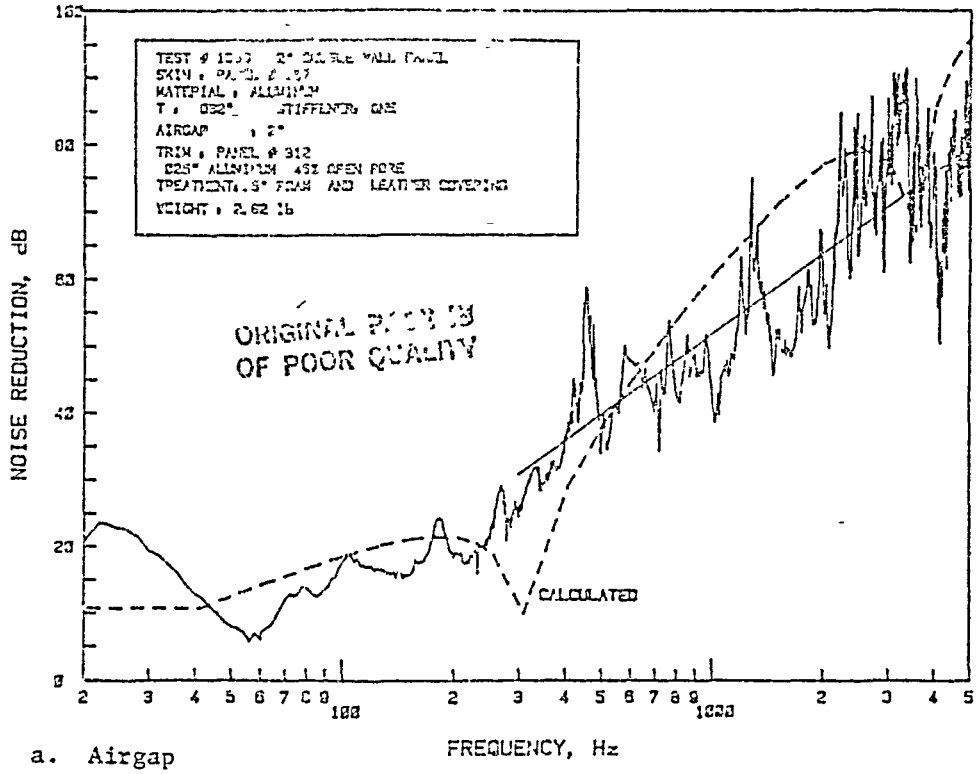

a. Airgap

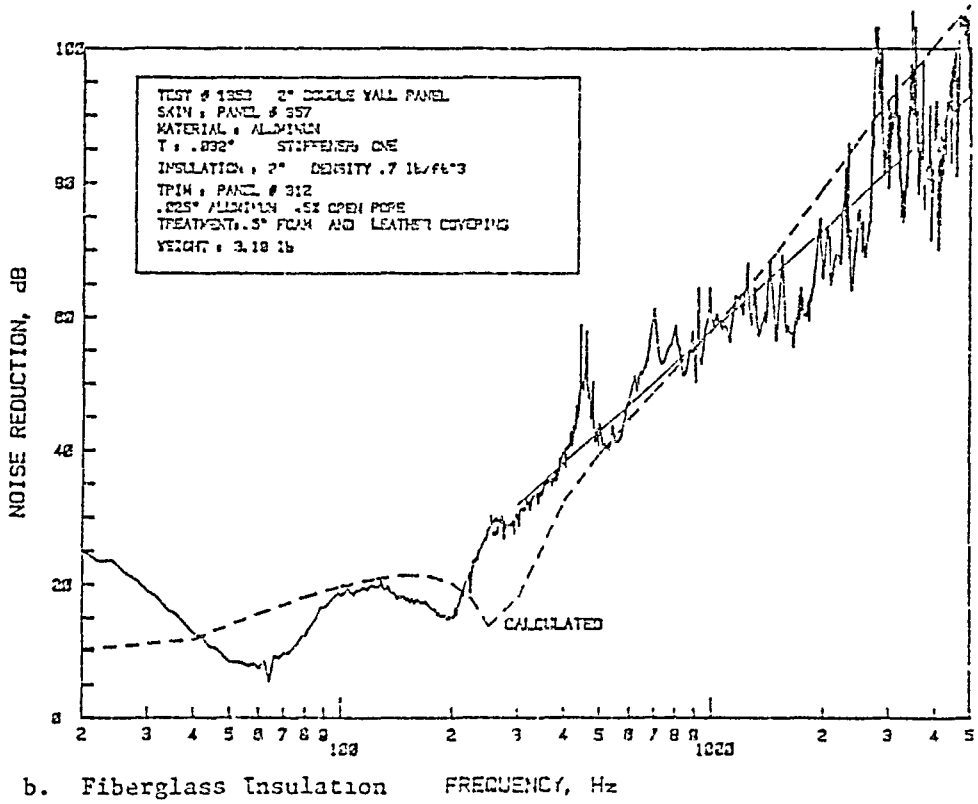

b. Fiberglass Insulation

Figure 4.5: Comparison of Experimental and Theoretical Noise Reduction Characteristics of Double-Wall Panel Made of Aluminum Skin (Panel 357) and Trim Panel 312; Panel Depth 2"

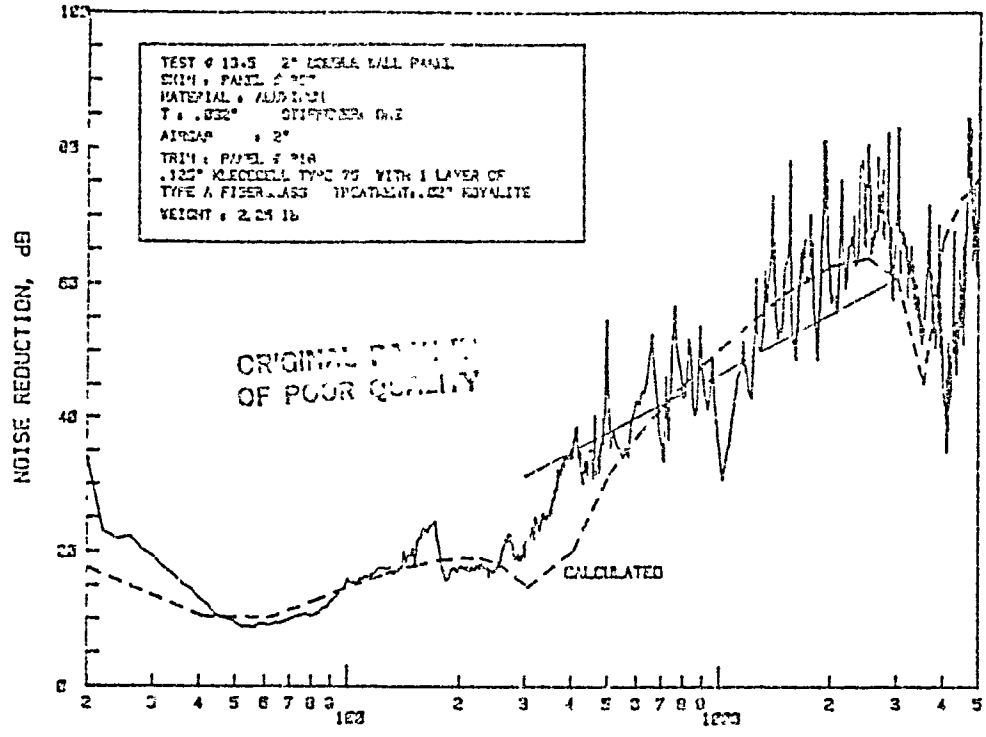

a. Airgap

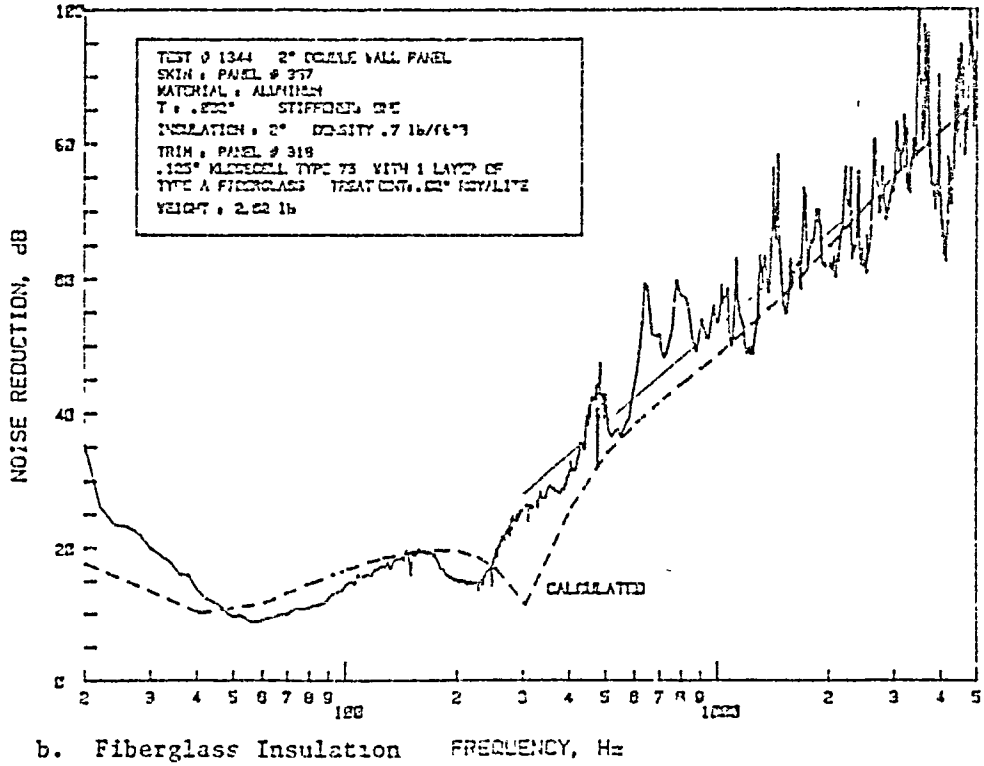

b. Fiberglass Insulation

Figure 4.6: Comparison of Experimental and Theoretical Noise Reduction Characteristics of Double-Wall Panel Made of Aluminum Skin (Panel 357) and Trim Panel 318; Panel Depth 2"

C-2

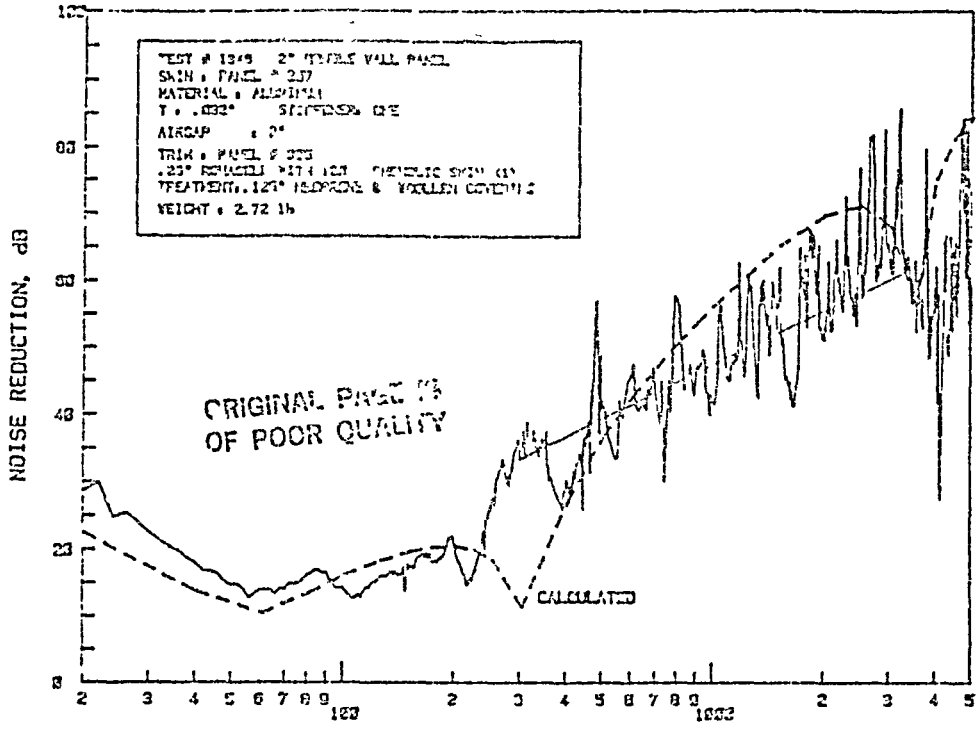

a. Airgap FREQUENCY, Hz

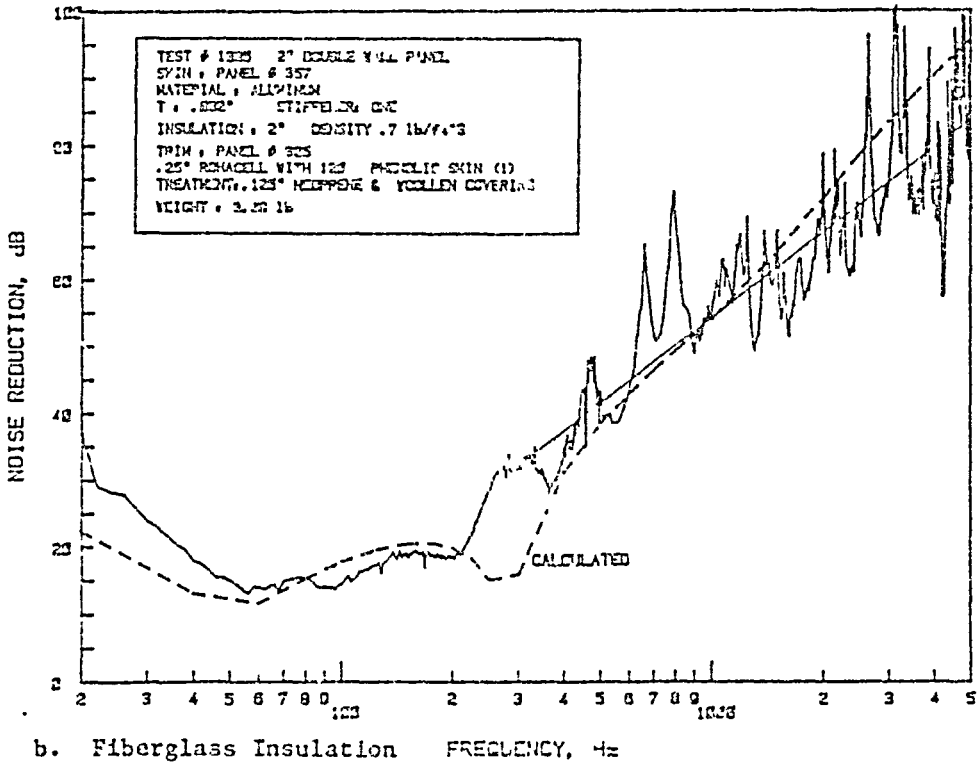

b. Fiberglass Insulation FREQUENCY, Hz

Figure 4.7: Comparison of Experimental and Theoretical Noise Reduction Characteristics of Double-Wall Panel Made of Aluminum Skin (Panel 357) and Trim Panel 325; Panel Depth 2"

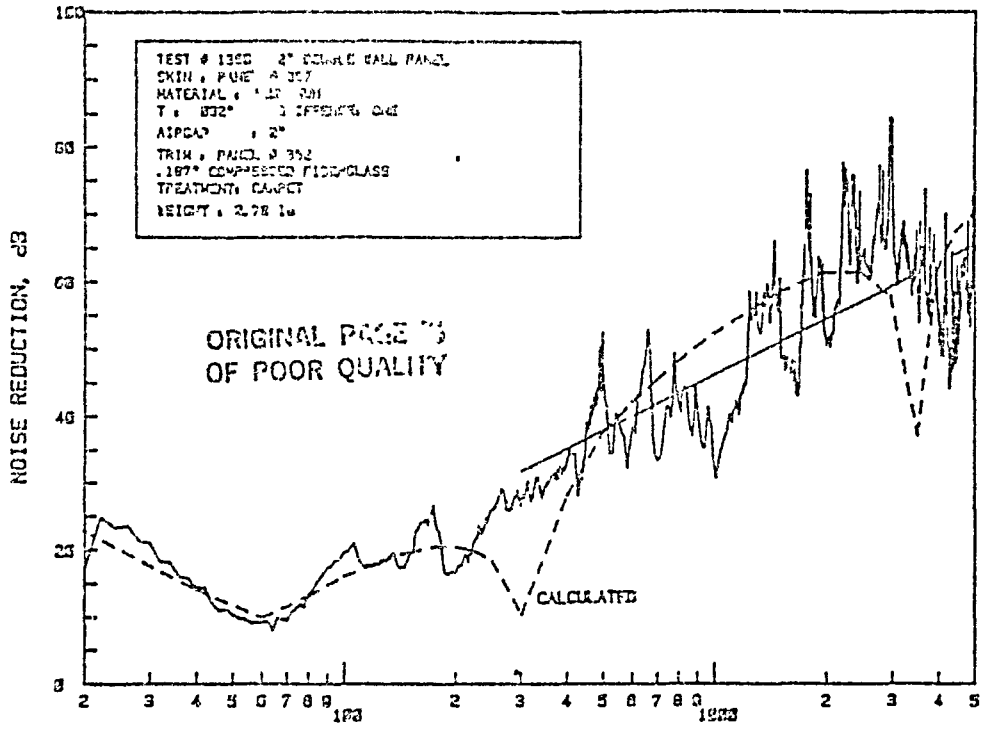

a. Airgap

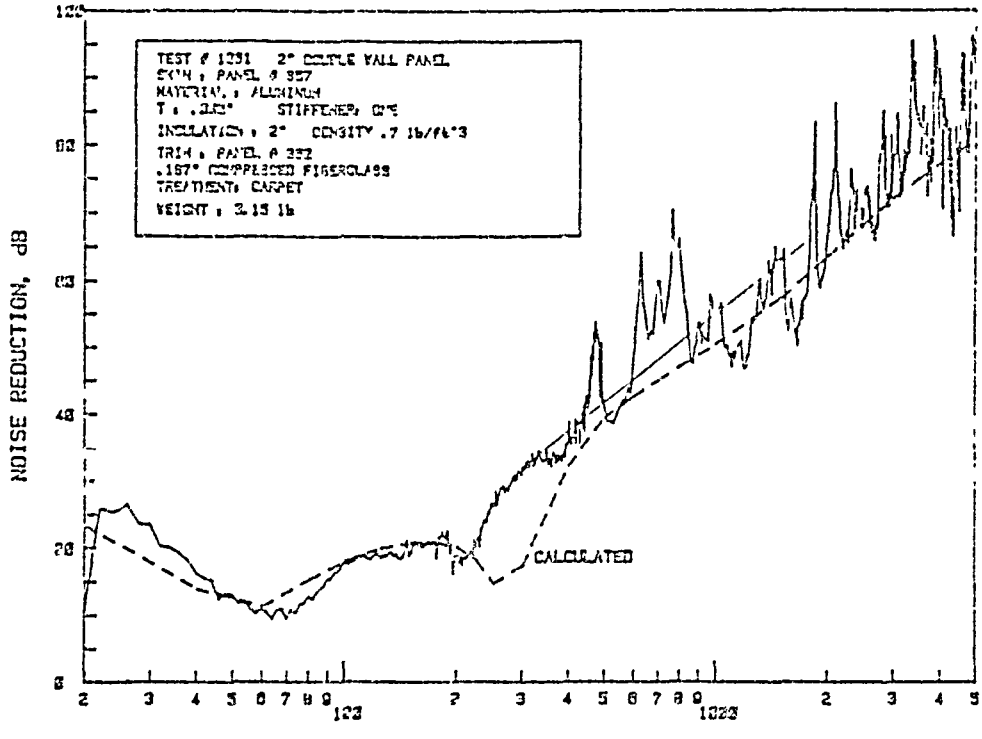

b. Fiberglass Insulation

Figure 4.8: Comparison of Experimental and Theoretical Noise Reduction Characteristics of Double-Wall Panel Made of Aluminum Skin (Panel 357) and Trim Panel 352; Panel Depth 2"

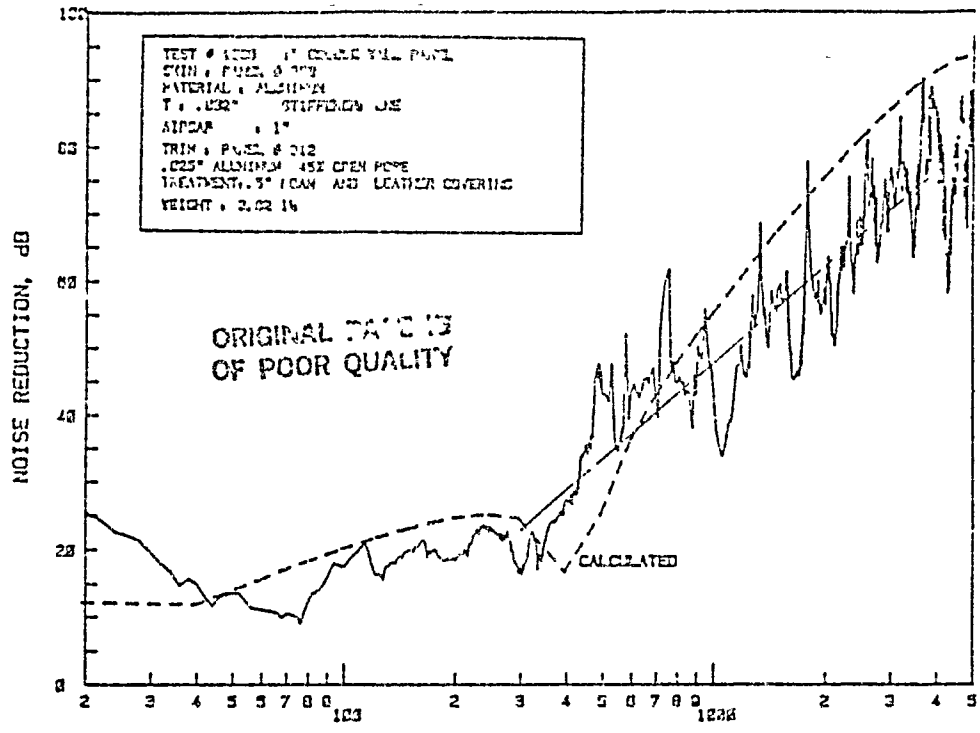

a. Airgap

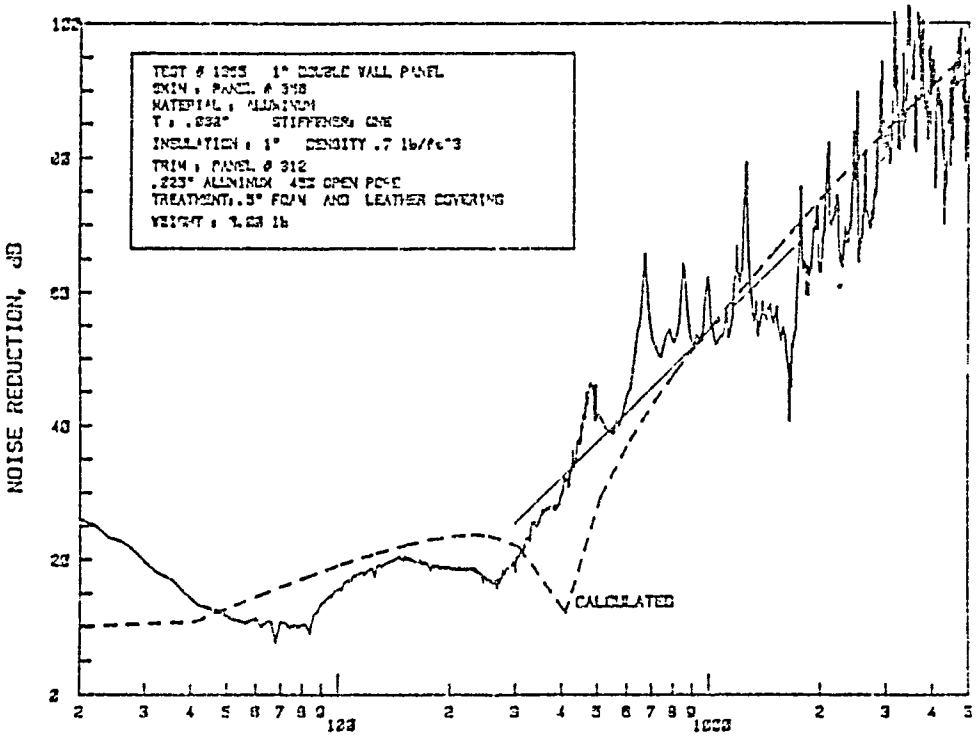

b. Fiberglass Insulation

Figure 4.9: Comparison of Experimental and Theoretical Noise Reduction Characteristics of Double-Wall Panel Made of Aluminum Skin (Panel 358) and Trim Panel 312; Panel Depth 1"

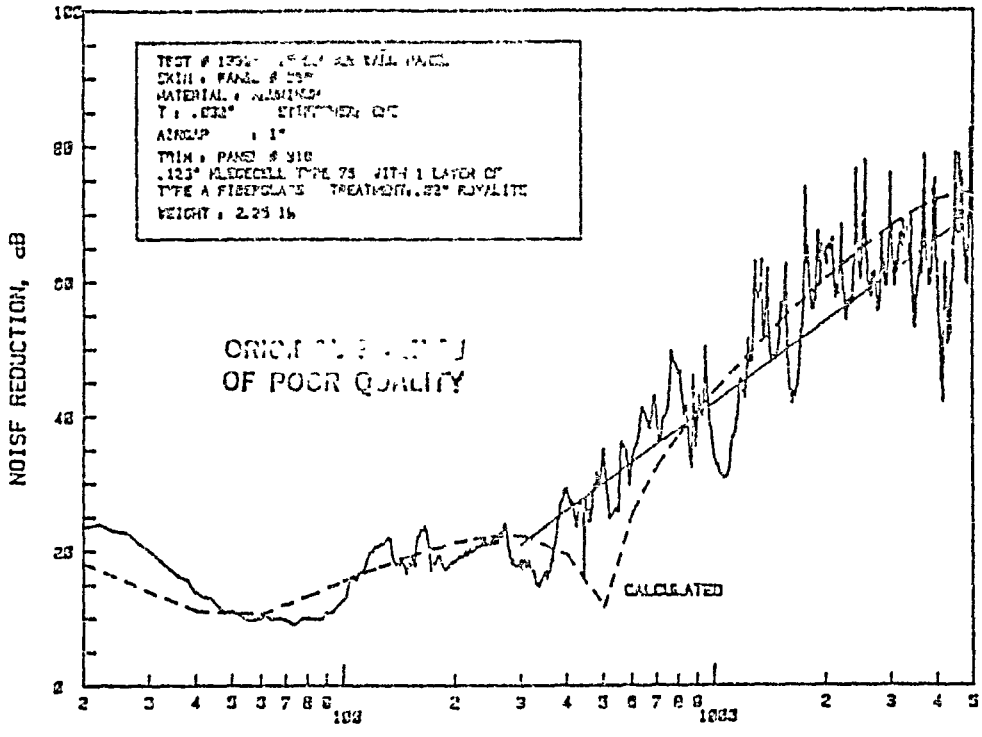

a. Airgap

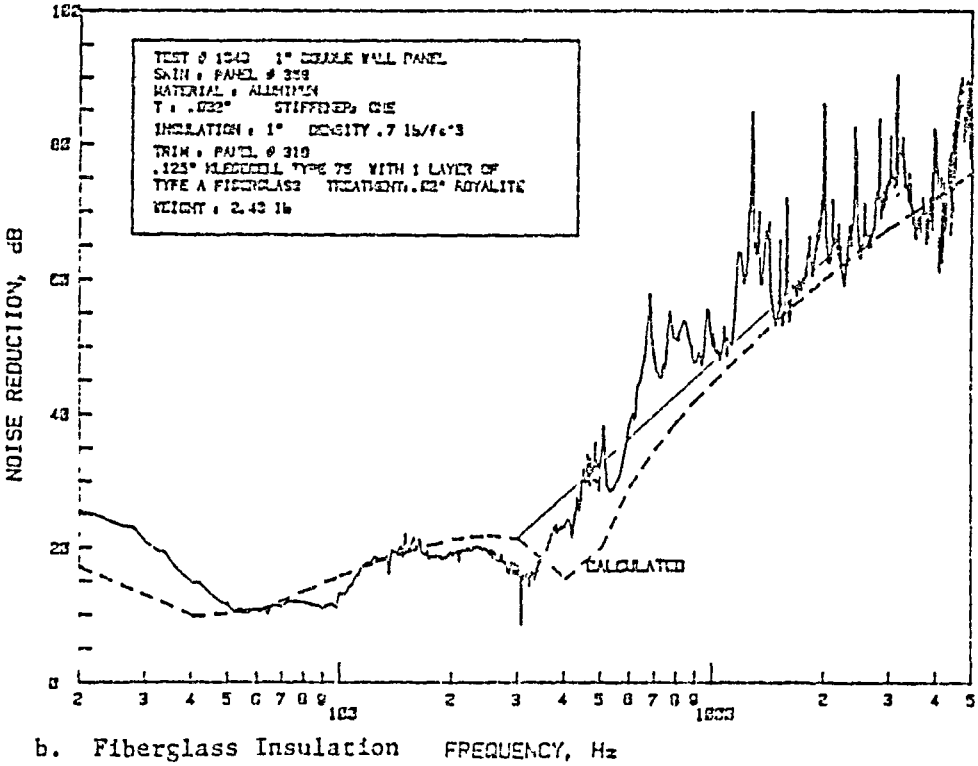

b. Fiberglass Insulation

Figure 4.10: Comparison of Experimental and Theoretical Noise Reduction Characteristics of Double-Wall Panel Made of Aluminum Skin (Panel 358) and Trim Panel 318; Panel Depth 1"

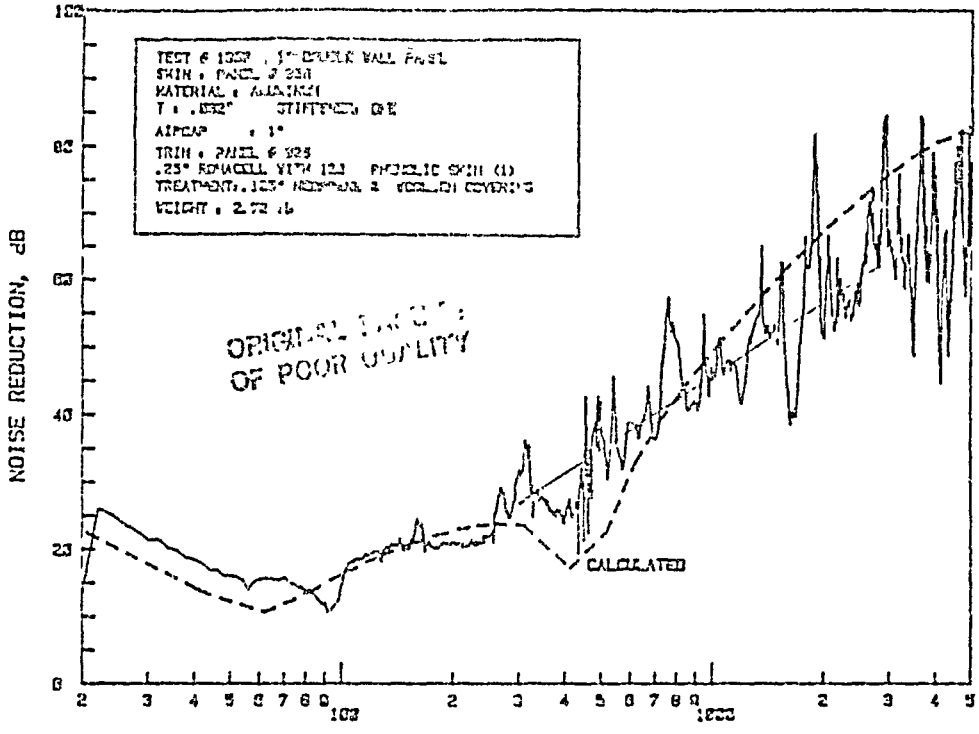

a. Airgap

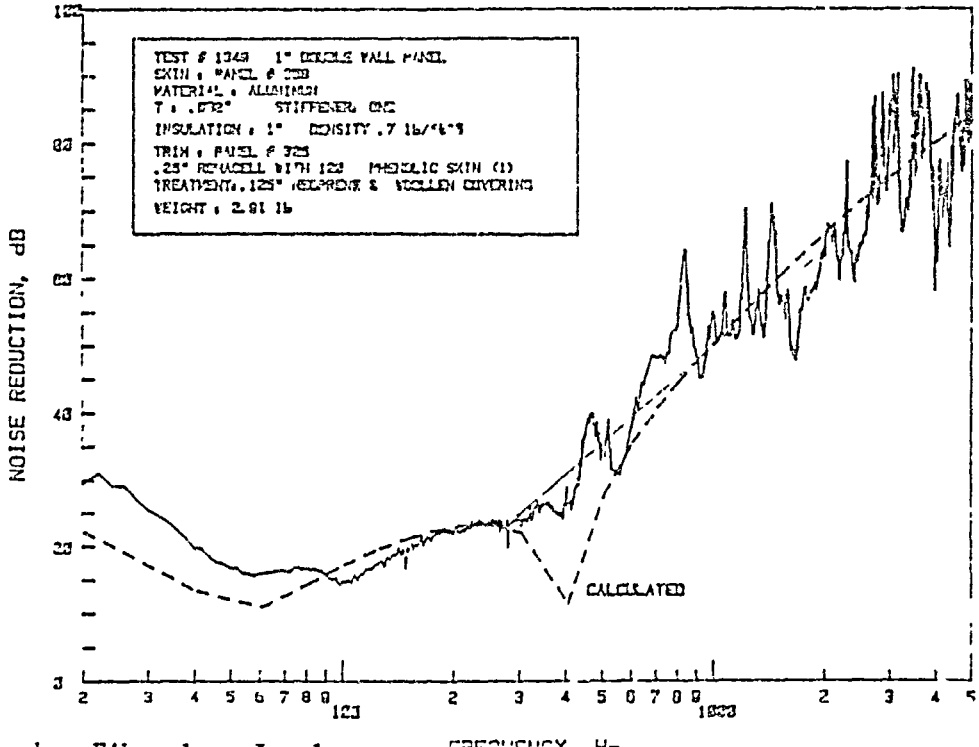

b. Fiberglass Insulation

Figure 4.11: Comparison of Experimental and Theoretical Noise Reduction Characteristics of Double-Wall Panel Made of Aluminum Skin (Panel 358) and Trim Panel 325; Panel Depth 1"

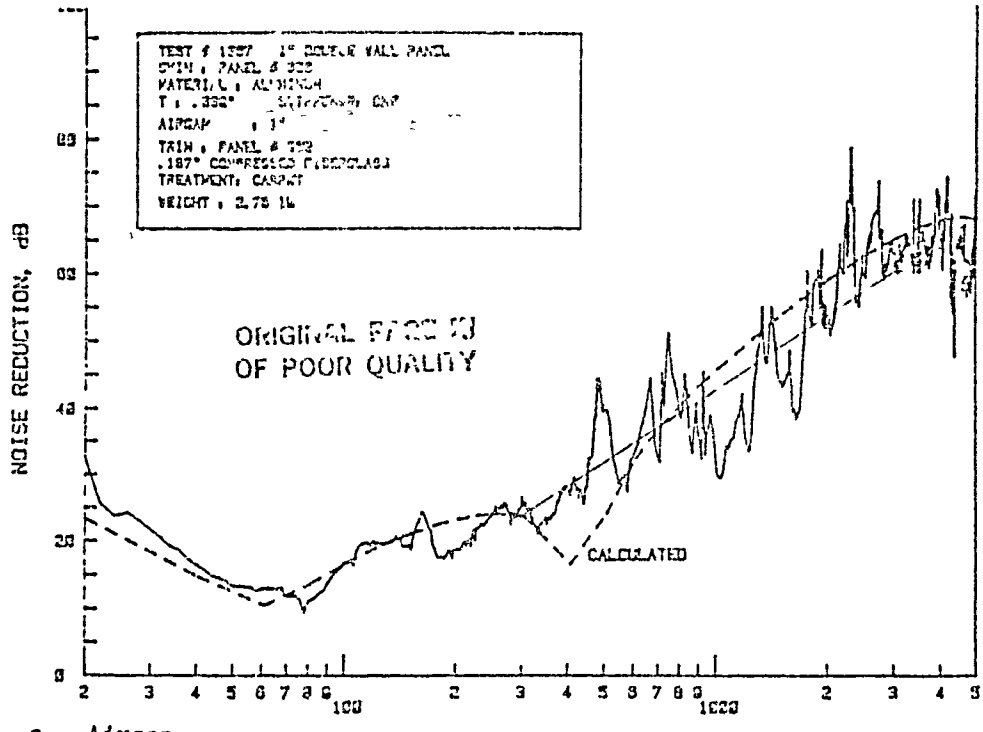

a. Airgap

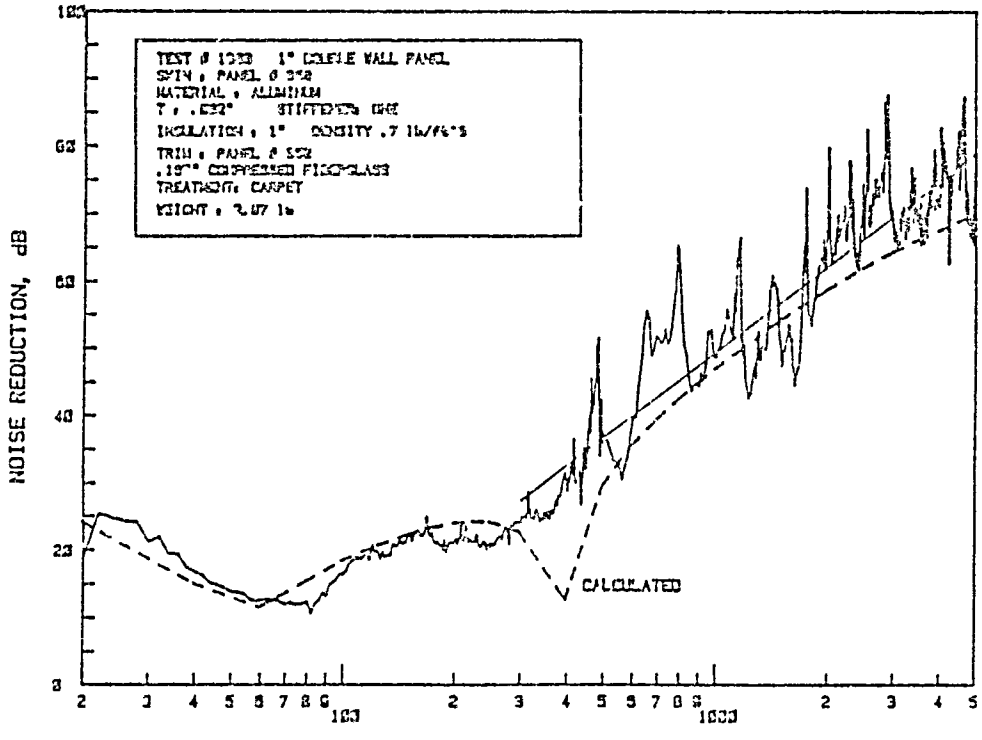

b. Fiberglass Insulation

Figure 4.12: Comparison of Experimental and Theoretical Noise Reduction Characteristics of Double-Wall Panel Made of Aluminum Skin (Panel 358) and Trim Panel 352; Panel Depth 1"

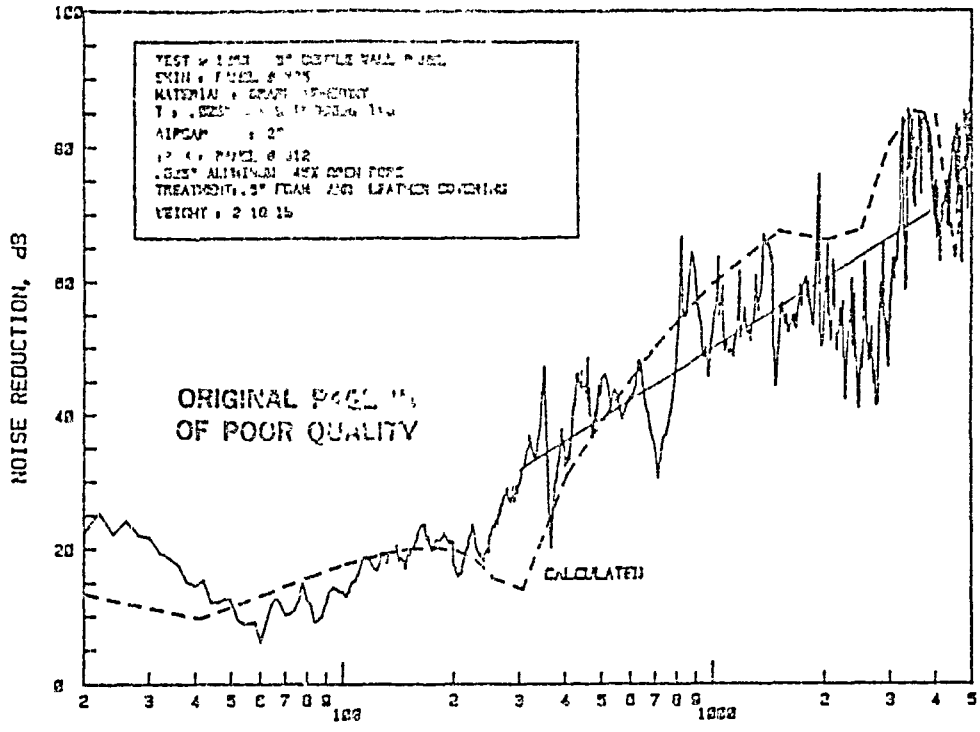

a. Airgap

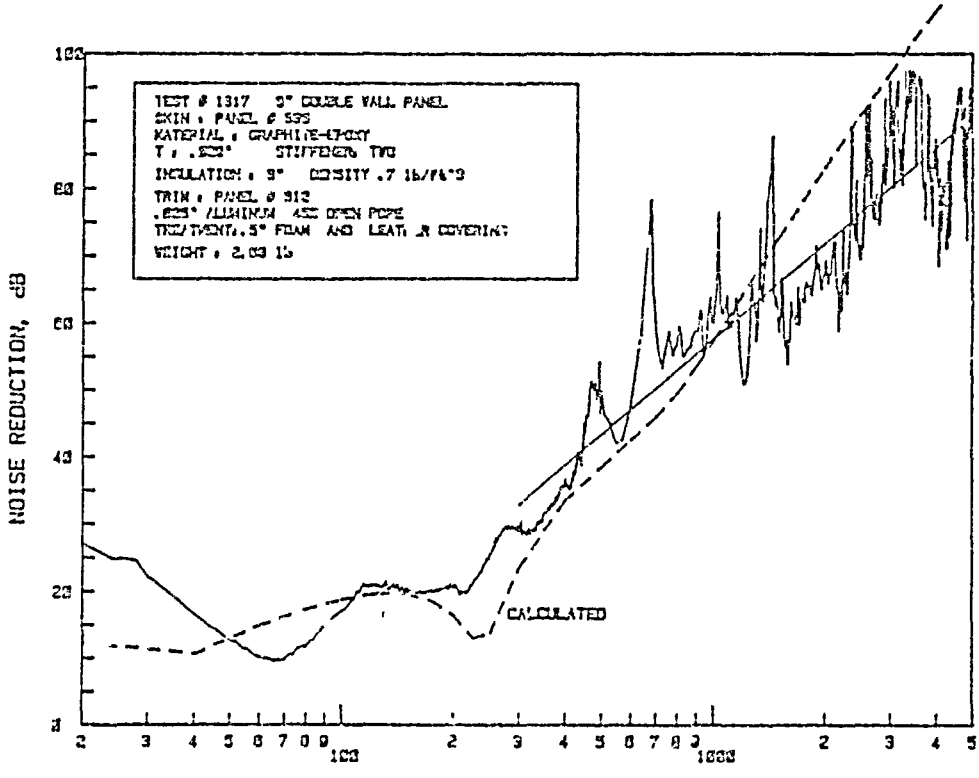

b. Fiberglass Insularion

Figure 4.13: Comparison of Experimental and Theoretical Noise Reduction Characteristics of Double-Wall Panel Made of Graphite-Epoxy Skin (Panel 335) and Trim Panel 312; Panel Depth 3"

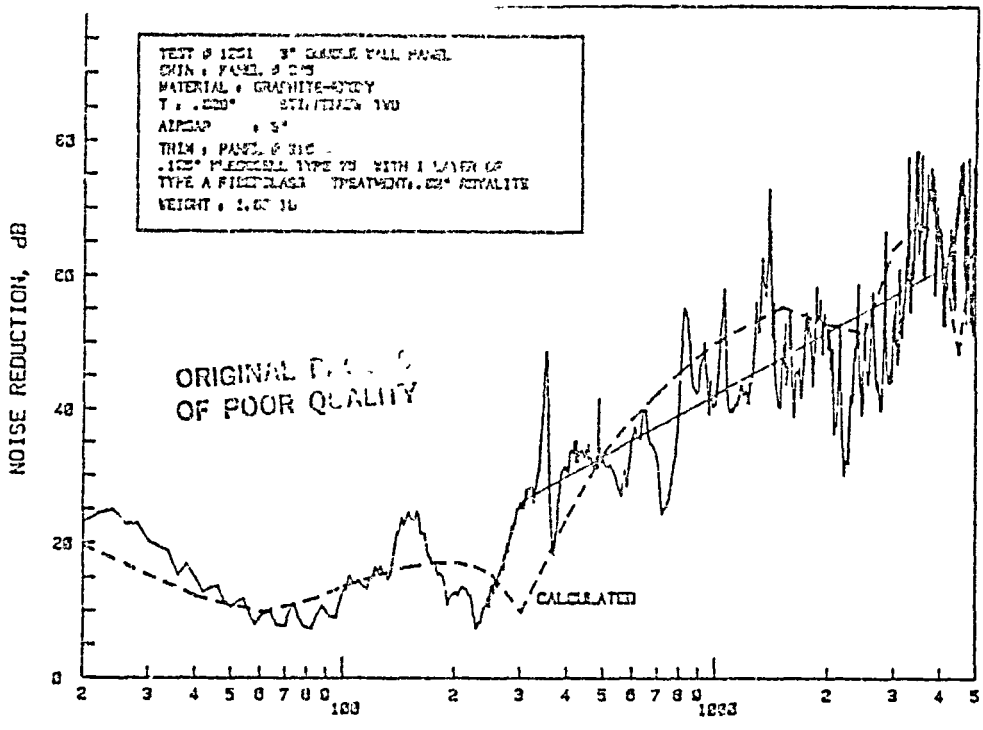

a. Airgap

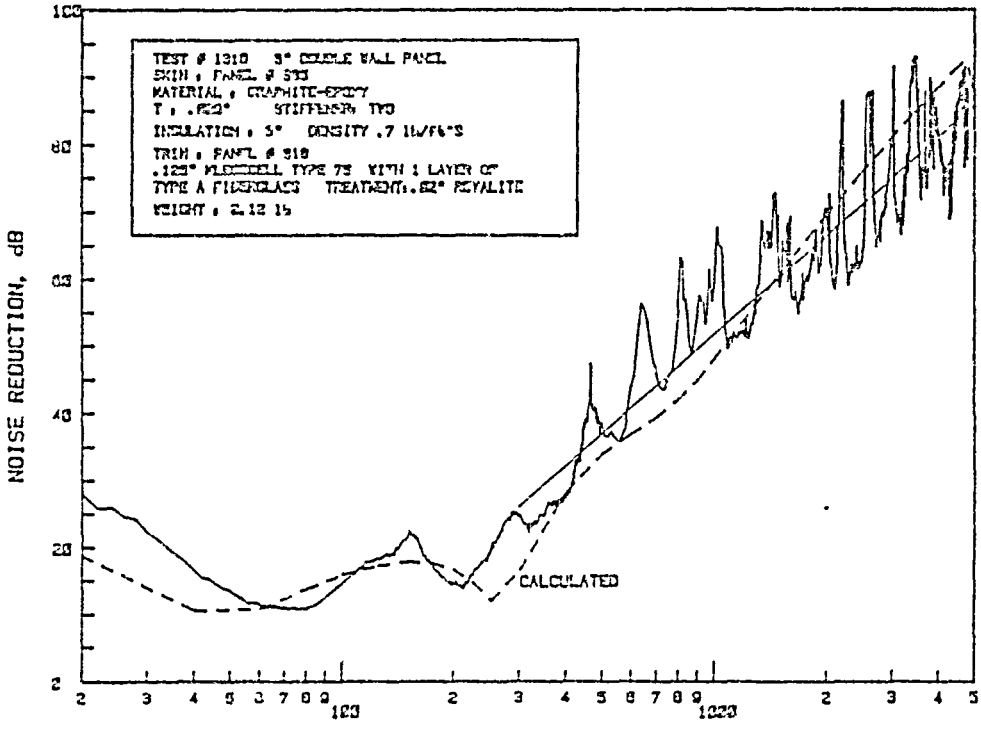

b. Fiberglass Insulation

Figure 4.14: Comparison of Experimental and Theoretical Noise Reduction Characteristics of Double-Wall Panel Made of Graphite-Epoxy Skin (Panel 335) and Trim Panel 318; Panel Depth 3"

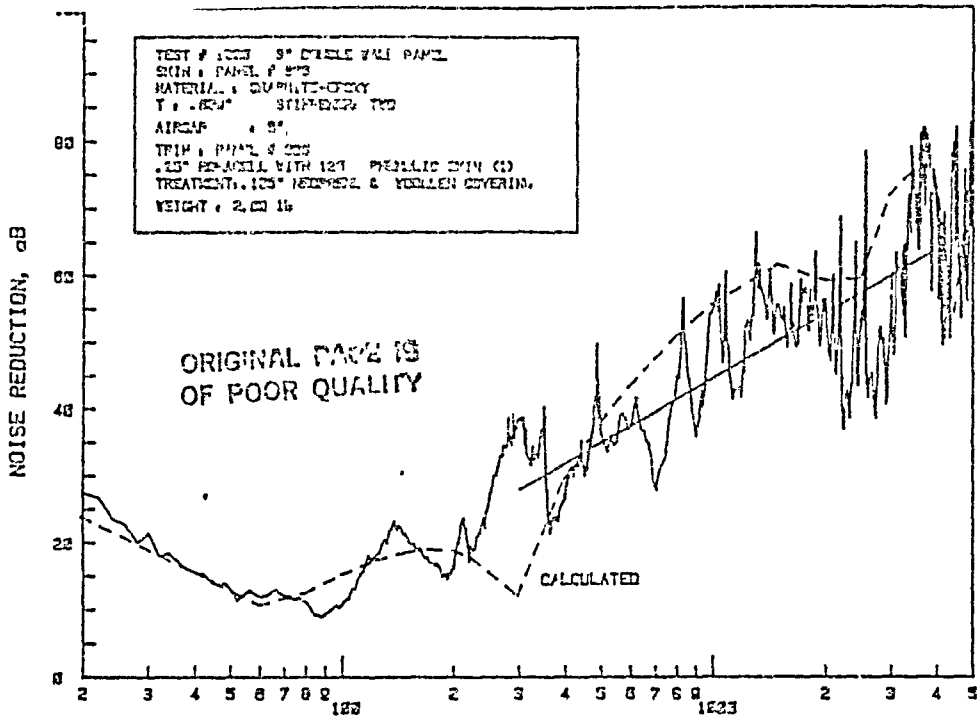

a. Airgap

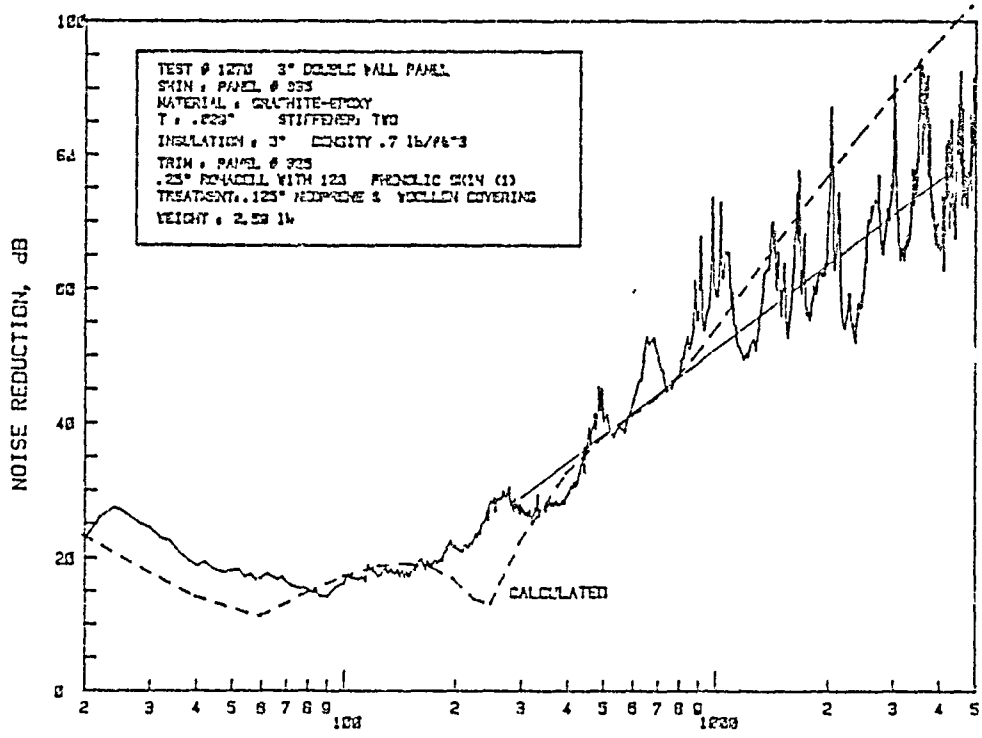

b. Fiberglass Insulation

Figure 4.13: Comparison of Experimental and Theoretical Noise Reduction Characteristics of Double-Wall Panel Made of Graphite-Epoxy Skin (Panel 335) and Trim Panel 325; Panel Depth 3"

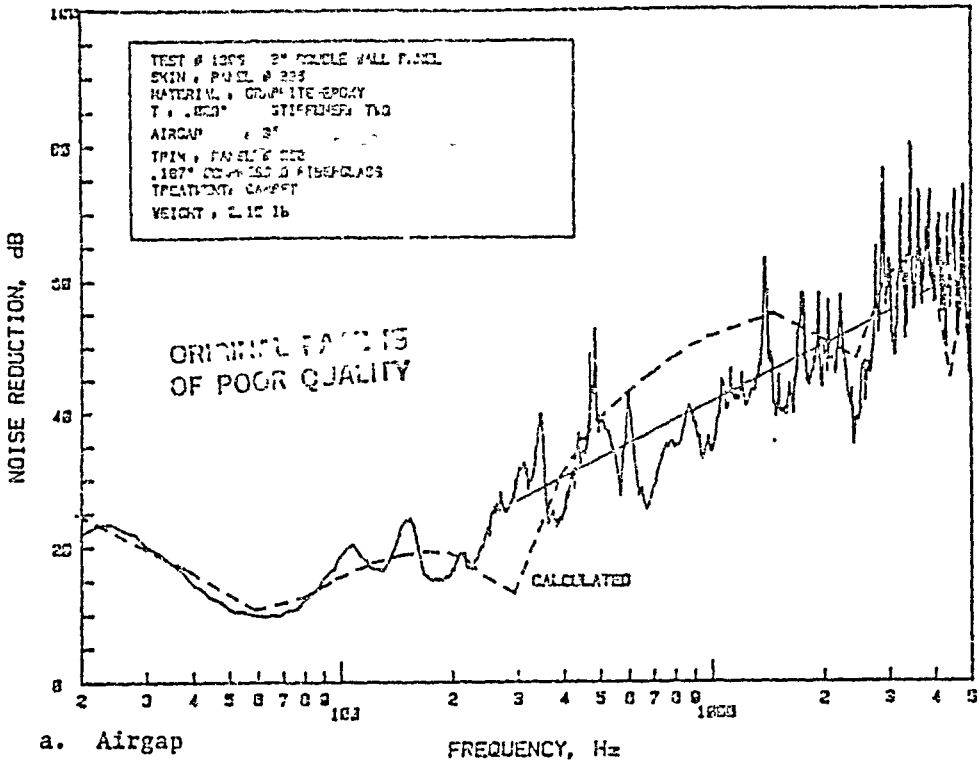

a. Airgap

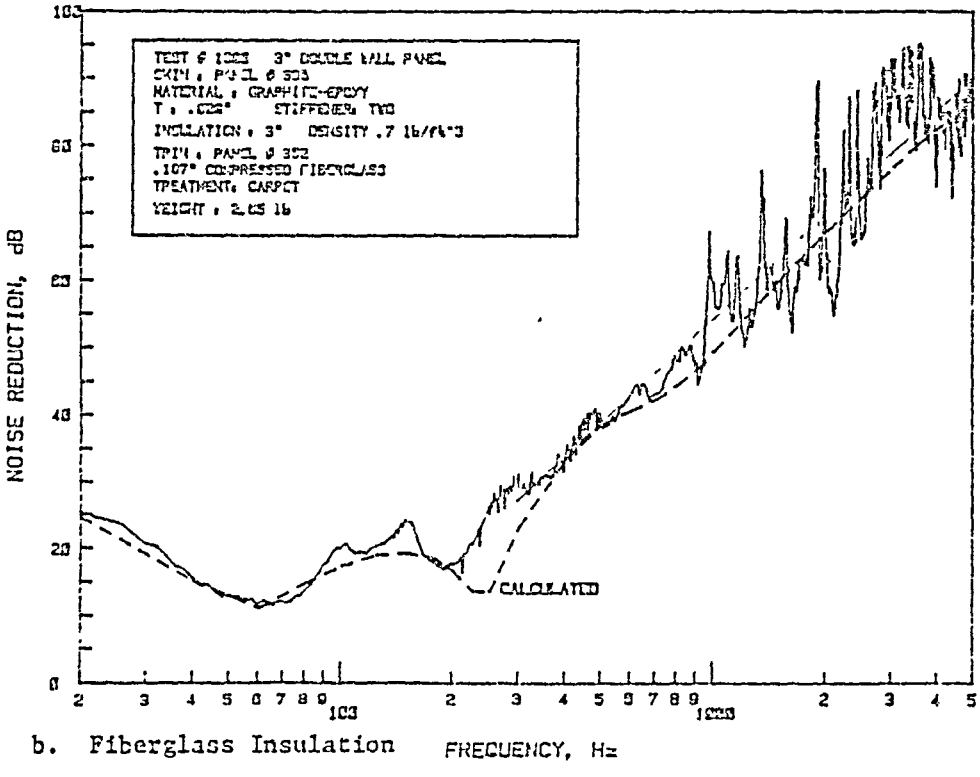

b. Fiberglass Insulation

Figure 4.16: Comparison of Experimental and Theoretical Noise Reduction Characteristics of Double-Wall Panel Made of Graphite-Epoxy Skin (Panel 335) and Trim Panel 352; Panel Depth 3"

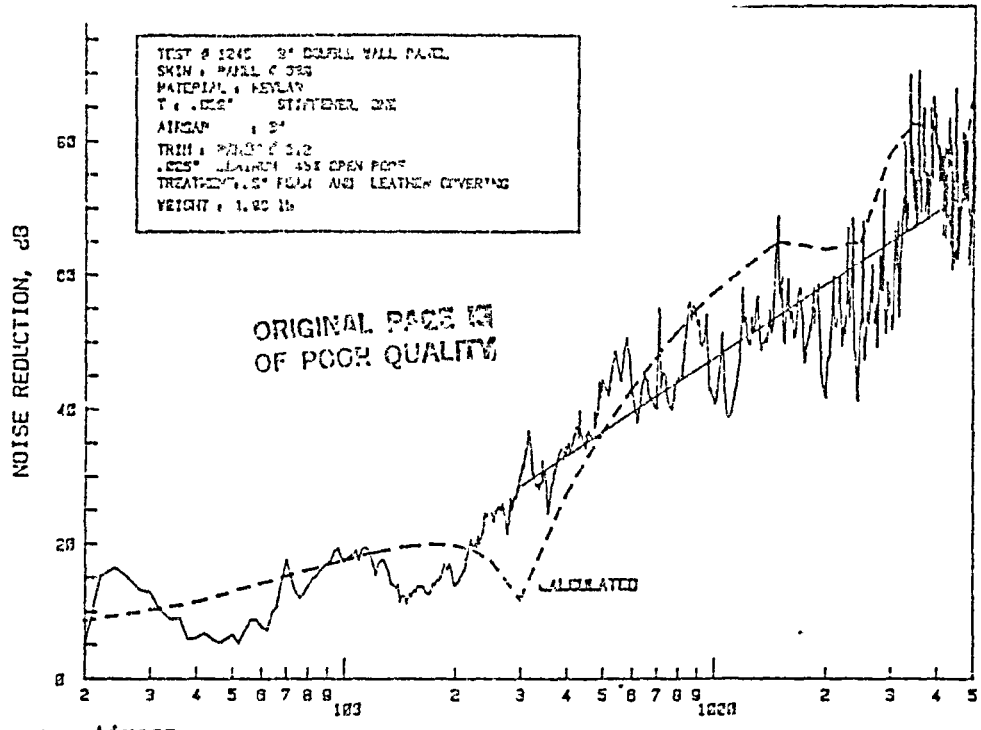

a. Airgap

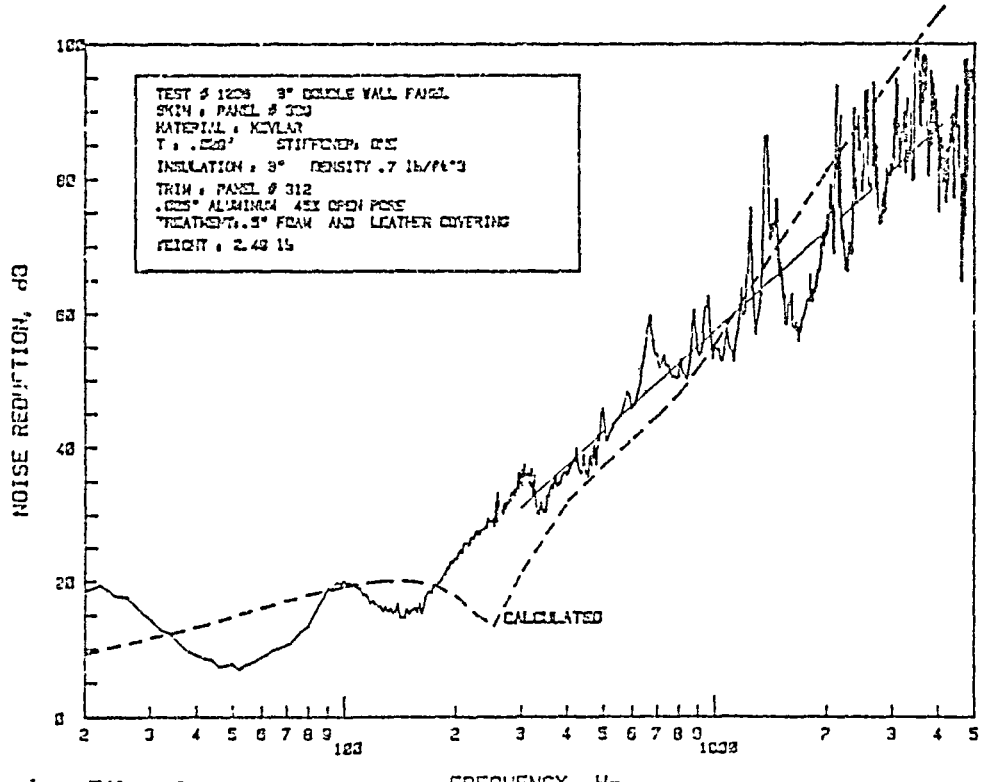

b. Fiberglass Insulation

Figure 4.17: Comparison of Experimental and Theoretical Noise Reduction Characteristics of Double-Wall Panel Made of Kevlar Skin (Panel 339) and Trim Panel 312; Panel Depth 3"

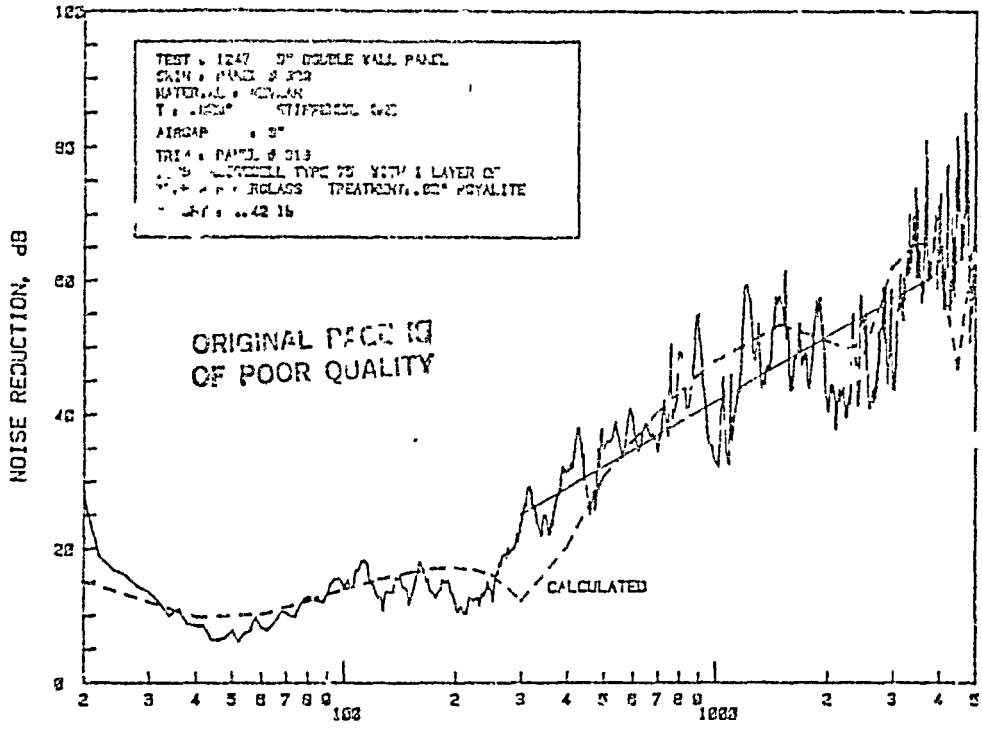

a. Airgap

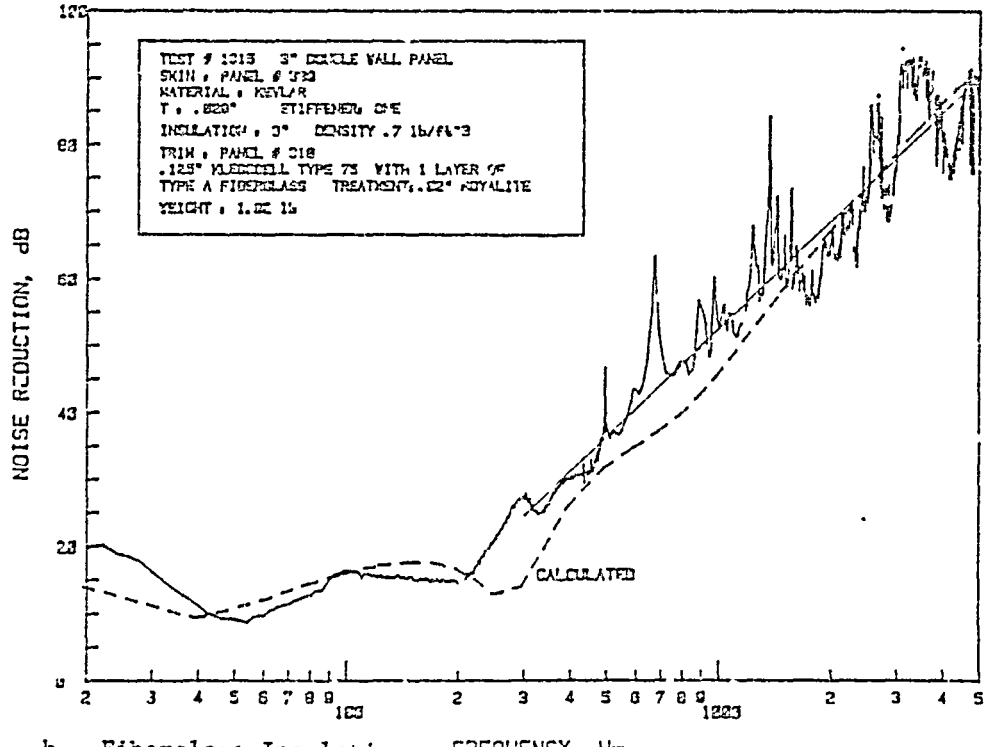

b. Fiberglass Insulation

Figure 4.18: Comparison of Experimental and Theoretical Noise Reduction Characteristics of Double-Wall Panel Made of Kevlar Skin (Panel 339) and Trim Panel 318; Panel Depth 3"

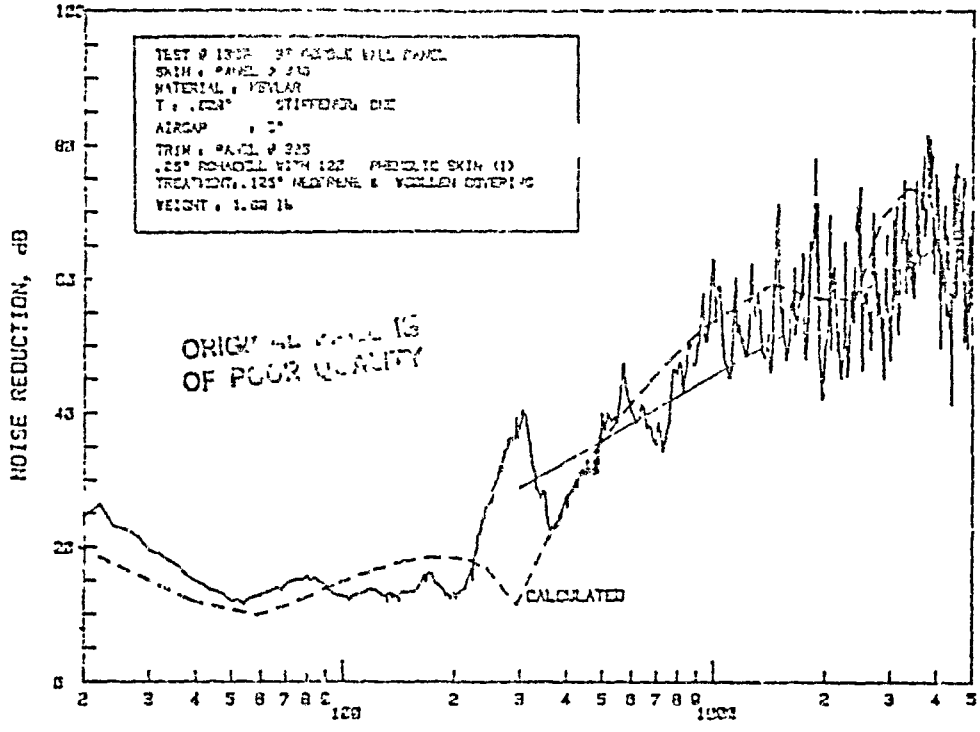

a. Airgap

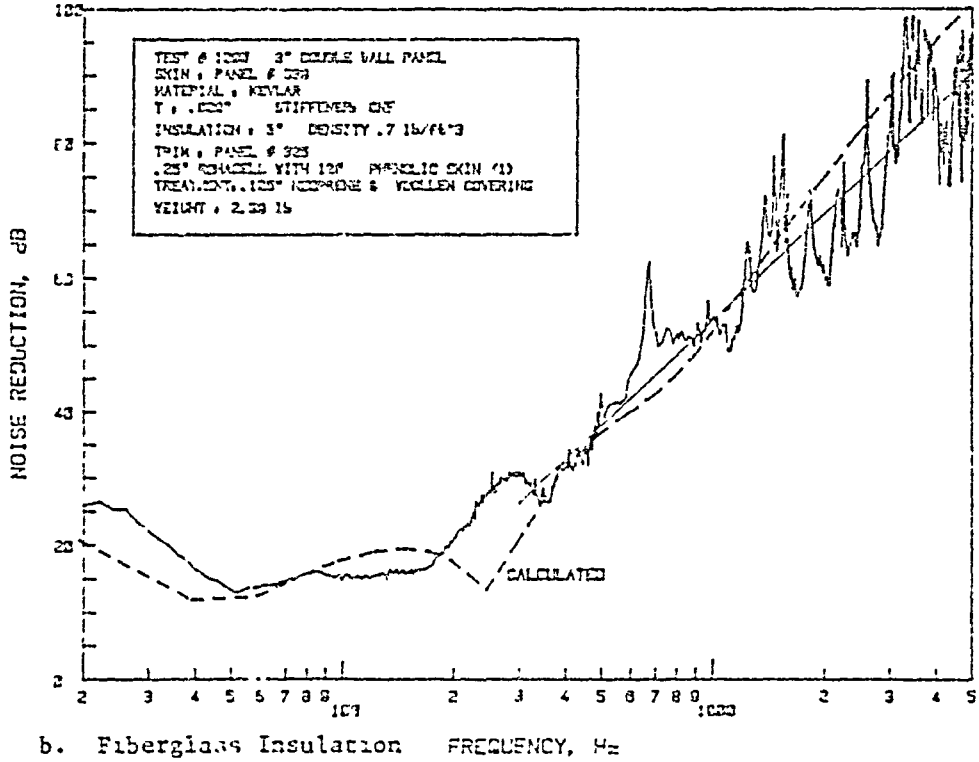

b. Fiberglass Insulation

Figure 4.19: Comparison of Experimental and Theoretical Noise Reduction Characteristics of Double-Wall Panel Made of Kevlar Skin (Panel 339) and Trim Panel 325; Panel Depth 3"

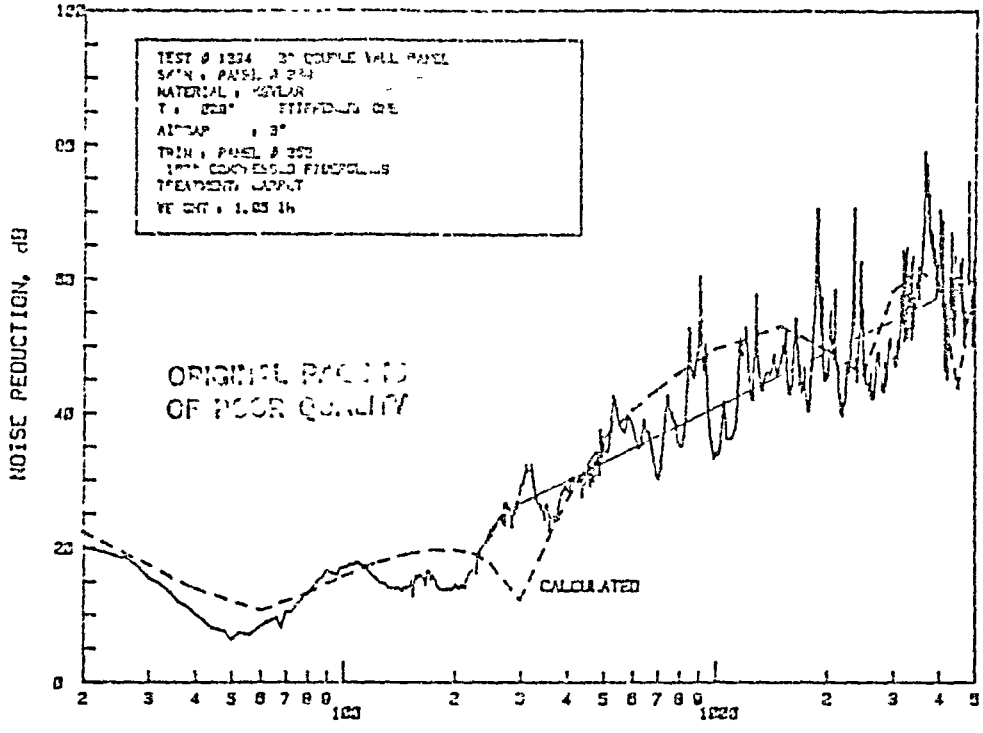

a. Airgap

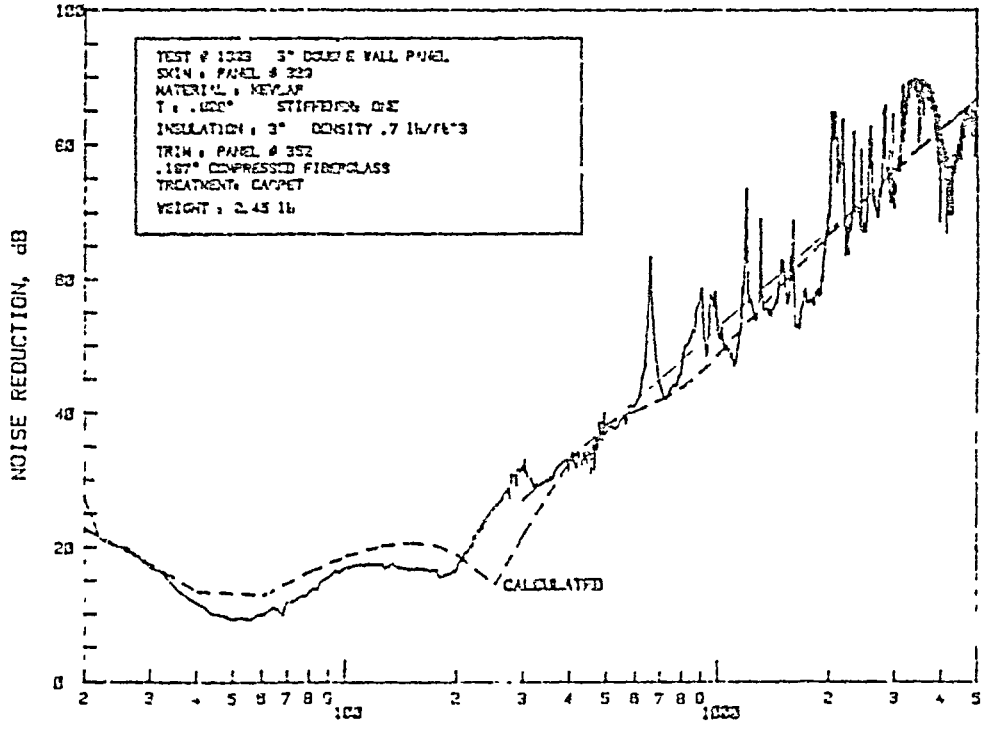

b. Fiberglass Insulation

Figure 4.20: Comparison of Experimental and Theoretical Noise Reduction Characteristics of Double-Wall Panel Made of Kevlar Skin (Panel 339) and Trim Panel 352; Panel Depth 3"

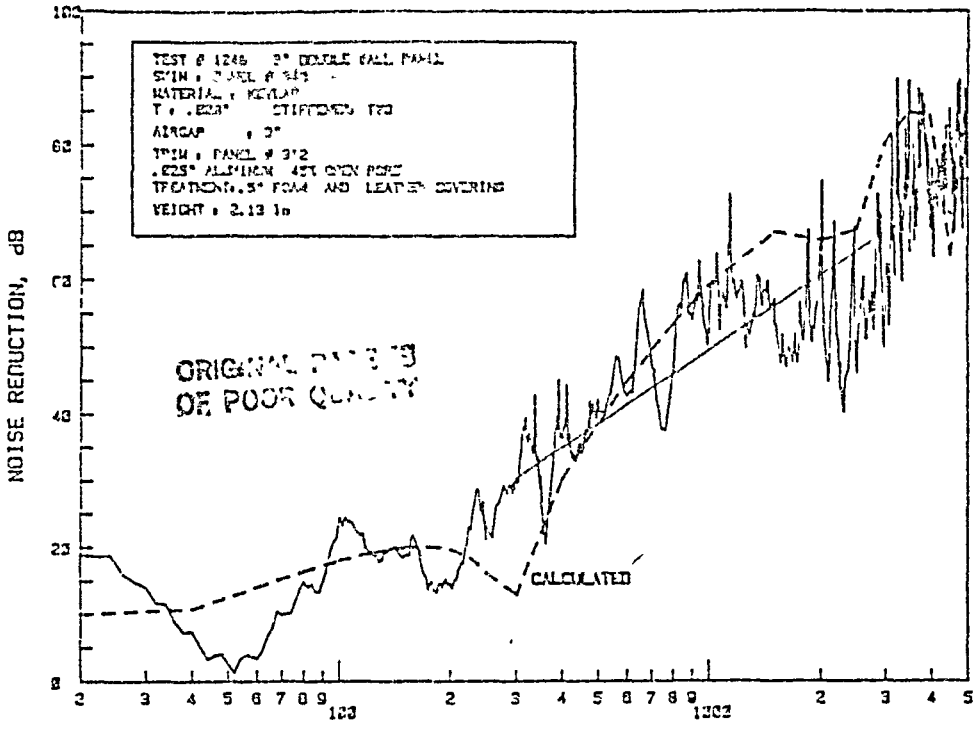

a. Airgap

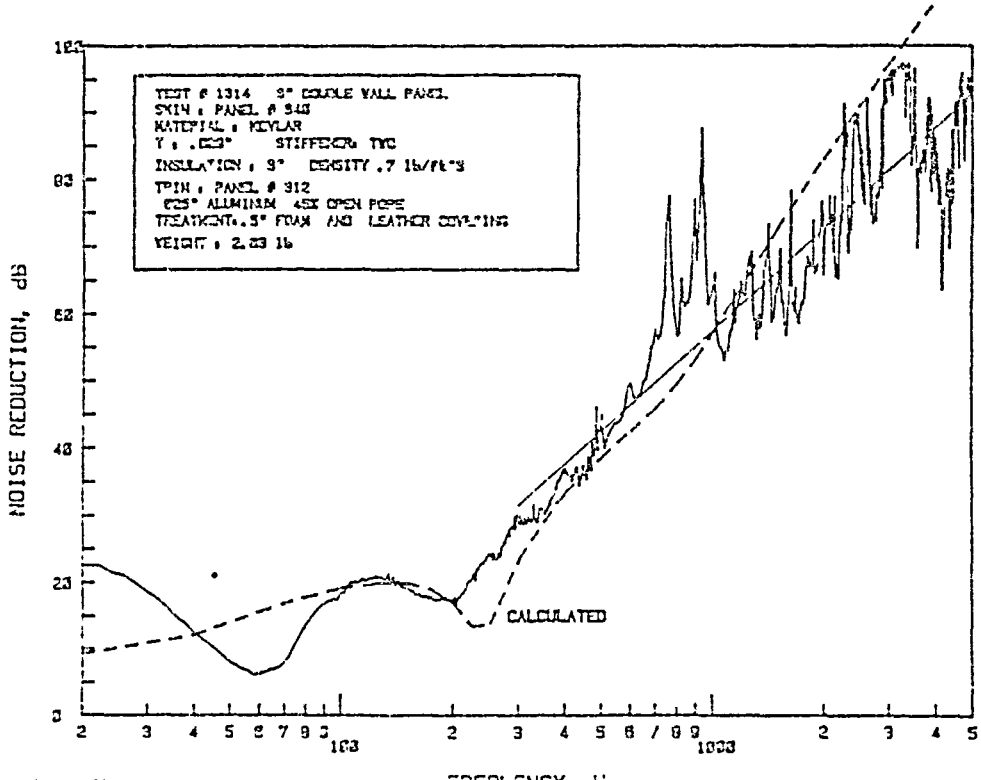

b. Fiberglass Insulation

Figure 4.21: Comparison of Experimental and Theoretical Noise Reduction Characteristics of Double-Wall Panel Made of Kevlar Skin (Panel 340) and Trim Panel 312; Panel Depth 3"

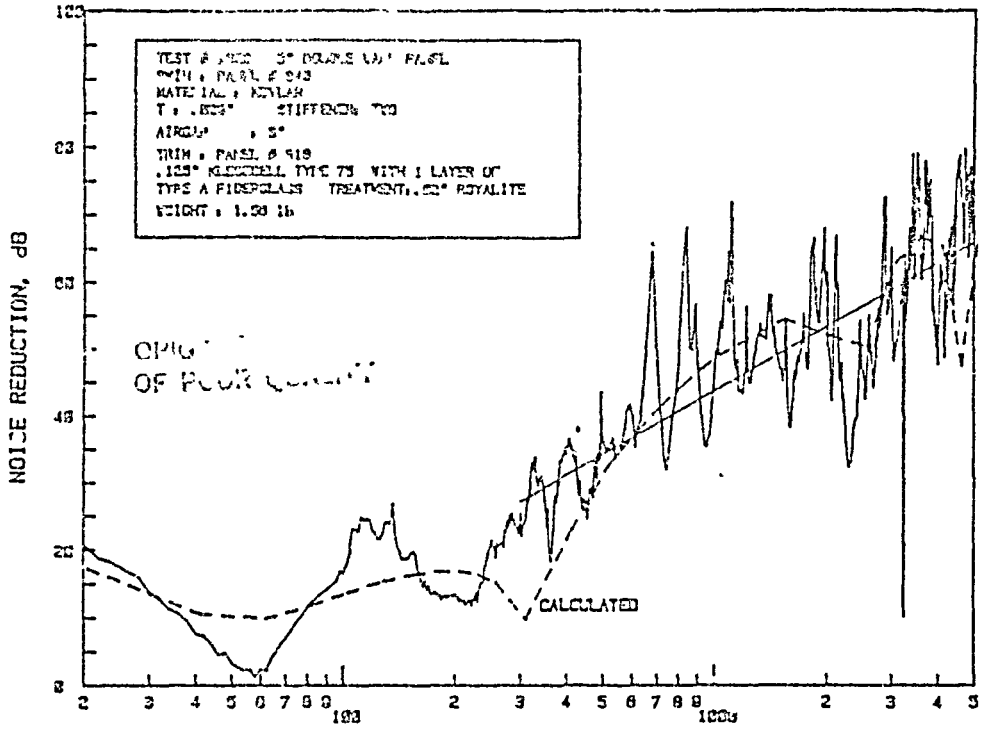

a. Airgap

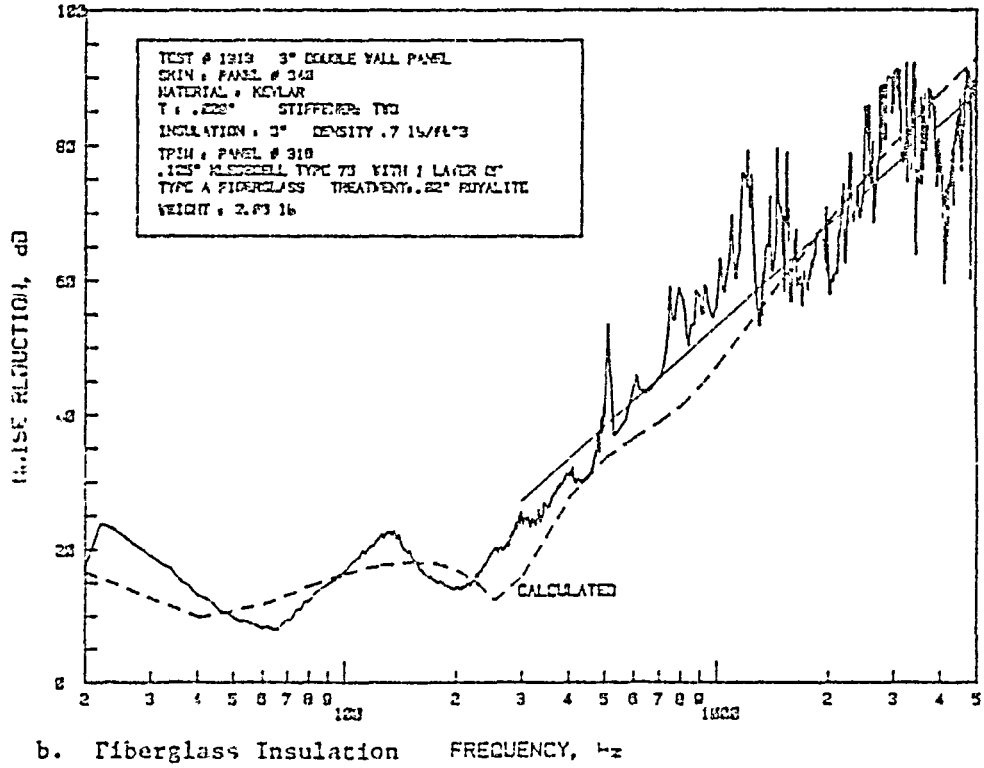

b. Fiberglass Insulation

Figure 4.22: Comparison of Experimental and Theoretical Noise Reduction Characteristics of Double-Wall Panel Made of Kevlar Skin (Panel 340) and Trim Panel 318; Panel Depth 3"

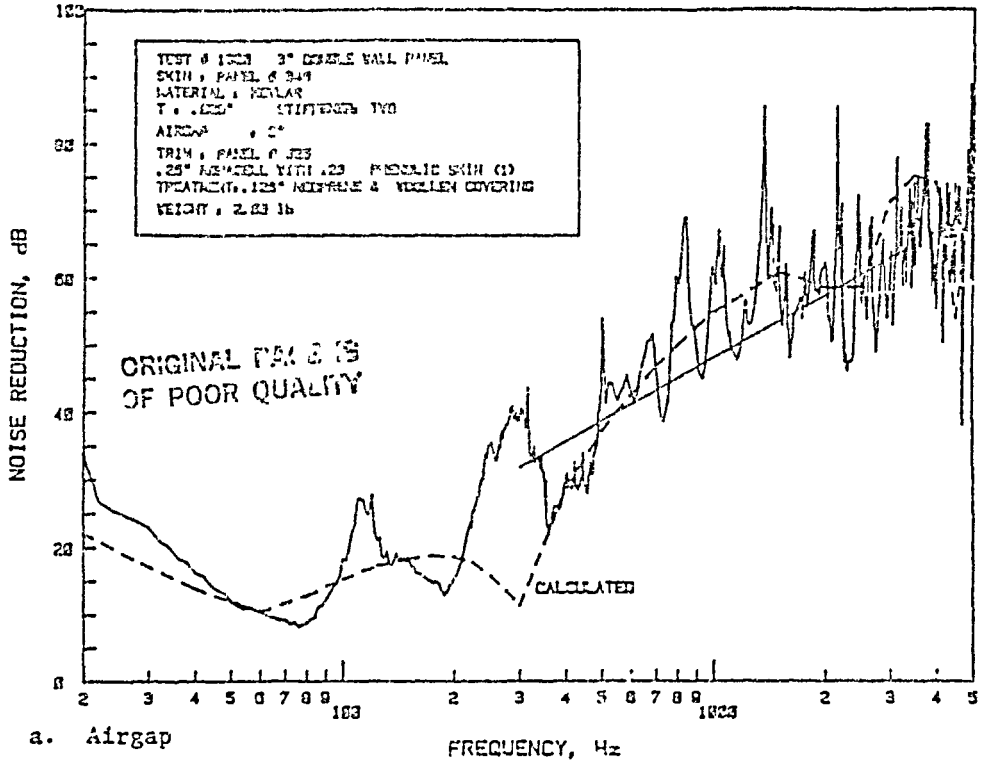

a. Airgap

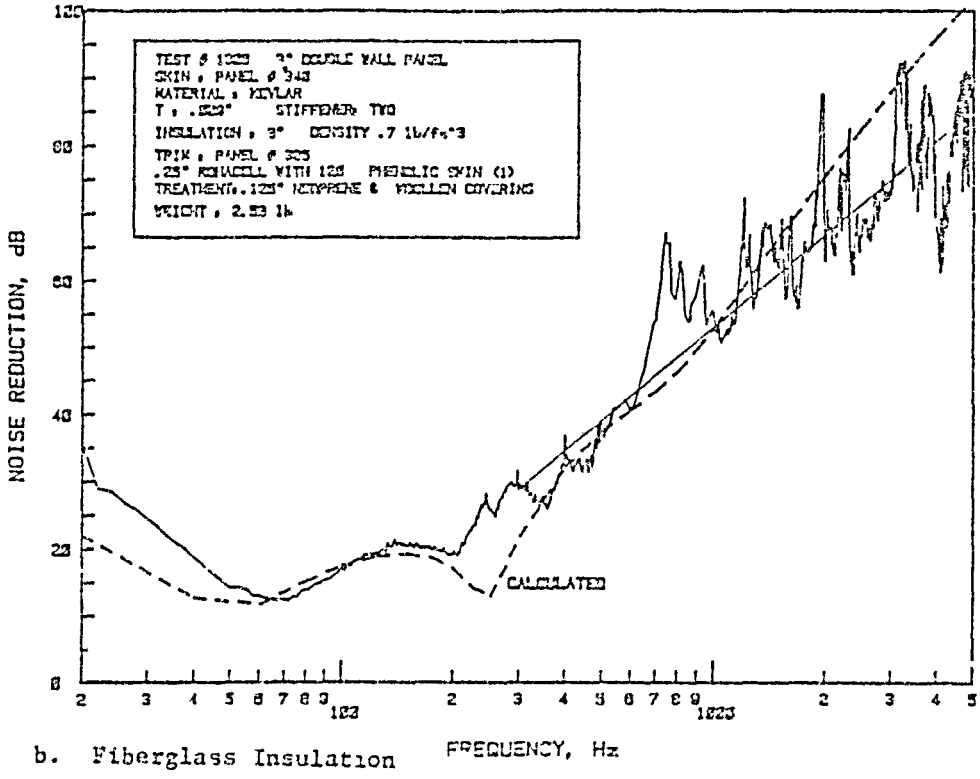

b. Fiberglass Insulation

Figure 4.23: Comparison of Experimental and Theoretical Noise Reduction Characteristics of Double-Wall Panel Made of Kevlar Skin (Panel 340) and Trim Panel 325; Panel Depth 3"

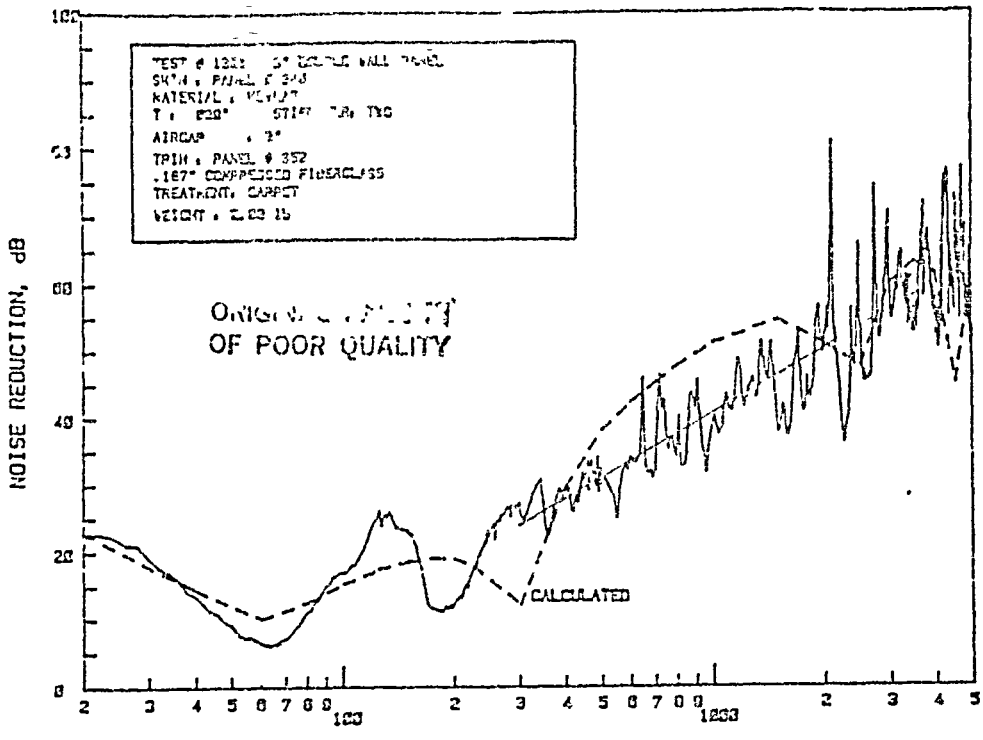

a. Airgap

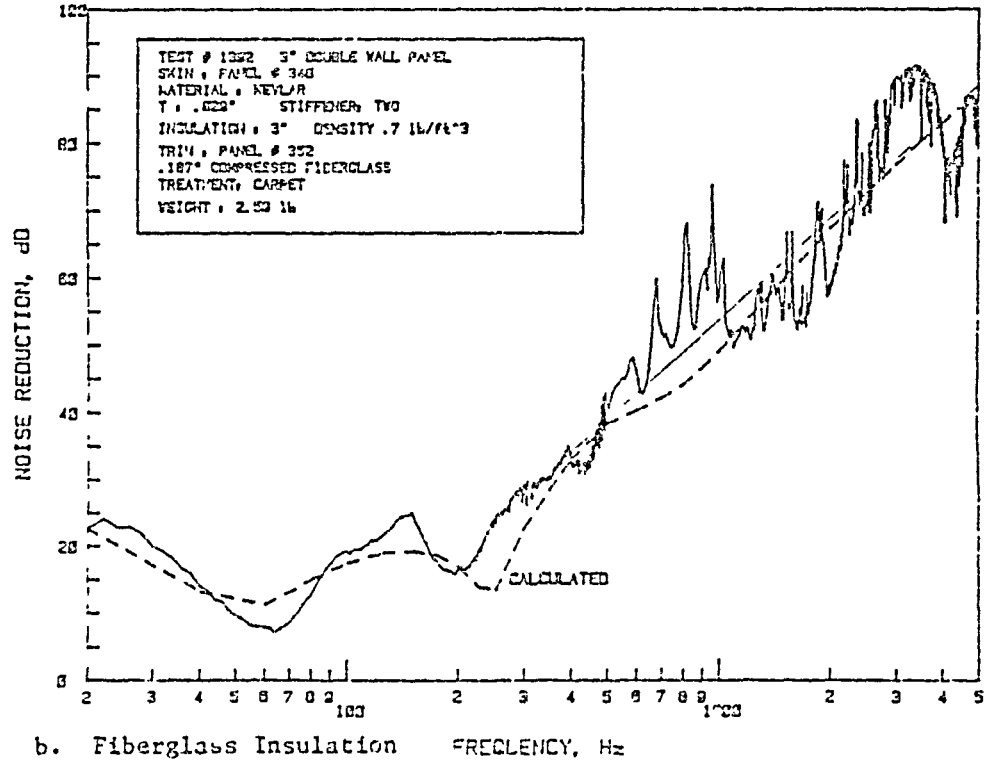

b. Fiberglass Insulation

Figure 4.24: Comparison of Experimental and Theoretical Noise Reduction Characteristics of Double-Wall Panel Made of Kevlar Skin (Panel 340) and Trim Panel 352; Panel Depth 3"

In general, it can be seen that the agreement is reasonable for most of the cases tested. Due to the single mode approximation used in the program, the higher order modes of the skin and the trim panel are not present. Also not present are the higher order cavity modes of the receiver cavity. As the theory does not ignore the higher harmonic of the double-wall panel-air-panel resonance frequencies, they are present and can be seen at higher panel depths without any insulation between the walls.

At low frequency region the calculated values agree well with the experimental double-wall results. These results are expected, since the input values are experimental, single-panel, fundamental resonance frequencies of skin and trim panels. This indicates that at low frequencies the transmission loss is a function of single-panel stiffness. This is true when the frequency is well below the fundamental resonance frequency of either the skin or the trim panel.

In the frequency region between 100 and 500 Hz, which is the region of greatest importance for general aviation interior aircraft noise, the fundamental skin or trim resonance frequency and the fundamental double-wall, panel-air-panel frequency occur. As can be seen, the theoretical values overpredict the measured values by a large value (75 Hz). The reason for this is not understood. Figure 4.25 shows the measured and the calculated double-wall resonance frequency as a function of the thickness of the double-wall panel. The effect of the panel depth on the measured and the caluclated resonance frequencies is the same; but somehow the experimental values are always lower by 75 to 100 Hz, depending upon the trim panel. At the time of

writing this report, this discrepancy is not resolved. Hence, around this frequency region, measured values of noise reduction do not agree with the calculated transmission loss values. However, the trends are the same.

In the high frequency region (above 500 Hz) the higher order panel modes and the cavity modes are not predicted. With airgaps the harmonics of panel-air-panel resonances are visible. The agreement with the test results depends on the trim panel and the depth of panel. Increase in panel depth decreases the fundamental panel-air-panel resonance by the same amount as the experimental results, as can be seen from Figure 4.25. At 3000 Hz frequency the calculated transmission loss dips at 2" depth because of this resonance frequency. This has also been observed in the experimental results. With the insulation no decrease in noise reduction is observed near the harmonic of the panel-air-panel resonance frequency. Whenever the theoretical results are above 90 dB, the difference between the experimental values and the theoretical values is large. This is due to the limitation of the dynamic range of the instrumentation.

The theoretical results overpredict the high frequency noise reduction of the double-wall panel with teim panel 312, and they underpredict the noise reduction of the double-wall panel with trim panel 352. This is because of the variation in the actual slope of the trim panels. The slope of panel 312 is 8 dB/octave, and that of panel 352 is nearly zero. These results indicate that the double-wall results even out these differences. Reasonably good fit is obtained when the slope is less than the theoretical 6 dB/octave slope. Hence

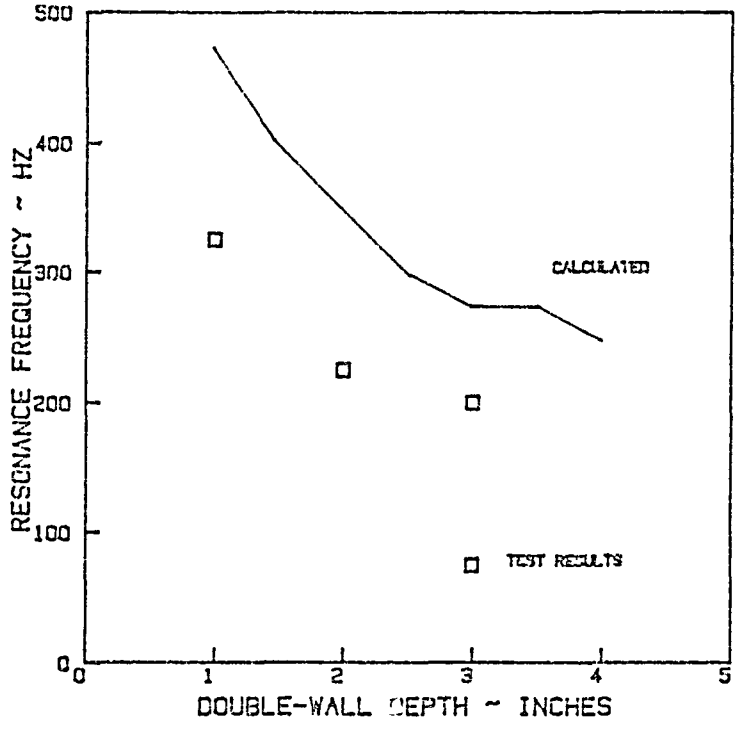

Figure 4.25: Comparison of Experimental and Theoretical Fundamental Panel-Air-Panel Resonance Frequency of the Double-Wall Panel

it can be concluded that the double wall acts as though the trim panel slope is somewhere between .5 and .8 times the theoretical slope.

CHAPTER 5

CONCLUSIONS AND RECOMMENDATIONS

In this report the experimental noise attenuation characteristics of flat, double-wall panels are presented. A simple, classical, sound transmission loss model has been developed for multilayered panels. The experimental results are compared with the theoretical results.

The results of the tests described in this report have demonstrated the following characteristics of the sound transmission through double-wall structures:

- The results of the tests agree, in general, with the simple theoretical model.
- At very low frequencies (below 100 Hz) the noise reduction is a function only of the stiffness of either skin or trim panel. Hence use of a double-wall panel presents no additional gain over use of the single-wall structure.
- At frequencies of 100 to 500 Hz, the overall noise reduction of the double-wall panel is normally lower than the noise reduction of the single panel with the same panel weight. However, the noise reduction at these frequencies is so much a function of the double-wall, panel-air-panel, resonance frequencies that any conclusion on the efficiency of the double wall without knowledge of the excitation frequency and the double-wall characteristics will not be valid. By proper designing of the double-wall panel treatment, the coincidence of the panel-air-panel resonance frequency and the excitation frequency may

be avoided. The double wall may also be designed to give a higher noise reduction at the excitation frequencies.

- In the high frequency region, even though the slope of the noise reduction curve of the double-wall panel exceeds that of the single-wall panel, the experimental values are lower than the theoretically predicted 12 dB/octave. One of the causes for the discrepancy is the assumption that the trim panel behaves like a limp panel following mass-law impedance.
- In particular for the double-wall panels investigated, the effect of the airgap depth in the high frequency region is negligible outside the range of the harmonics of the panel-air-panel resonance frequencies.
- Of the skin panels tested, the aluminum skin panel offers higher high-frequency noise reduction by virtue of its greater mass. At low frequencies, graphite-epoxy panels have up to 7 dB higher noise reduction than the Kevlar panels. One-to-one comparison between these panels is not possible, due to the varied nature of the thickness and the stiffener characteristics. The effect of an additional stiffener in the skin panel is to increase the low-frequency noise reduction by about 4 dB. The additional stiffener has a negligible effect on the noise reduction at high frequencies.
- The effect of the fiberglass insulation in the low-frequency region is small and at times slightly negative.
- In the high frequency region the installation of the fiberglass insulation damps out the resonance effects and also

increases the noise reduction due to the viscous losses. This increase is directly proportional to the insulation thickness.

- The effect of the trim panel is not significant in the low frequency region. Increase in the trim panel mass results in a slightly lower noise reduction.
- At high frequencies the base material and the treatment of the trim panel play a major role in the noise reduction characteristics of both double-wall and single-wall panels. Of the trim panels tested, panels with .5" foam as part of the treatment had the best noise reduction in the high frequency region, even after consideration of their increased mass.
- Due to the instrument limitation, the effect of very high trim panel density on the high frequency noise reduction could not be accurately determined. However, as the noise reduction is well above 80 dB, it is considered that this may not be worthwhile.
- Simple, classical, multilayered transmission loss theory predicts the double-wall transmission loss reasonably well if the actual single-wall data, including the slope of the trim panel noise reduction curve, are input. The theoretical double-wall results do not match with the experimental results when the trim panel slope differs very much from the mass-law slope.

- One of the major deficiencies of this program is the determination of the fundamental panel-air-panel resonance. Even though the experimental values follow the same trend as the theoretical values, they are 75 to 100 Hz lower. The reason for this is yet to be determined.

Based on the results, it is recommended that the computer model and the test procedure be studied to find the cause for the mismatch between the experimental and the theoretical results. It is also recommended that additional tests be conducted to quantify the various trim panel parameters such as the base material characteristics and the treatment.

LIST OF REFERENCES

1. Navaneethan, R.; Hunt, J.; Quayle, B.; "Study of the Damping Characteristics of General Aviation Aircraft Panels and Development of Computer Programs to Calculate the Effectiveness of Interior Noise Control Treatment: Part I," KU-FRL-417-19, Flight Research Laboratory, University of Kansas Center for Research, Inc., Lawrence, KS, December 1982.
2. Navaneethan, R.; "User's Guide to Multilayer Sound Transmission Loss Program " KU-FRL-417-20, Flight Research Laboratory, University of Kansas Center for Research, Inc., Lawrence, KS, January 1983.
3. Henderson, T. D.; "Design of an Acoustic Panel Test Facility," KU-FRL-317-3, Flight Research Laboratory, University of Kansas Center for Research, Inc., Lawrence, KS, August 1977.
4. Grosveld, F.; and van Aken, J.; "Investigation of the Characteristics of an Acoustic Panel Test Facility," KU-FRL-317-9, Flight Research Laboratory, University of Kansas Center for Research, Inc., Lawrence, KS, September 1978.
5. Laméris, J.; Stevenson, S.; Street, B.; "Study of Noise Reduction Characteristics of Composite Fiber-reinforced Panels, Interior Panel Configurations, and the Application of Tuned Damper Concept," KU-FRL-417-18, Flight Research Laboratory, University of Kansas Center for Research, Inc., Lawrence, KS, March 1982.
6. Beranek, L. L.; Noise and Vibration Control, McGraw-Hill Book Co., New York, N.Y., 1971.

7. Grosveld, F.; Navaneethan, R.; "Noise Reduction Characteristics of Flat, General Aviation Type Dual Pane Windows," KU-FRL-417-12, Flight Research Laboratory, University of Kansas Center for Research, Inc., Lawrence, KS, February 1980.

8. Rennison, D. C., et al.; "Interior Noise Control Prediction STudy for High-Speed Propeller Driven Aircraft," NASA CR 159200, NASA, September 1979.

9. Revell, J. D.; Balena, F. J.; and Koval, L. R.; "Analytical Study of Interior Noise Control by Fuselage Design Techniques on High-Speed Propeller Driven Aircraft," NASA CR 159222, July 1978.

APPENDIX A

DETAIL AND CHARACTERISTICS OF THE KU-FRL ACOUSTIC TEST FACILITY

The design and construction details of the KU-FRL acoustic test facility have been described in Reference 3. Reference 4 describes the investigation carried out to determine the characteristics of the test facility. Salient features from these report are presented below.

A.1 DESIGN AND CONSTRUCTION DETAILS

The test facility consists of two chambers: the source chamber and the receiver chamber. The test panel is mounted between these two chambers. The source chamber--consisting of a massive brick wall, a concrete collar, and a steel box--contains nine evenly spaced loudspeakers. This chamber can be considered to be a speaker box. Its purpose is to support the speakers and to prevent sound radiation to the rear and the sides. It contains sound absorbing materials to minimize standing waves. These waves can induce undesirable speaker-sound radiation characteristics. A small distance, about one inch, separates the test panel from the front side of the speaker baffle. This arrangement prevents standing waves between the baffle and the test panel at frequencies in the range of interest, 20 - 5000 Hz. Other standing waves, parallel to the panel and the speaker baffle, could disturb the desired uniformity of excitation at the panel surface. The strength of these waves, however, is reduced by sound absorbing material, which nearly fills all the space between the baffle and the test panel. The receiving chamber is an acoustic termination, which absorbs almost all the sound energy. To facilitate the installation

of test specimens between this termination and the speaker box, the receiving chamber is mounted on wheels and rests on a steel table. Figures A.1 and A.2 show the details.

The test-specimen size is 20 inches by 20 inches. One inch along the edges is used to clamp the test specimen between the two chambers. This leaves an exposed area of 18 inches by 18 inches. This is the maximum size of the test specimen that can be tested at this facility.

The loudspeakers can be driven by an amplified signal from a pure tone generator, a frequency sweep oscillator, a random noise generator, or a tape recording of in-flight boundary layer fluctuations (Figure A.3). An equalizer is included in the sound generation system to obtain a reasonably flat input spectrum. The noise measuring system includes two 1/4" or 1/2" B&K microphones, one on each side of the test panel. The output signals of the microphones are fed to a (narrow band) real-time analyzer. The resulting spectra are transferred to an H-8 microcomputer where they are stored on floppy disks. The data is then transferred to the KU-FRL MINC computer through the phone lines, where noise reduction curves are plotted using an HP 7225B plotter.

The facility has a series of adaptors which are used to test the noise reduction characteristics at different angles of incidence. In addition a tension device is available which permits investigation under uniaxial or biaxial (tensile) stresses. To test the effect of pressurization on the sound transmission loss of a panel, a depressurization system has been installed. With this system the pressure in the source chamber can be reduced. At present all tests are being conducted at ambient temperature (68 to 72 degrees F).

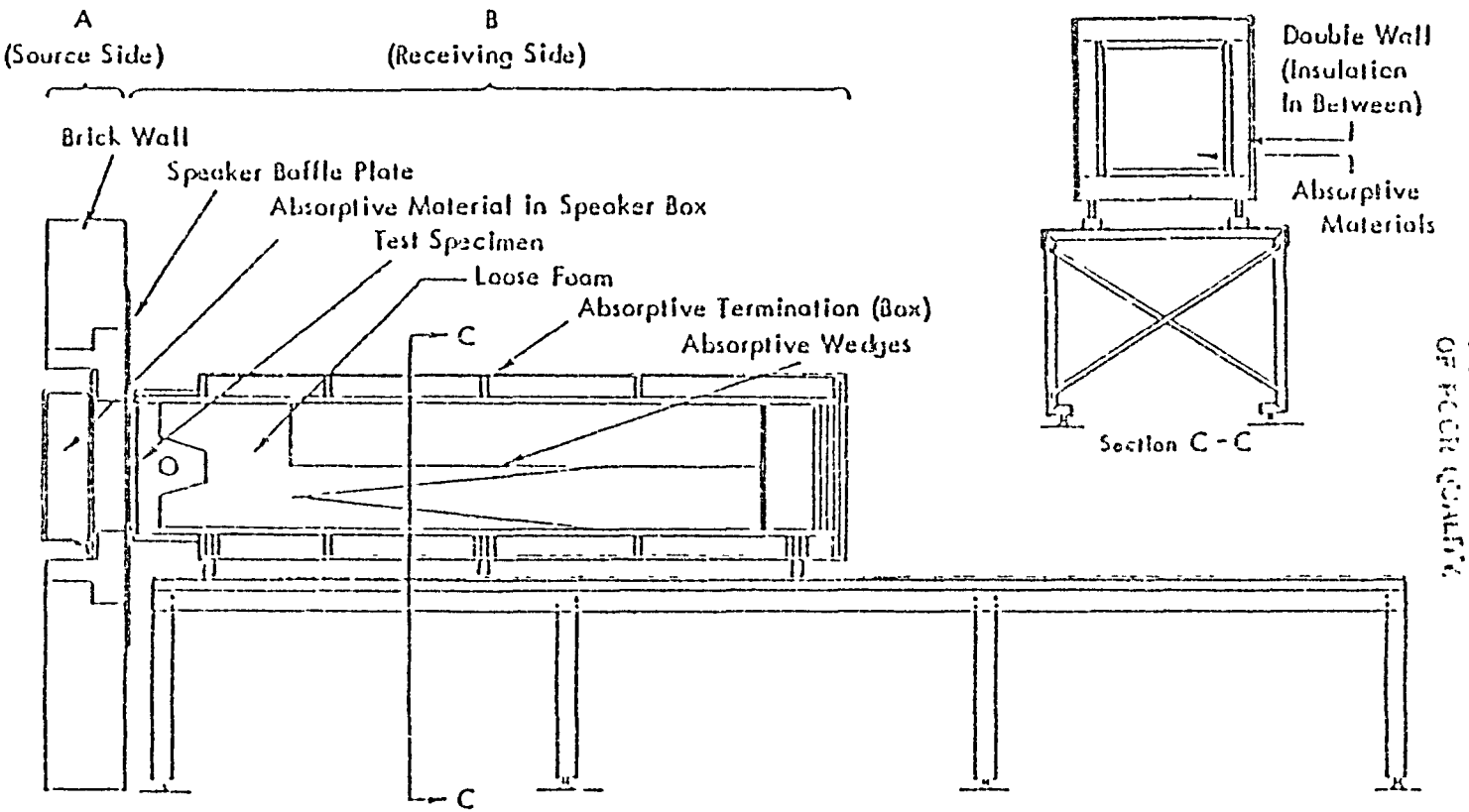

Figure A.1: KU-FRL Acoustic Test Facility

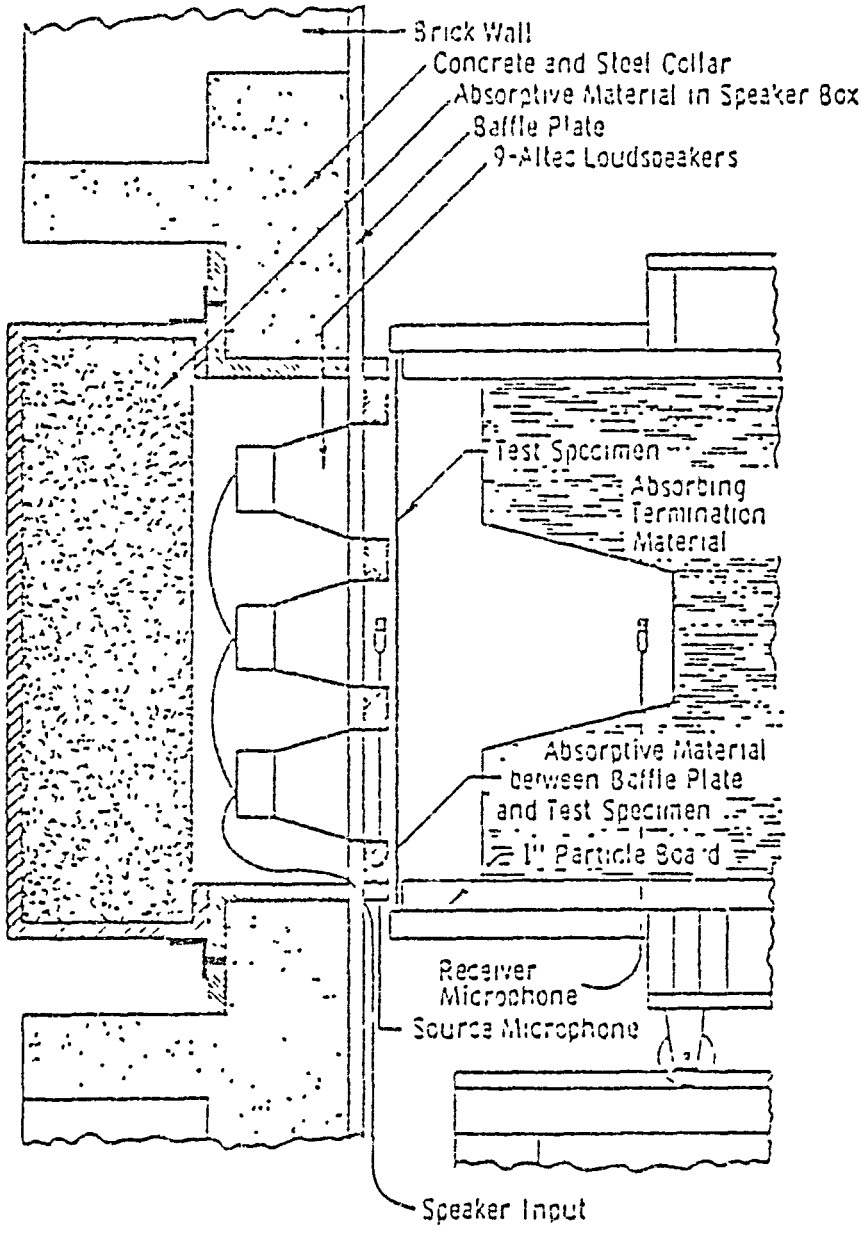

Figure A.2: KU-FRL Acoustic Test Facility--Placement of Test Specimen

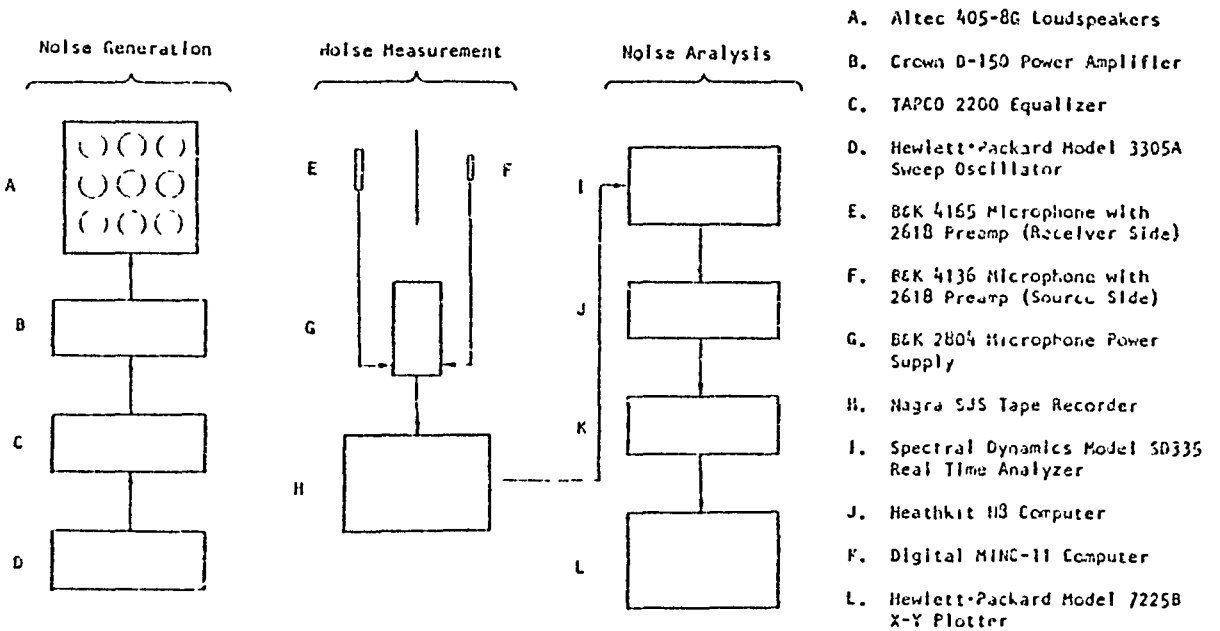

Figure A.3: General Arrangement of Electronic Equipment

A.2 CHARACTERISTICS OF THE TEST FACILITY

Several investigations were carried out to determine accurately the characteristics of this test facility. The results are described in References 3 and 4. Notable conclusions are given below.

1. At high frequencies using a standard panel, the slope of the noise reduction curve obtained corresponds to that predicted by mass law (i.e., 6 dB/octave). However, actual values are overpredicted by at least 3 to 4 dB.
2. The plane wave approximation is justified only below a frequency of 800 Hz at short distances from the speaker baffle. However, this variation seems to have not much effect on the slope of the noise reduction curve. It is also justified over the entire frequency range tested (20 to 5000 Hz) if the distance from the source is at least 34 inches.
3. Although all the walls have been covered very carefully with high quality absorption material, standing waves have not been fully prevented.
4. In addition, the reflections from the side walls affect the signal measured by the receiver microphone. These reflections and the standing waves result in additional peaks and dips in the measured spectra, when narrow-band analysis is carried out.
5. The use of a sweep oscillator with a very slow sweep rate is a satisfactory substitute to measure sound transmission through aircraft structures.

6. Each of the nine speakers has its own frequency response characteristics.

7. The effect of the possible reflections off the back panel of the receiving chamber is so low that it is within the experimental scatter.

8. Removal of the back panel of the source chamber affects the results below 60 Hz.

9. The air in the closed cavity backing the test specimen acts as an additional stiffness, raising the fundamental panel resonance frequency. For a simple panel the analytical model gives an accurate account (within 5% accuracy) of this effect.

10. The edge conditions of the test panel are somewhere between simply supported and clamped, and this complicates any comparison of measured and theoretical values in the low-frequency region. In the high-frequency region, presence of the cavity resonances and the sound absorption capability of the sound absorption materials complicate comparison of measured sound transmission with theoretical predictions. However, the results from the facility agree with the results from classical transmission loss theory when higher modes are neglected.

APPENDIX B

EXPERIMENTAL NOISE REDUCTION DATA OF DOUBLE-WALL STRUCTURES

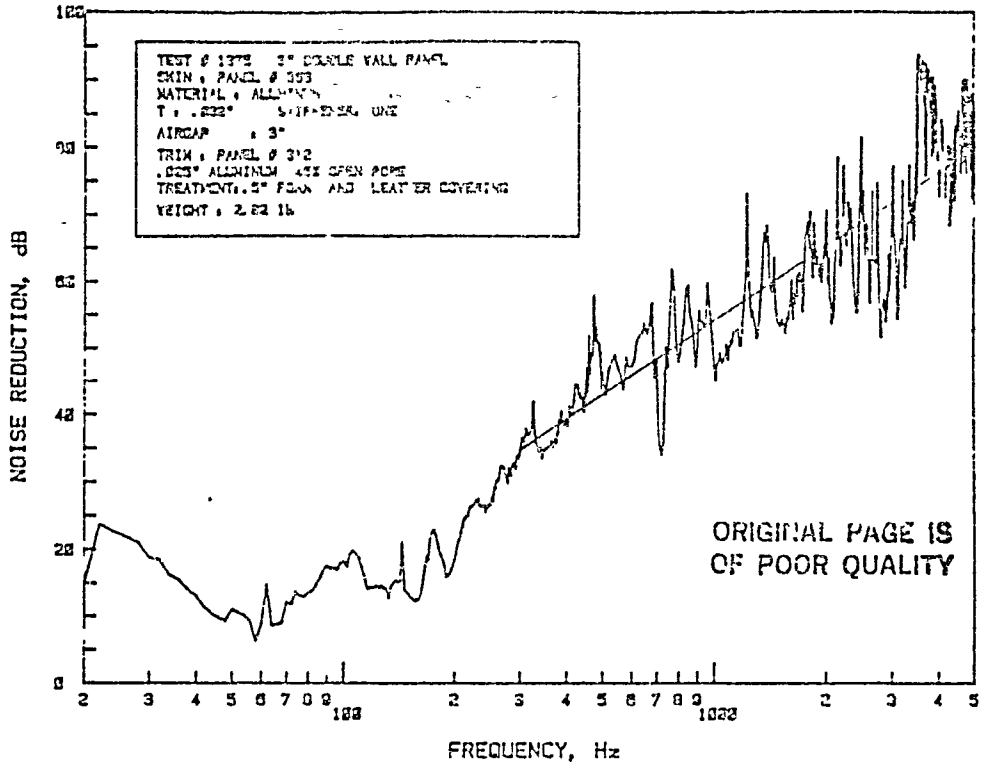

a. Airgap

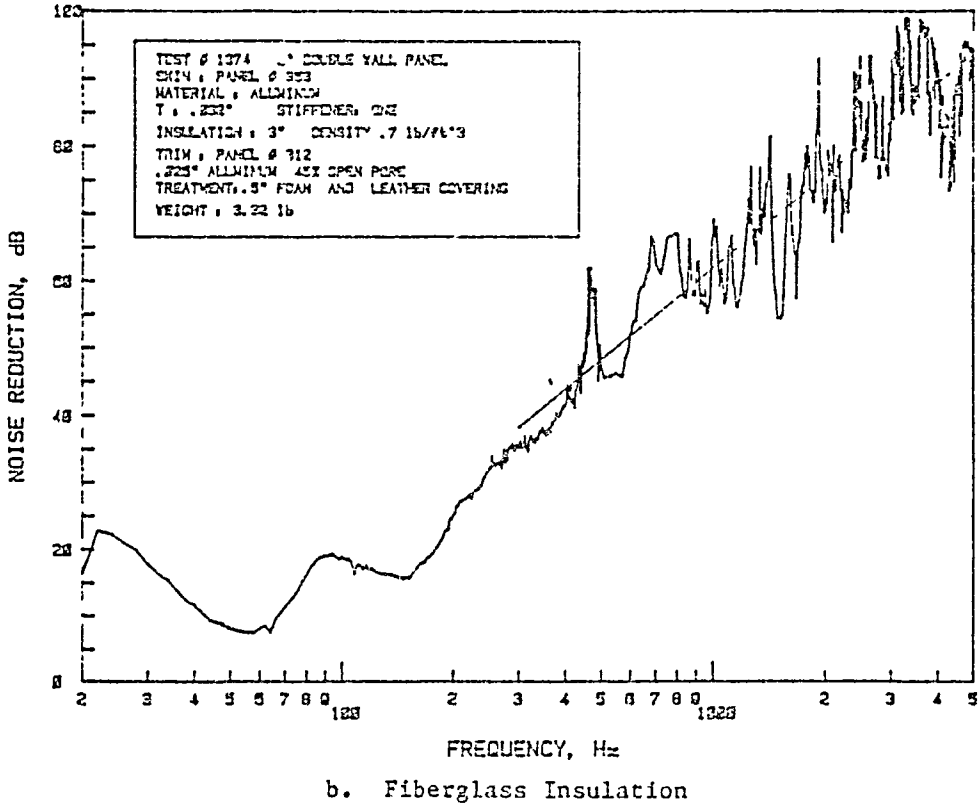

b. Fiberglass Insulation

Figure B.1: Noise Reduction Characteristics of Double-Wall Panel Made of Aluminum Skin Panel 353 and Trim Panel 312; Panel Depth 3"

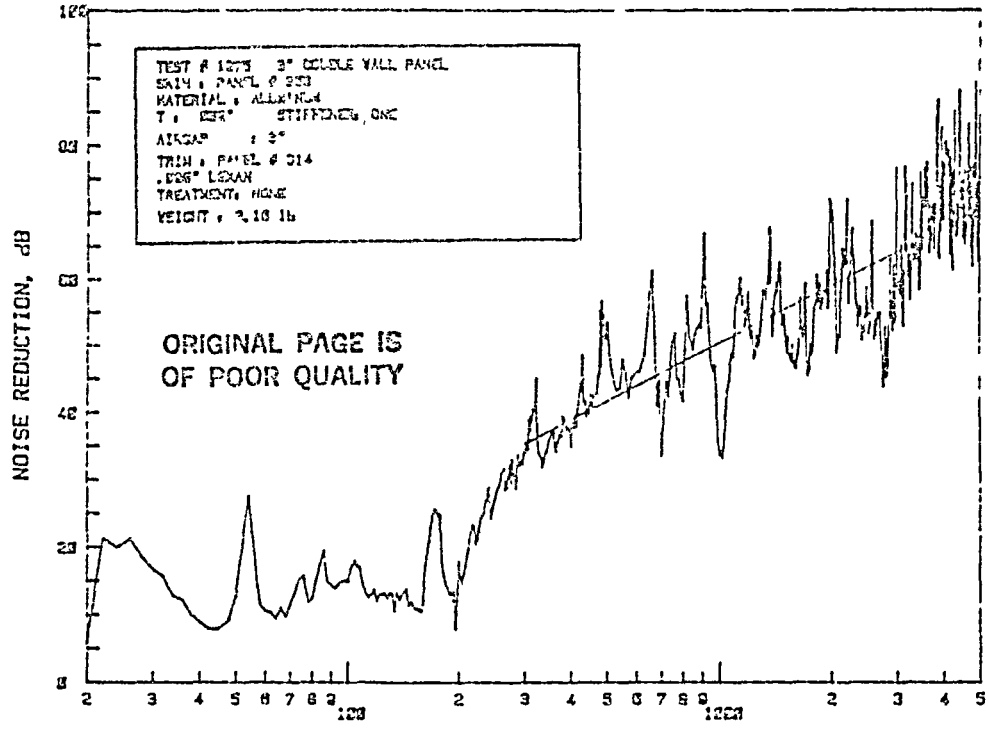

a. Airgap

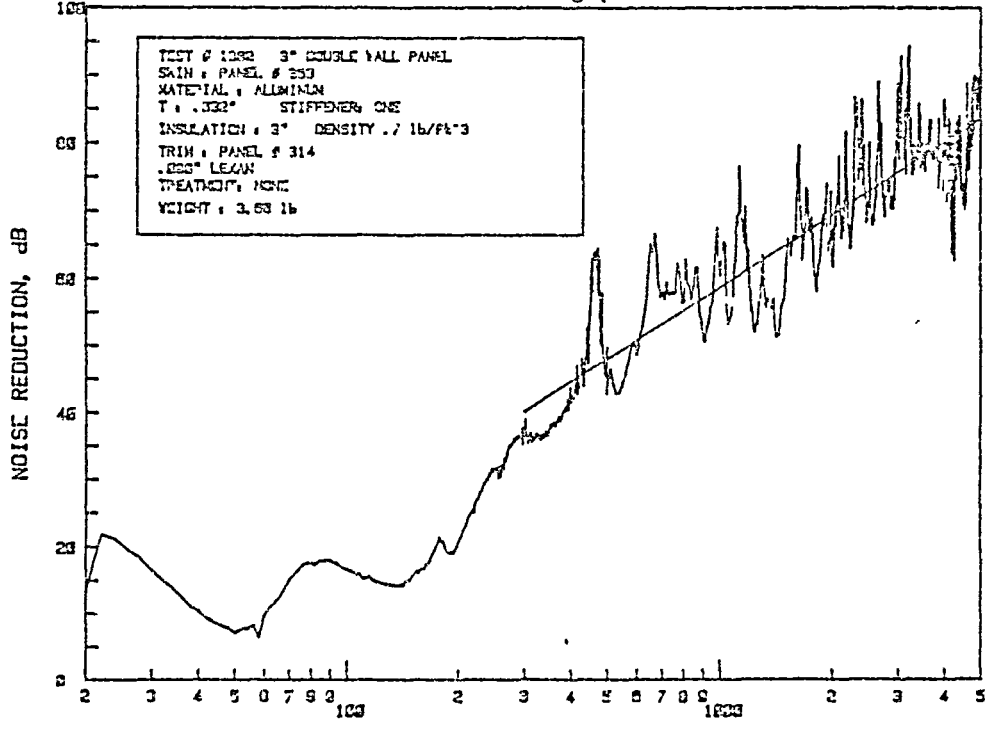

b. Fiberglass Insulation

Figure B.2: Noise Reduction Characteristics of Double-Wall Panel Made of Aluminum Skin Panel 353 and Trim Panel 314; Panel Depth 3"

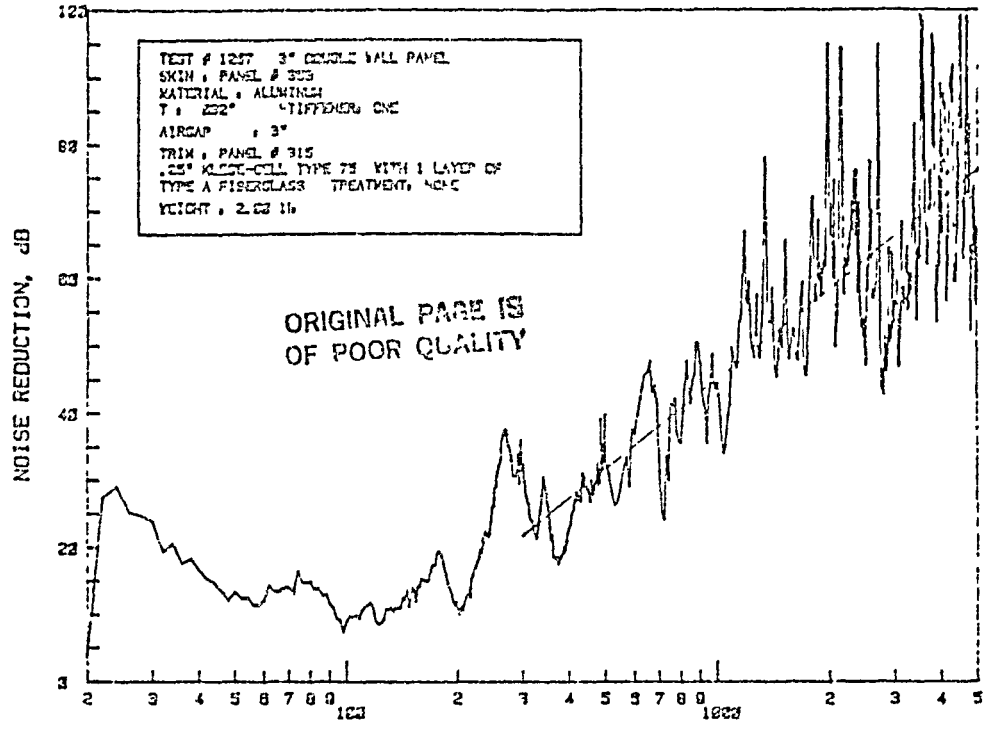

a. Airgap

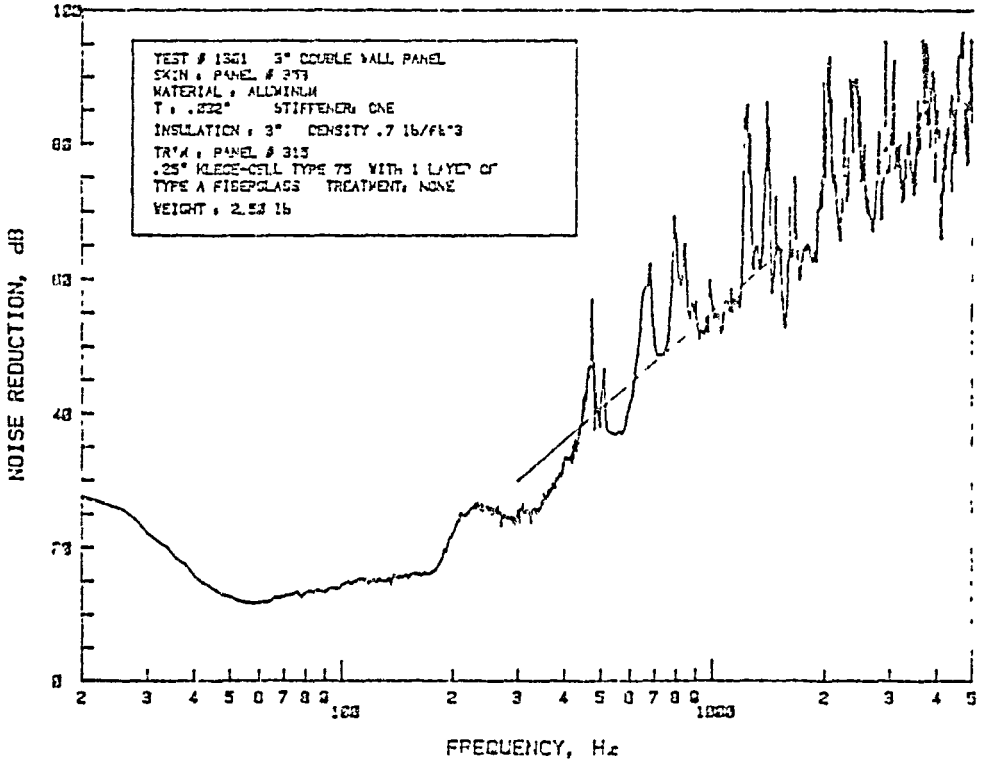

b. Fiberglass Insulation

Fibure B.3: Noise Reduction Characteristics of Double-Wall Panel Made of Aluminum Skin Panel 353 and Trim Panel 315; Panel Depth 3"

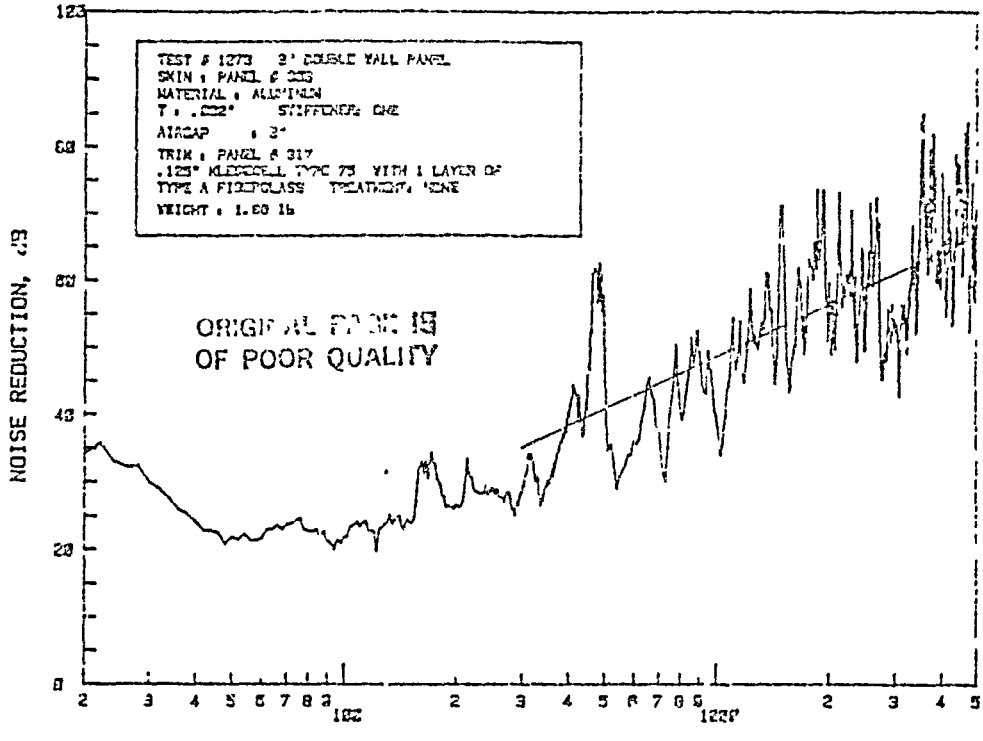

a. Airgap

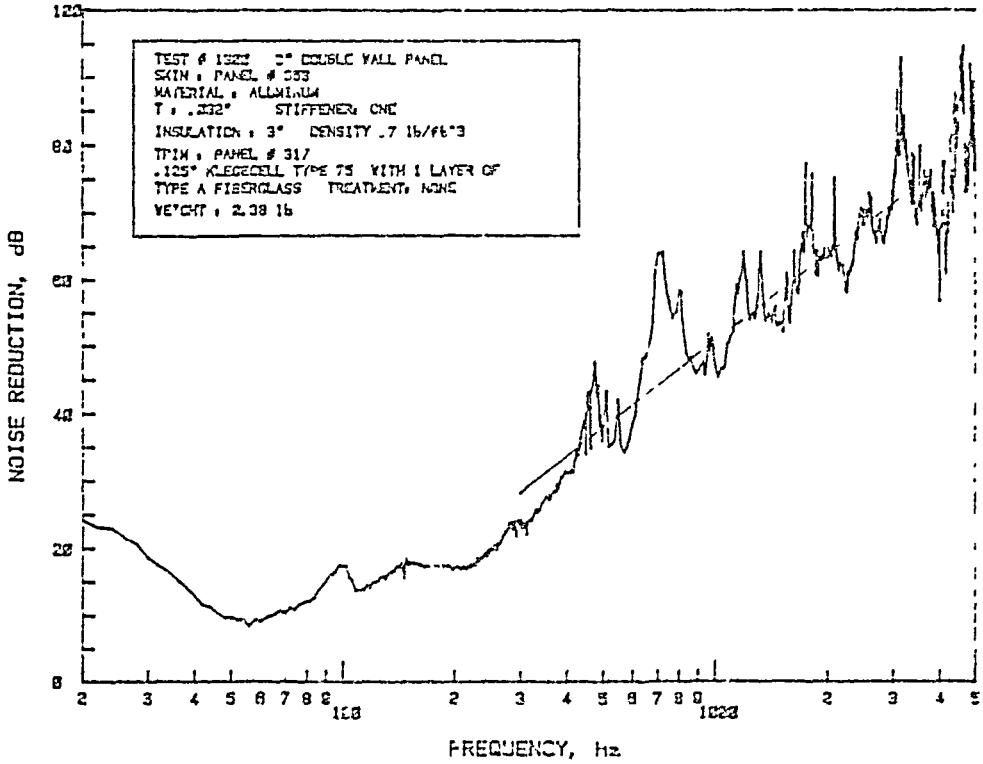

b. Fiberglass Insulation

Figure B.4: Noise Reduction Characteristcs of Double-Wall Panel Made of Aluminum Skin Panel 353 and Trim Panel 317; Panel Depth 3"

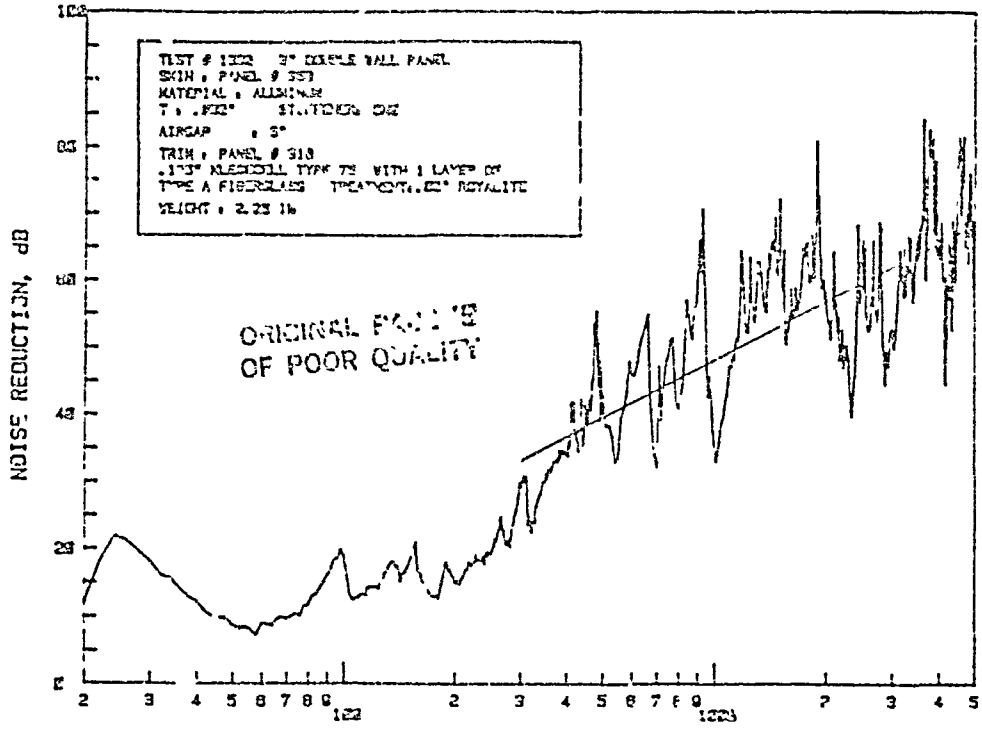

a. Airgap

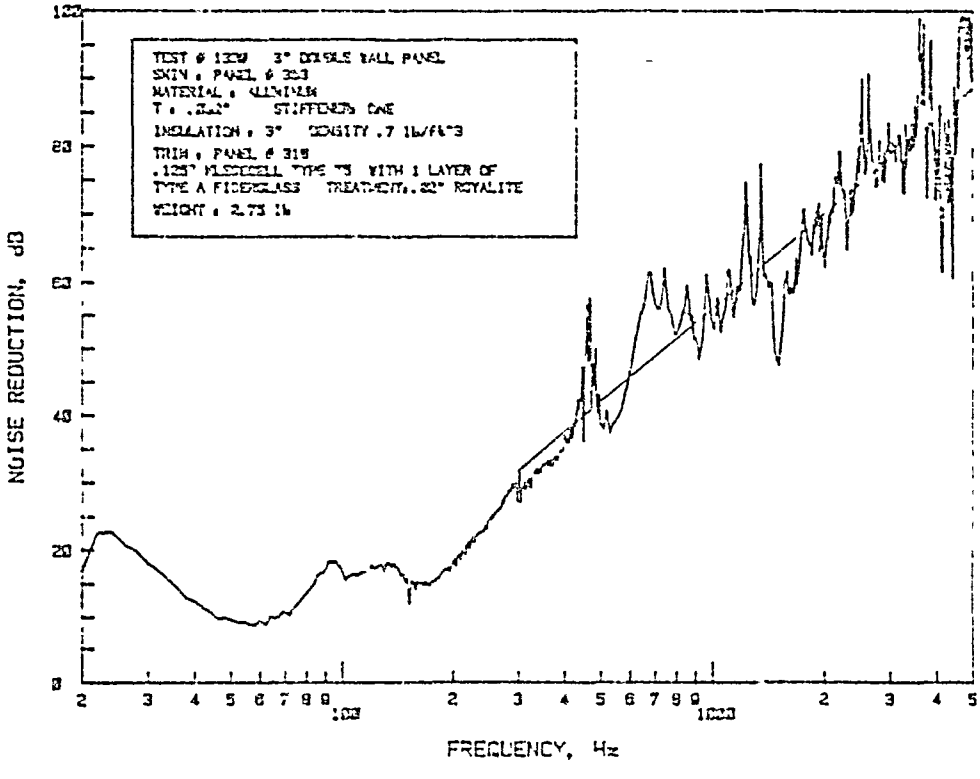

b. Fiberglass Insulation

Figure B.5: Noise Reduction Characteristics of Double-Wall Panel Made of Aluminum Skin Panel 353 and Trim Panel 318; Panel Depth 3"

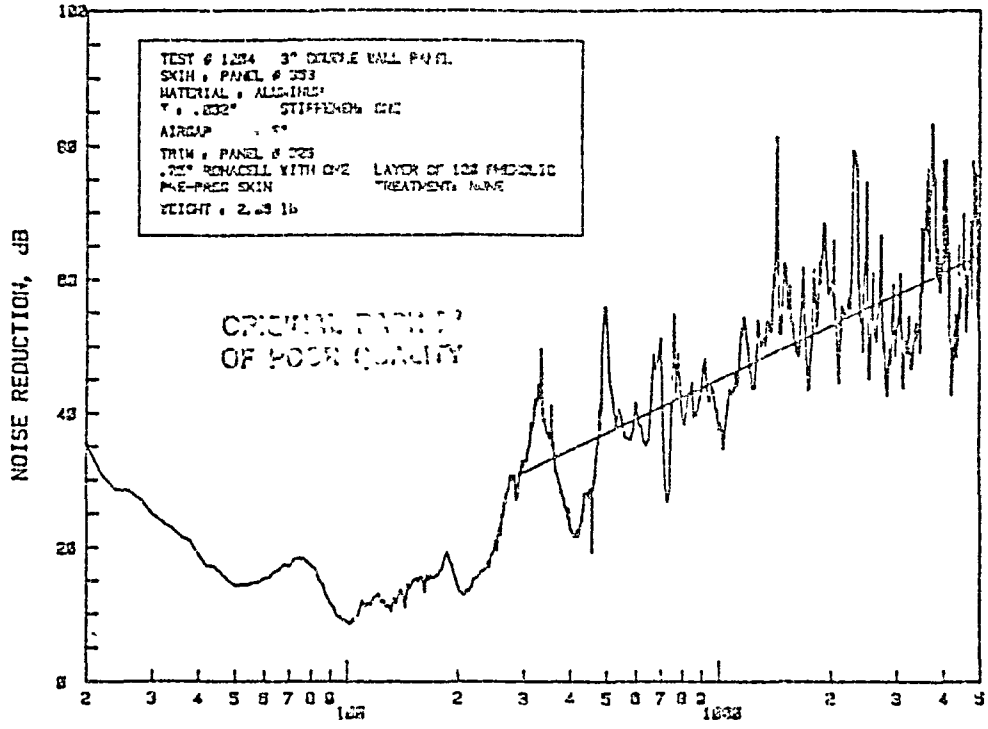

a. Airgap

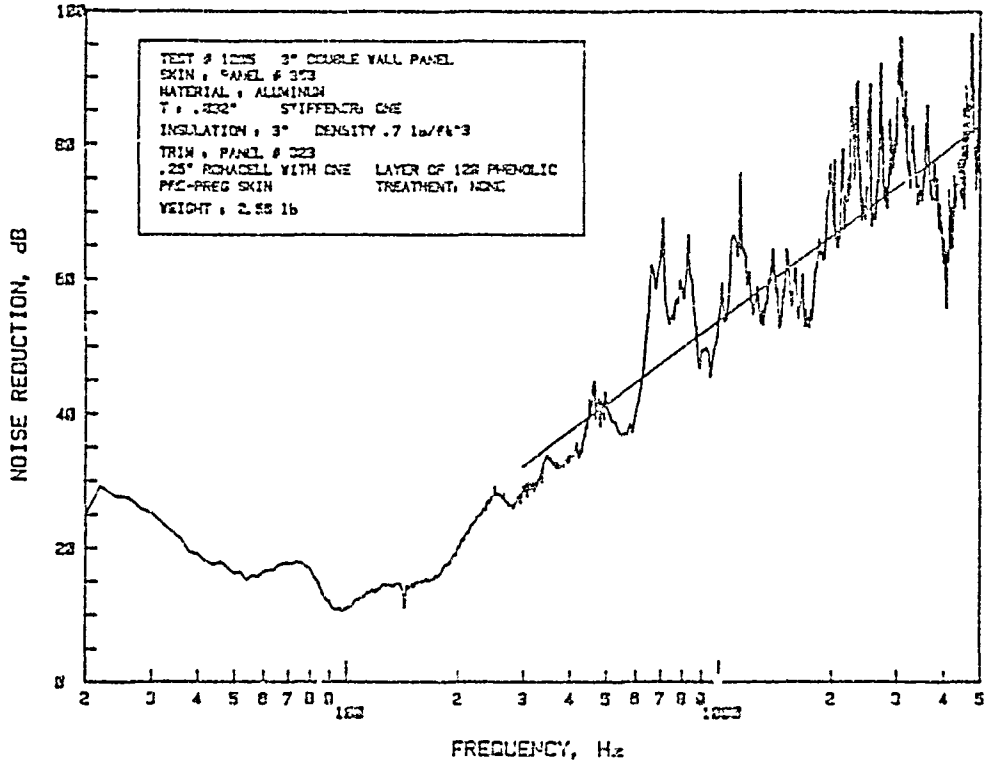

b. Fiberglass Insulation

Figure B.6: Noise Reduction Characteristics of Double-Wall Panel Made of Aluminum Skin Panel 353 and Trim Panel 323; Panel Depth 3"

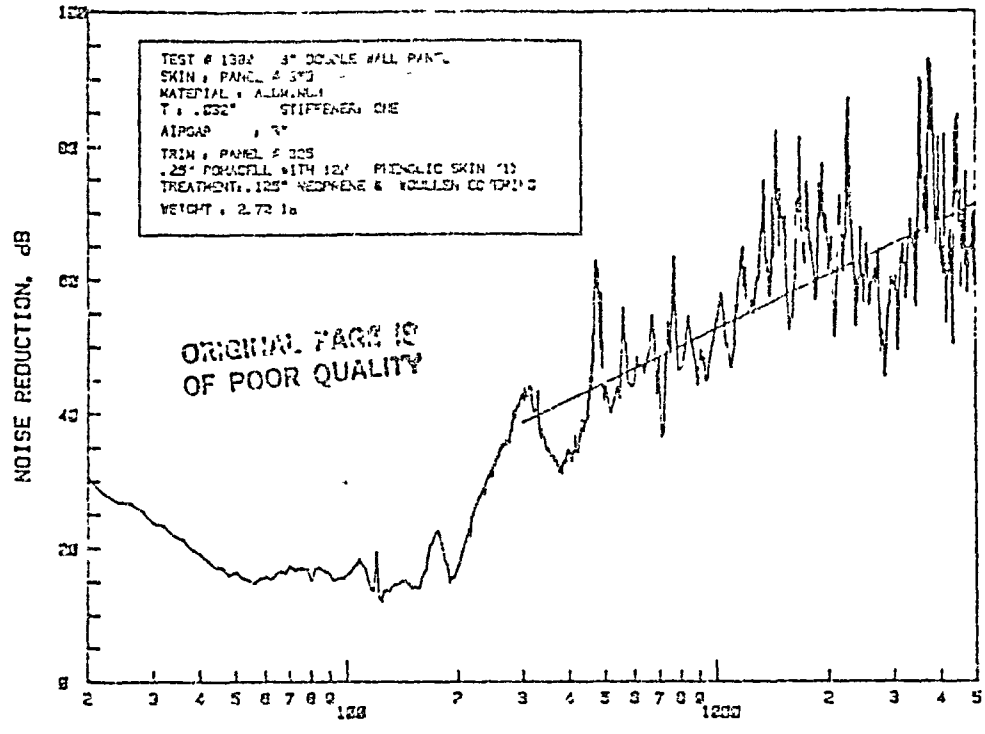

a. Airgap

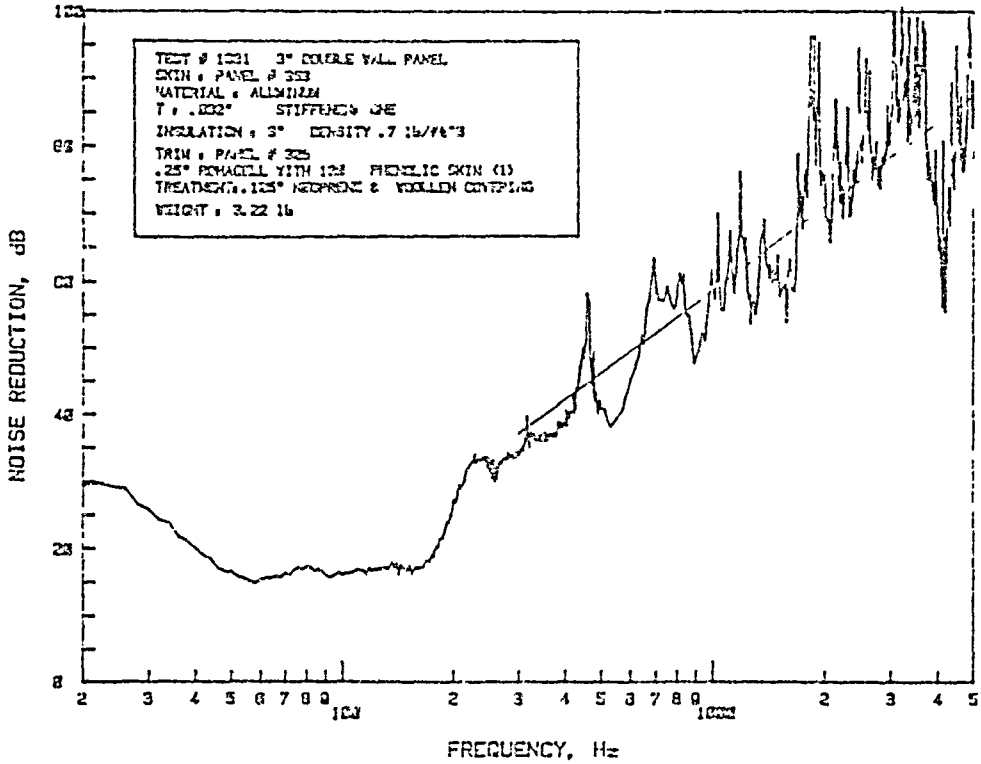

b. Fiberglass Insulation

Figure B.7: Noise Reduction Characteristics of Double-Wall Panel Made of Aluminum Skin Panel 353 and Trim Panel 325; Panel Depth 3"

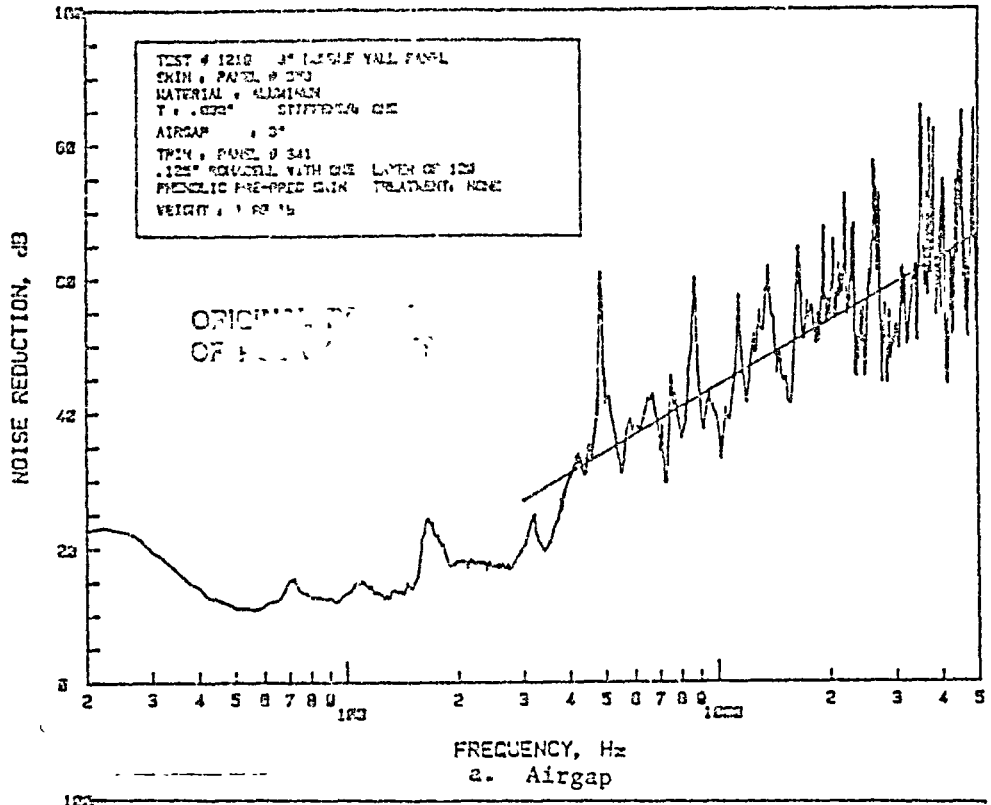

a. Airgap

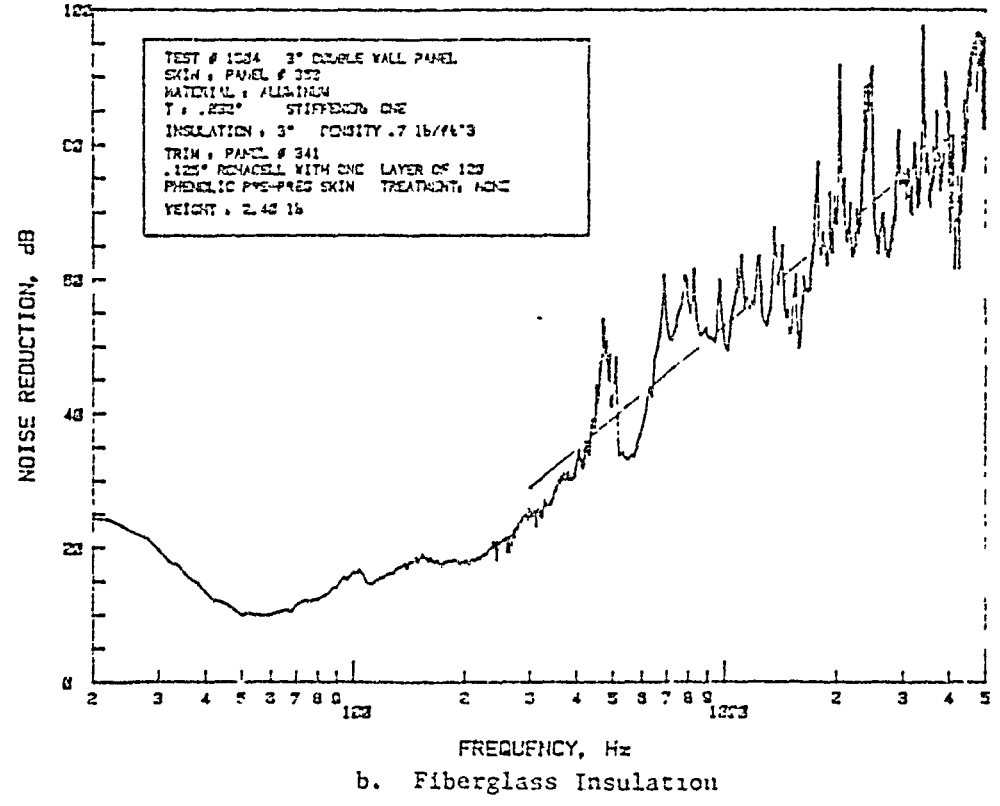

b. Fiberglass Insulation

Figure B.8: Noise Reduction Characteristics of Double-Wall Panel Made of Aluminum Skin Panel 353 and Trim Panel 341; Panel Depth 3"

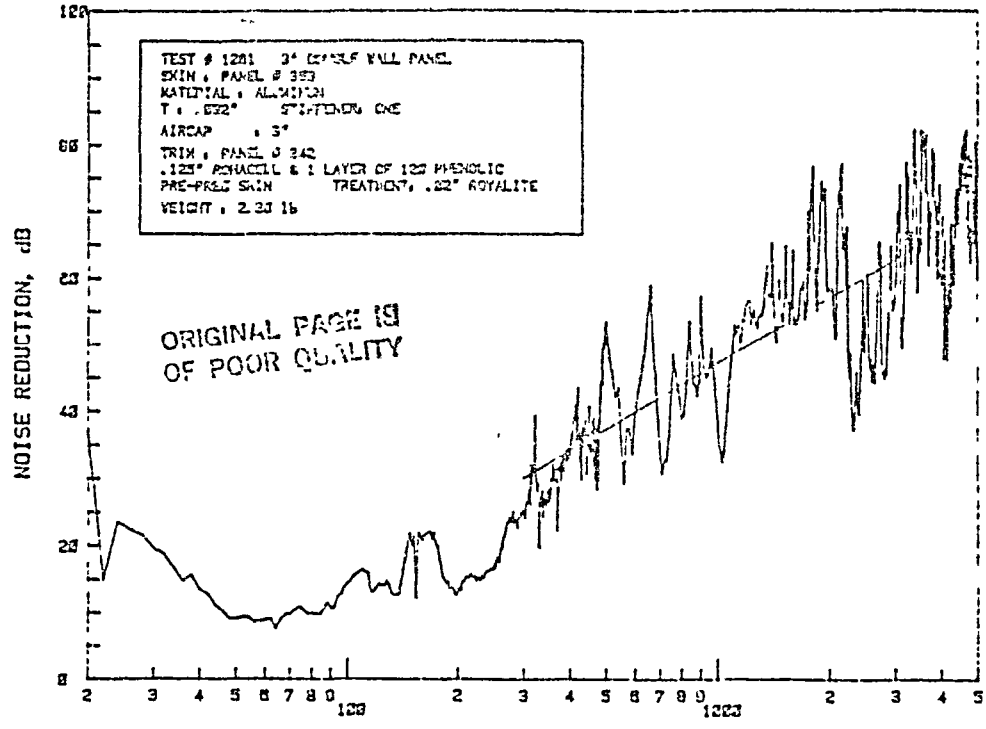

a. Airgap

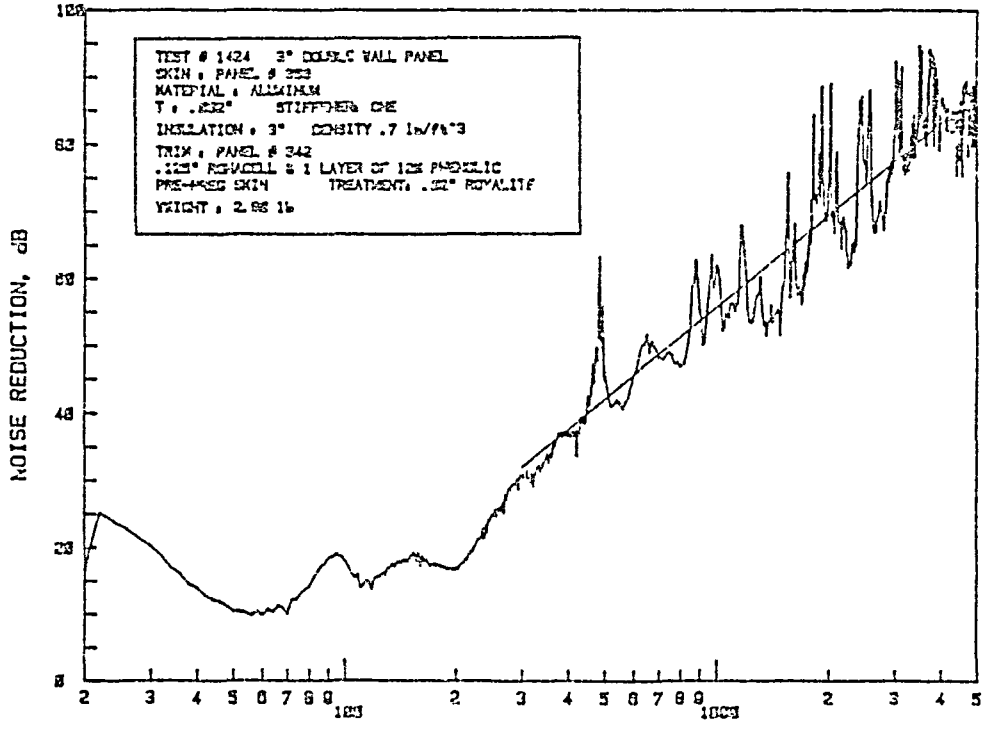

b. Fiberglass Insulation

Figure B.9: Noise Reduction Characteristics of Double-Wall Panel Made of Aluminum Skin Panel 353 and Trim Panel 342; Panel Depth 3"

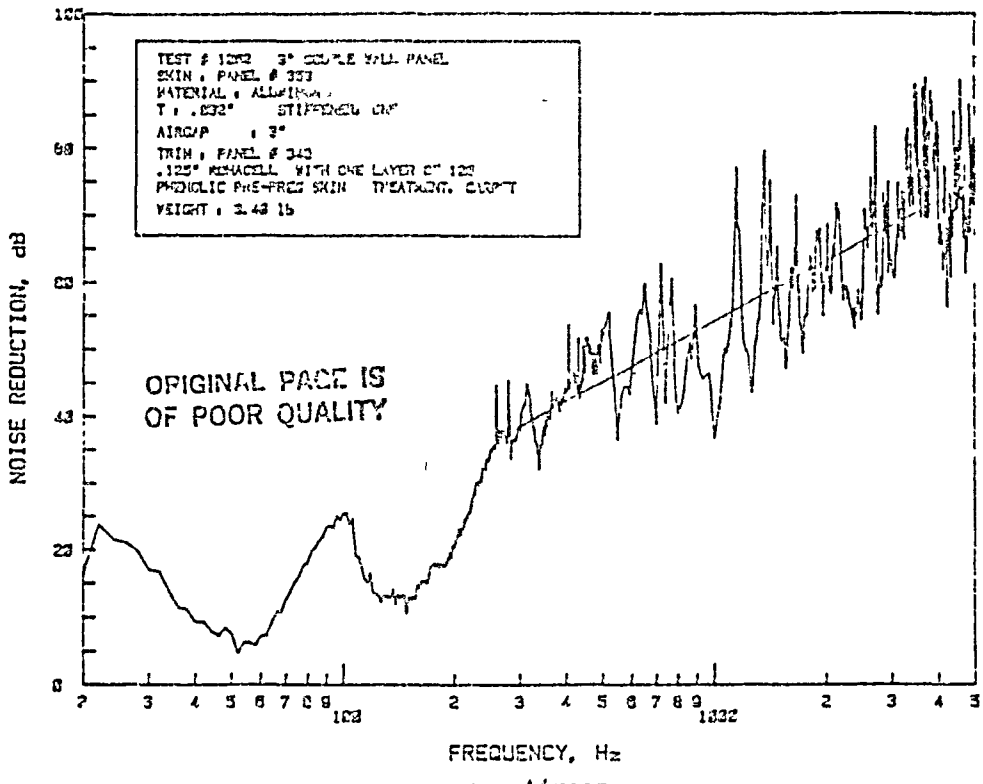

a. Airgap

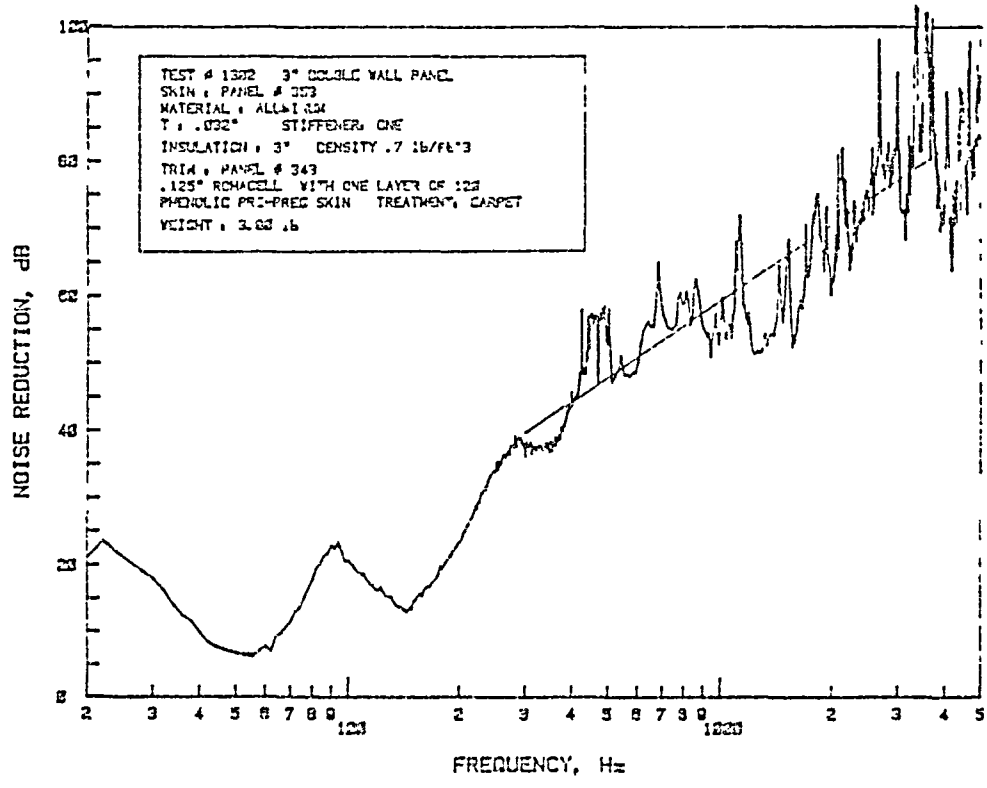

b. Fiberglass Insulation

Figure B.10: Noise Reduction Characteristics of Double-Wall Panel Made of Aluminum Skin Panel 353 and Trim Panel 343; Panel Depth 3"

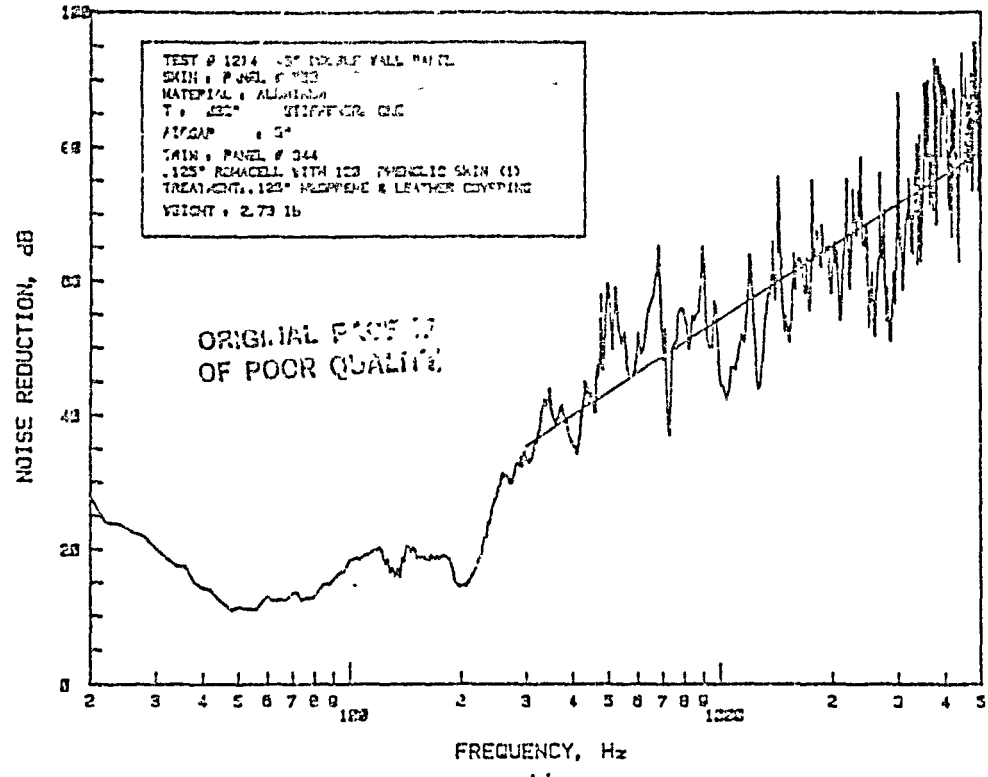

a. Airgap

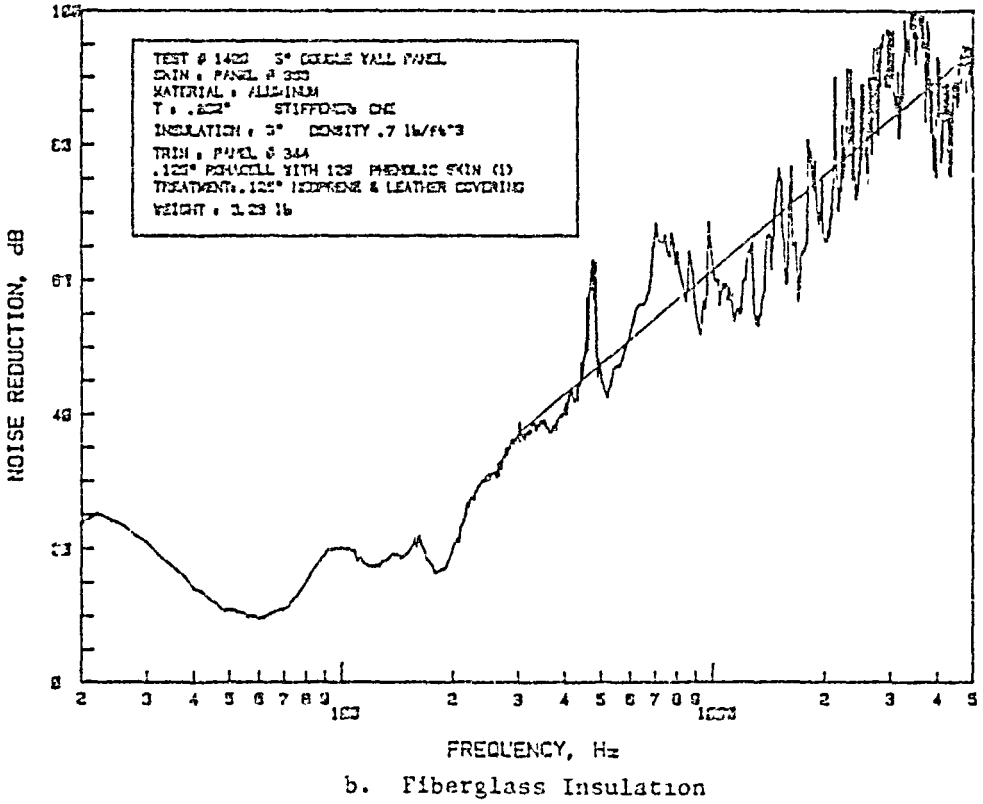

b. Fiberglass Insulation

Figure B.11: Noise Reduction Characteristics of Double-Wall Panel Made of Aluminum Skin Panel 353 and Trim Panel 344; Panel Depth 3"

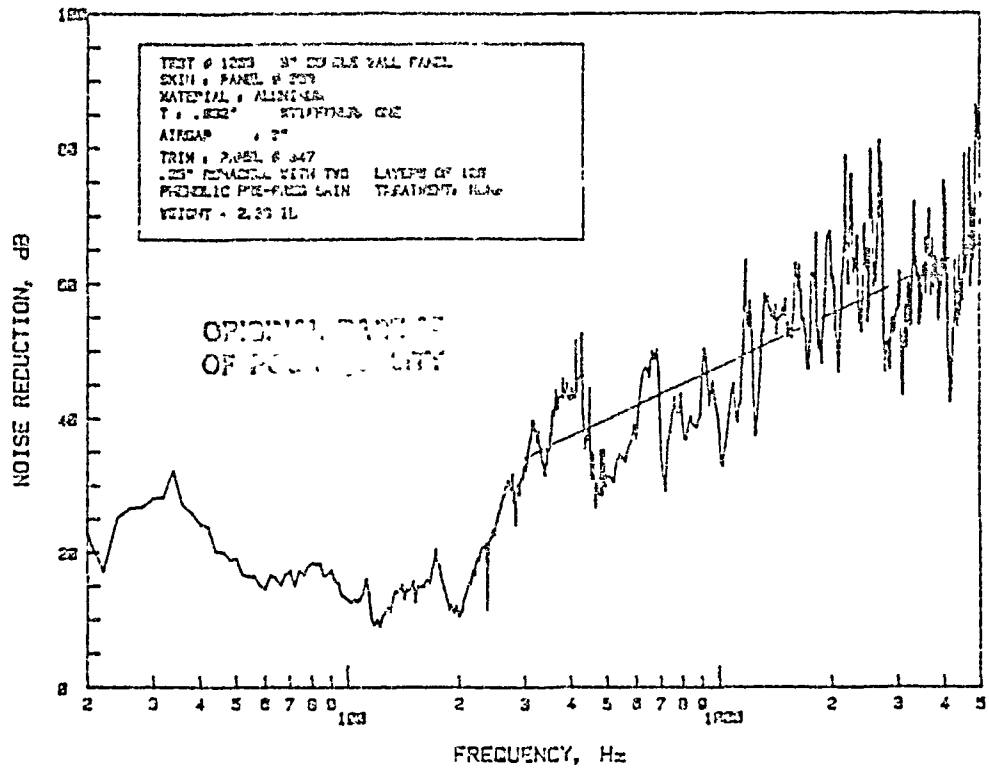

a. Airgap

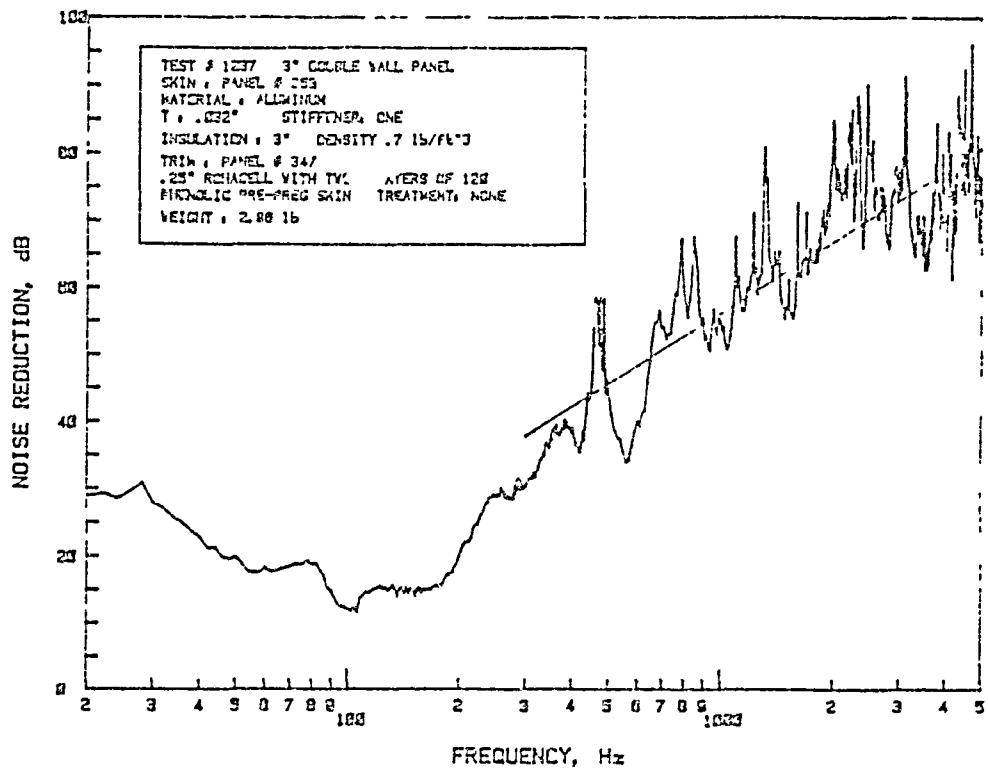

b. Fiberglass Insulation

Figure B.12: Noise Reduction Characteristics of Double-Wall Panel Made of Aluminum Skin Panel 353 and Trim Panel 347; Panel Depth 3"

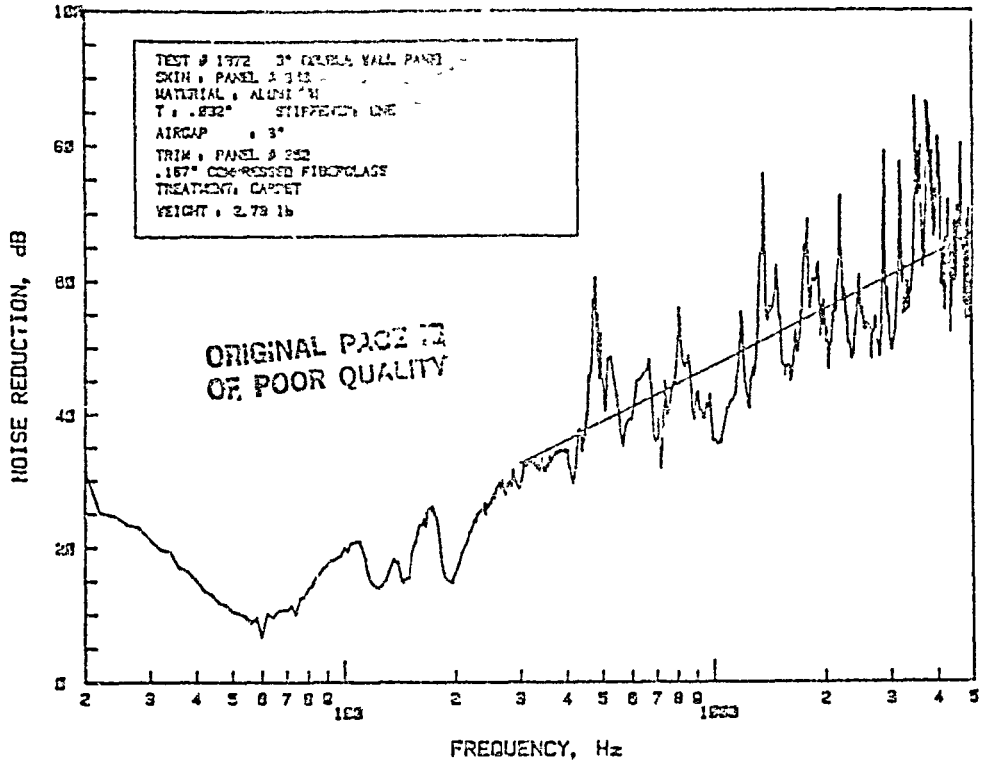

a. Airgap

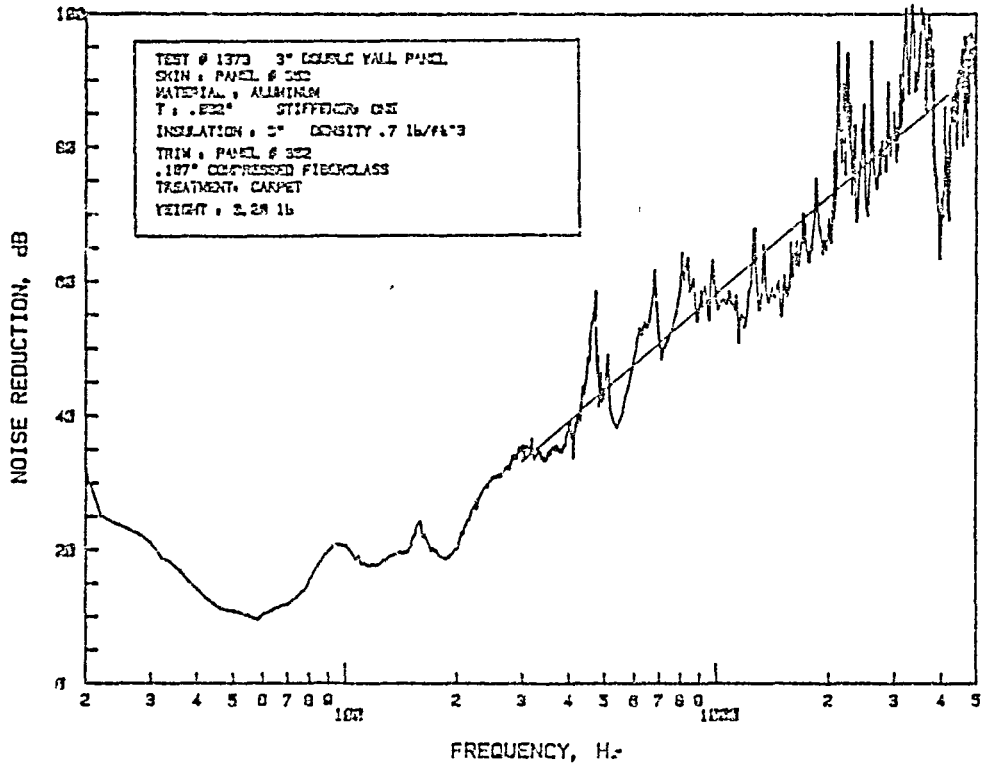

b. Fiberglass Insulation

Figure B.13: Noise Reduction Characteristics of Double-Wall Panel Made of Aluminum Skin Panel 353 and Trim Panel 352; Panel Depth 3"

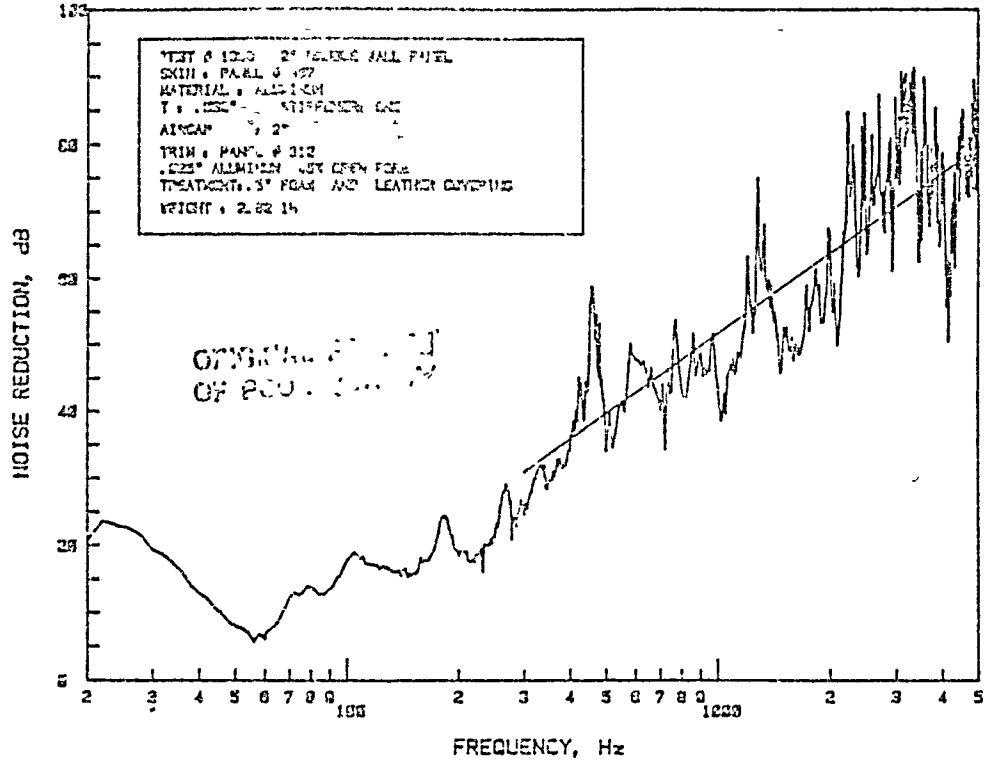

a. Airgap

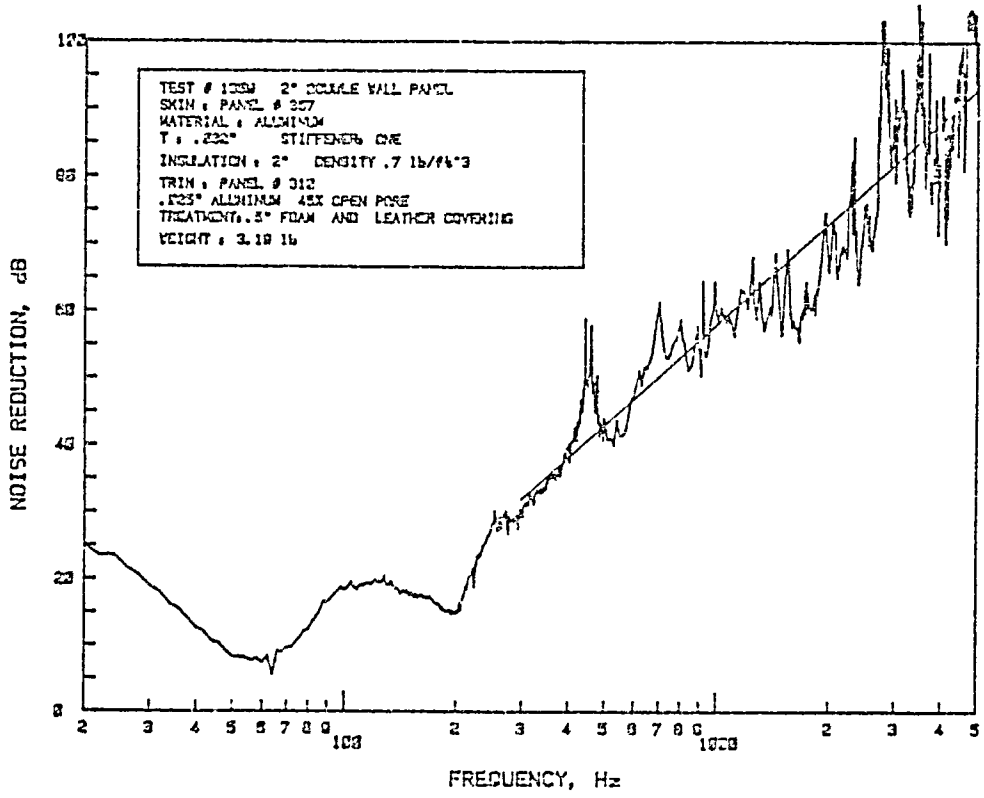

b. Fiberglass Insulation

Figure B.14: Noise Reduction Characteristics of Double-Wall Panel Made of Aluminum Skin Panel 357 and Trim Panel 312; Panel Depth 2"

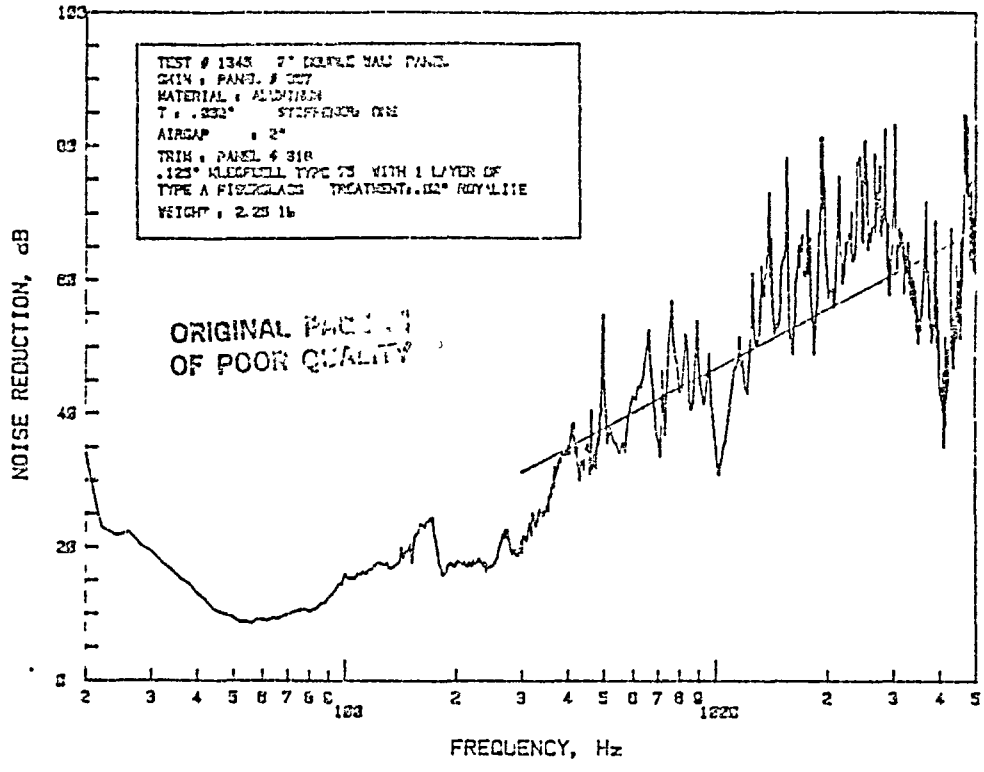

a. Airgap

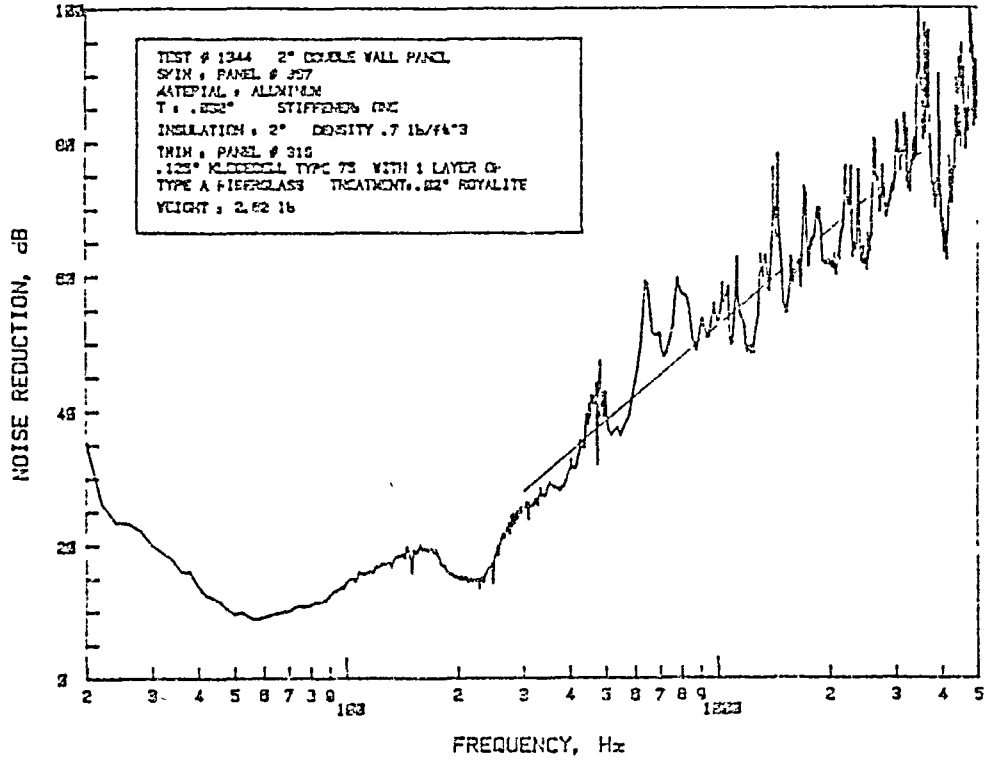

b. Fiberglass Insulation

Figure B.15: Noise Reduction Characteristics of Double-Wall Panel Made of Aluminum Skin Panel 357 and Trim Panel 318; Panel Depth 2"

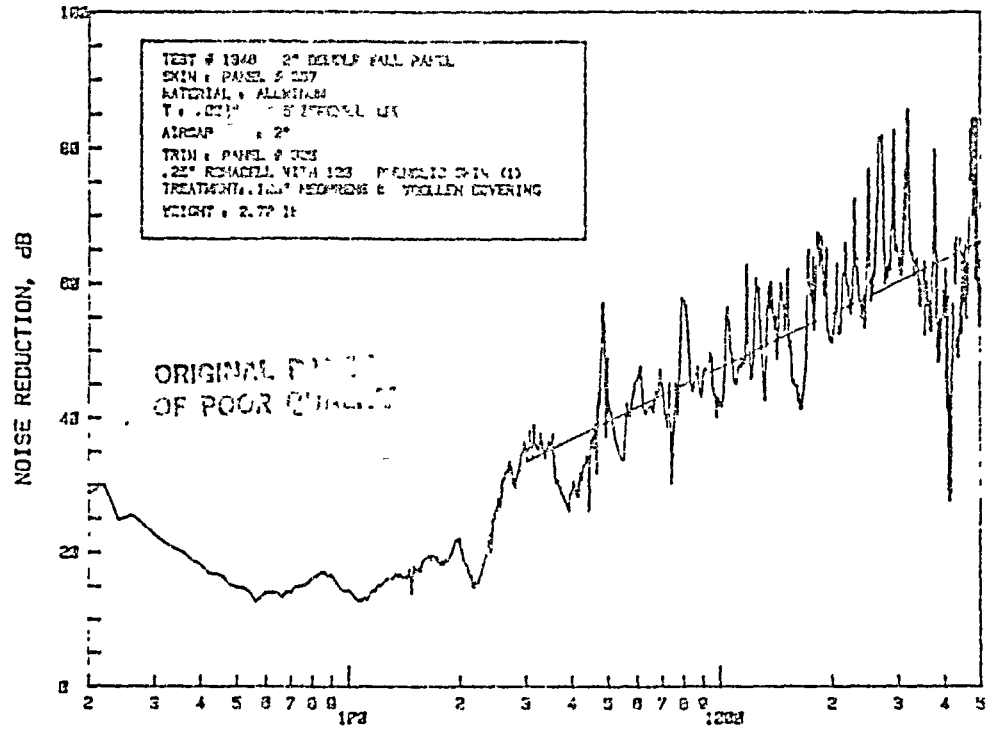

a. Airgap

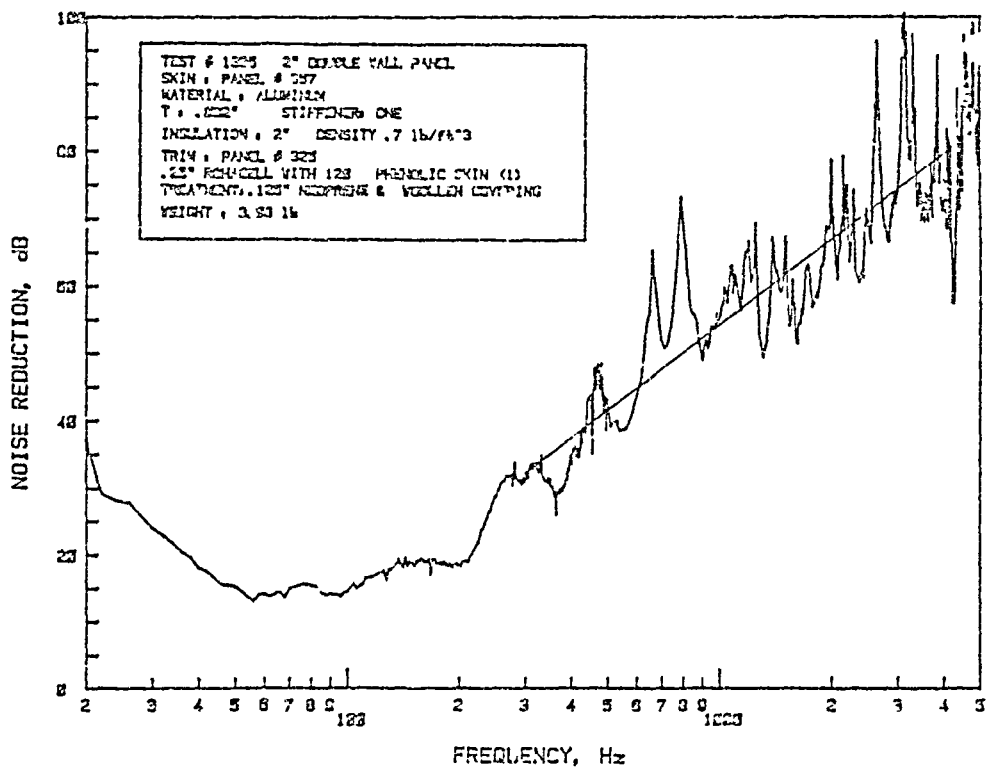

b. Fiberglass Insulation

Figure B.16: Noise Reduction Characteristics of Double-Wall Panel Made of Aluminum Skin Panel 357 and Trim Panel 325; Panel Depth 2"

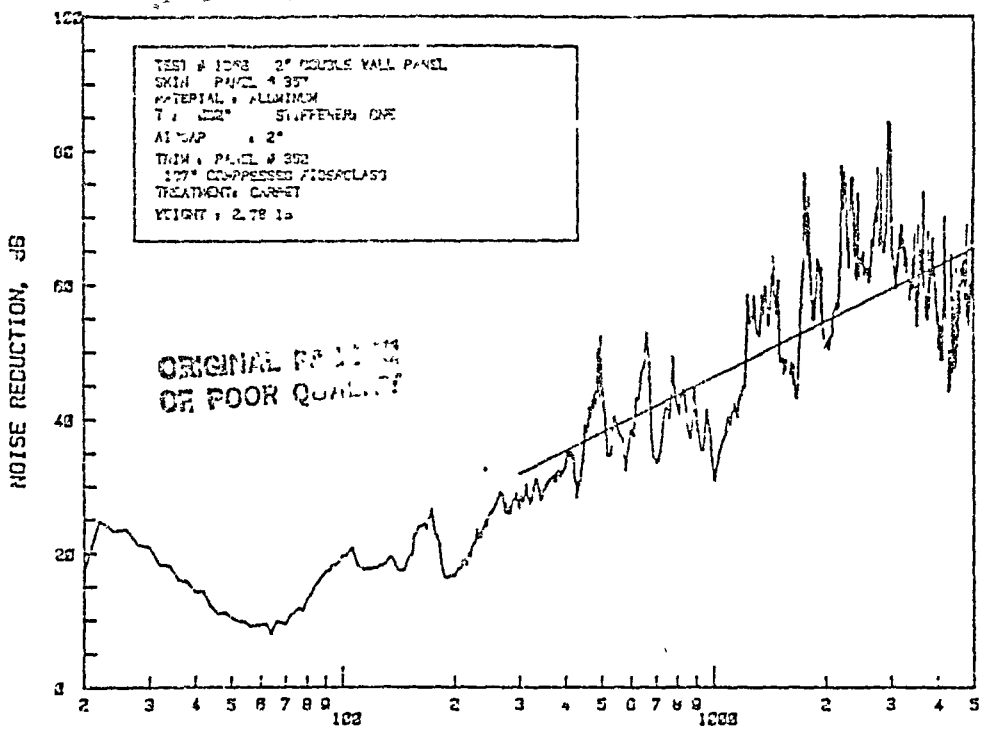

a. Airgap

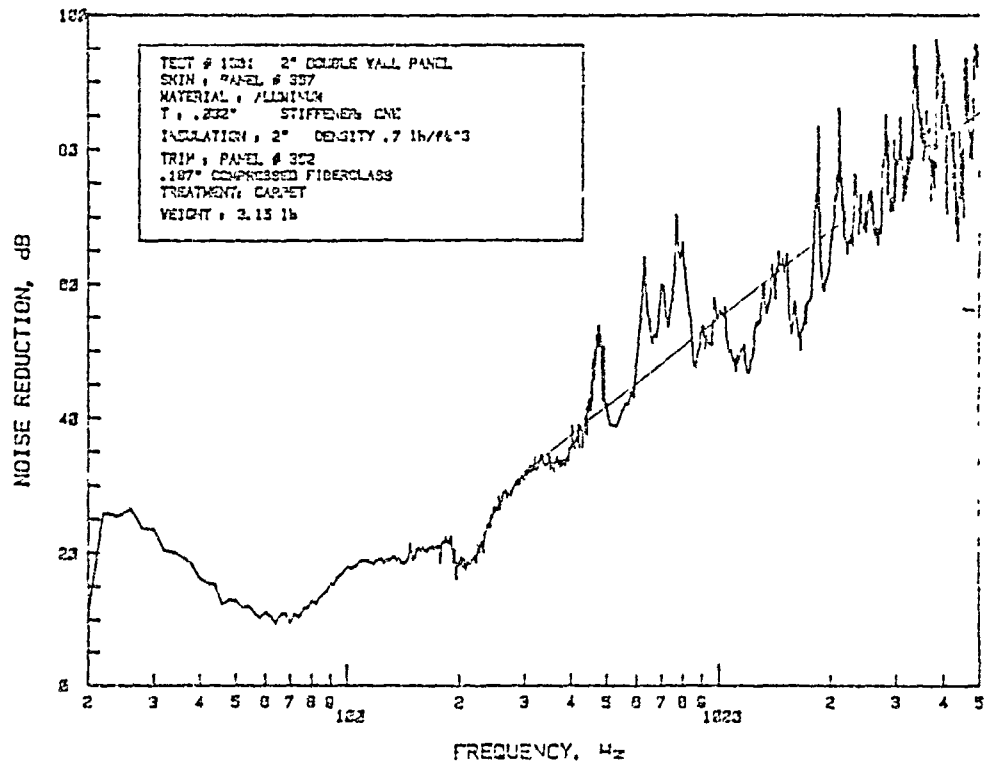

b. Fiberglass Insulation

Figure B.17: Noise Reduction Characteristics of Double-Wall Panel Made of Aluminum Skin Panel 357 and Trim Panel 352; Panel Depth 2"

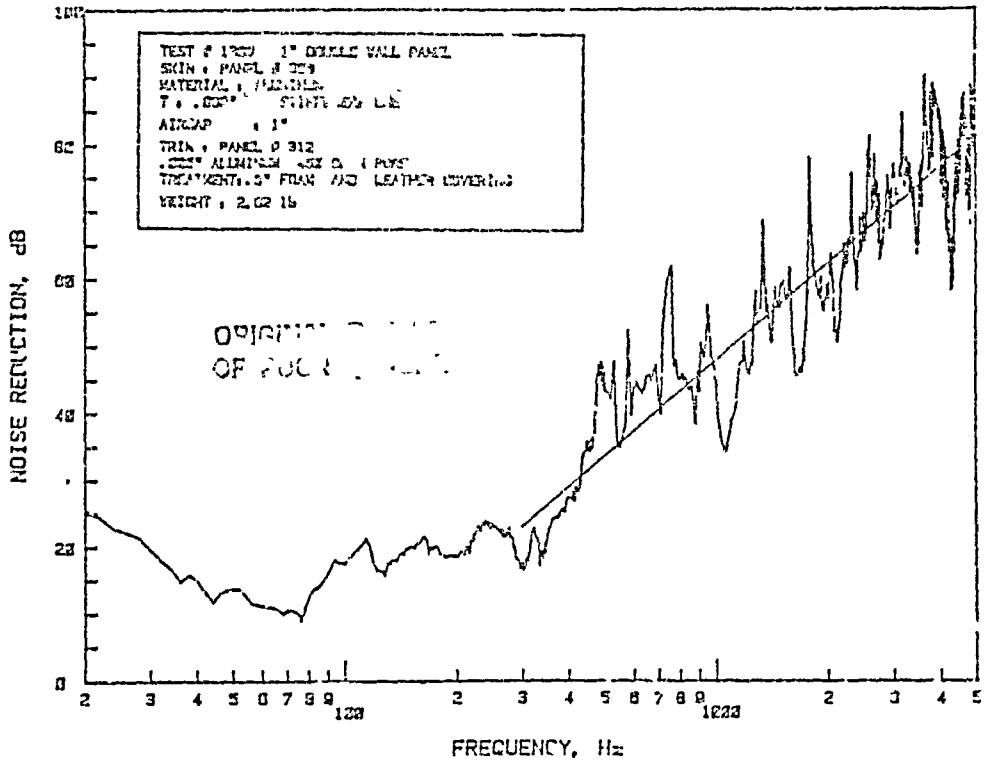

a. Airgap

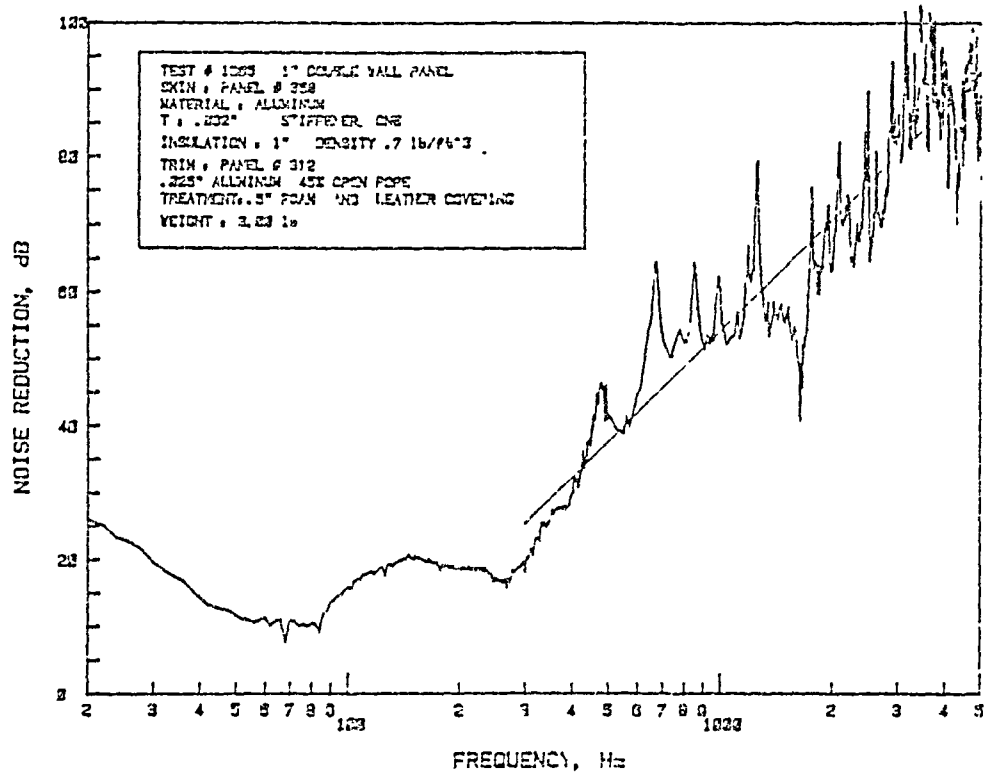

b. Fiberglass Insulation

Figure B.18: Noise Reduction Characteristics of Double-Wall Panel Made of Aluminum Skin Panel 358 and Trim Panel 312; Panel Depth 1"

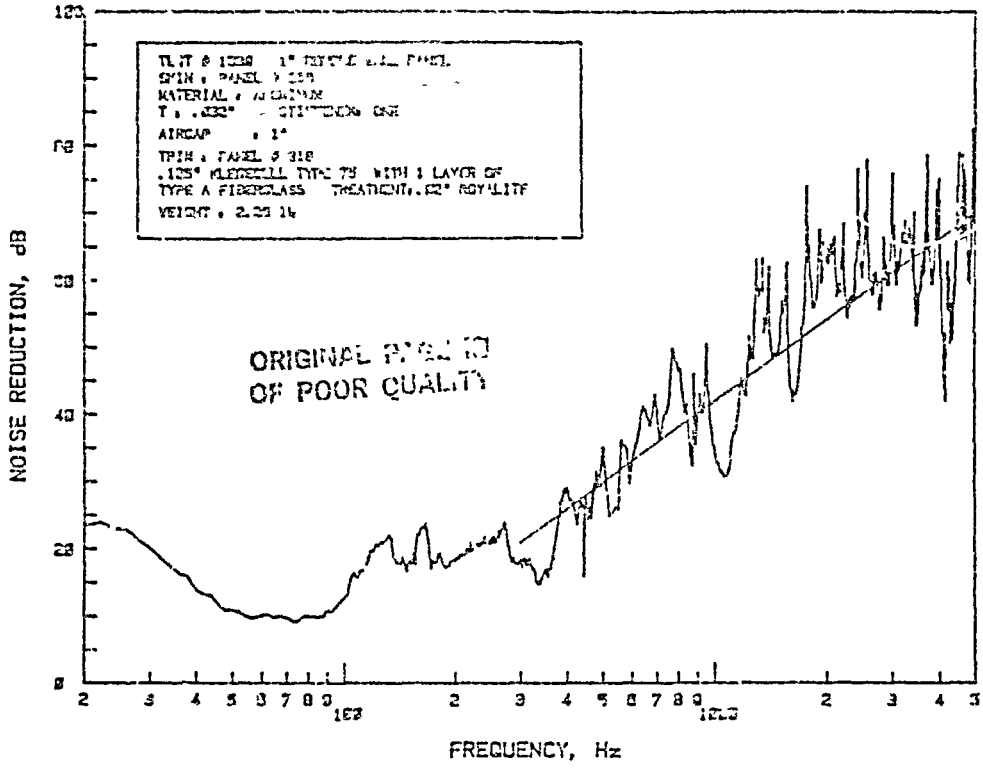

a. Airgap

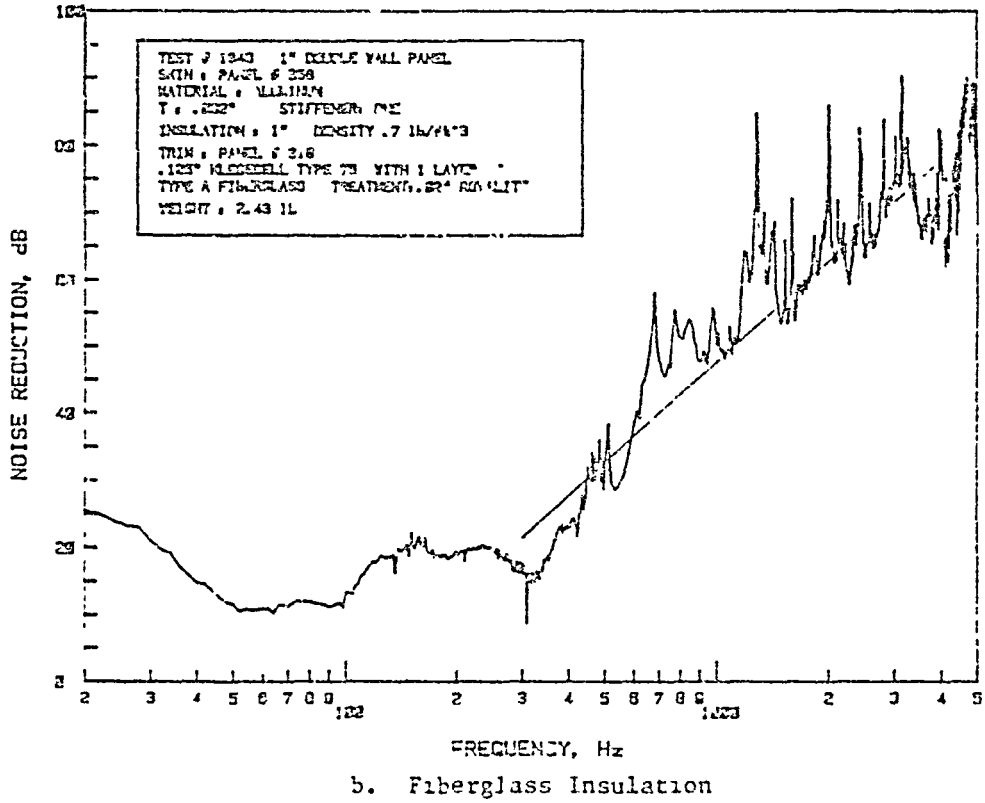

b. Fiberglass Insulation

Figure B.19: Noise Reduction Characteristics of Double-Wall Panel Made of Aluminum Skin Panel 353 and Trim Panel 318; Panel Depth 1"

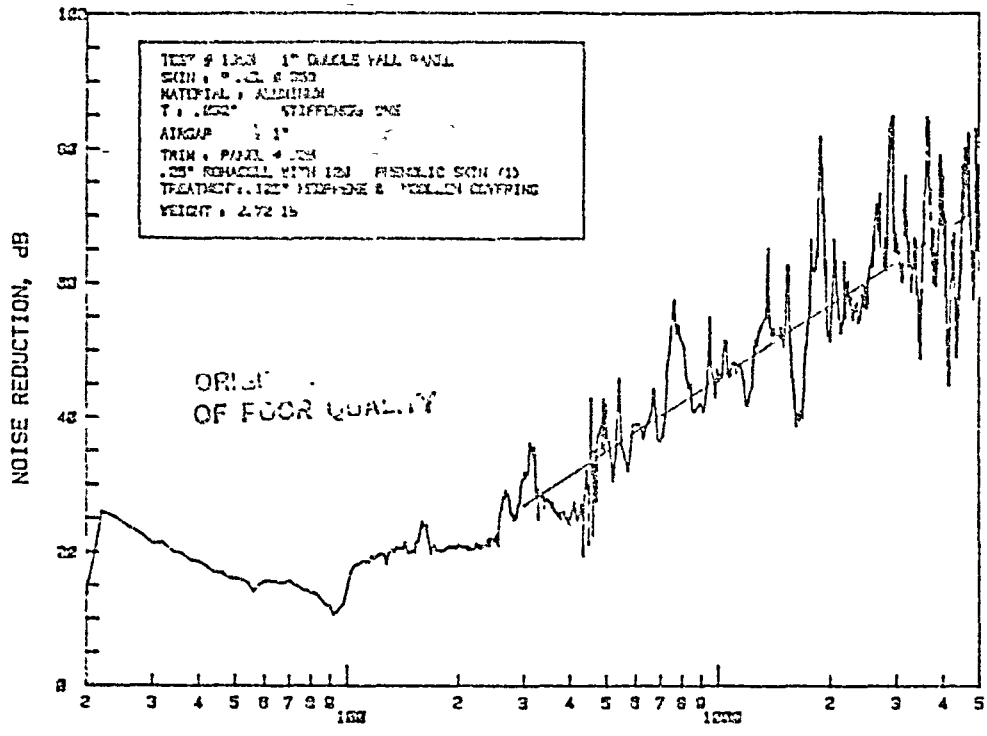

a. Airgap

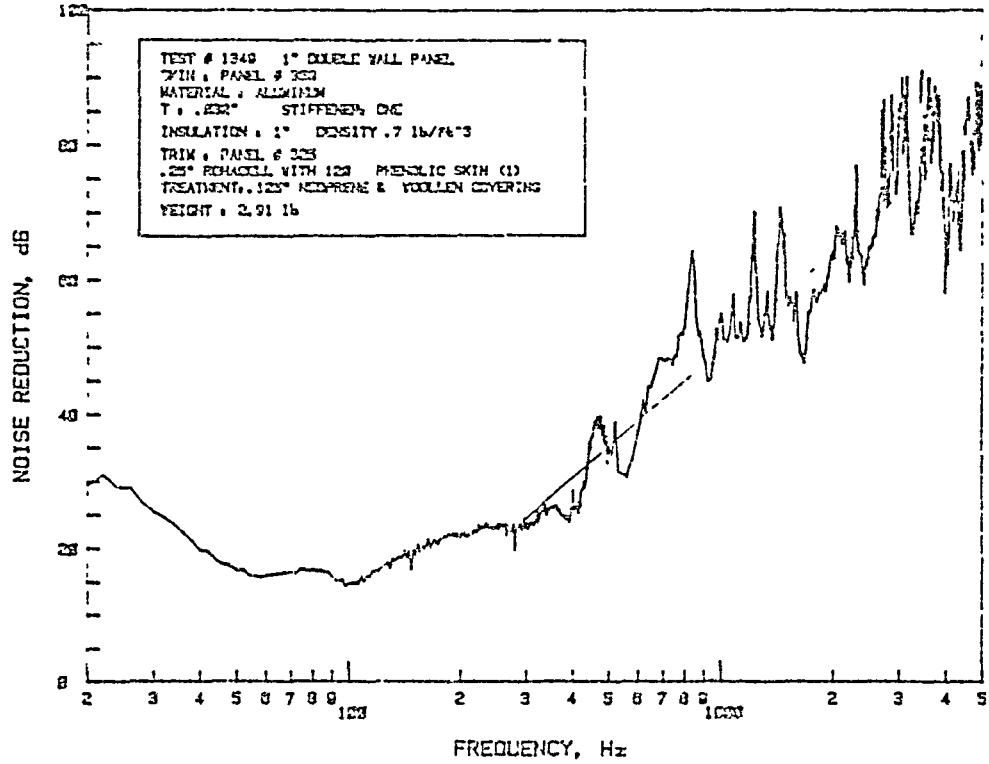

b. Fiberglass Insulation

Figure B.20: Noise Reduction Characteristics of Double-Wall Panel Made of Aluminum Skin Panel 358 and Trim Panel 325; Panel Depth 1"

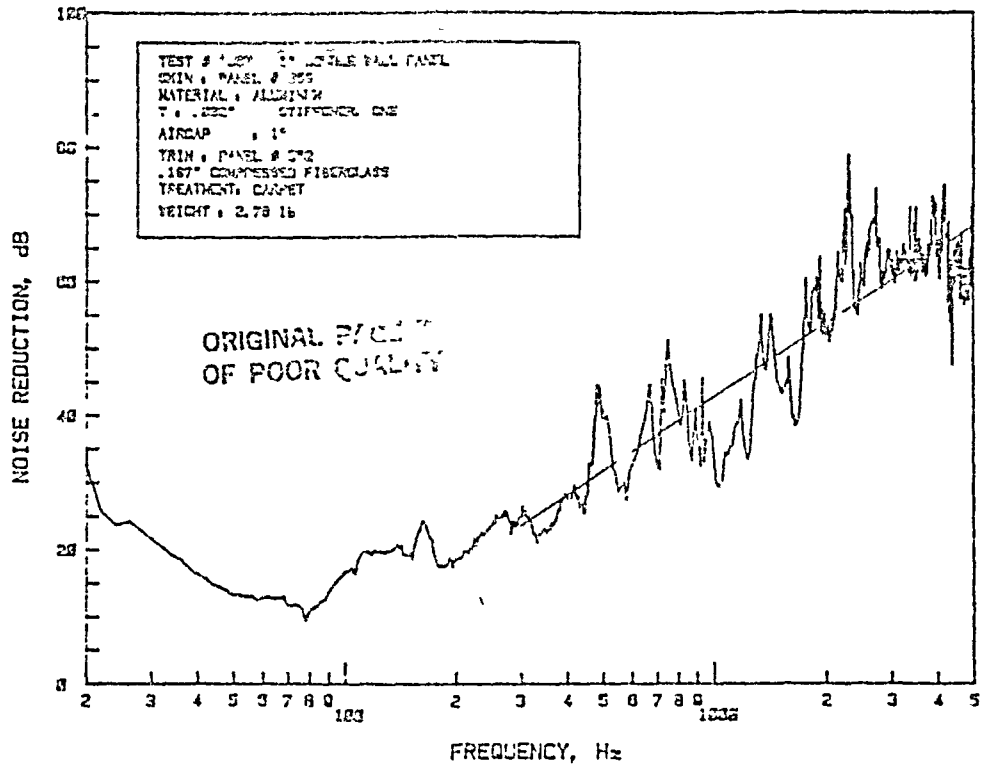

a. Airgap

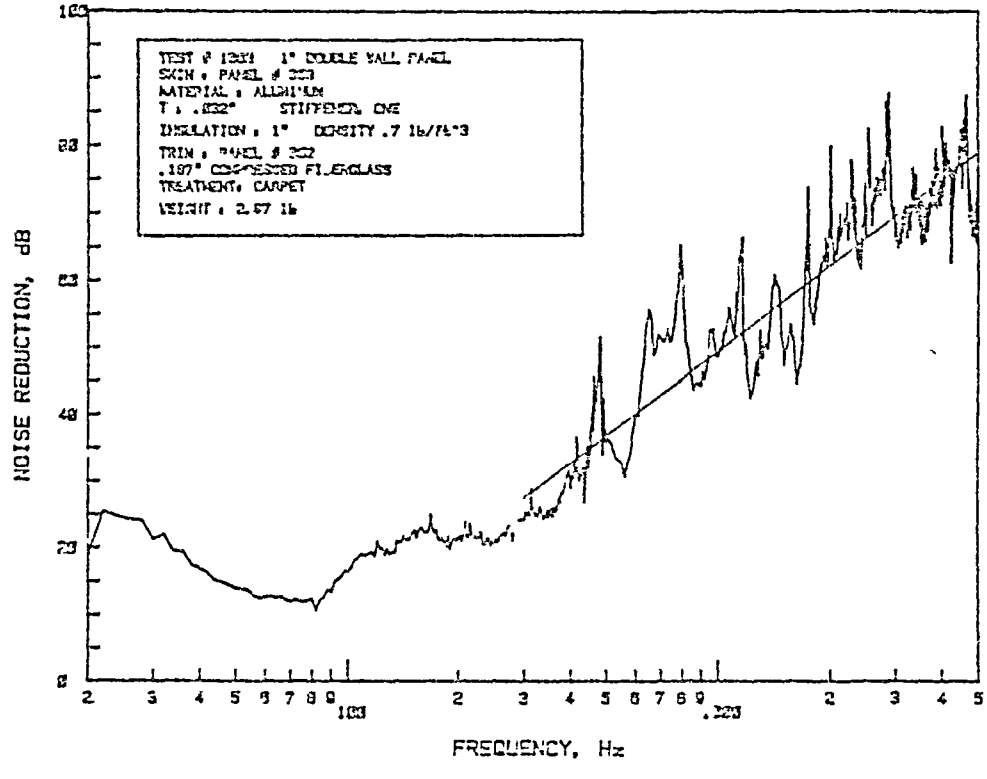

b. Fiberglass Insulation

Figure B.21: Noise Reduction Characteristics of Double-Wall Panel Made of Aluminum Skin Panel 353 and Trim Panel 352; Panel Depth 1"

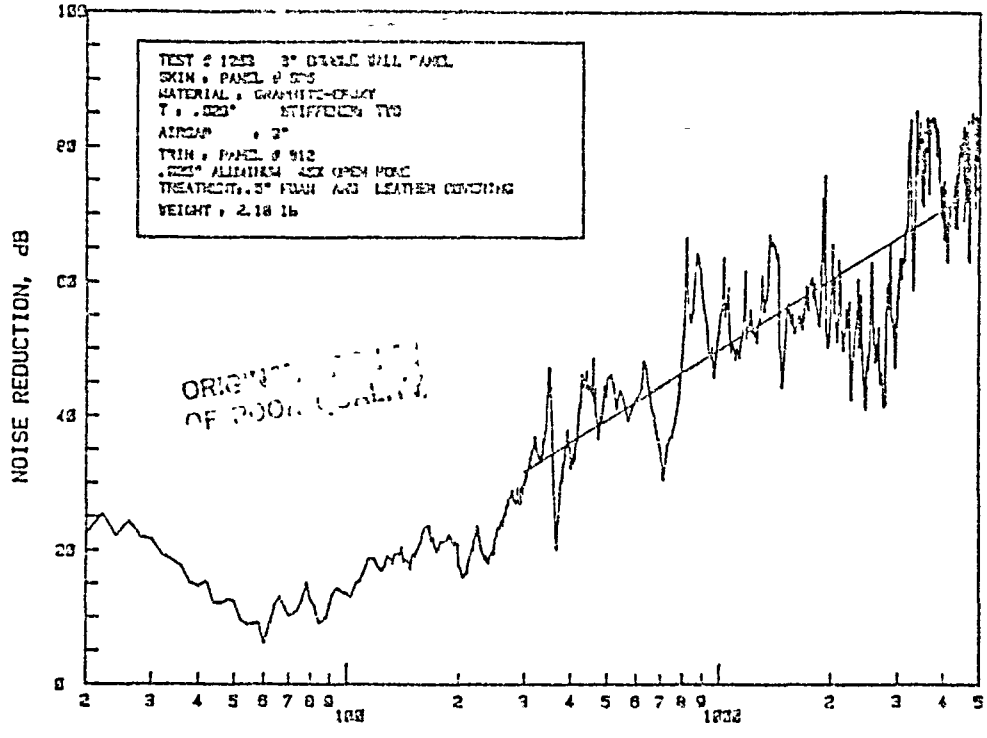

a. Airgap

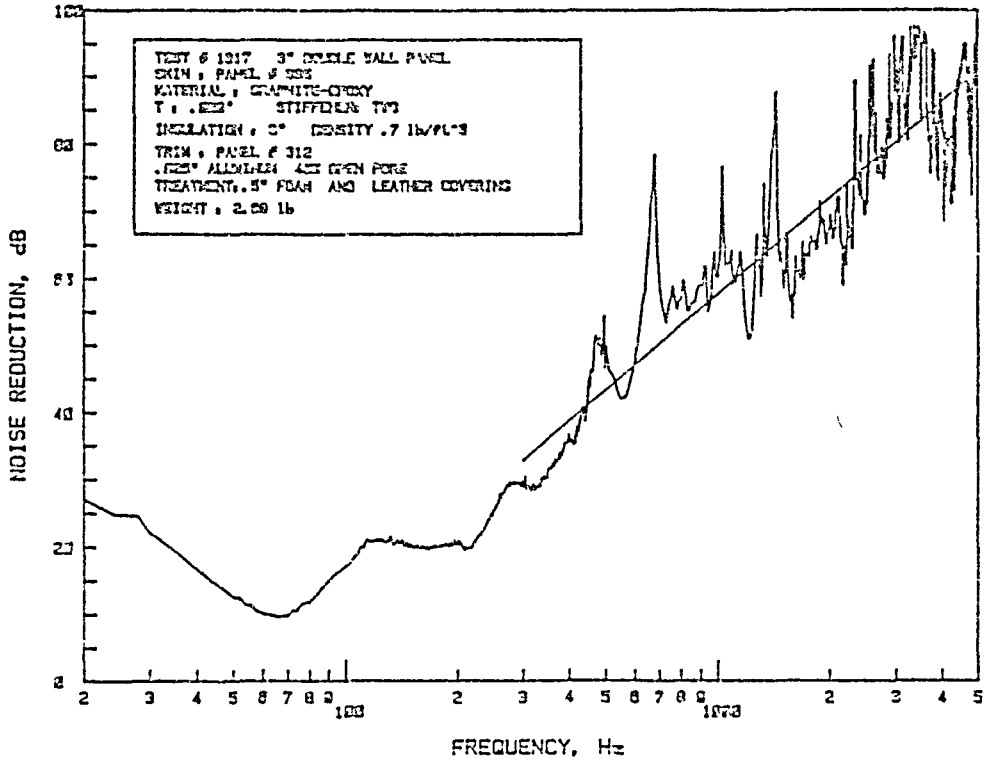

b. Fiberglass Insulation

Figure B.22: Noise Reduction Characteristics of Double-Wall Panel Made of Graphite-Epoxy Skin Panel 335 and Trim Panel 312; Panel Depth 3"

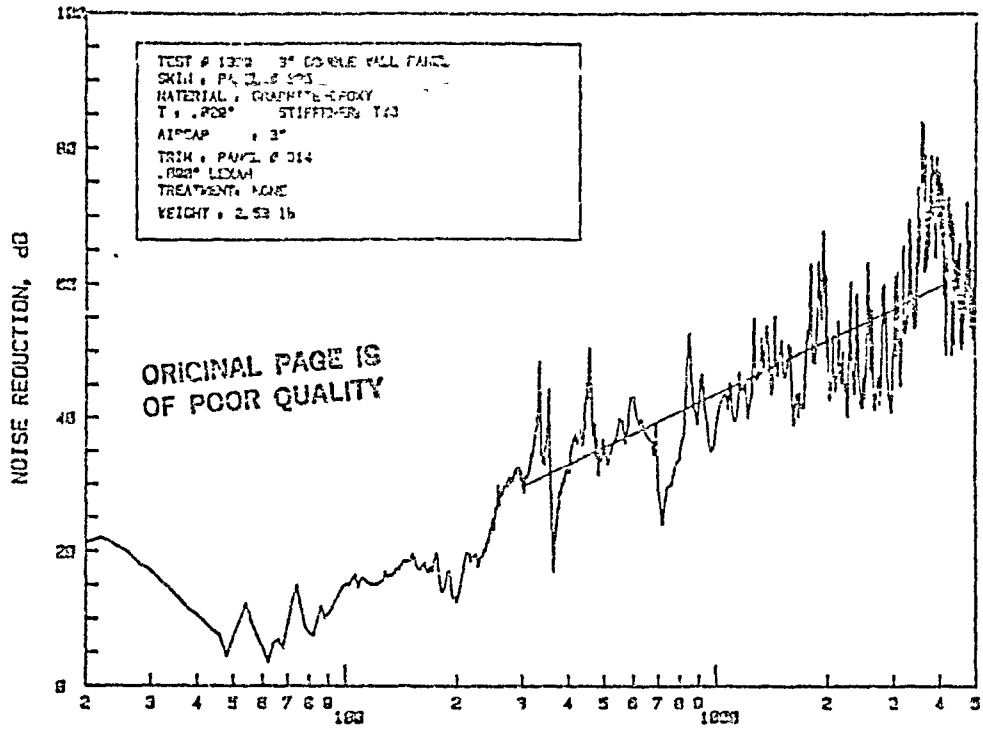

a. Airgap

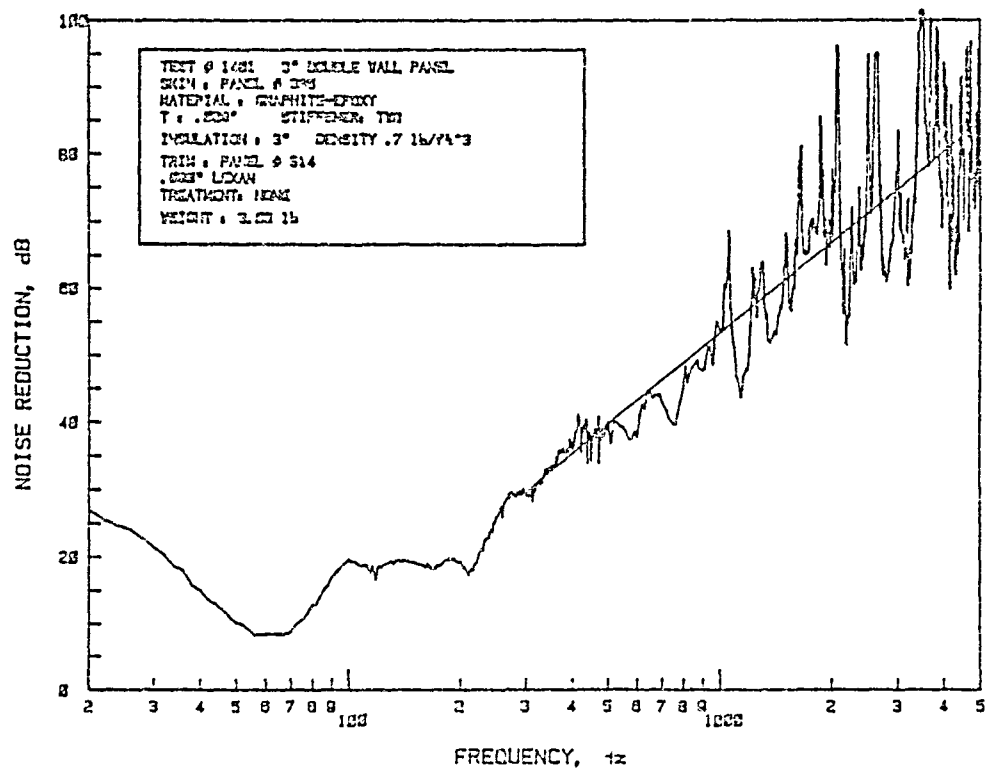

b. Fiberglass Insulation

Figure B.23: Noise Reduction Characteristics of Double-Wall Panel Made of Graphite-Epoxy Skin Panel 335 and Trim Panel 314; Panel Depth 3"

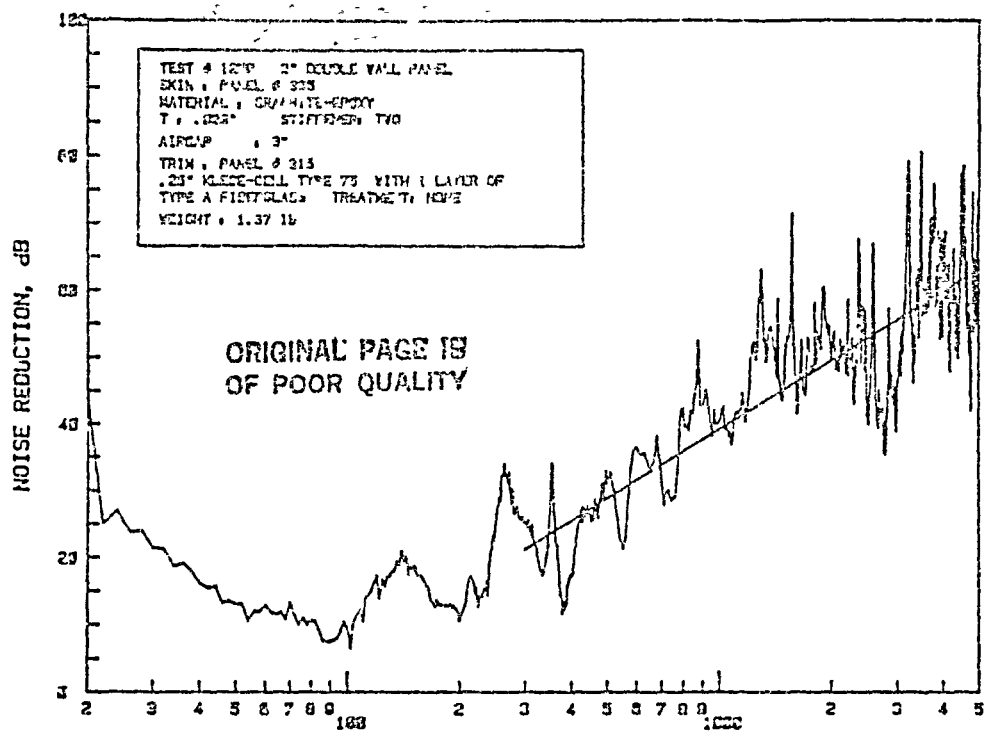

a. Airgap

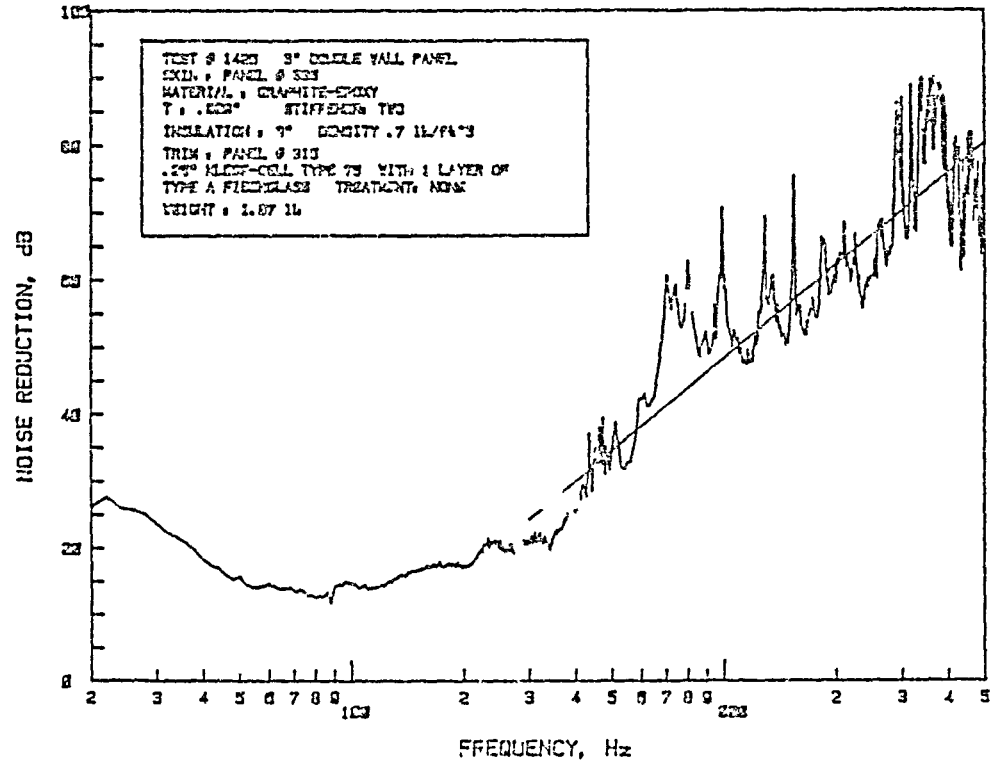

b. Fiberglass Insulation

Figure B.24· Noise Reduction Characteristics of Double-Wall Panel Made of Graphite-Epoxy Skin Panel 335 and Trim Panel 315; Panel Depth 3"

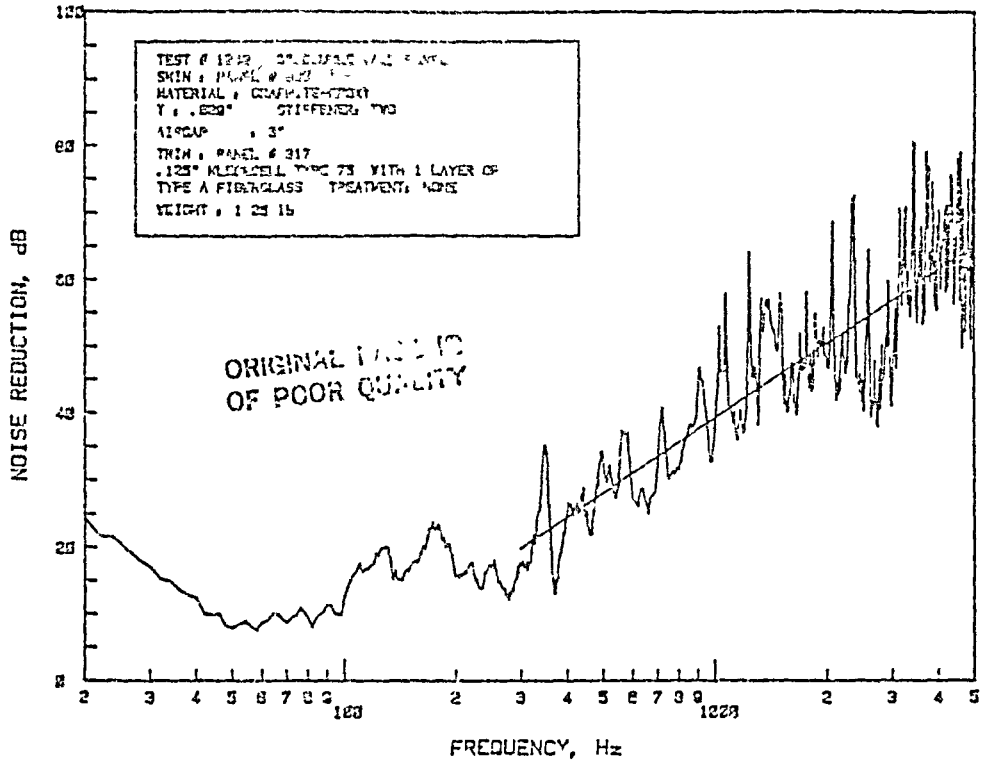

a. Airgap

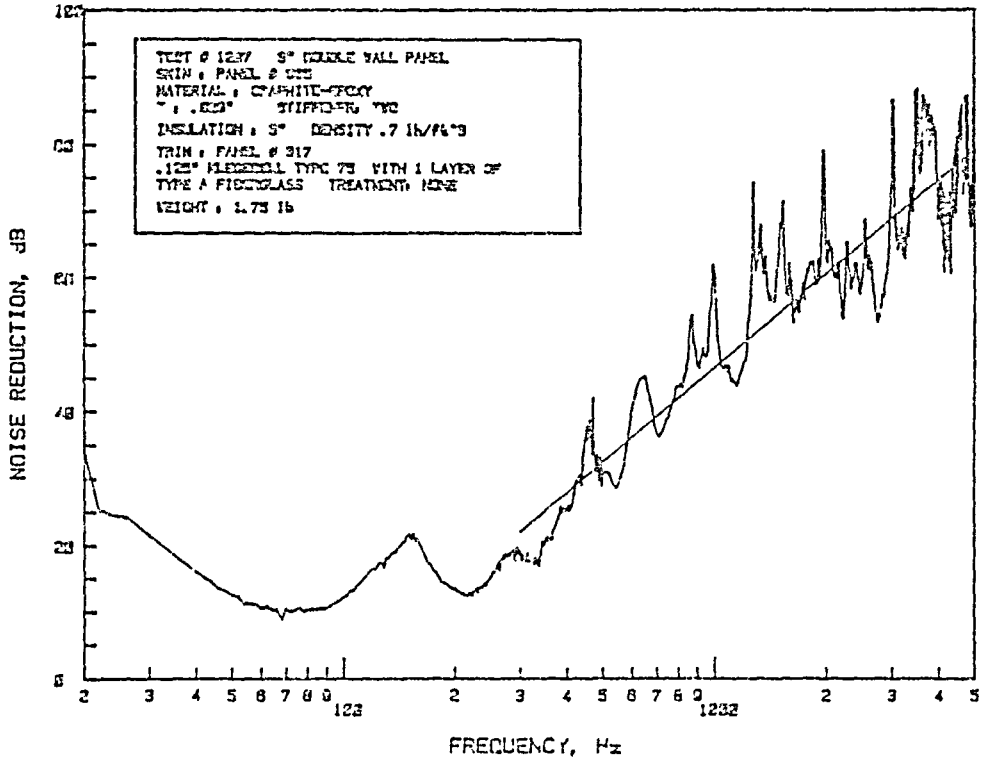

b. Fiberglass Insulation

Figure B.25: Noise Reduction Characteristics of Double-Wall Panel Made of Graphite-Epoxy Skin Panel 335 and Trim Panel 317. Panel Depth 3"

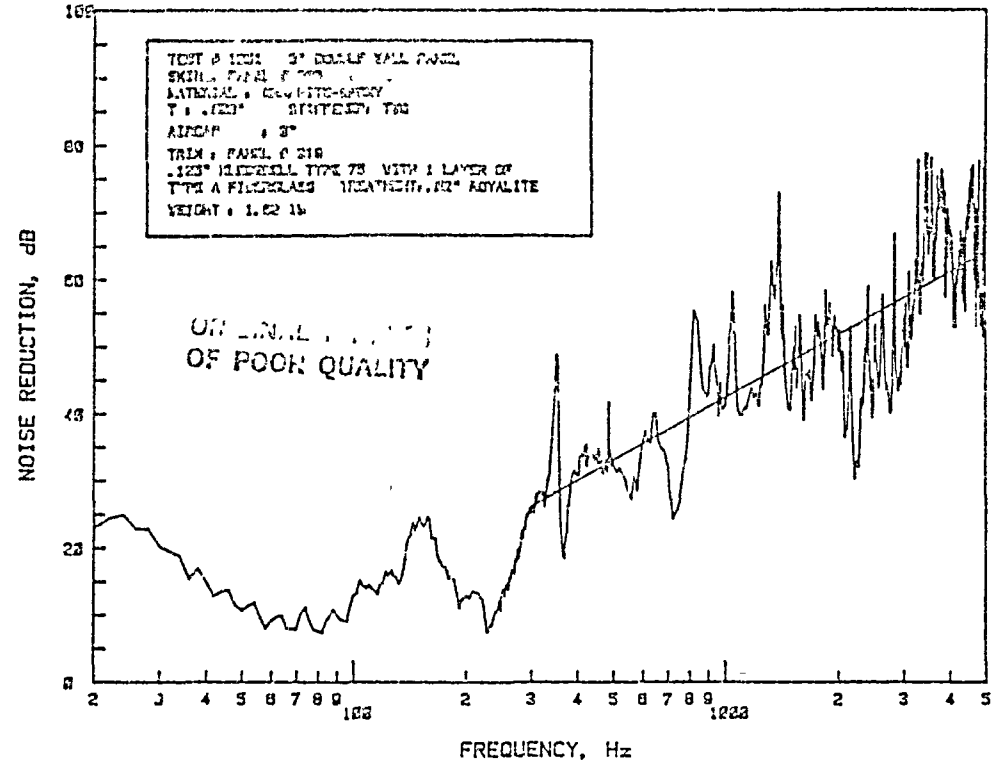

a. Airgap

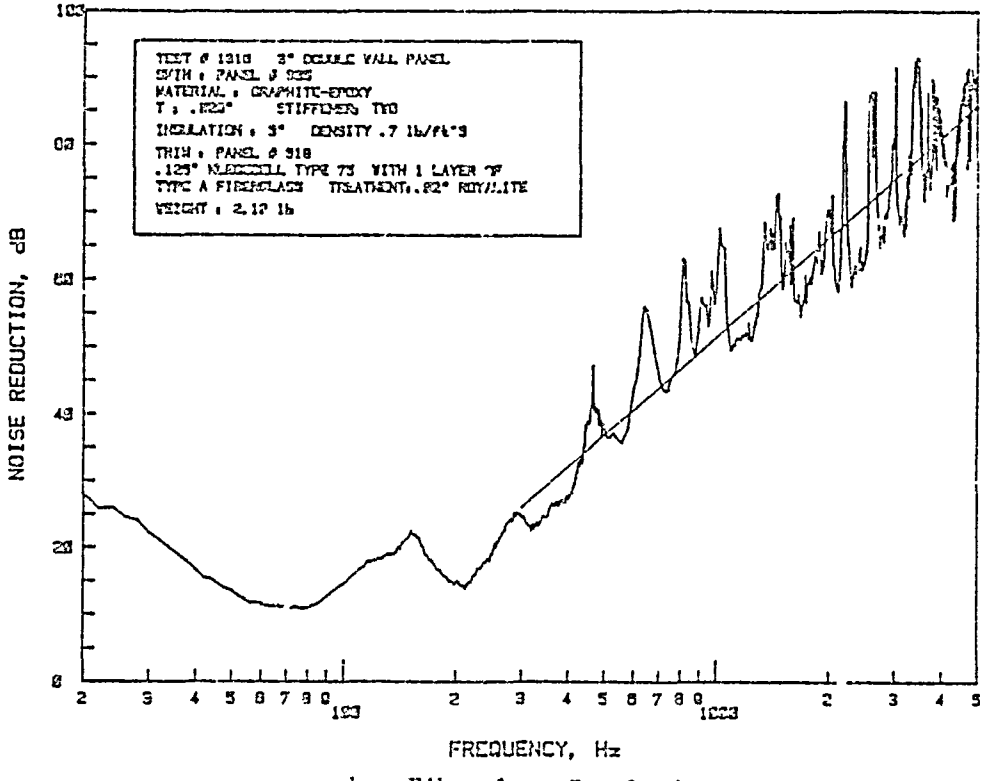

b. Fiberglass Insulation

Figure B.26: Noise Reduction Characteristics of Double-Wall Panel Made of Graphite-Epoxy Skin Panel 335 and Trim Panel 318; Panel Depth 3"

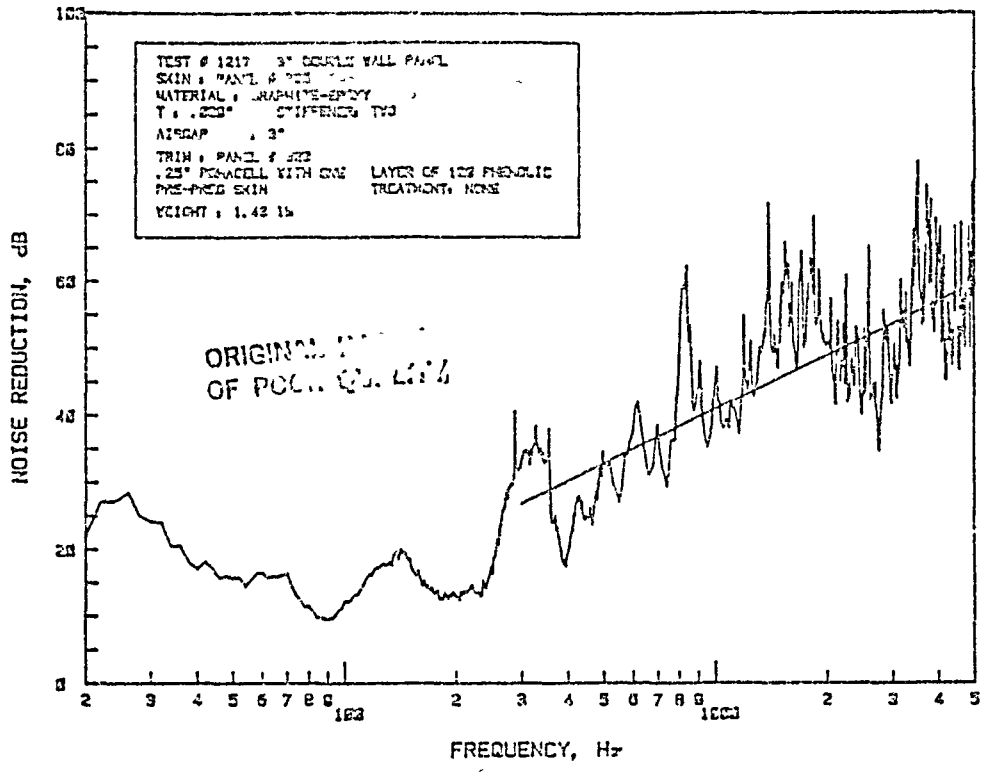

a. Airgap

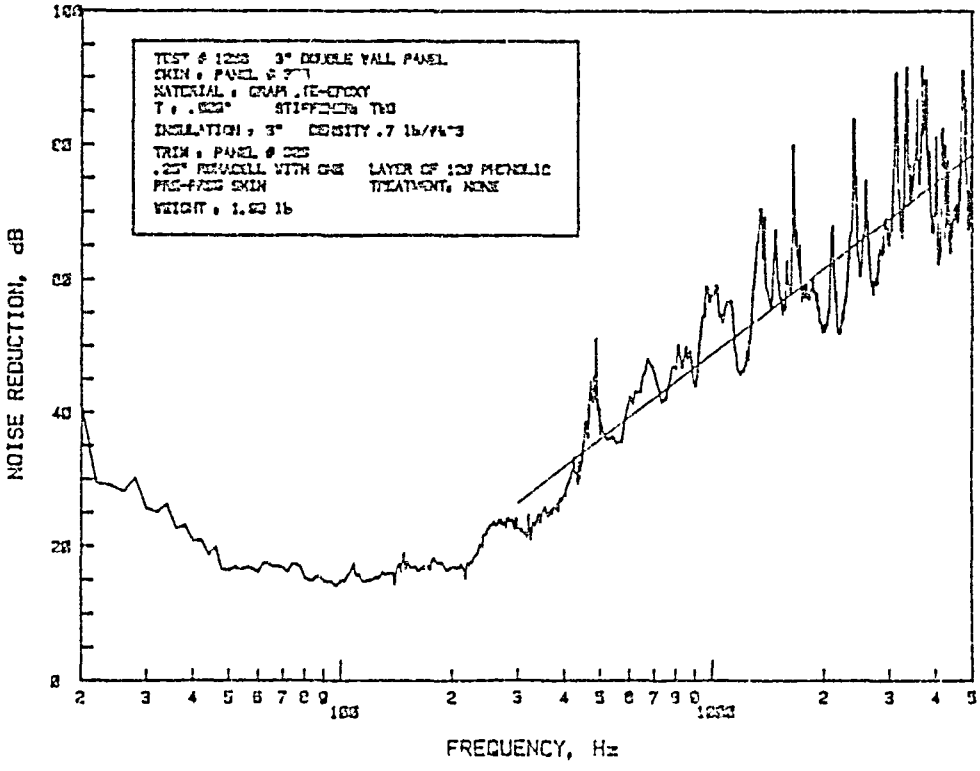

b. Fiberglass Insulation

Figure B.27: Noise Reduction Characteristics of Double-Wall Panel Made of Graphite-Epoxy Skin Panel 335 and Trim Panel 323; Panel Depth 3"

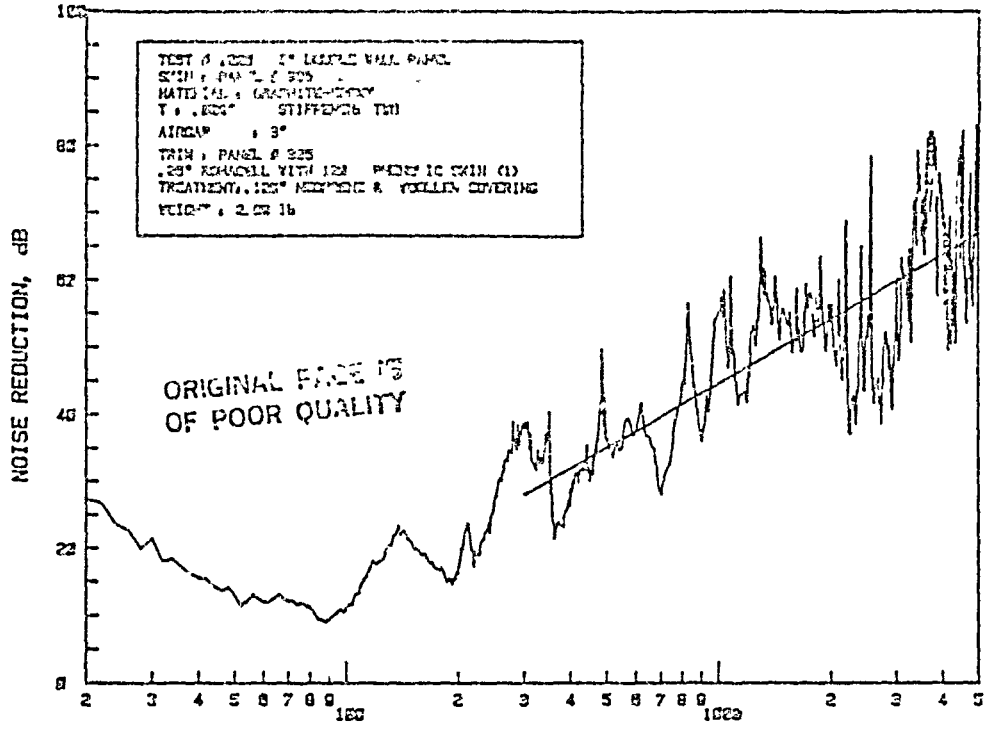

a. Airgap

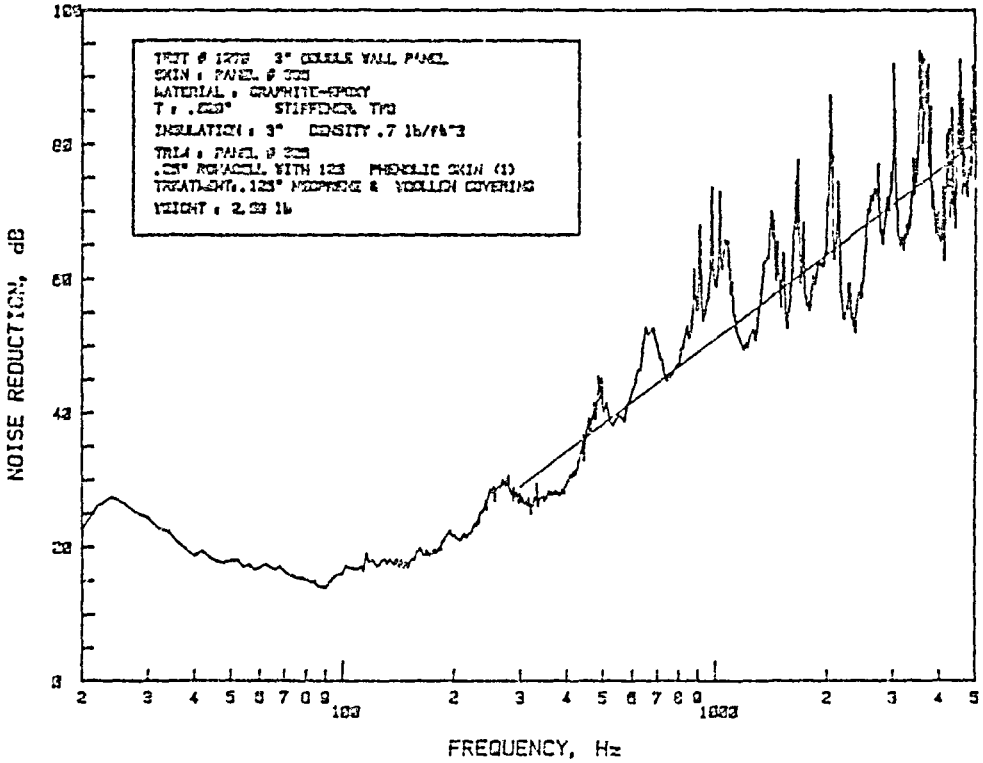

b. Fiberglass Insulation

Figure B.28: Noise Reduction Characteristics of Double-Wall Panel Made of Graphite-Epoxy Skin Panel 335 and Trim Panel 325; Panel Depth 3"

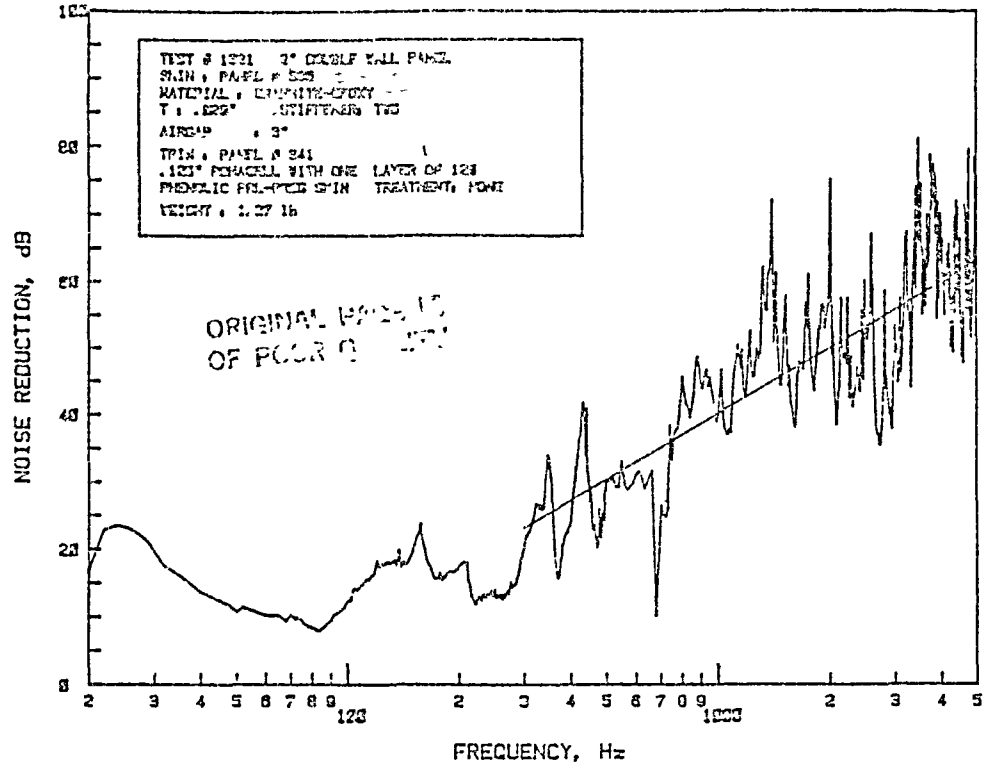

a. Airgap

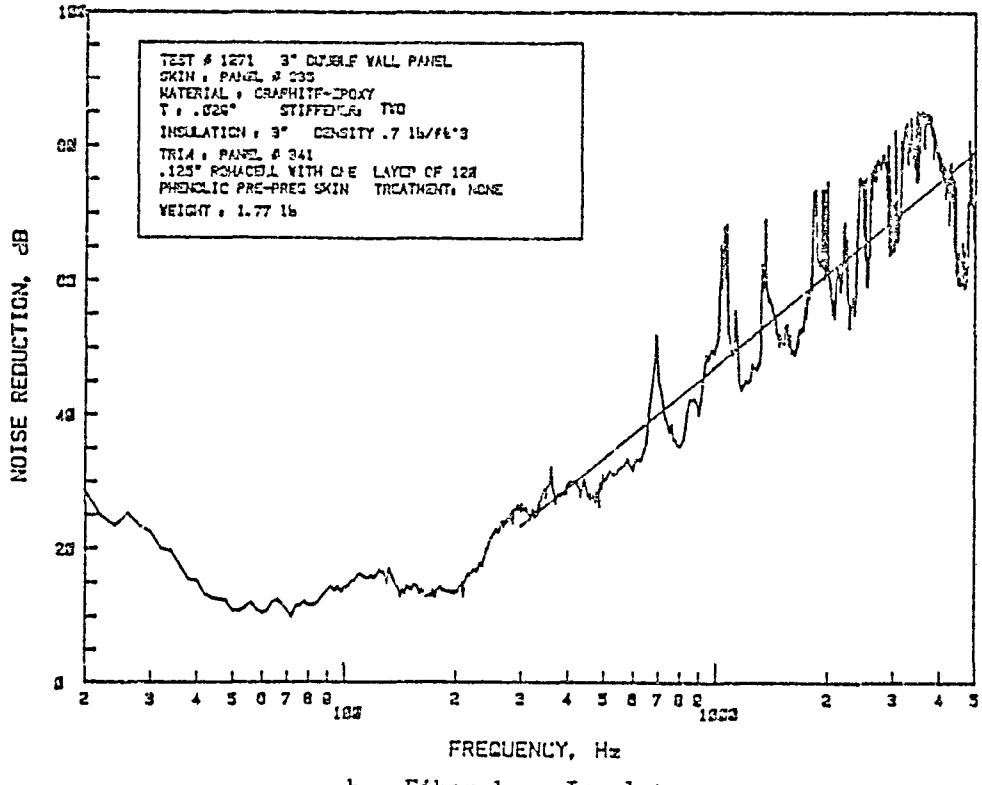

b. Fiberglass Insulation

Figure B.29: Noise Reduction Characteristics of Double-Wall Panel Made of Graphite-Epoxy Skin Panel 335 and Trim Panel 341, Panel Depth 3"

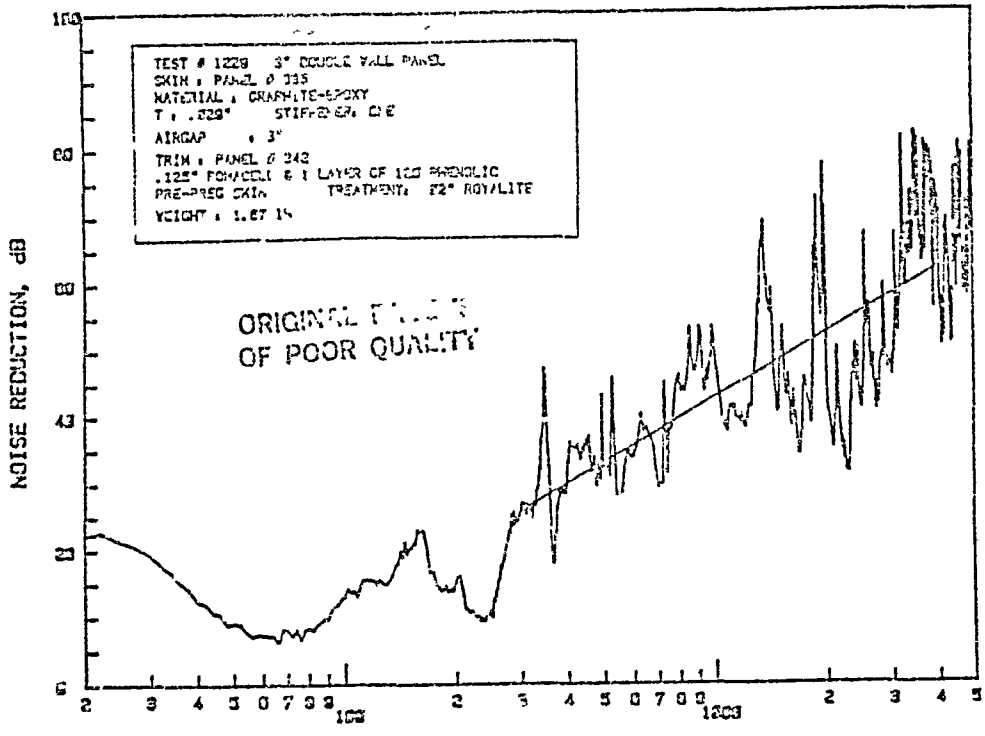

a. Airgap

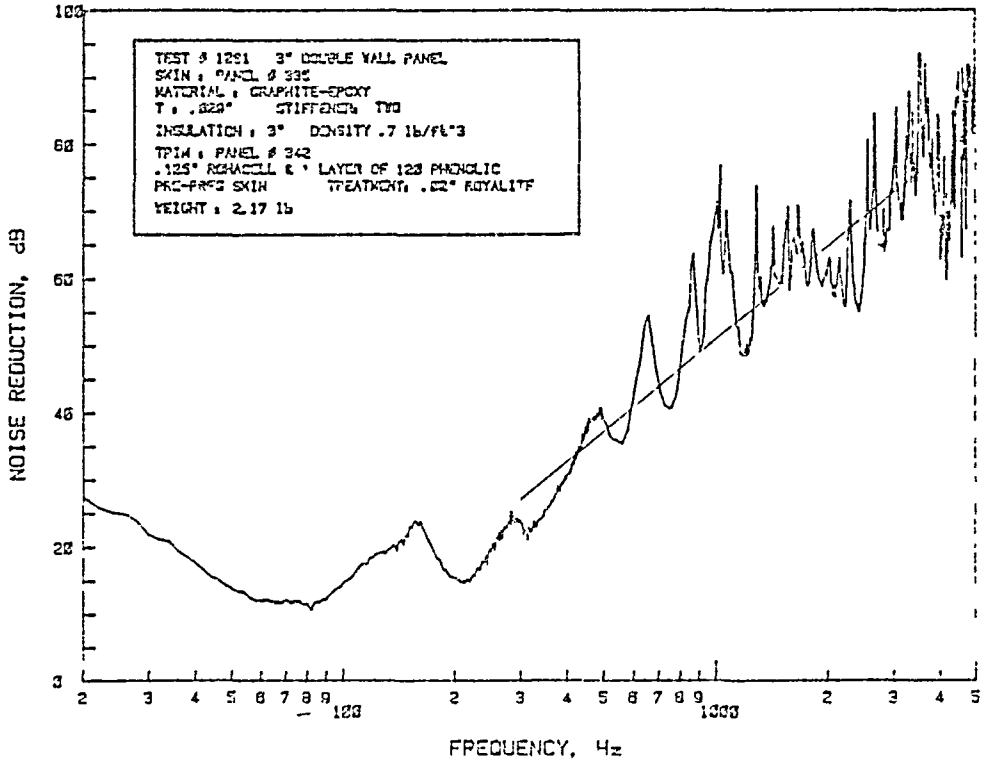

b. Fiberglass Insulation

Figure B.30: Noise Reduction Characteristics of Double-Wall Panel Made of Graphite-Epoxy Skin Panel 335 and Trim Panel 342; Panel Depth 3"

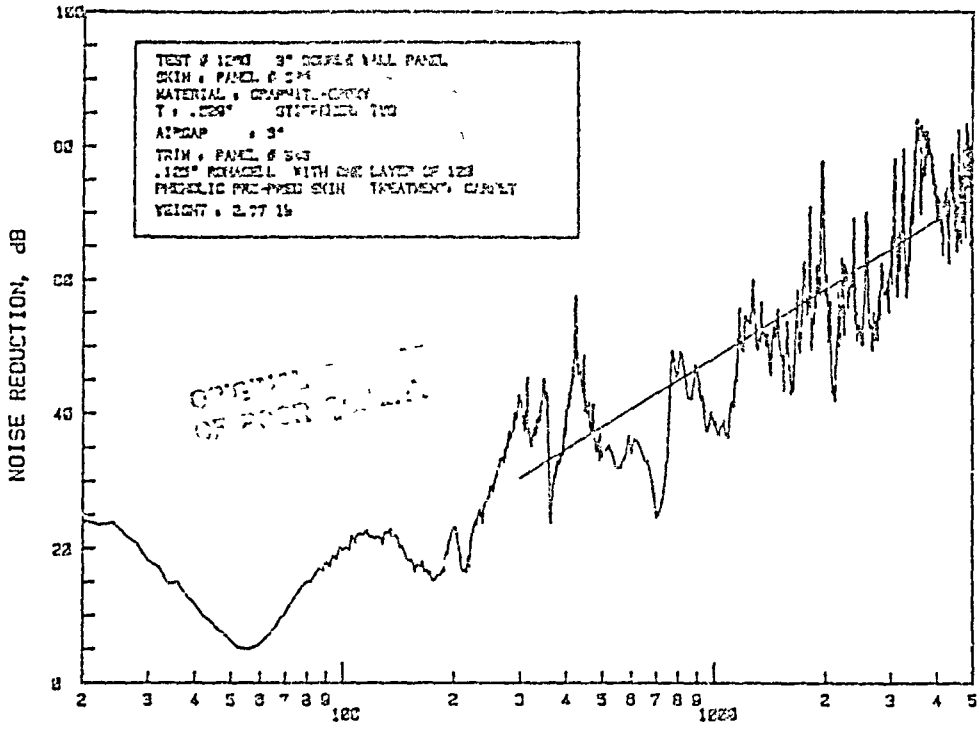

a. Airgap

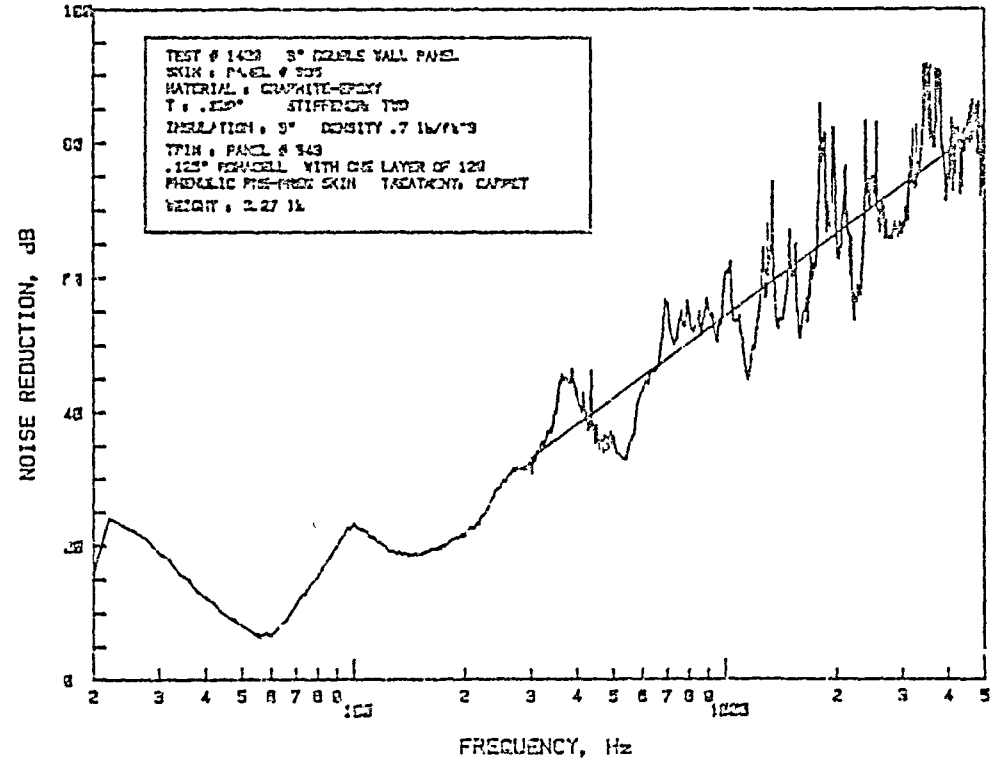

b. Fiberglass Insulation

Fibure B.31: Noise Reduction Characteristics of Double-Wall Panel Made of Graphite-Epoxy Skin Panel 335 and Trim Panel 343; Panel Depth 3"

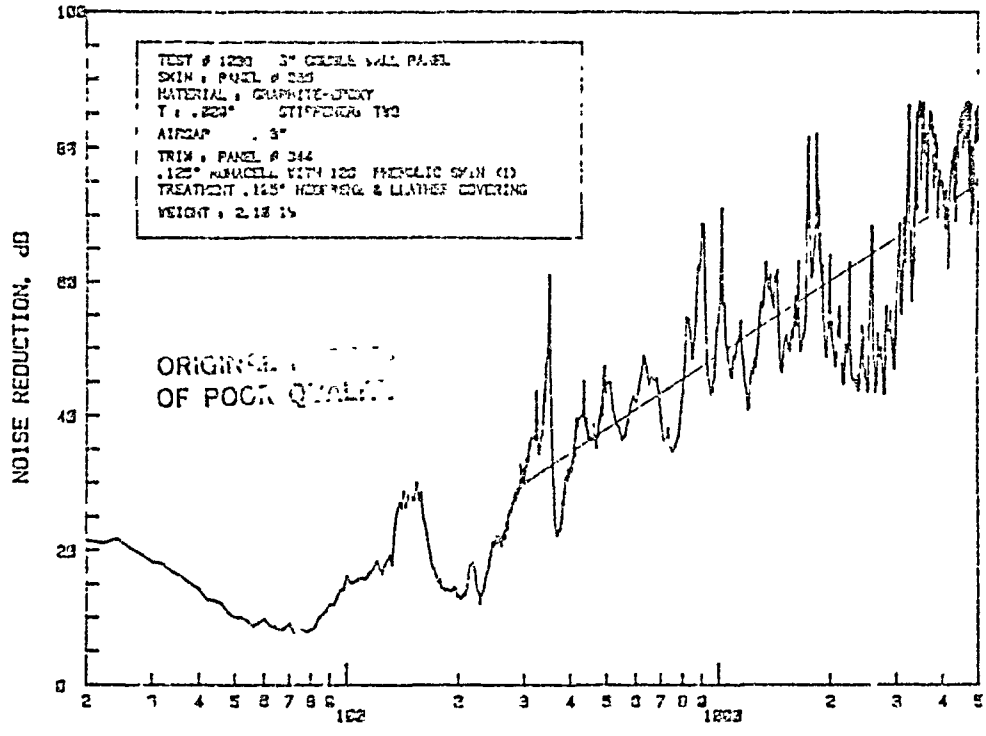

a. Airgap

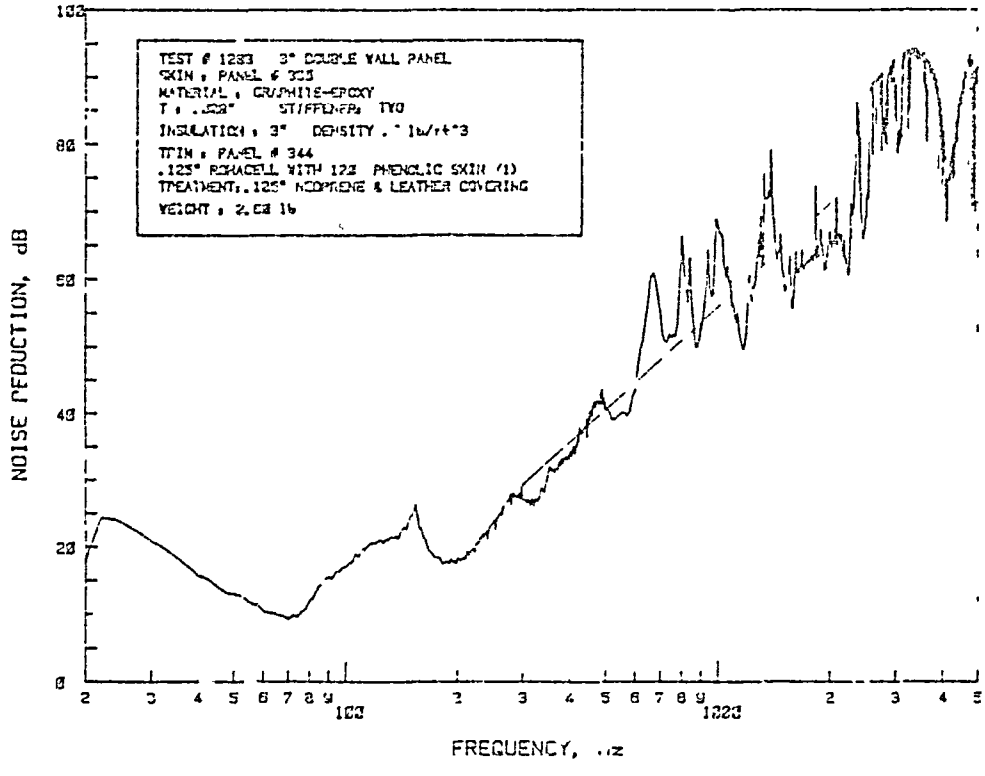

b. Fiberglass Insulation

Figure B.32: Noise Reduction Characteristics of Double-Wall Panel Made of Graphite-Epoxy Skin Panel 335 and Trim Panel 344; Panel Depth 3"

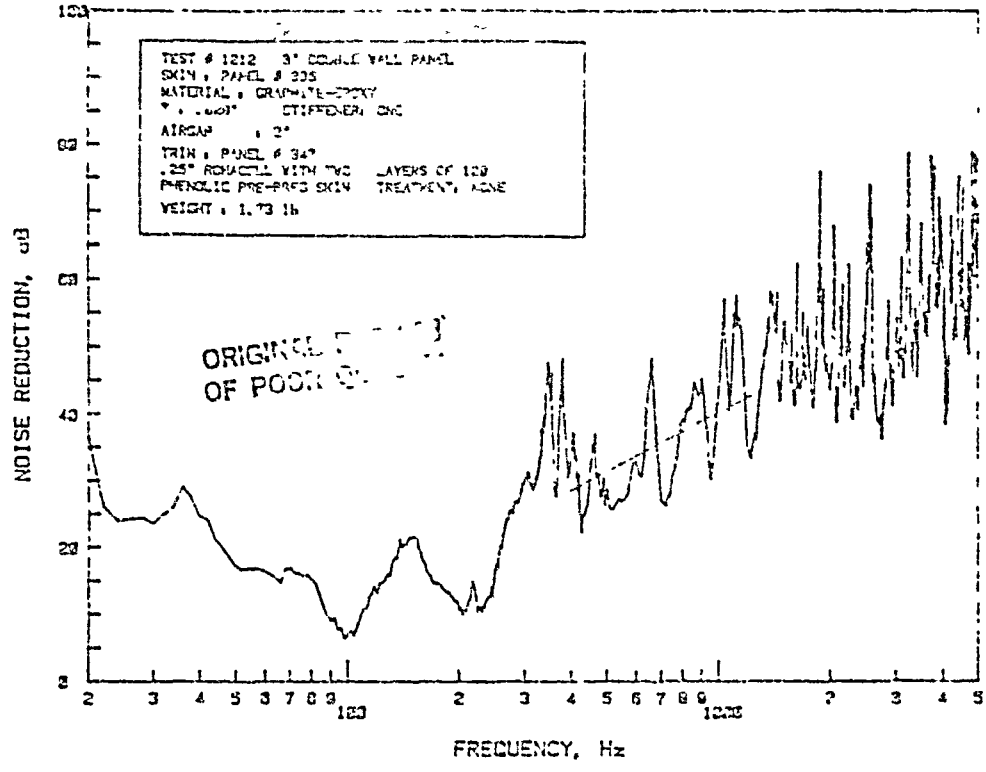

a. Airgap

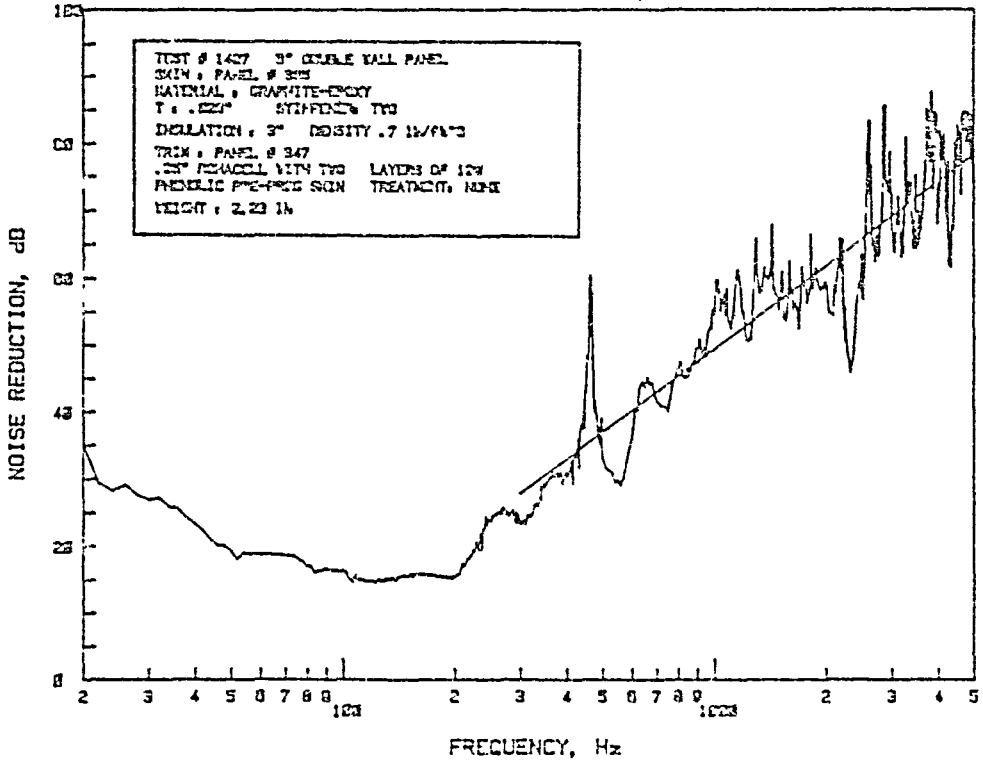

b. Fiberglass Insulation

Figure B.33: Noise Reduction Characteristics of Double-Wall Panel Made of Graphite-Epoxy Skin Panel 335 and Trim Panel 347; Panel Depth 3"

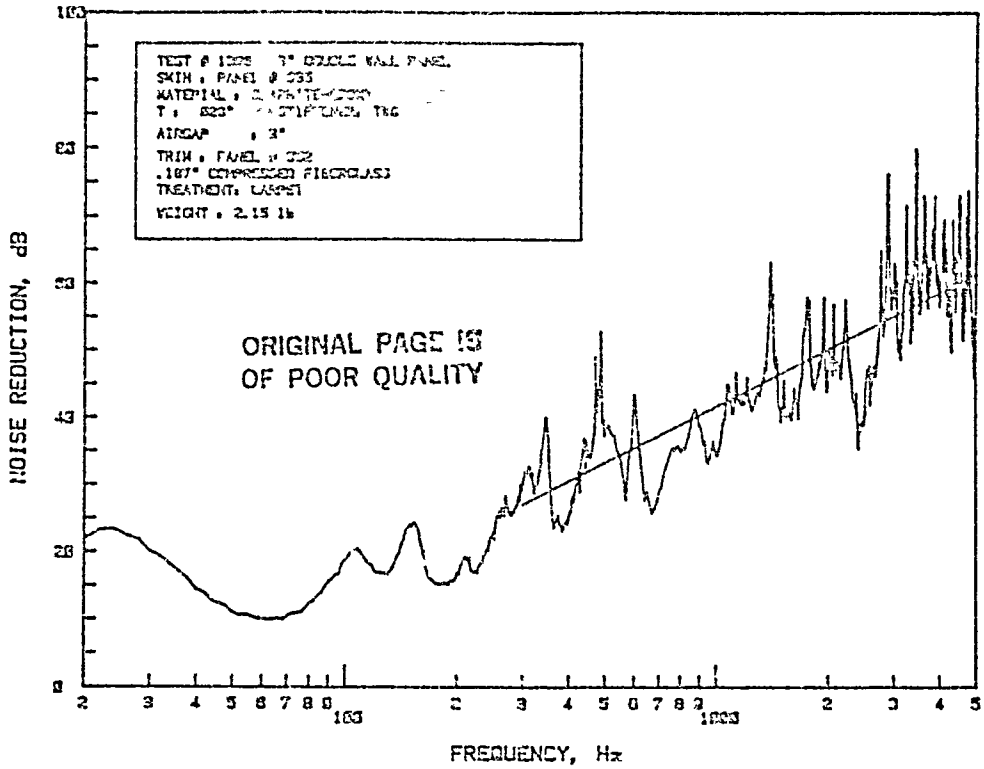

a. Airgap

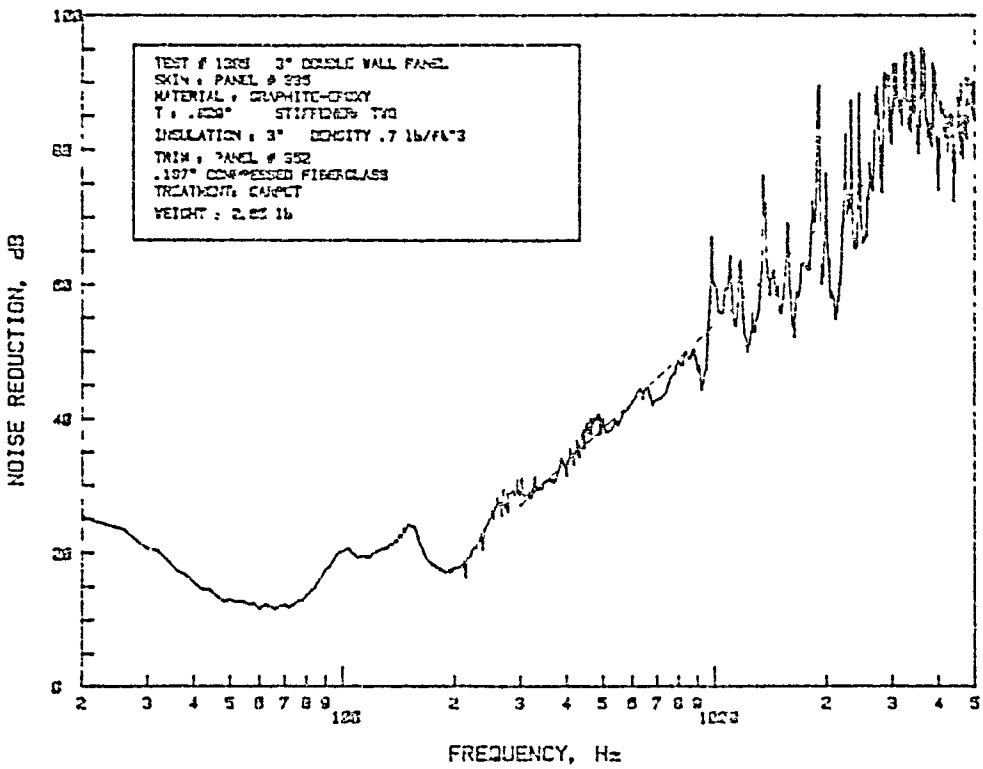

b. Fiberglass Insulation

Figure B.34: Noise Reduction Characteristics of Double-Wall Panel Made of Graphite-Epoxy Skin Panel 335 and Trim Panel 352; Panel Depth 3"

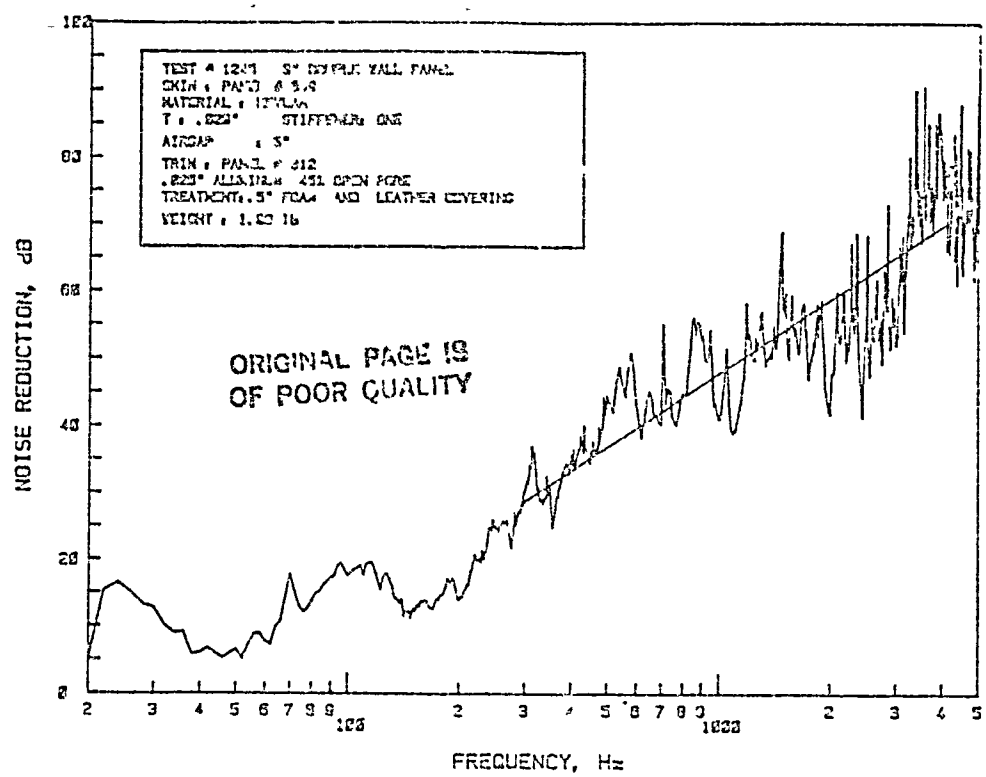

a. Airgap

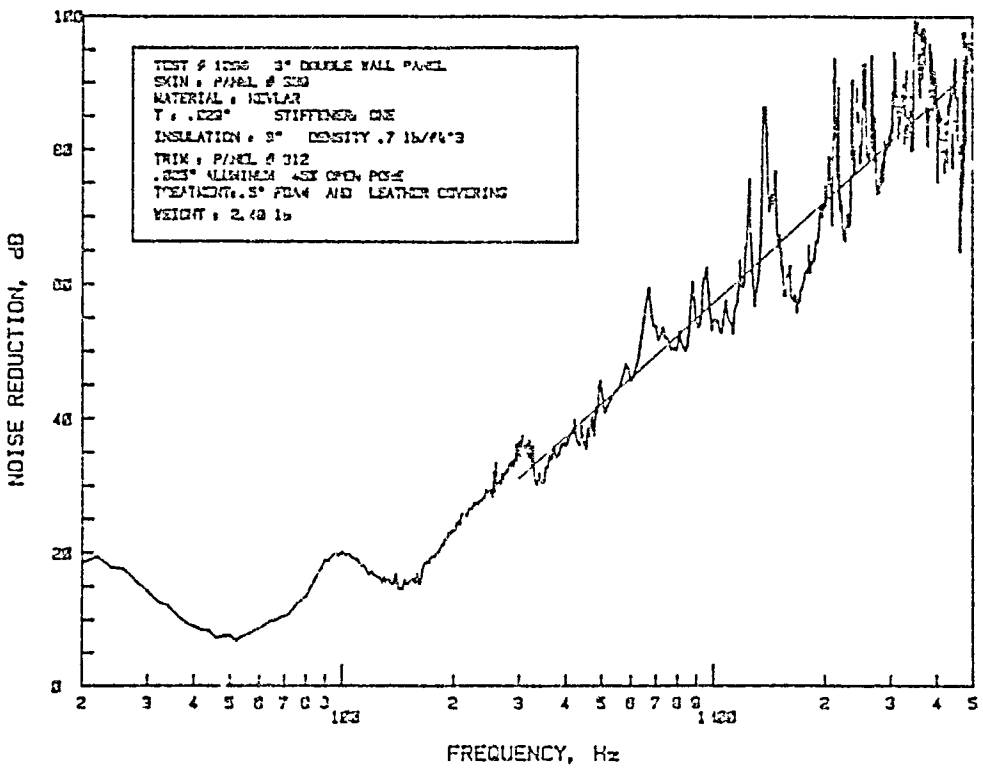

b. Fiberglass Insulation

Figure B.35: Noise Reduction Characteristics of Double-Wall Panel Made of Kevlar Skin Panel with One Hat Stiffener (Panel 339) and Trim Panel 312; Panel Depth 3"

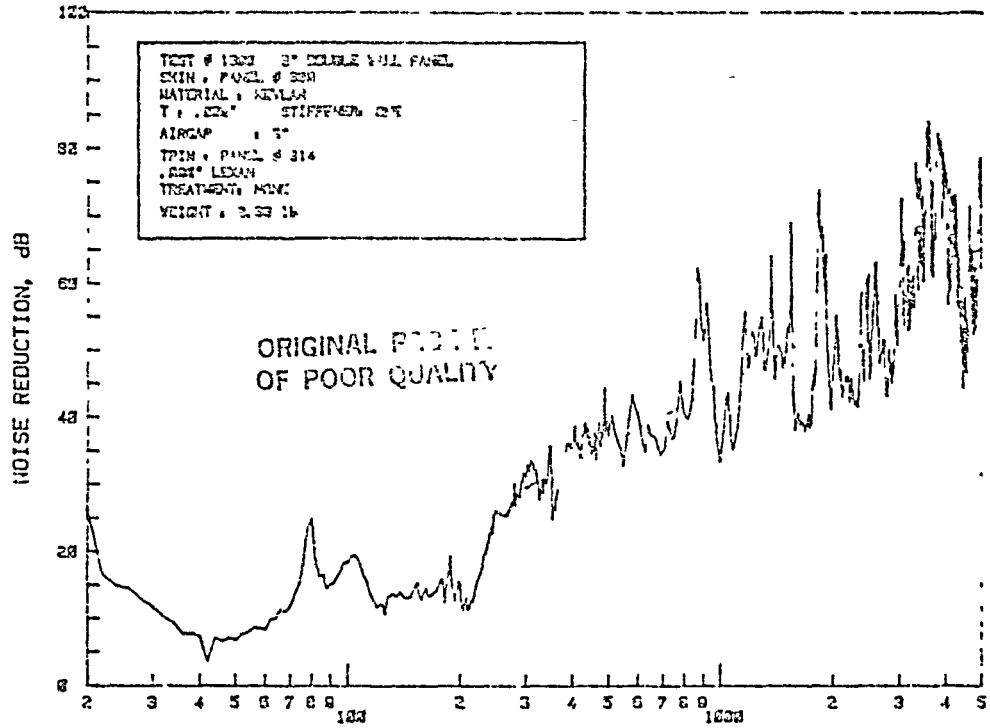

a. Airgap

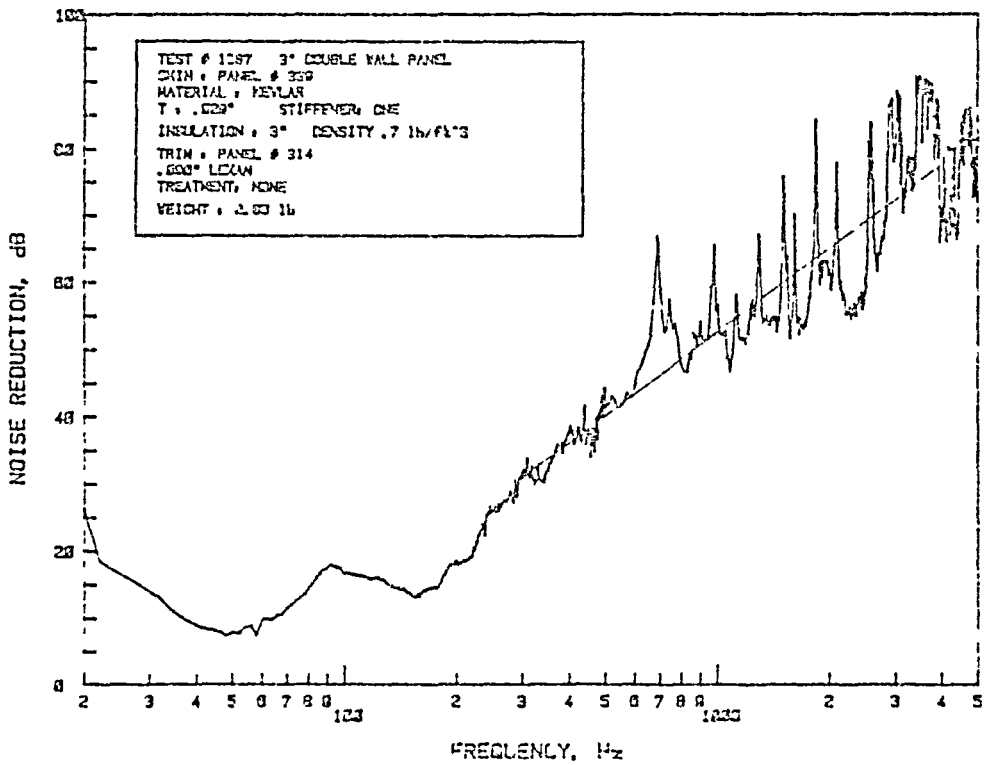

b. Fiberglass Insulation

Figure B.36: Noise Reduction Characteristics of Double-Wall Panel Made of Kevlar Skin Panel with One Hat Stiffener (Panel 339) and Trim Panel 314; Panel Depth 3"

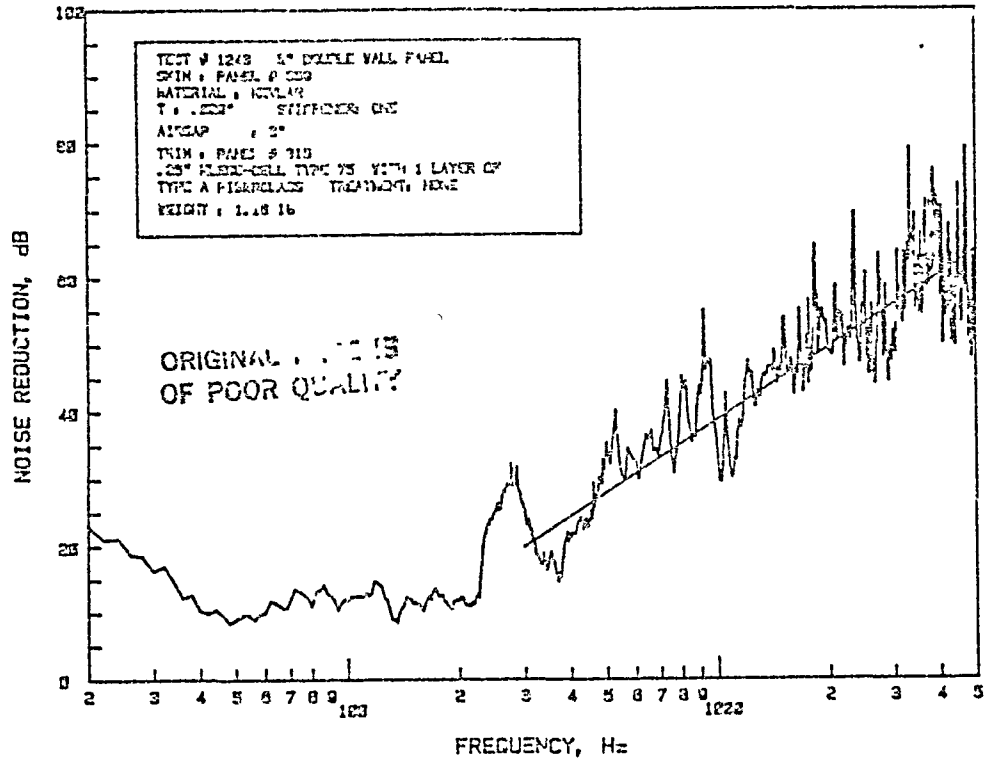

a. Airgap

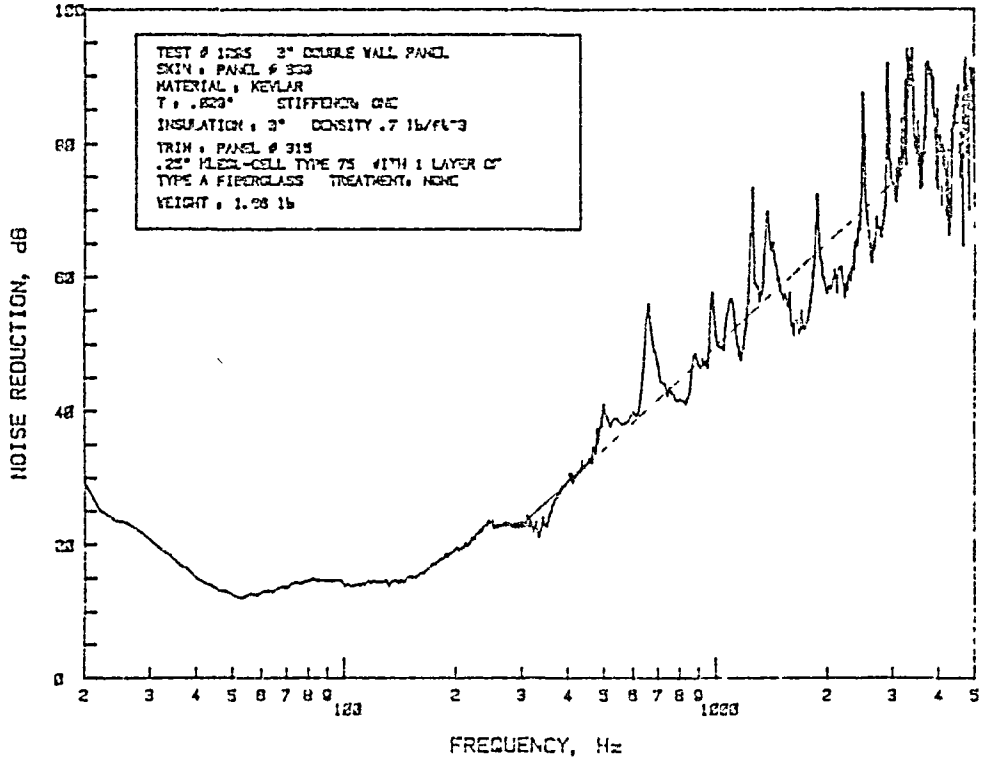

b. Fiberglass Insulation

Figure B.37: Noise Reduction Characteristics of Double-Wall Panel Made of Kevlar Skin Panel with One Hat Stiffener (Panel 339) and Trim Panel 315; Panel Depth 3"

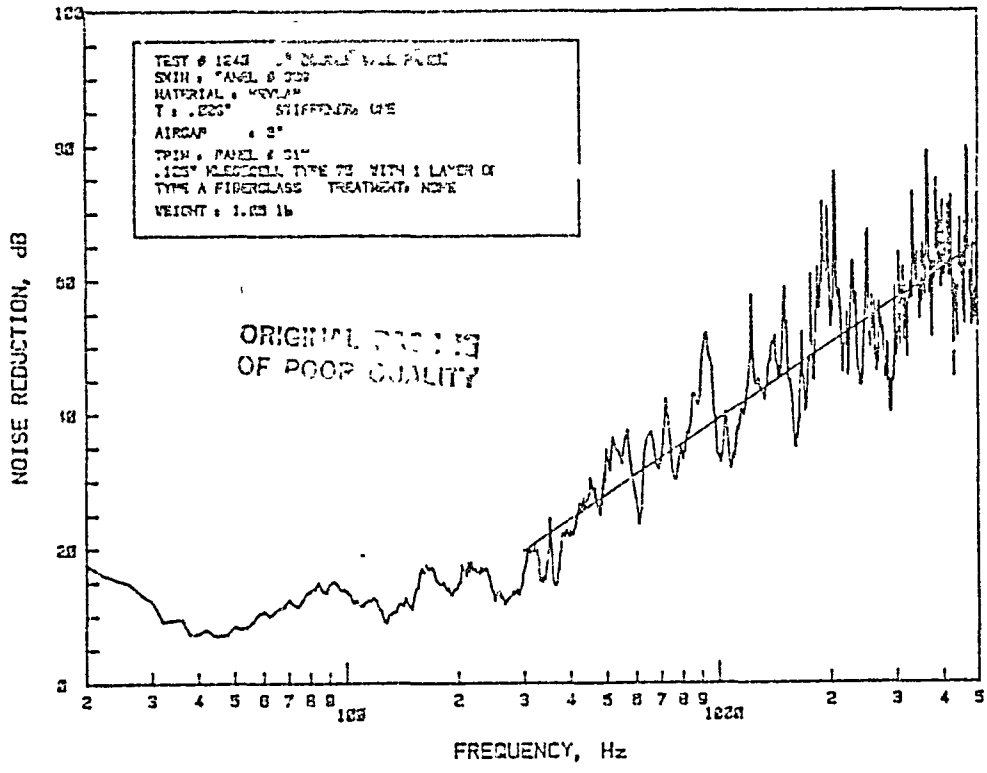

a. Airgap

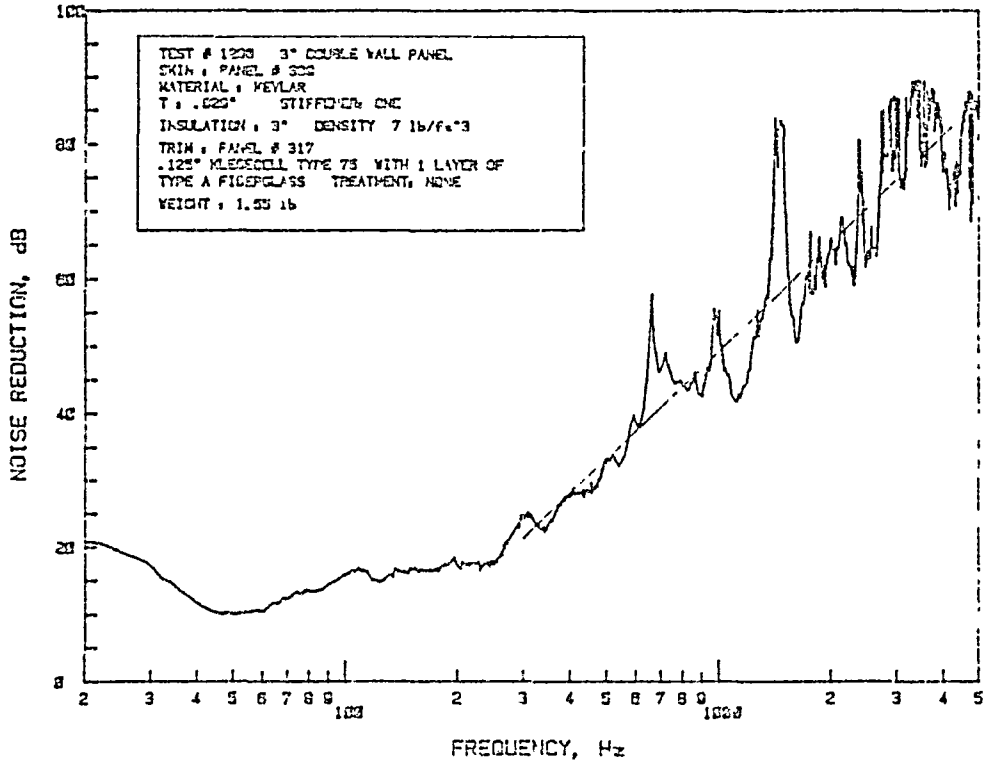

b. Fiberglass Insulation

Figure B.38: Noise Peduction Characteristics of Double-Wall Panel Made of Kevlar Skin Panel with One Hat Stiffener (Panel 339) and Trim Panel 317; Panel Depth 3"

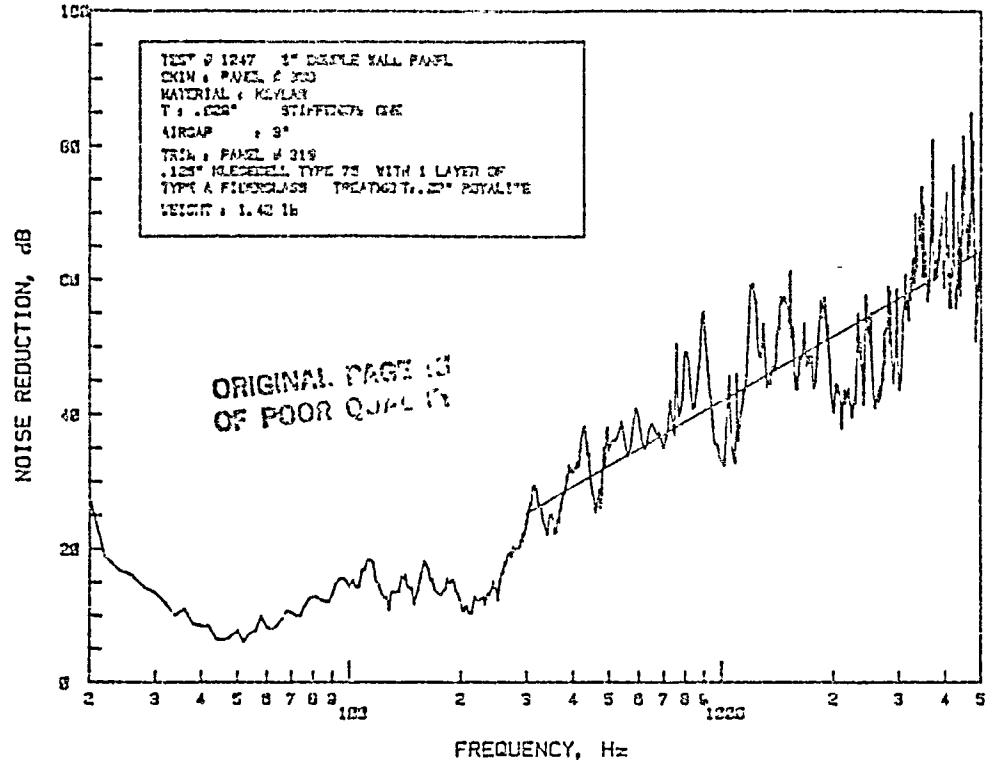

a. Airgap

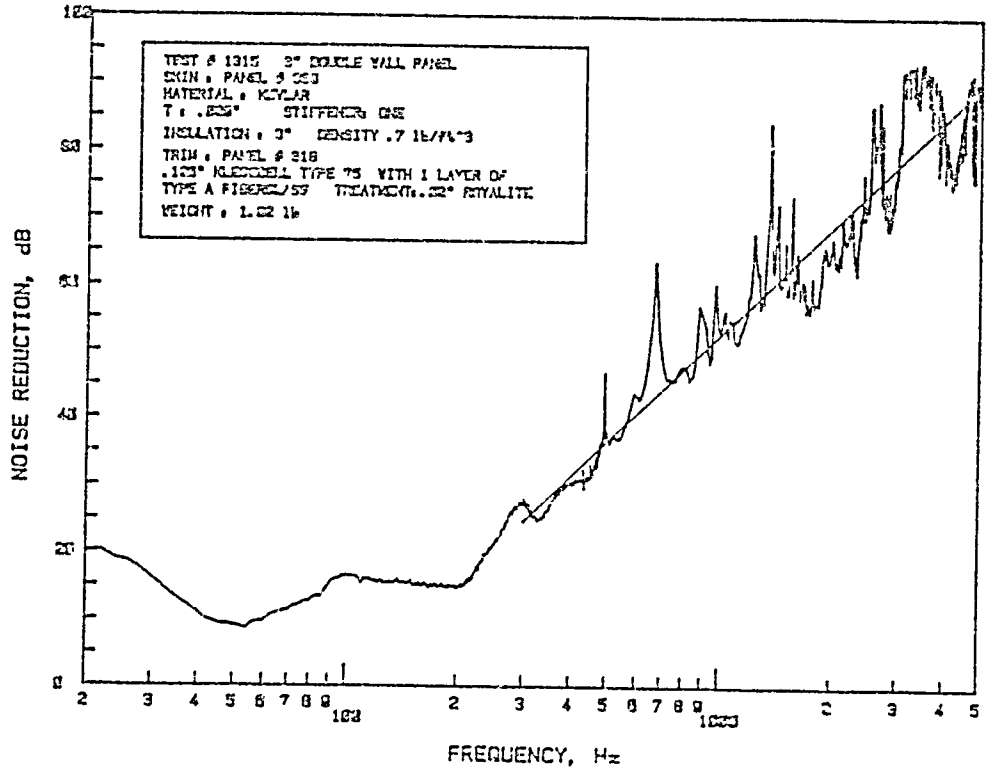

b. Fiberglass Insulation

Figure B.39: Noise Reduction Characteristics of Double-Wall Panel Made of Kevlar Skin Panel with One Hat Stiffener (Panel 339) and Trim Panel 318: Panel Depth 3"

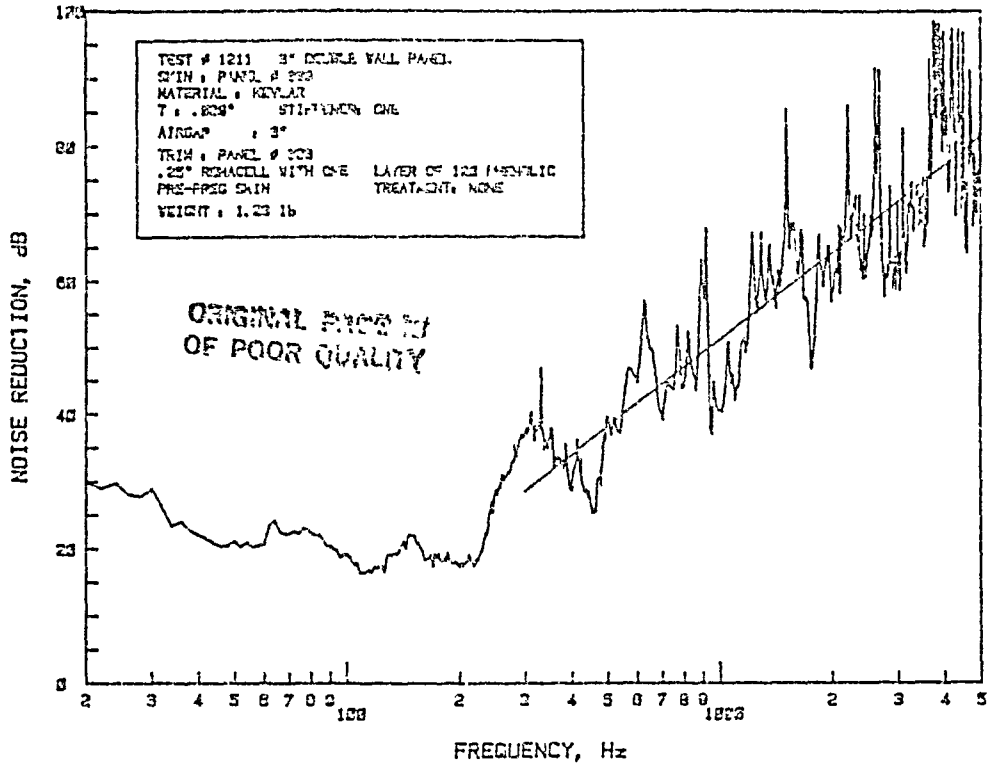

a. Airgap

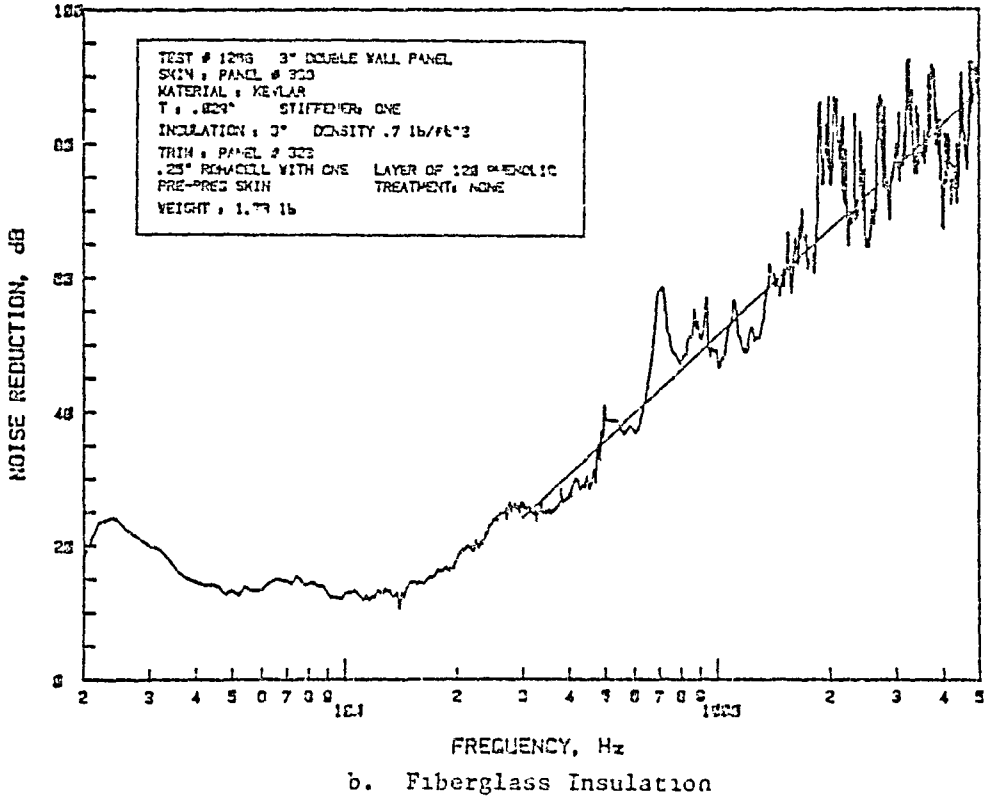

b. Fiberglass Insulation

Figure B.40: Noise Reduction Characteristics of Double-Wall Panel Made of Kevlar Skin Panel with One Hat Stiffener (Panel 339) and Trim Panel 323; Panel Depth 3"

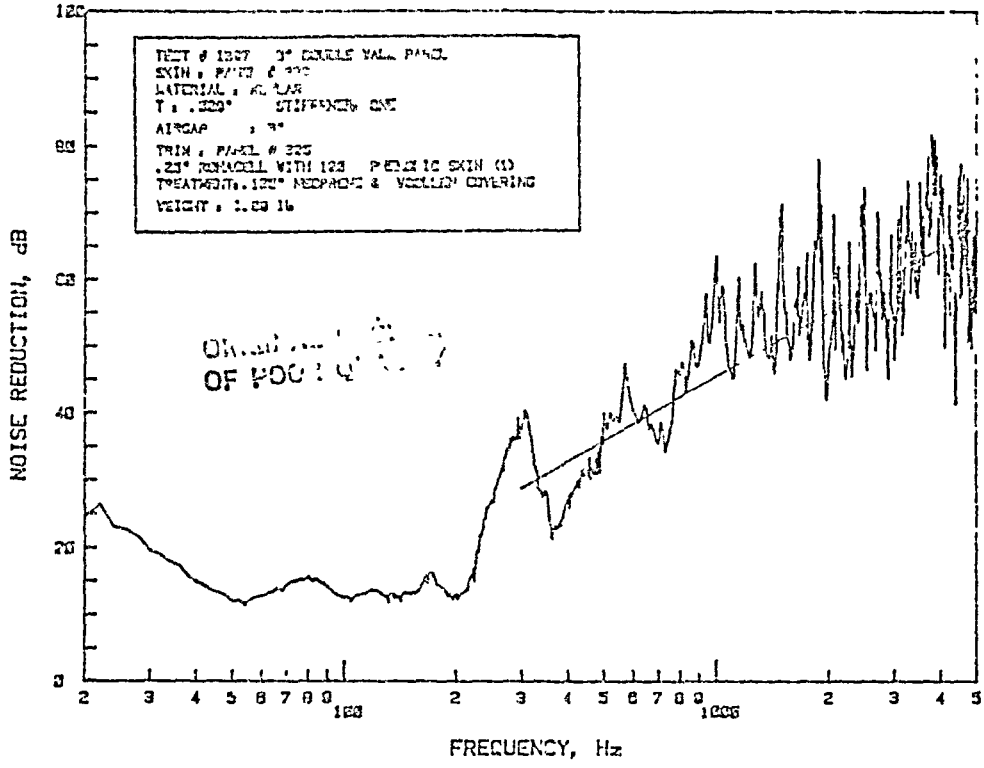

a. Airgap

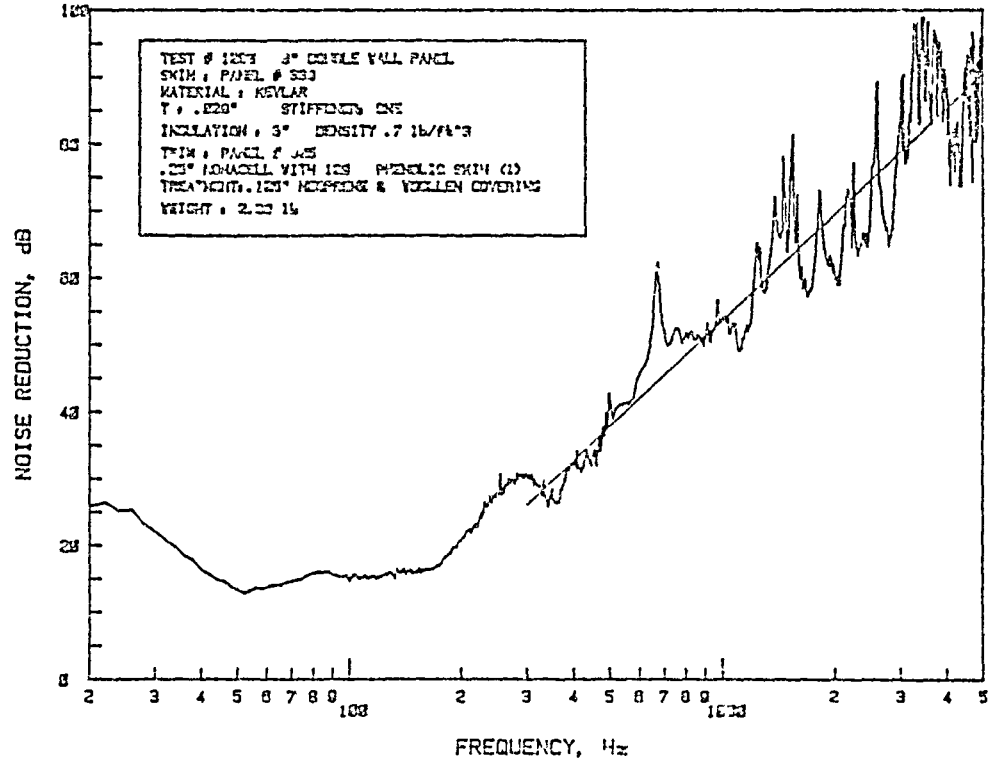

b. Fiberglass Insulation

Figure B.41: Noise Reduction Characteristics of Double-Wall Panel Made of Kevlar Skin Panel with One Hat Stiffener (Panel 339) and Trim Panel 325; Panel Depth 3"

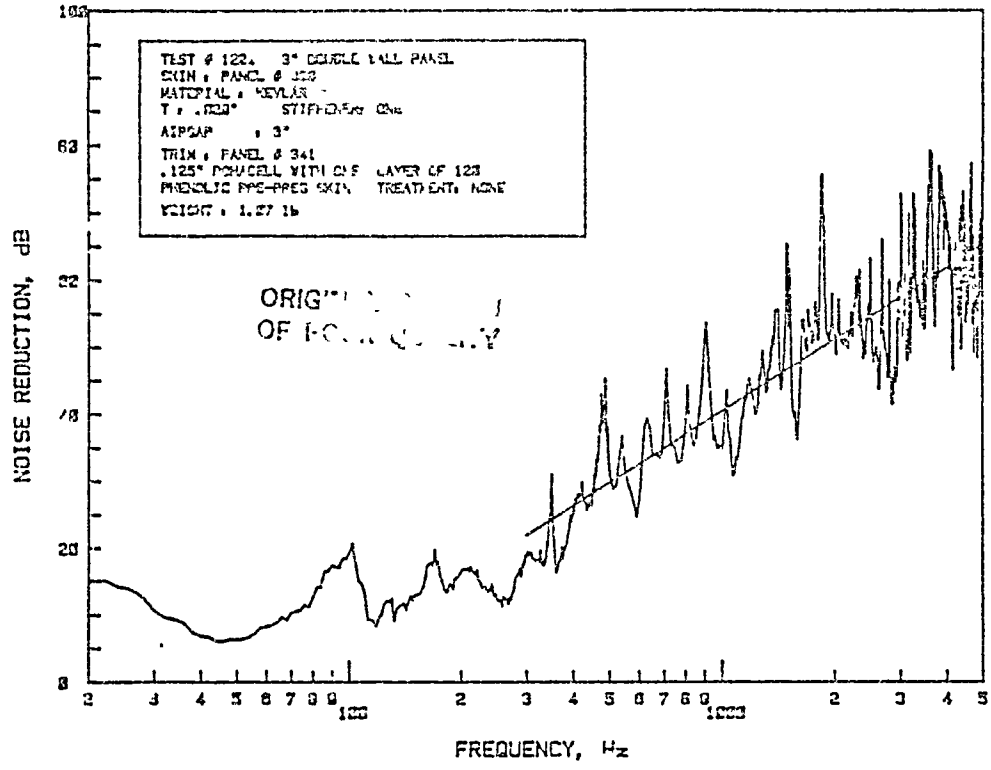

a. Airgap

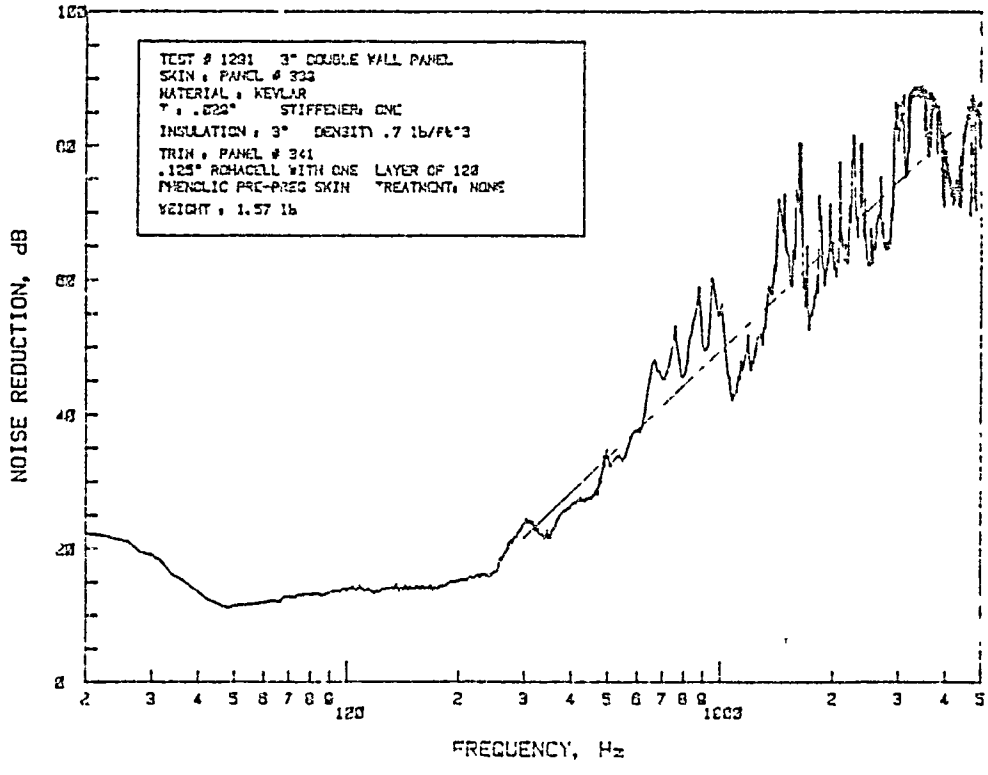

b. Fiberglass Insulation

Figure B.42: Noise Reduction Characteristics of Double-Wall Panel Made of Kevlar Skin Panel with One Hat Stiffener (Panel 339) and Trim Panel 341; Panel Depth 3"

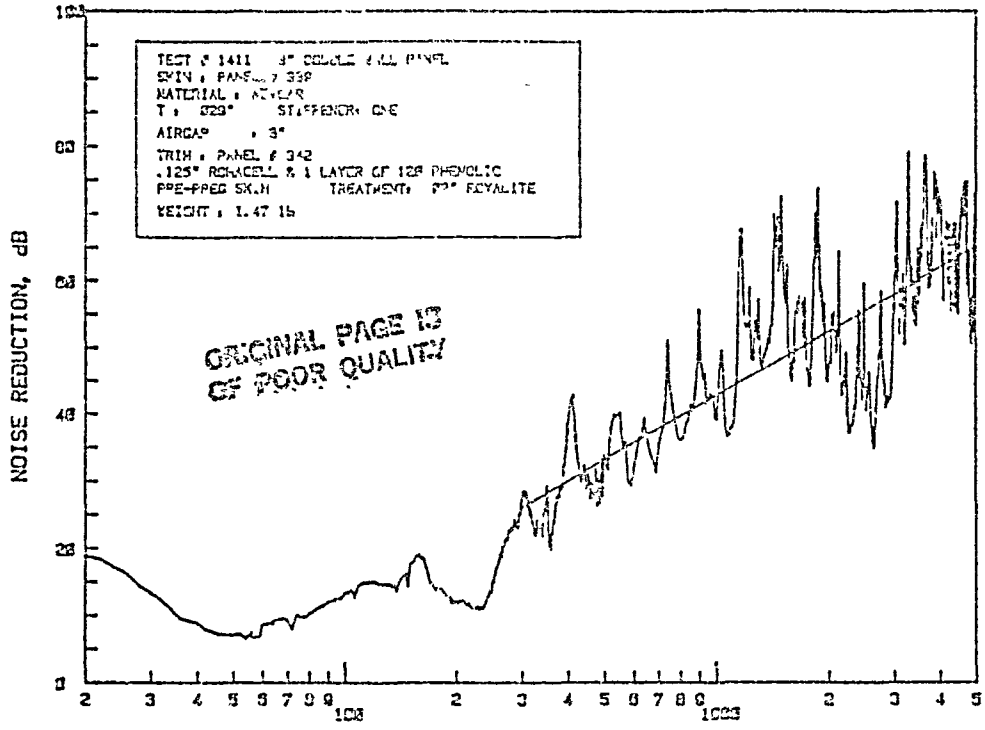

a. Airgap

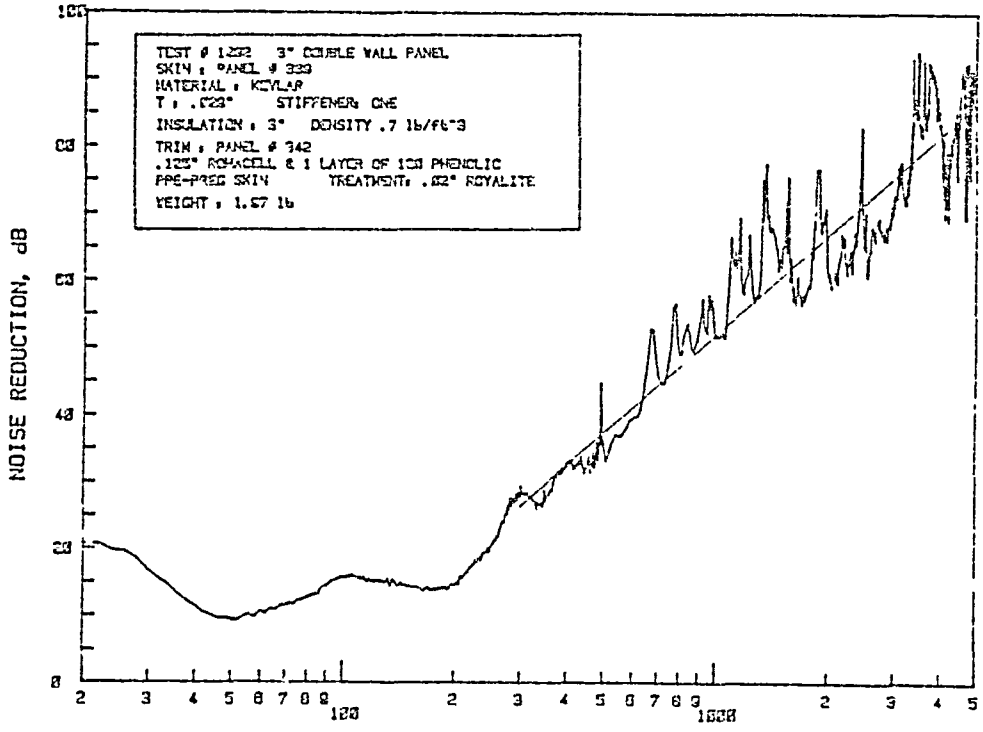

b. Fiberglass Insulation

Figure B.43: Noise Reduction Characteristics of Double-Wall Panel Made of Kevlar Skin Panel with ne Hat Stiffener (Panel 339) and Trim Panel 342; Panel Depth 3"

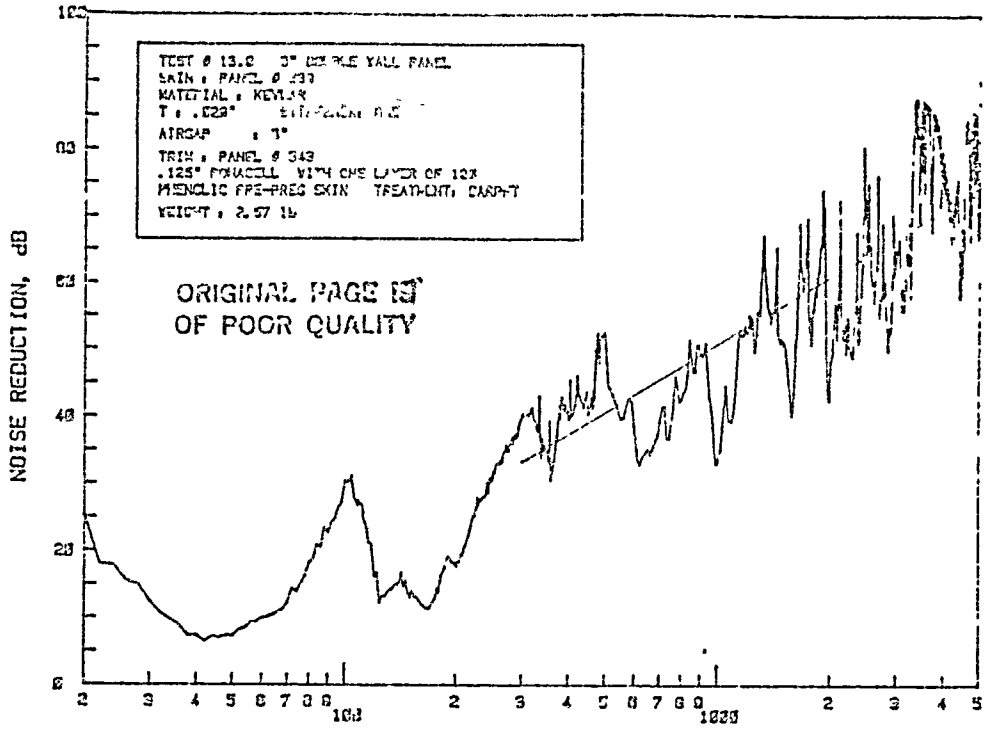

a. Airgap

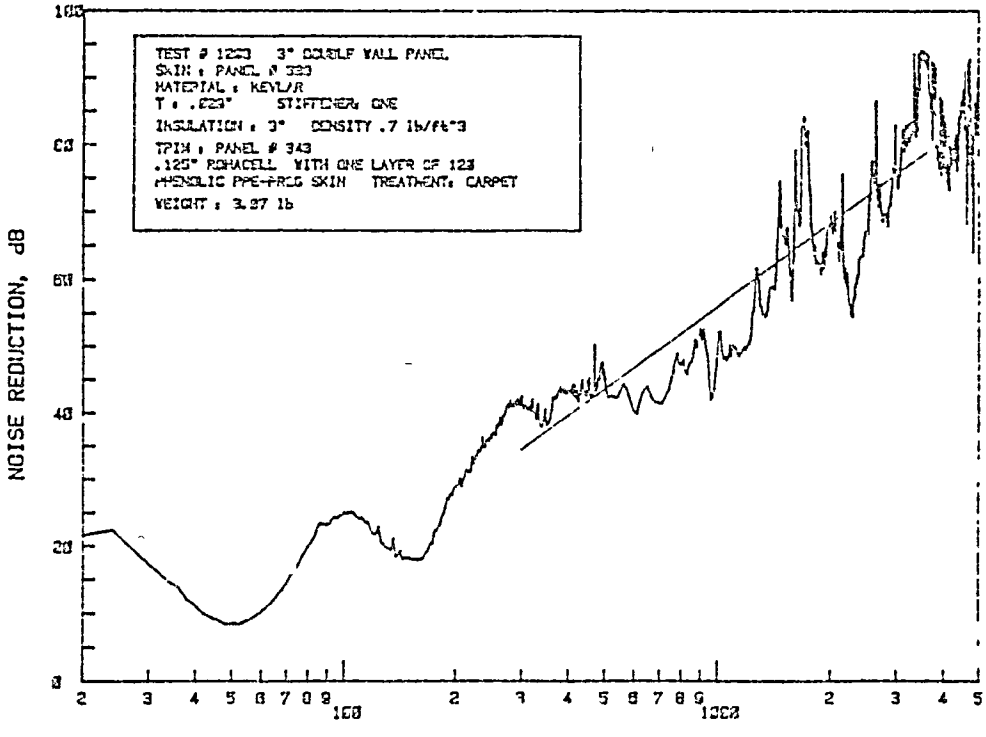

b. Fiberglass Insulation

Figure B.44: Noise Reduction Characteristics of Double-Wall Panel Made of Kevlar Skin Panel with One Hat Stiffener (Panel 339) and Trim Panel 343; Panel Depth 3"

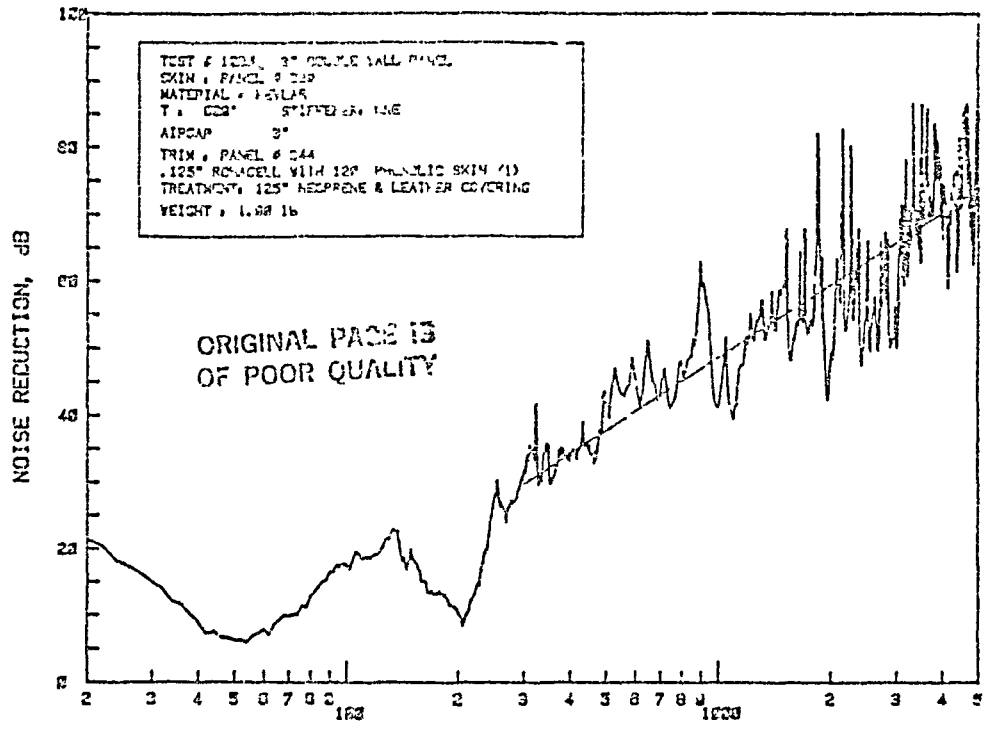

a. Airgap

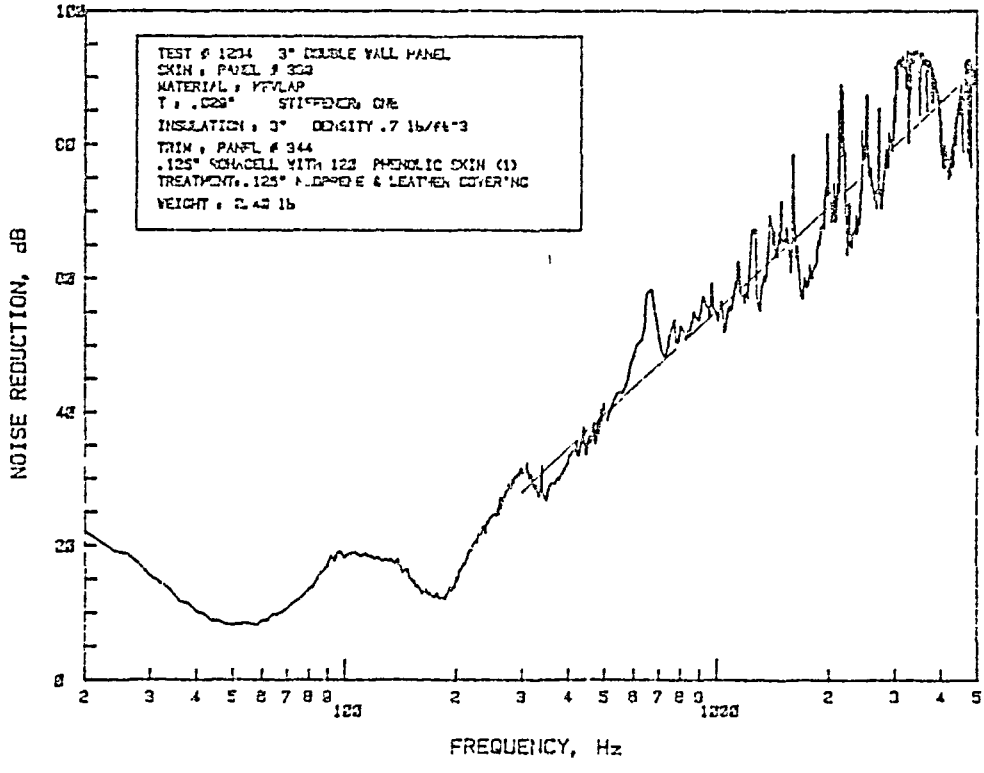

b. Fiberglass Insulation

Figure B.45: Noise Reduction Characteristics of Double-Wall Panel Made of Kevlar Skin Panel with One Hat Stiffener (Panel 339) and Trim Panel 344; Panel Depth 3"

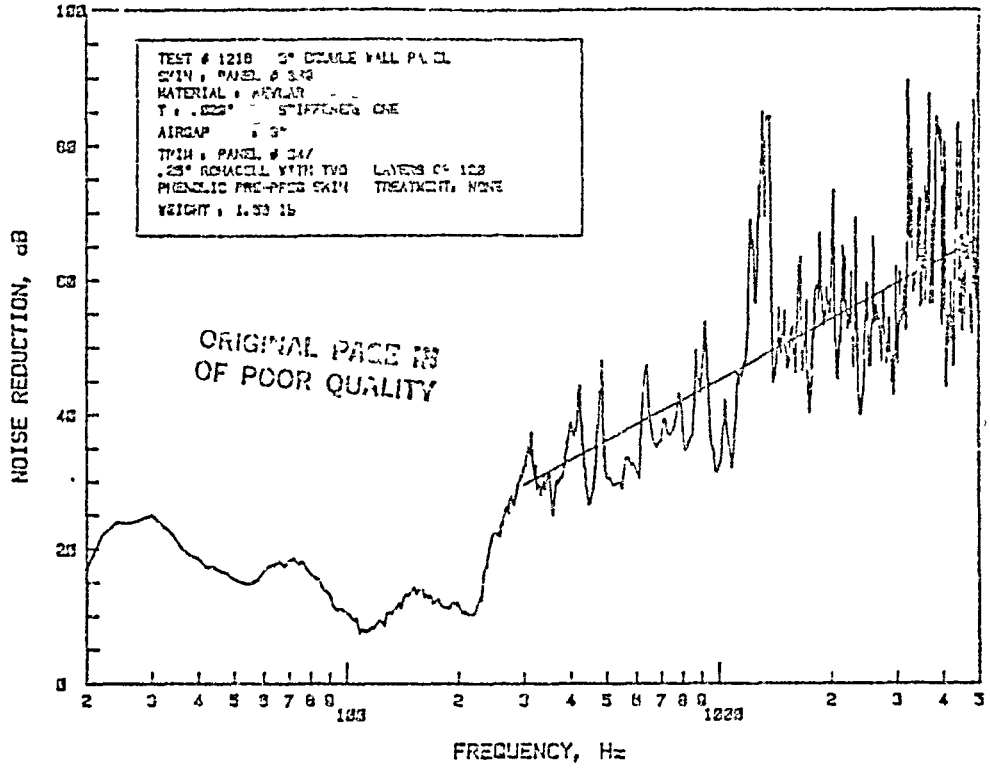

a. Airgap

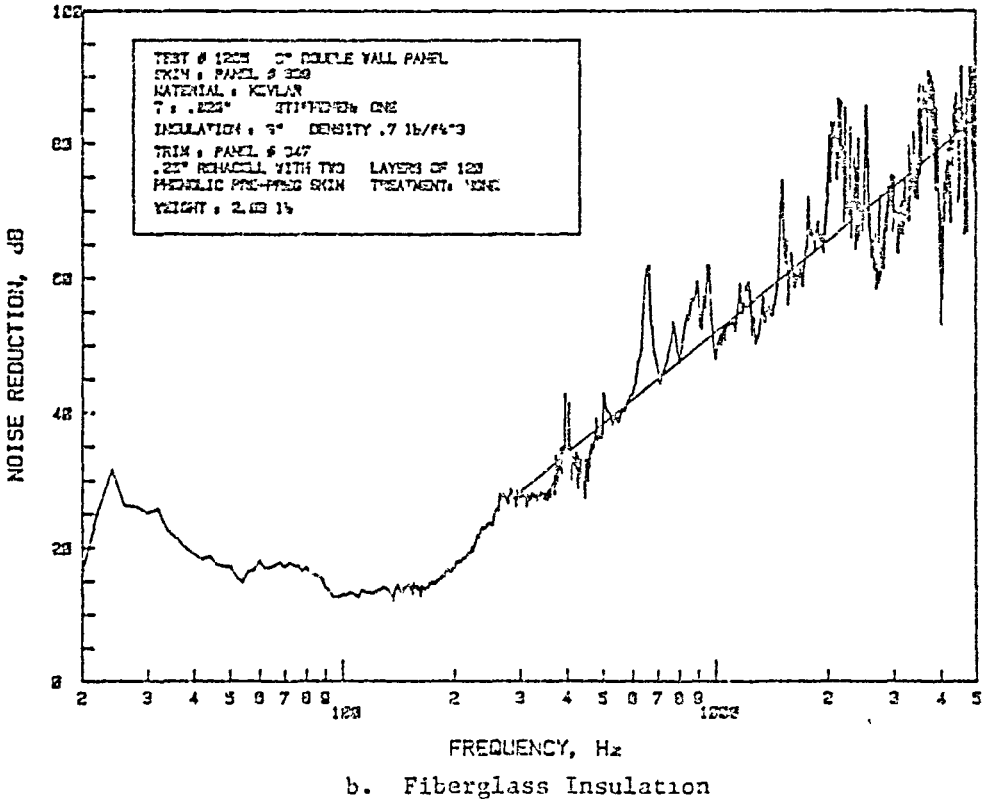

b. Fiberglass Insulation

Figure B.46: Noise Reduction Characteristics of Double-Wall Panel Made of Kevlar Skin Panel with One Hat Stiffener (Panel 339) and Trim Panel 347; Panel Depth 3"

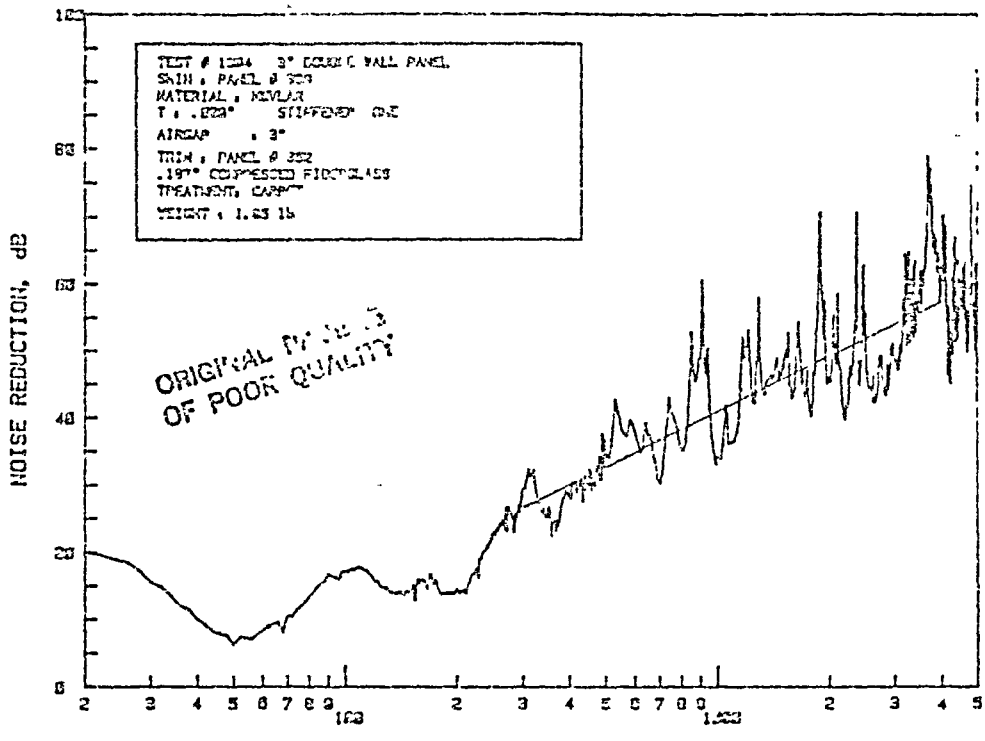

a. Airgap

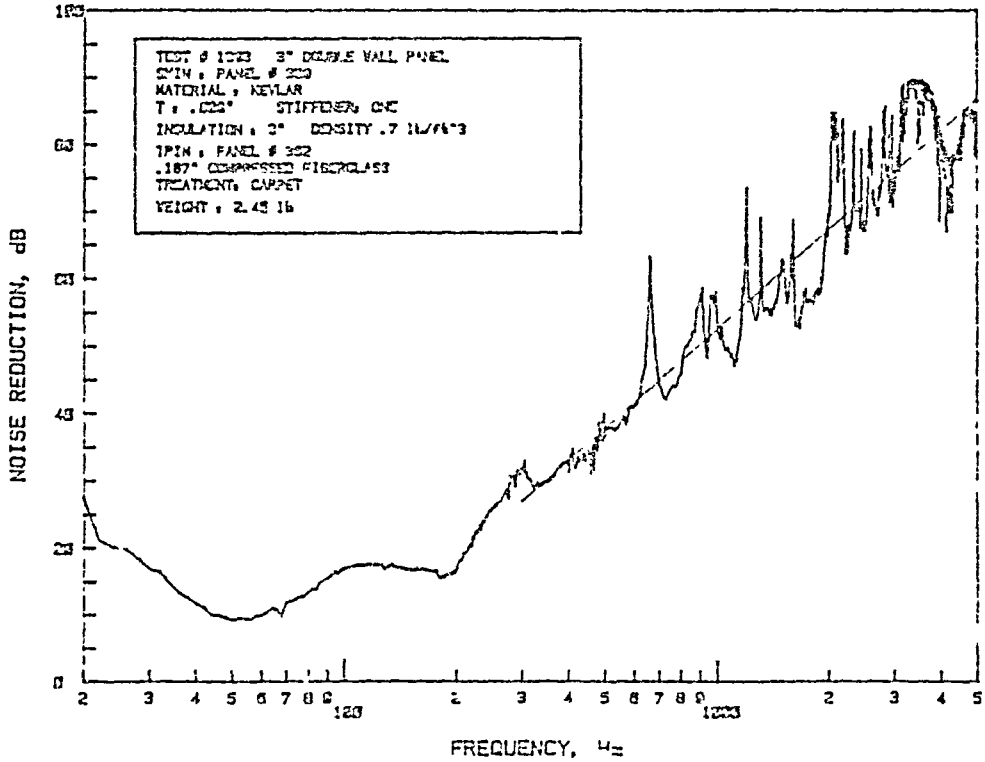

b. Fiberglass Insulation

Figure B.47: Noise Reduction Characteristics of Double-Wall Panel Made of Kevlar Skin Panel with One Hat Stiffener (Panel 339) and Trim Panel 352; Panel Depth 3"

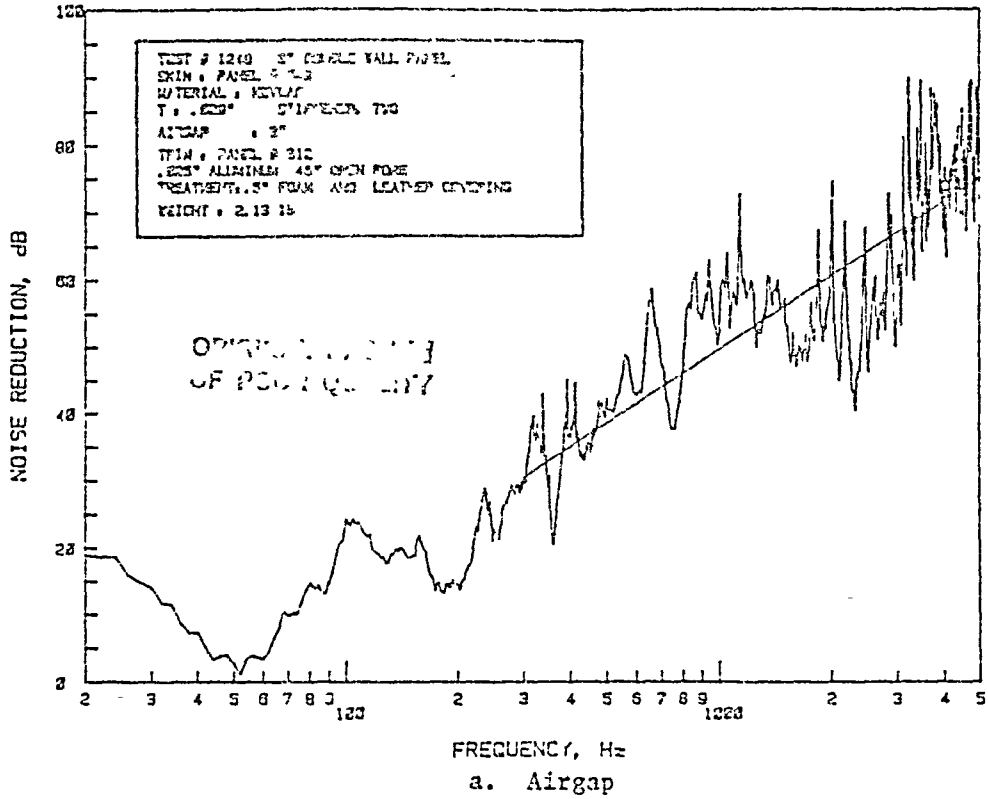

a. Airgap

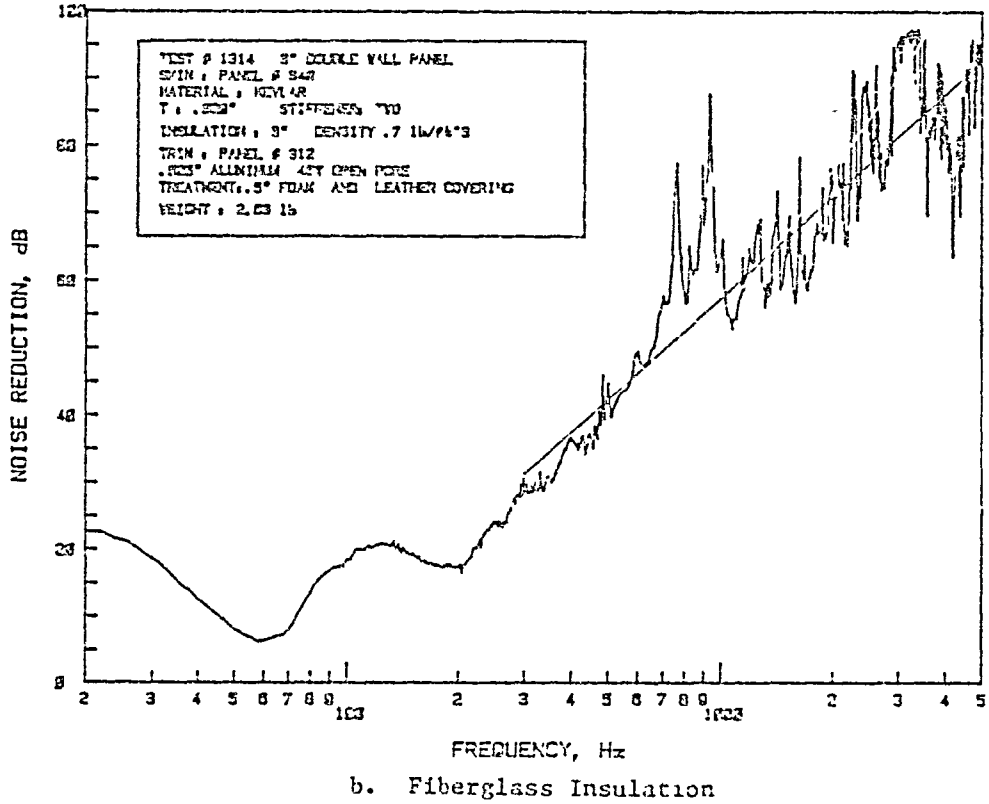

b. Fiberglass Insulation

Figure 3: Noise Reduction Characteristics of Double-Wall Panel Made of Kevlar Skin Panel with Two Hat Stiffeners (Panel 340) and Trim Panel 312; Panel Depth 3"

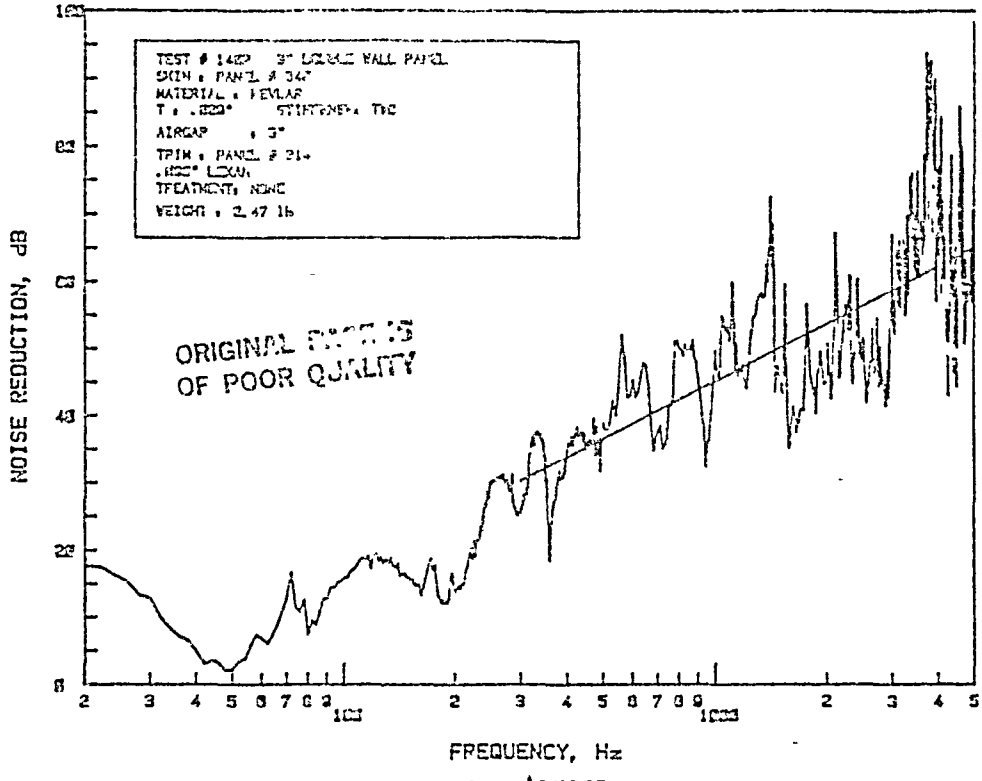

a. Airgap

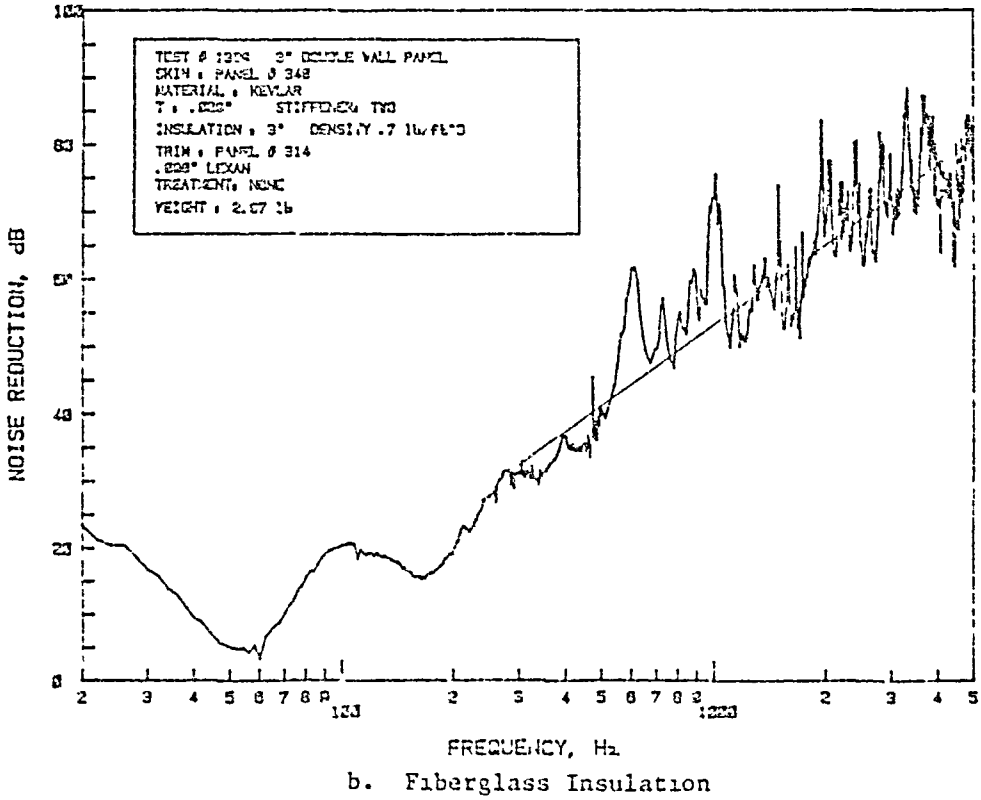

b. Fiberglass Insulation

Figure B.49: Noise Reduction Characteristics of Double-Wall Panel Made of Kevlar Skin Panel with Two Hat Stiffeners (Panel 340) and Trim Panel 314; Panel Depth 3"

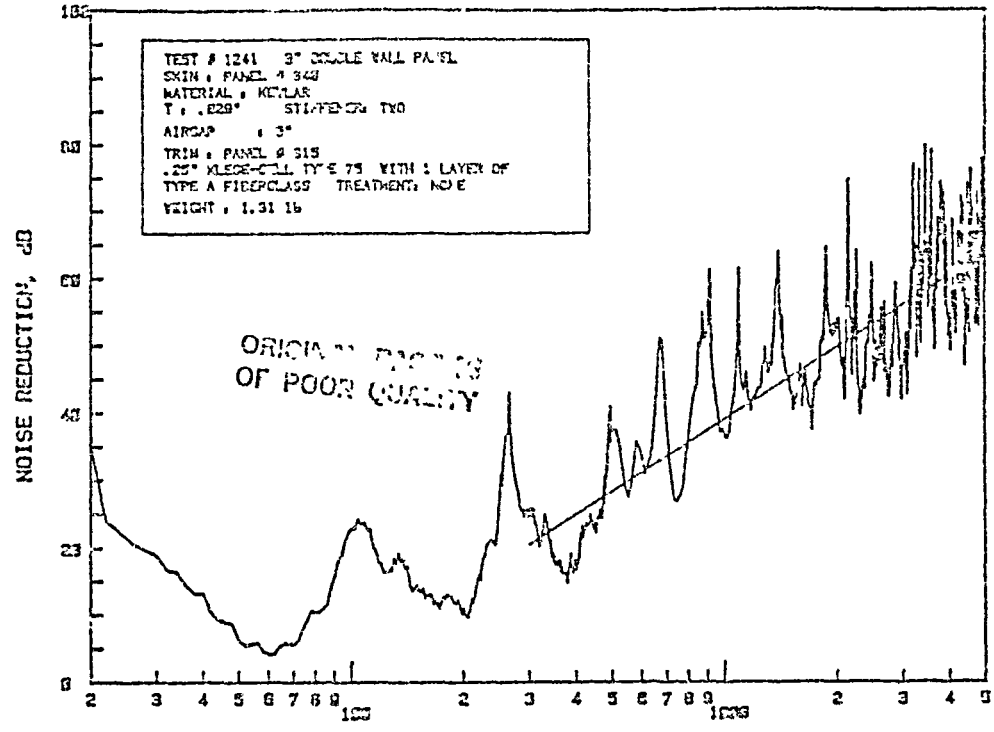

a. Airgap

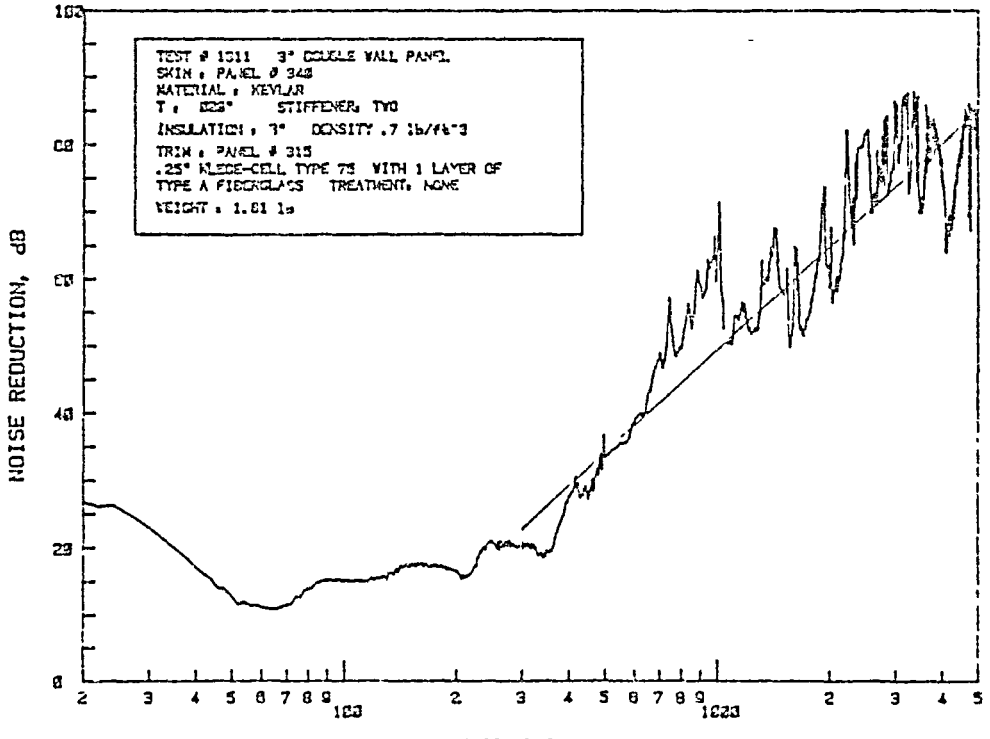

b. Fiberglass Insulation

Figure B.50: Noise Reduction Characteristics of Double-Wall Panel Made of Kevlar Skin Panel with Two Hat Stiffeners (Panel 340) and Trim Panel 315; Panel Depth 3"

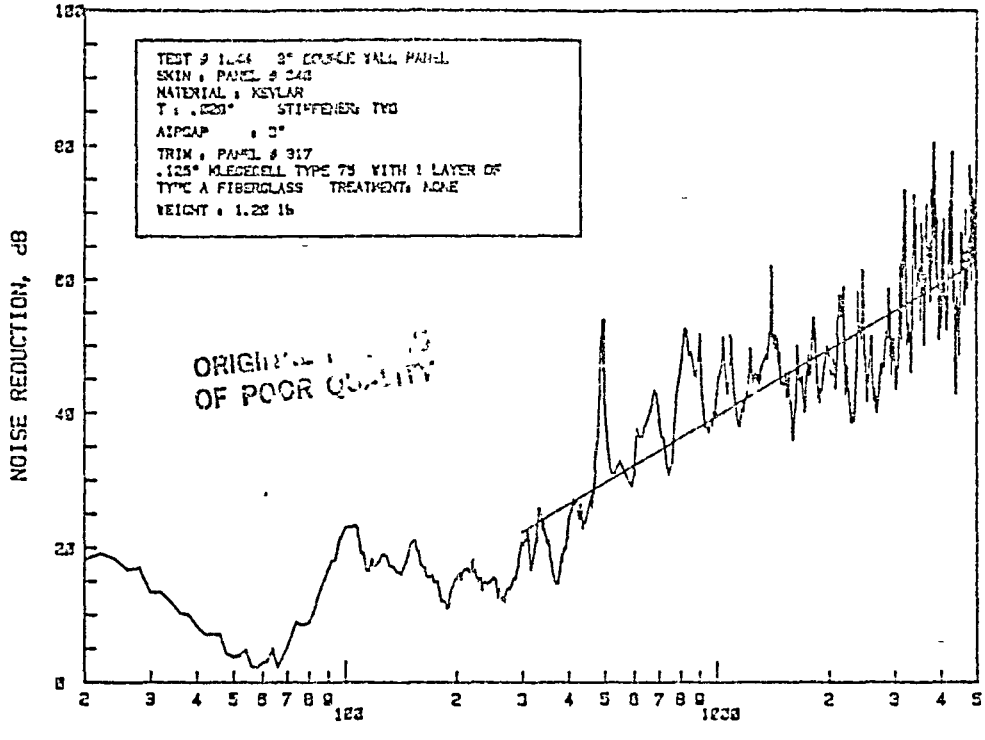

a. Airgap

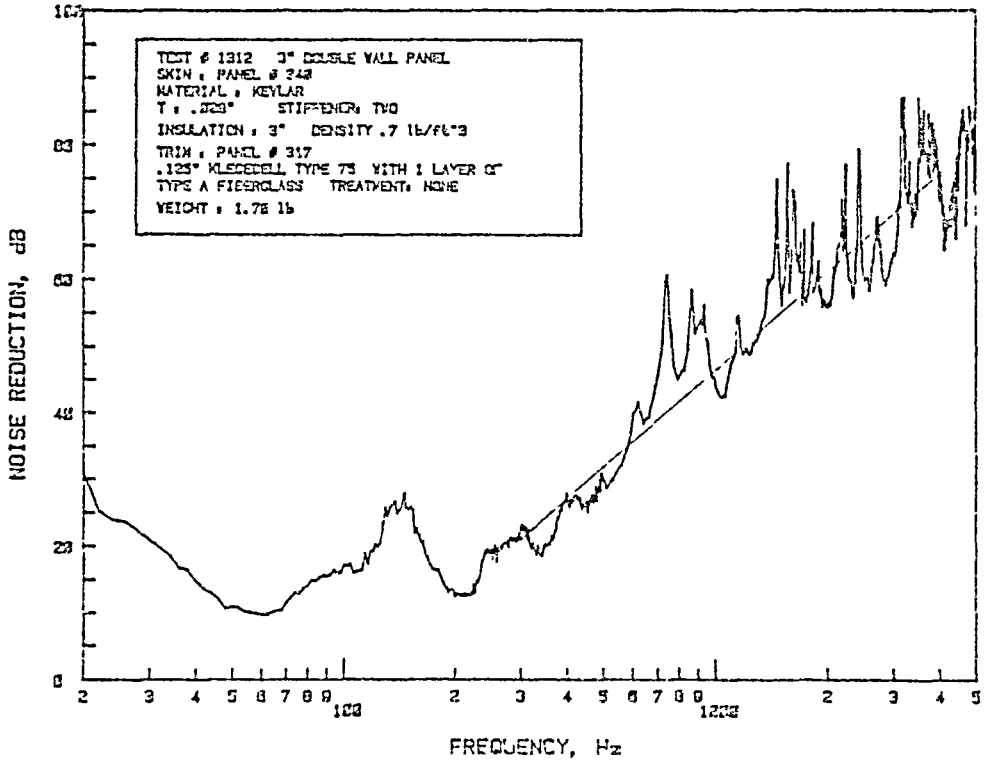

b. Fiberglass Insulation

Figure B.51: Noise Reduction Characteristics of Double-Wall Panel Made of Kevlar Skin Panel with Two Hat Stiffeners (Panel 340) and Trim Panel 317; Panel Depth 3"

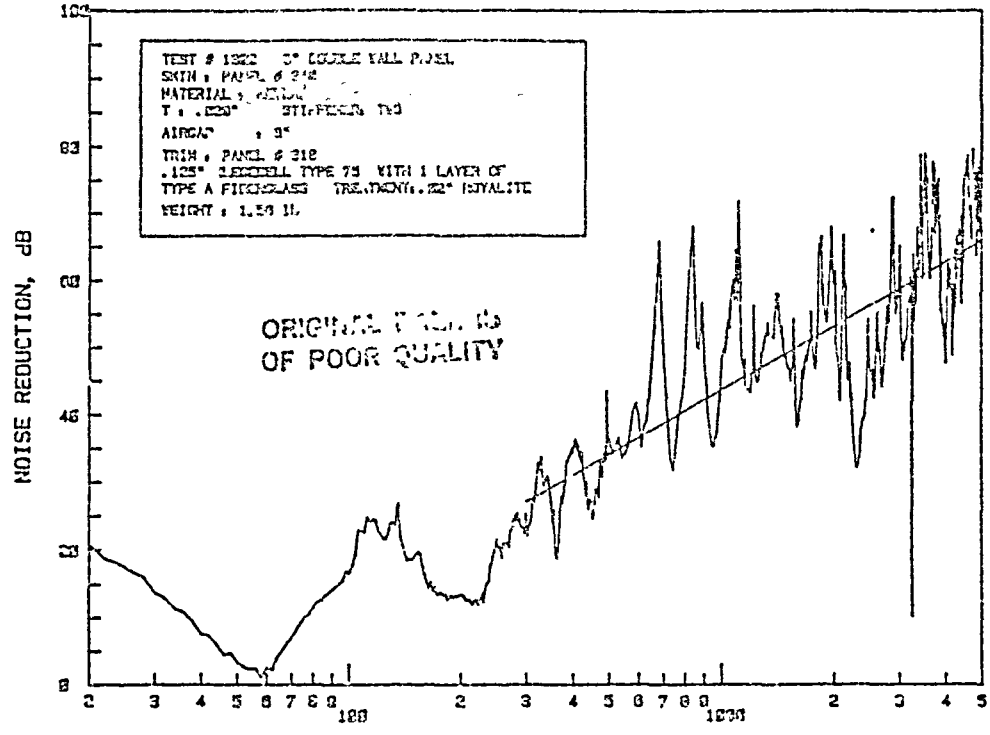

a. Airgap

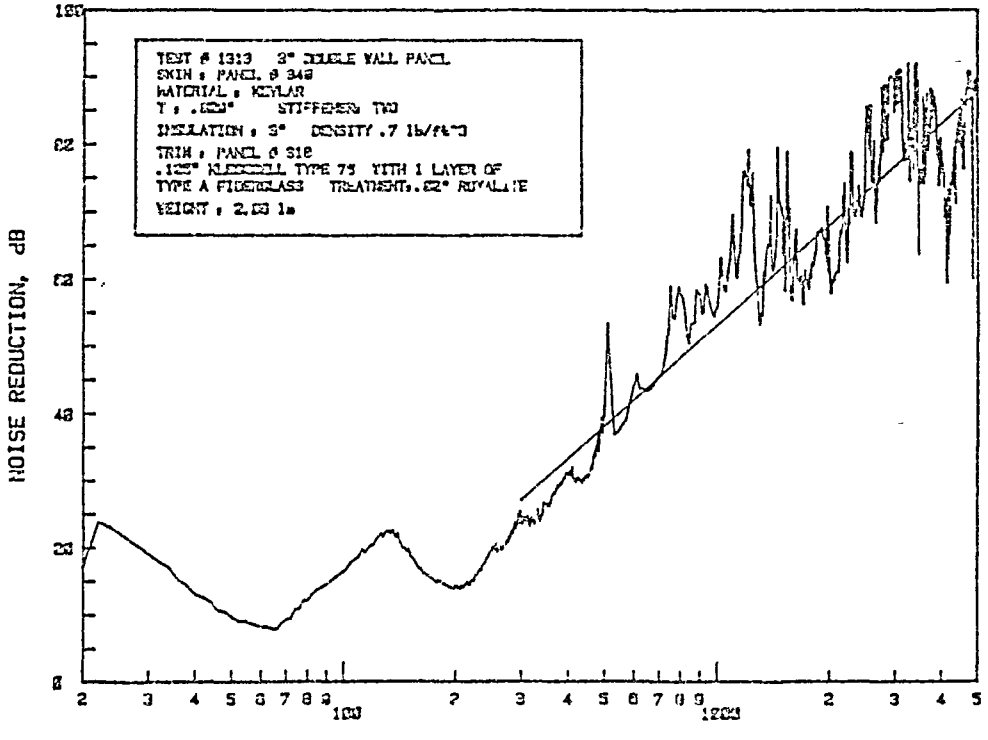

b. Fiberglass Insulation

Figure B.52: Noise Reduction Characteristics of Double-Wall Panel Made of Kevlar Skin Panel with Two Hat Stiffeners (Panel 340) and Trim Panel 318; Panel Depth 3"

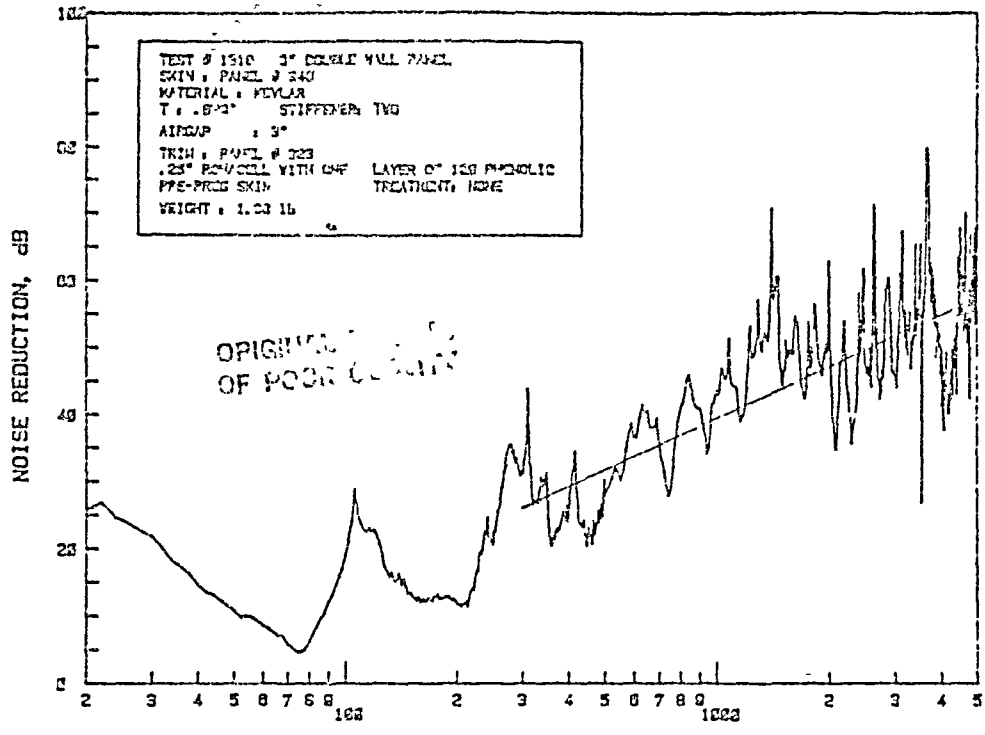

a. Airgap

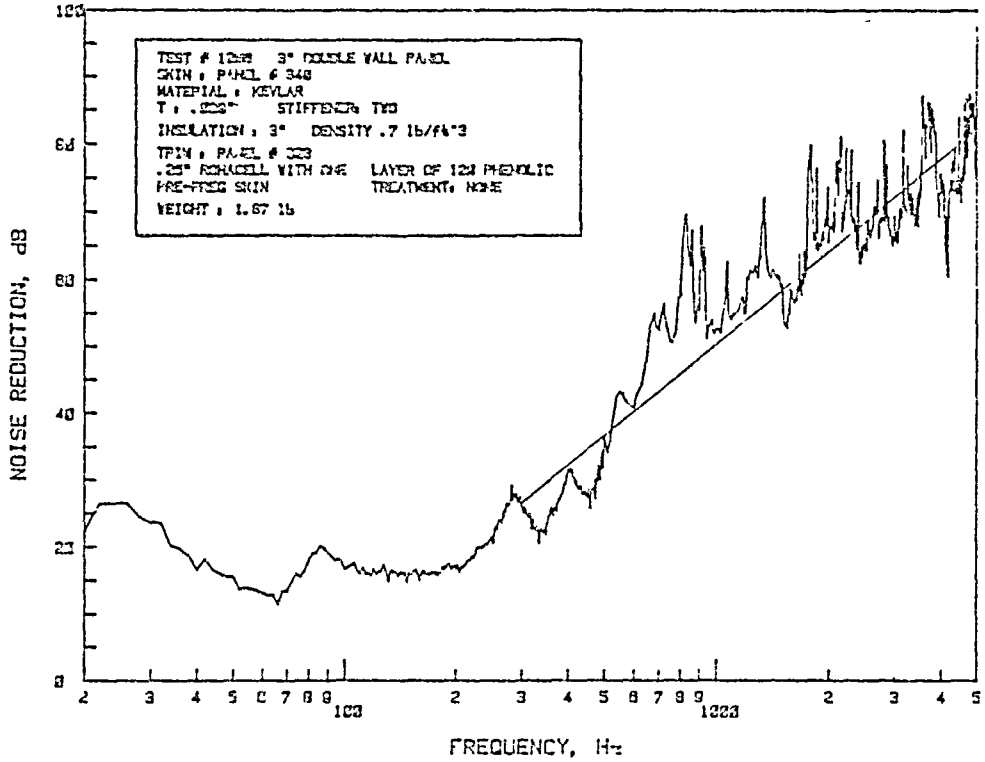

b. Fiberglass Insulation

Figure B.53: Noise Reduction Characteristics of Double-Wall Panel Made of Kevlar Skin Panel with Two Hat Stiffeners (Panel 340) and Trim Panel 323; Panel Depth 3"

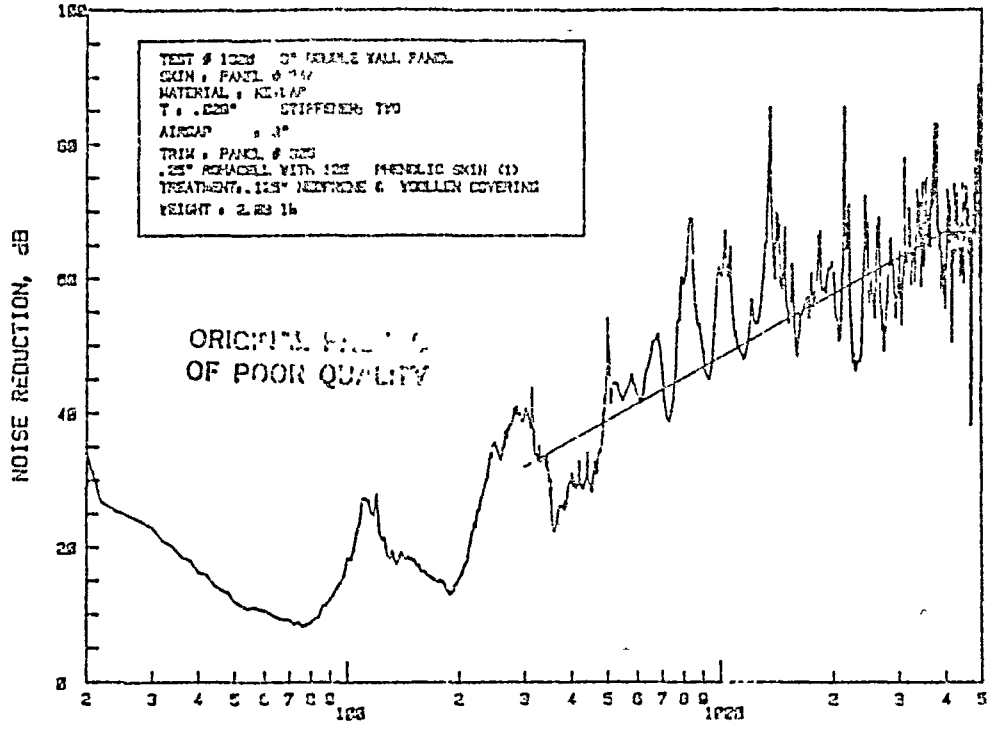

a. Airgap

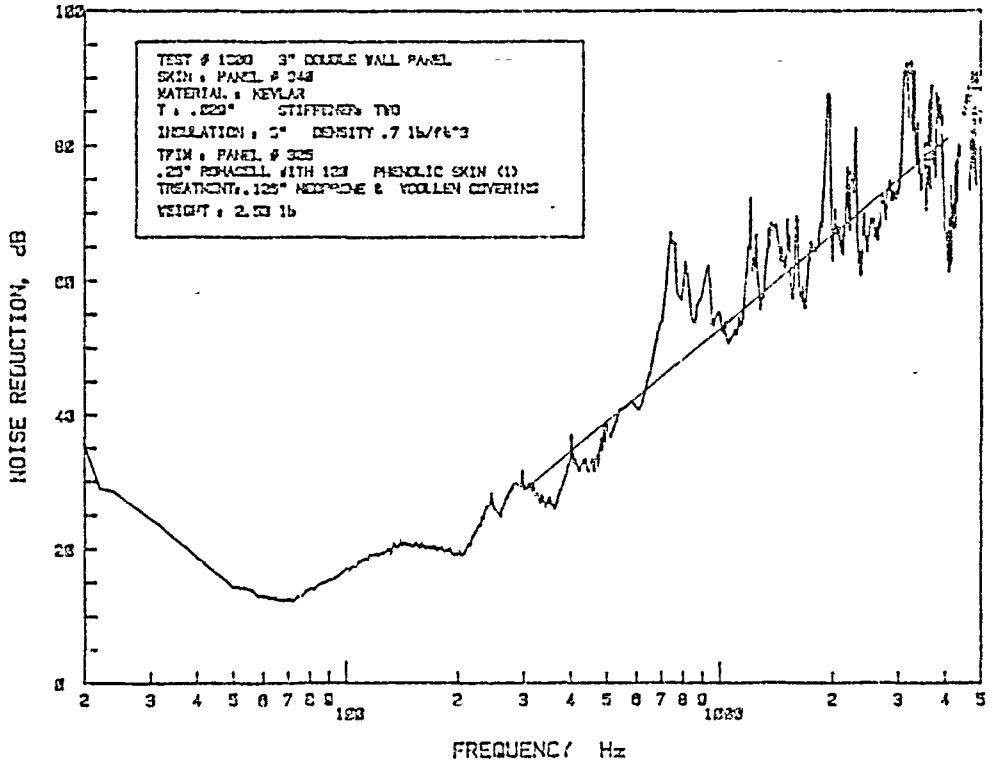

b. Fiberglass Insulation

Figure B.54: Noise Reduction Characteristics of Double-Wall Panel Made of Kevlar Skin Panel with Two Hat Stiffeners (Panel 340) and Trim Panel 325; Panel Depth 3"

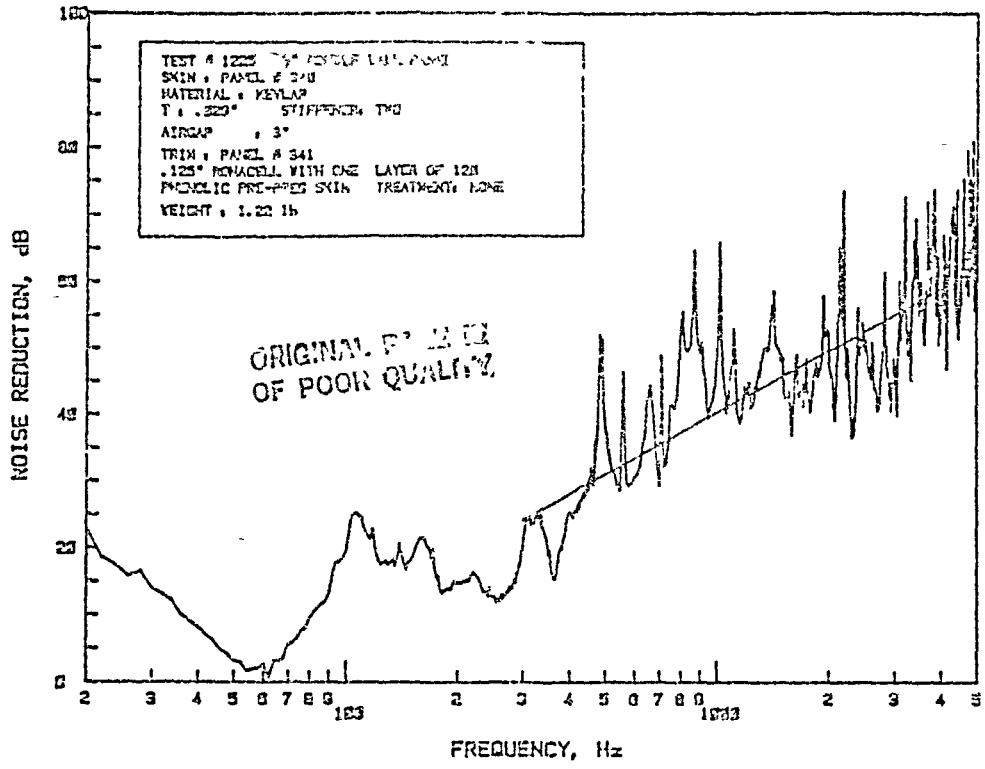

a. Airgap

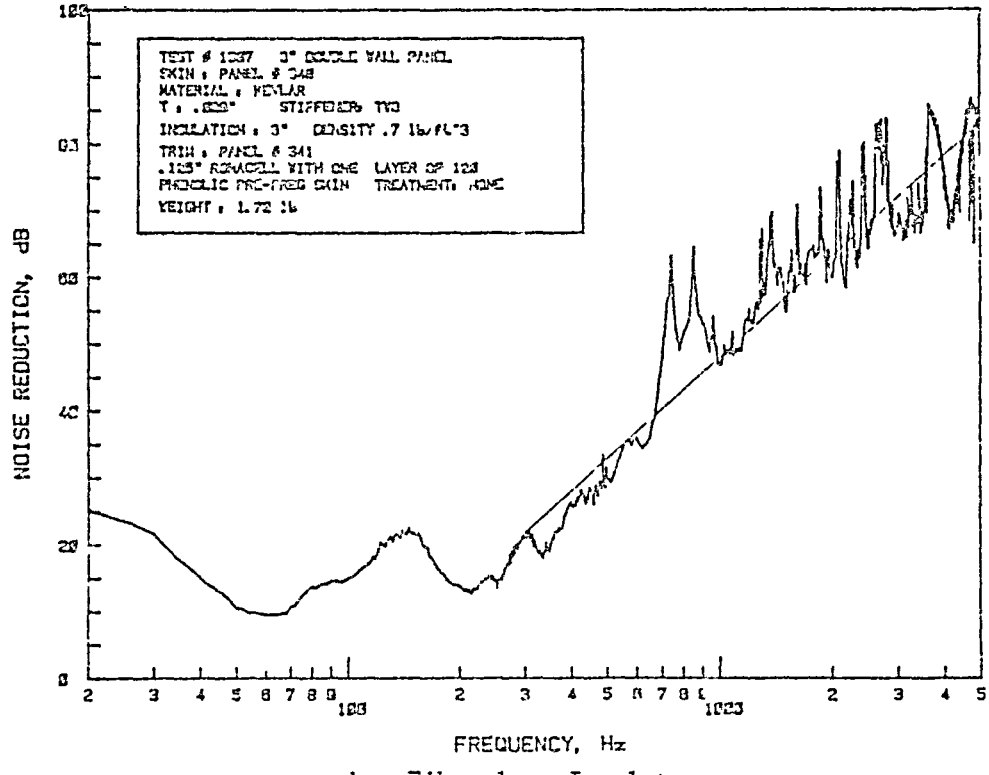

b. Fiberglass Insulation

Figure B.55: Noise Reduction Characteristics of Double-Wall Panel Made of Kevlar Skin Panel with Two Hat Stiffeners (Panel 340) and Trim Panel 341; Panel Depth 3"

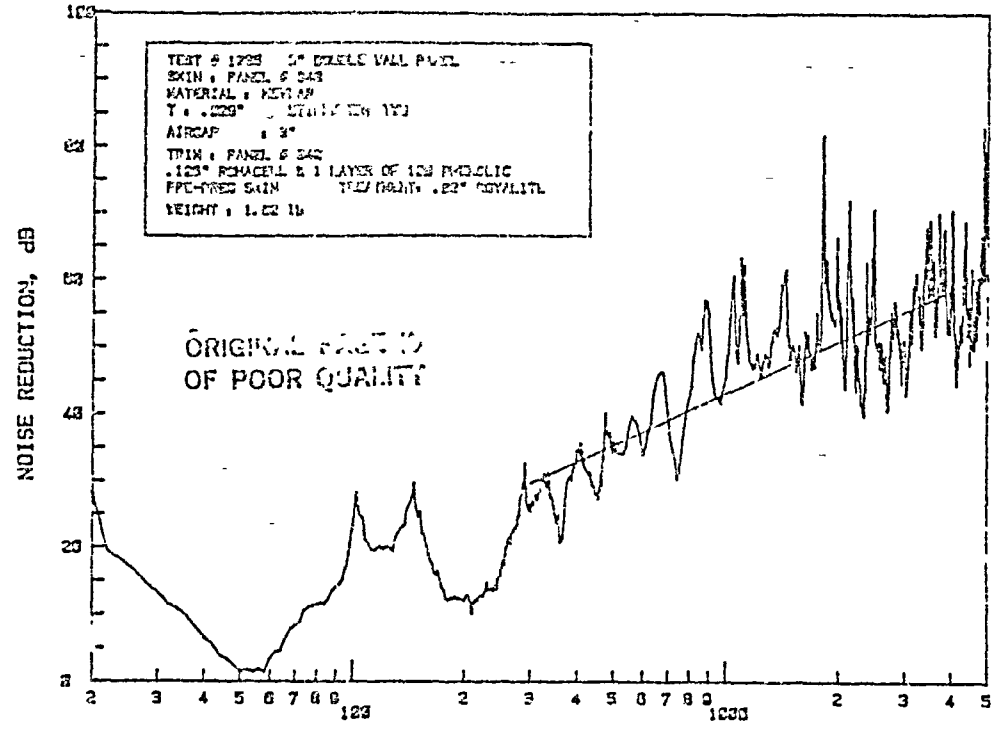

a. Airgap

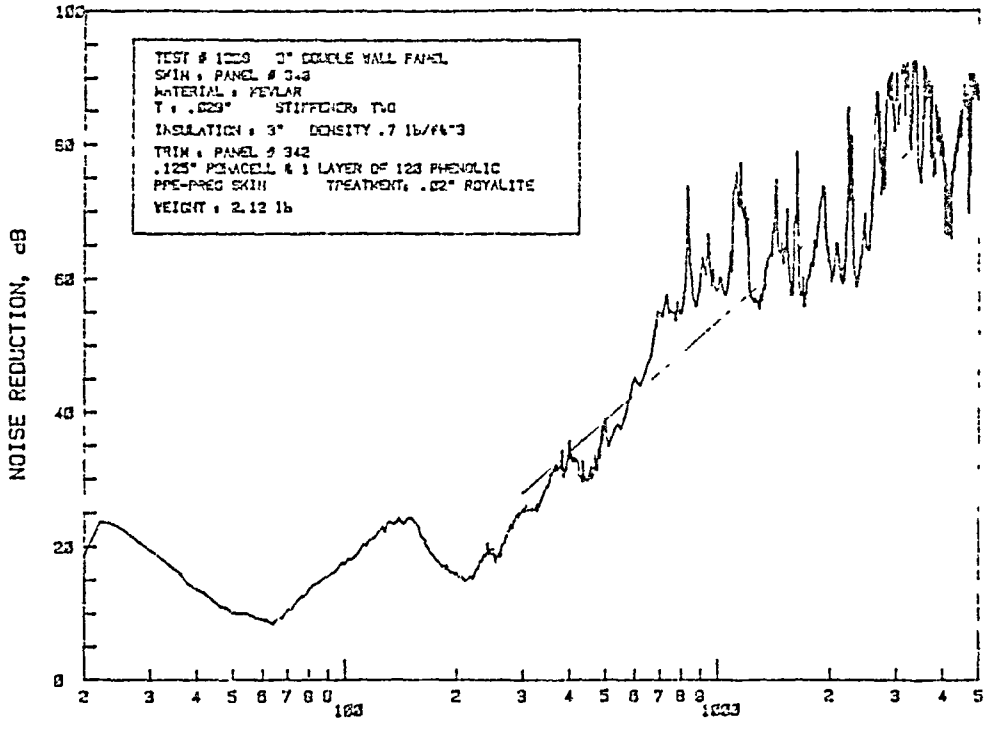

b. Fiberglass Insulation

Figure B.56: Noise Reduction Characteristics of Double-Wall Panel Made of Kevlar Skin Panel with Two Hat Stiffeners (Panel 340) and Trim Panel 342; Panel Depth 3"

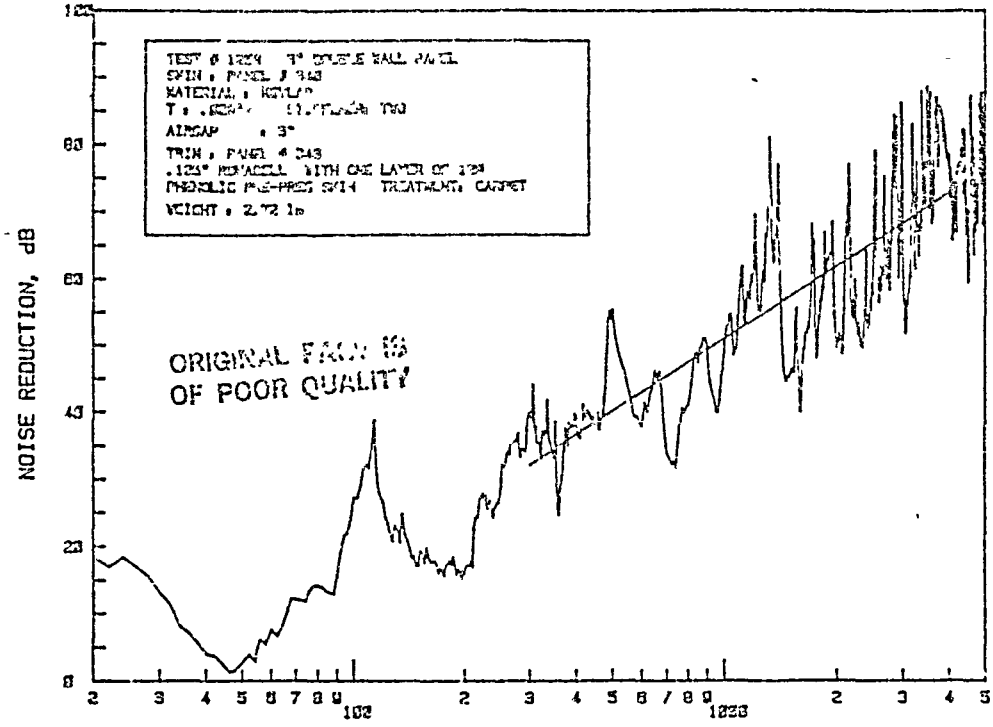

a. Airgap

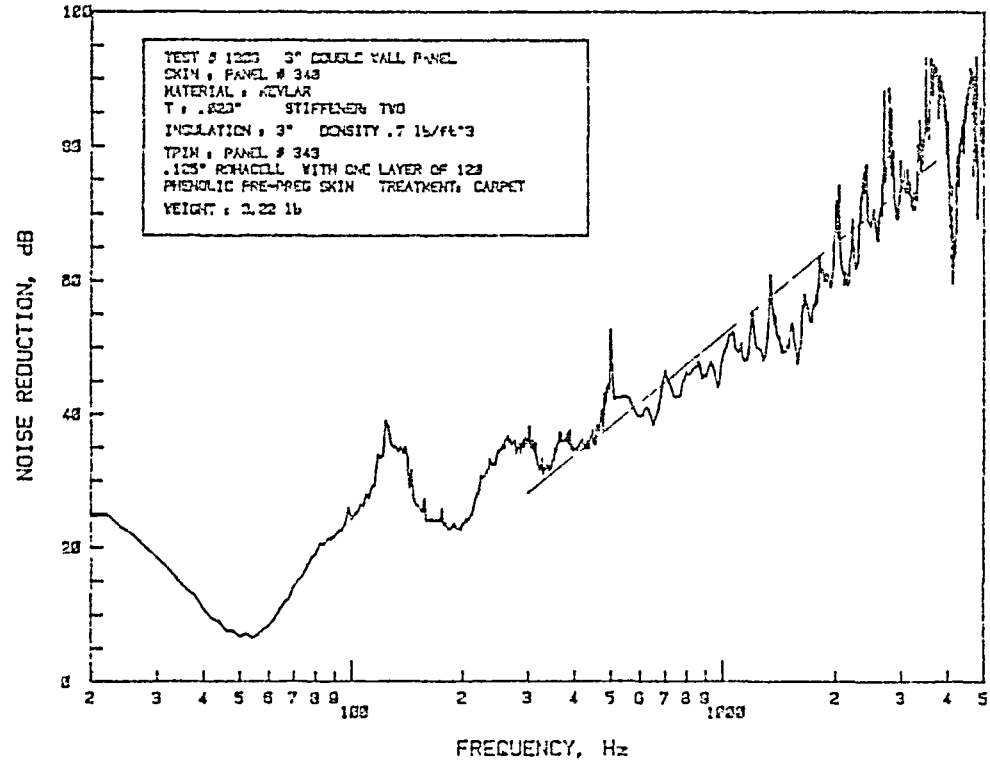

b. Fiberglass Insulation

Figure B.57: Noise Reduction Characteristics of Double-Wall Panel Made of Kevlar Skin Panel with Two Hat Stiffeners (Panel 340) and Trim Panel 343, Panel Depth 3"

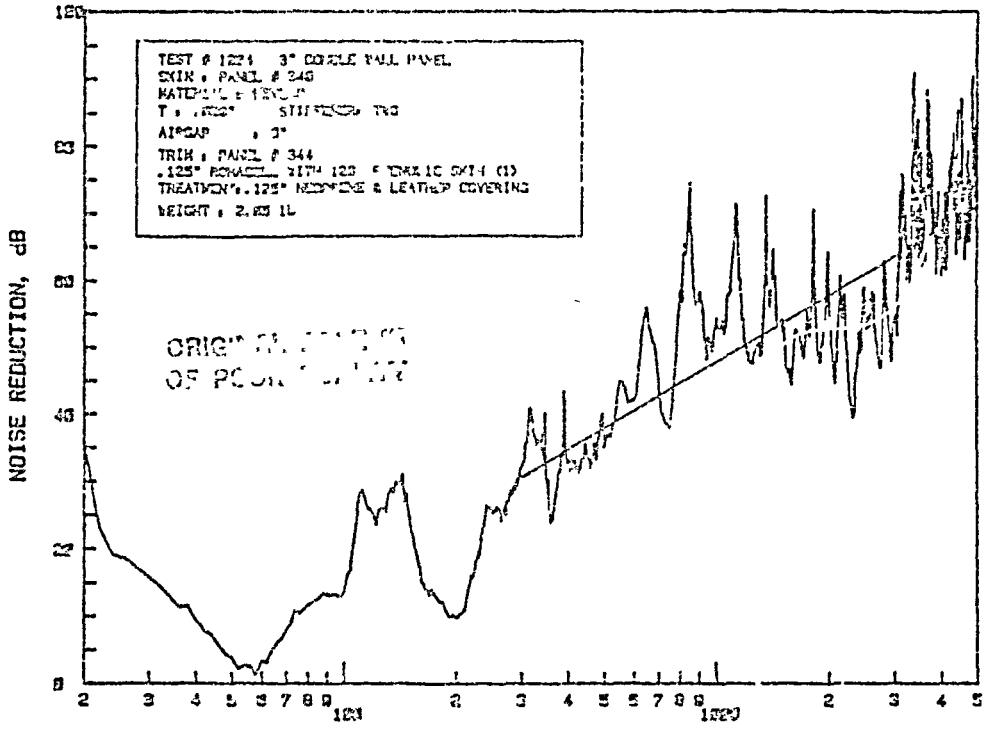

a. Airgap

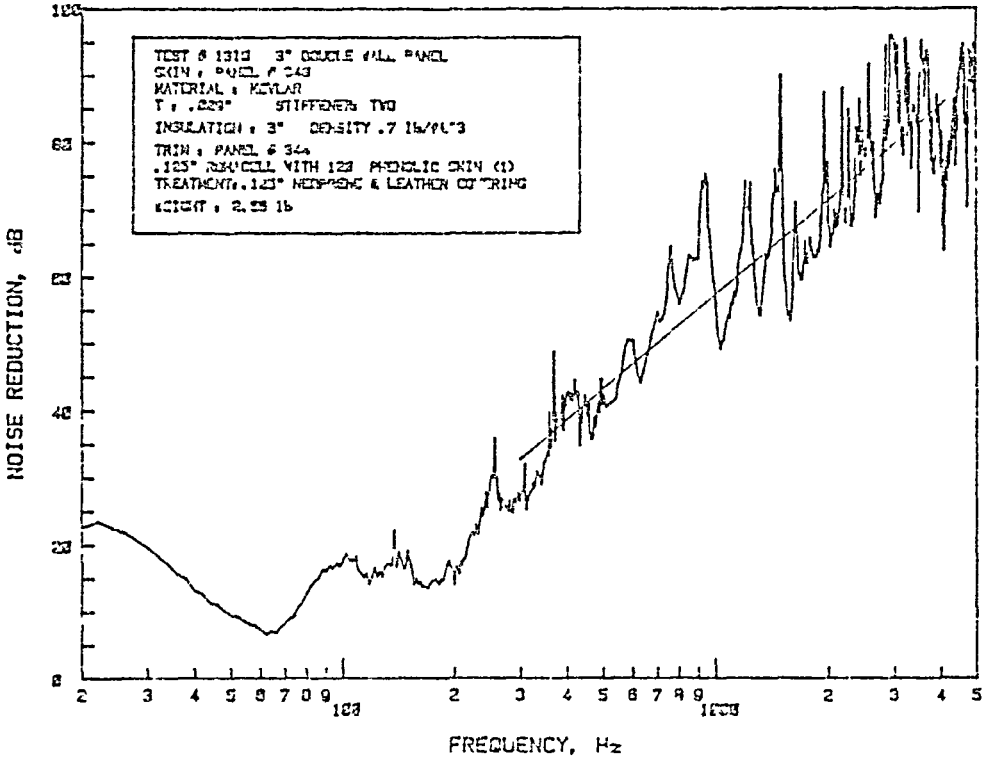

b. Fiberglass Insulation

Figure B.58: Noise Reduction Characteristics of Double-Wall Panel Made of Kevlar Skin Panel with Two Hat Stiffeners (Panel 340) and Trim Panel 344; Panel Depth 3"

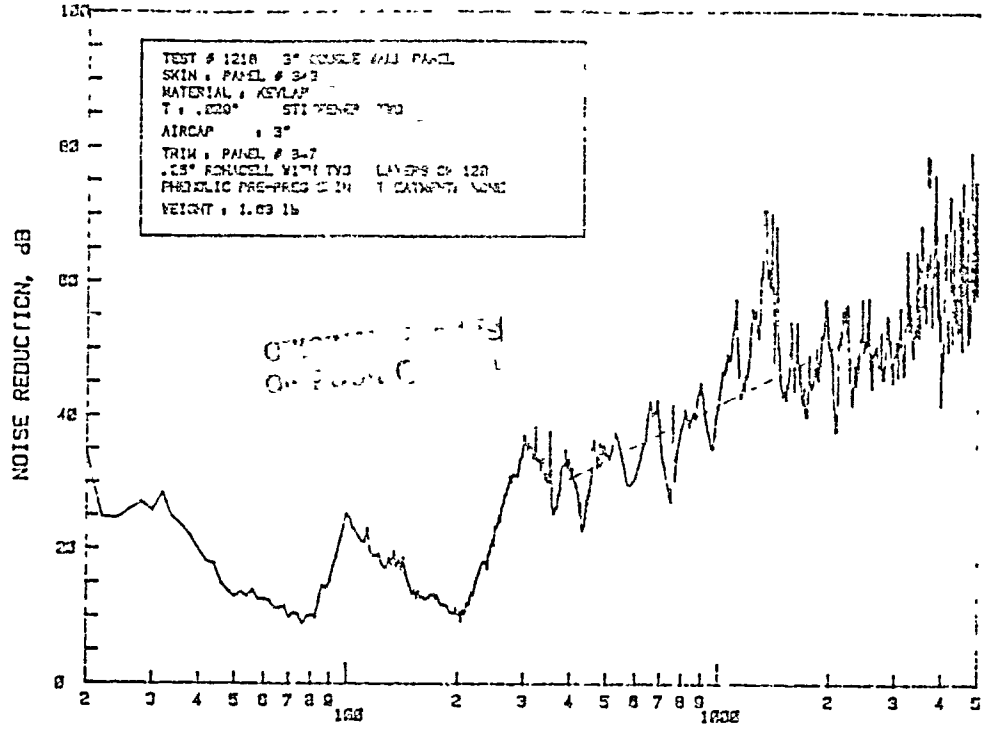

a. Airgap

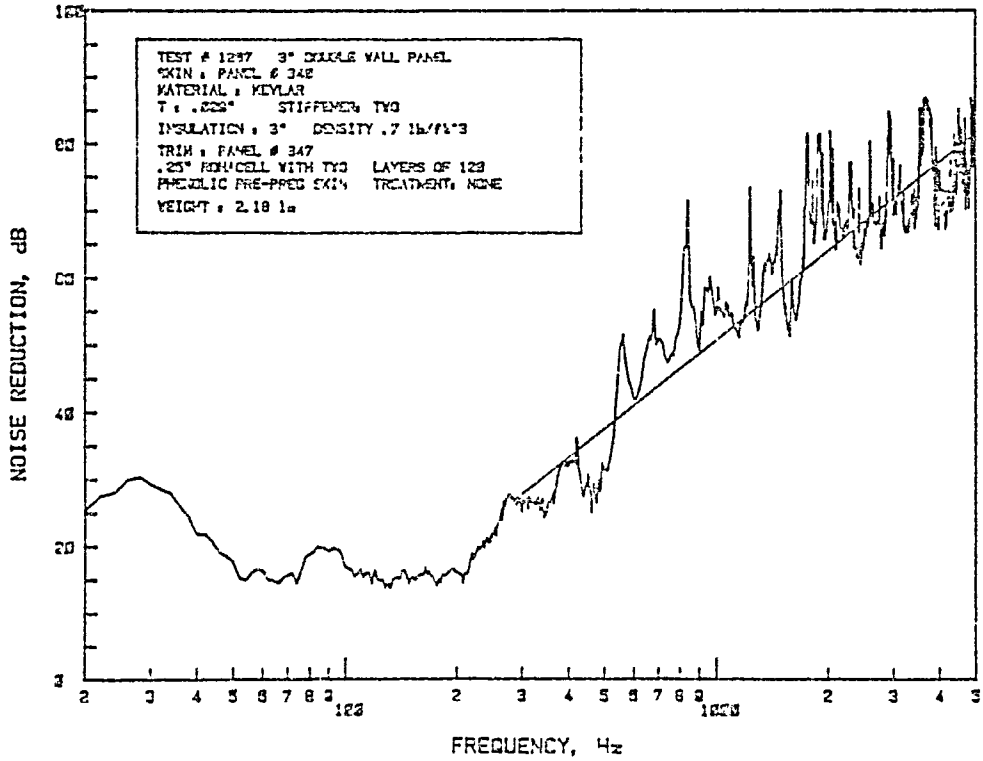

b. Fiberglass Insulation

Figure B.59: Noise Reduction Characteristics of Double-Wall Panel Made of Kevlar Skin Panel with Two Hat Stiffeners (Panel 340) and Trim Panel 347; Panel Depth 3"

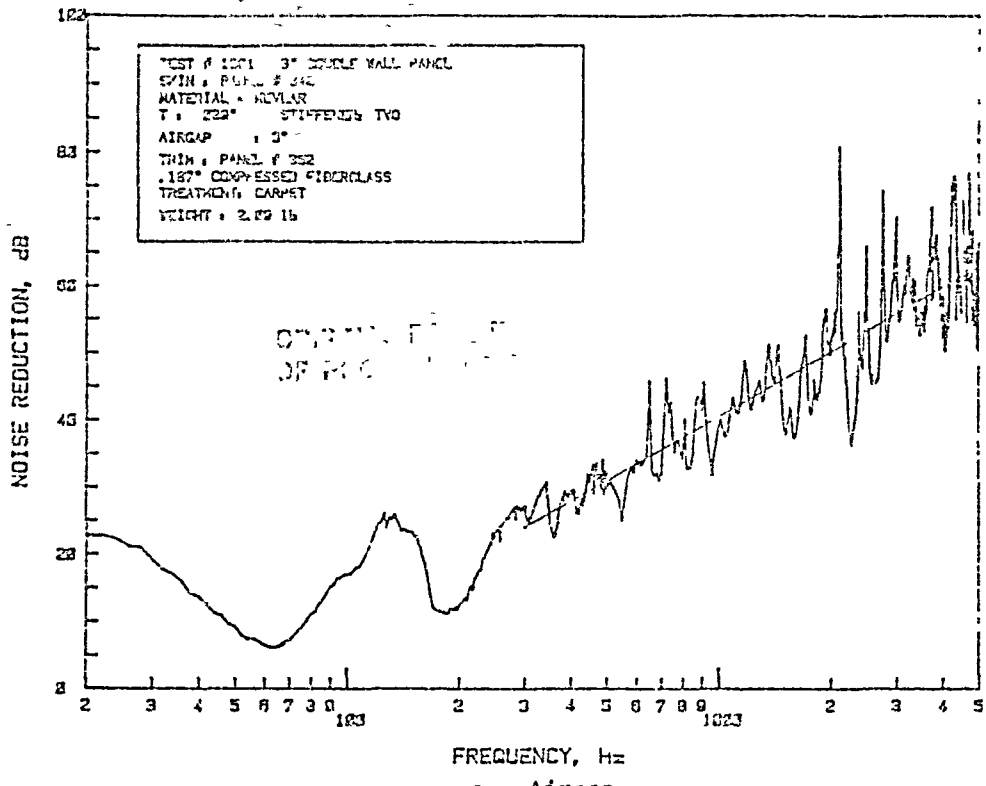

a. Airgap

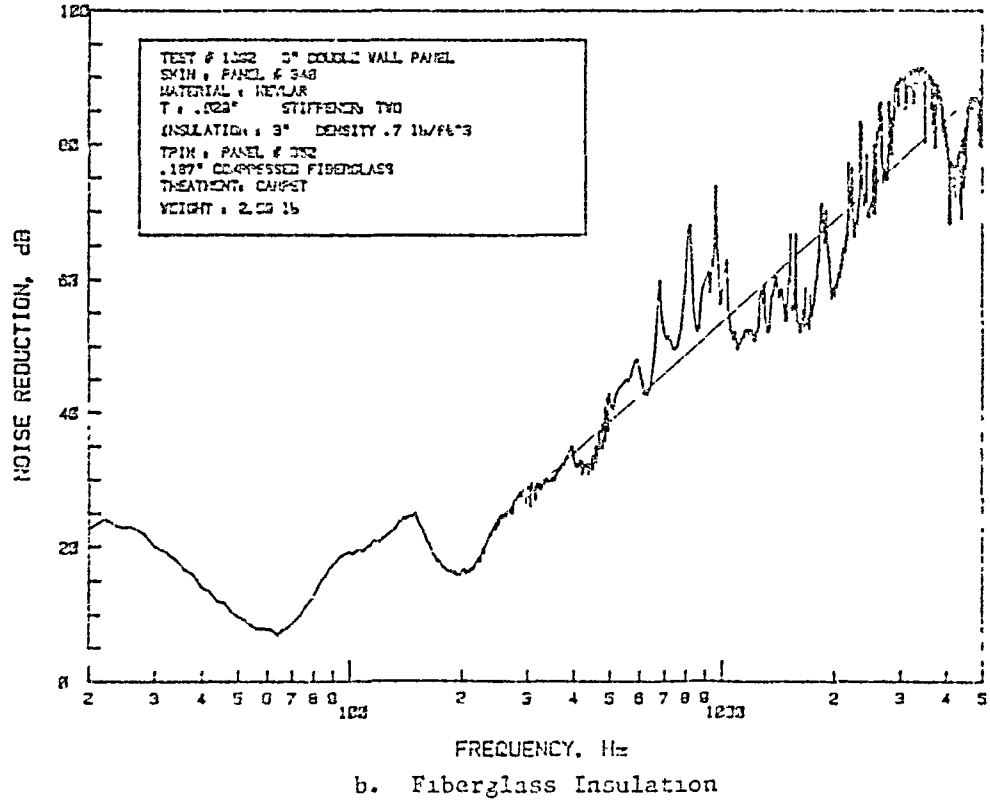

b. Fiberglass Insulation

Figure B.60: Noise Reduction Characteristics of Double-Wall Panel Made of Kevlar Skin Panel with Two Hat Stiffeners (Panel 340) and Trim Panel 352; Panel Depth 3"

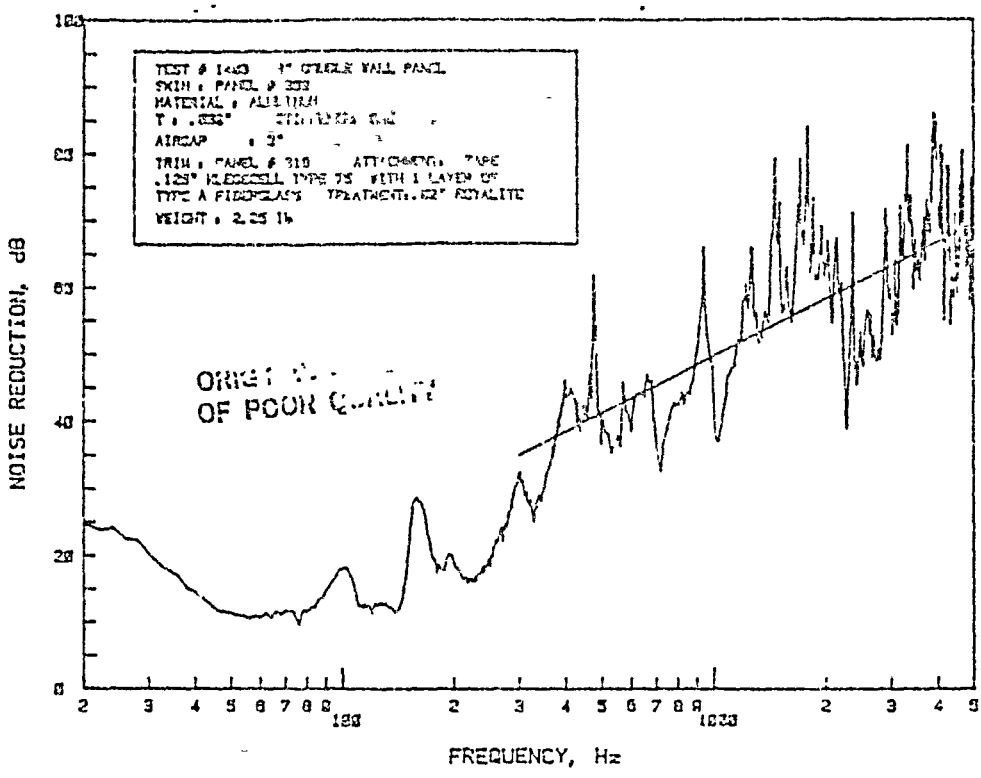

a. Airgap

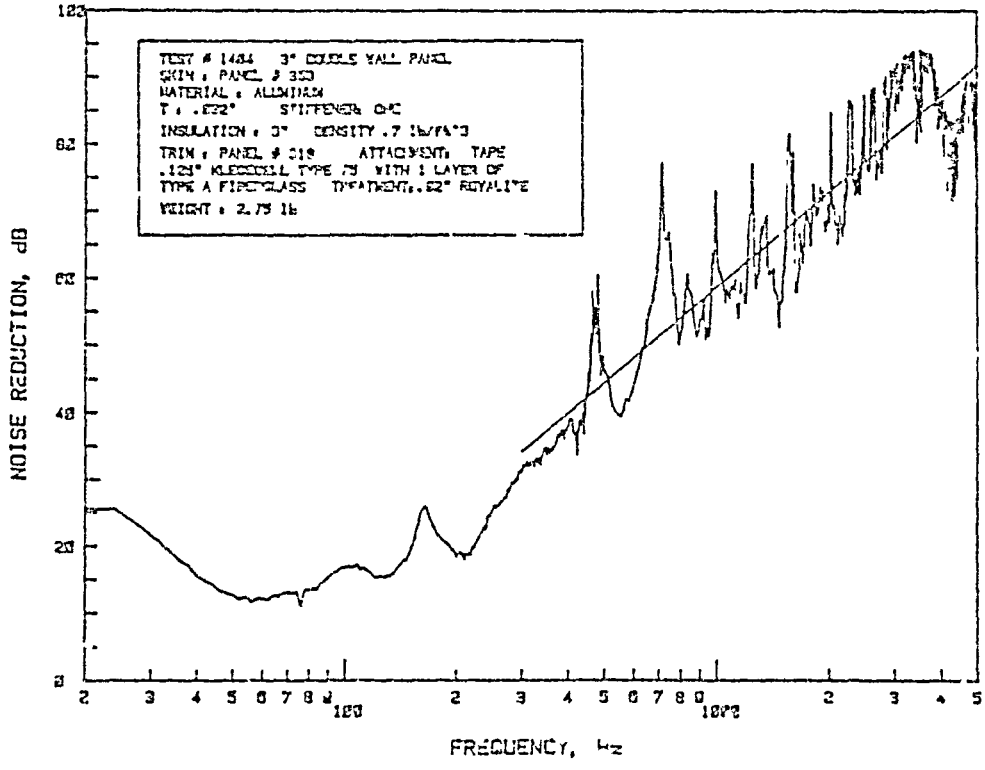

b. Fiberglass Insulation

Figure 8.61: Noise Reduction Characteristics of Double-Wall Panel Made of Aluminum Skin Panel 353 and "Floating" Trim Panel 318; Panel Depth 3"

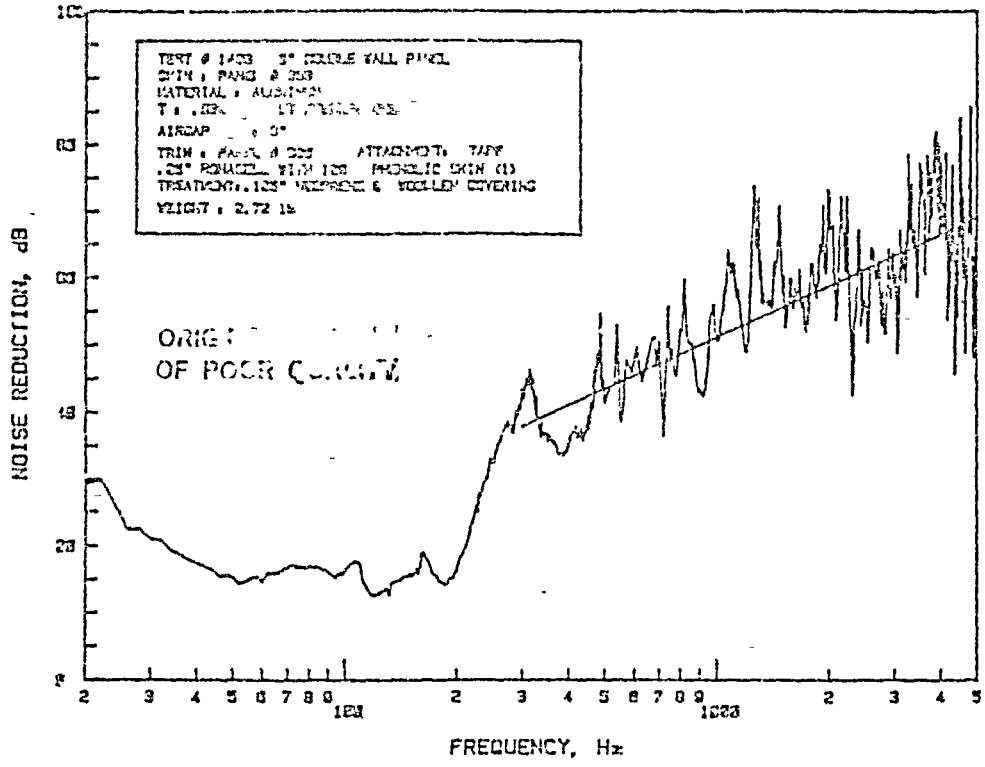

a. Airgap

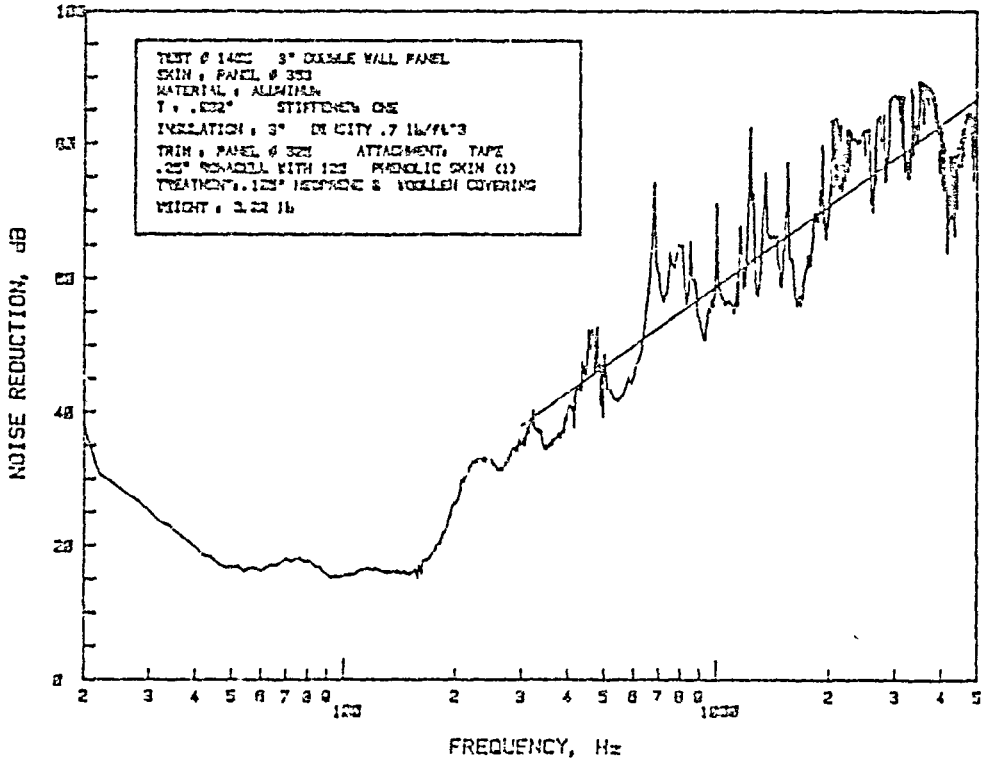

b. Fiberglass Insulation

Figure B.62: Noise Reduction Characteristics of Double-Wall Panel Made of Aluminum Skin Panel 353 and "Floating" Trim Panel 325; Panel Depth 3"

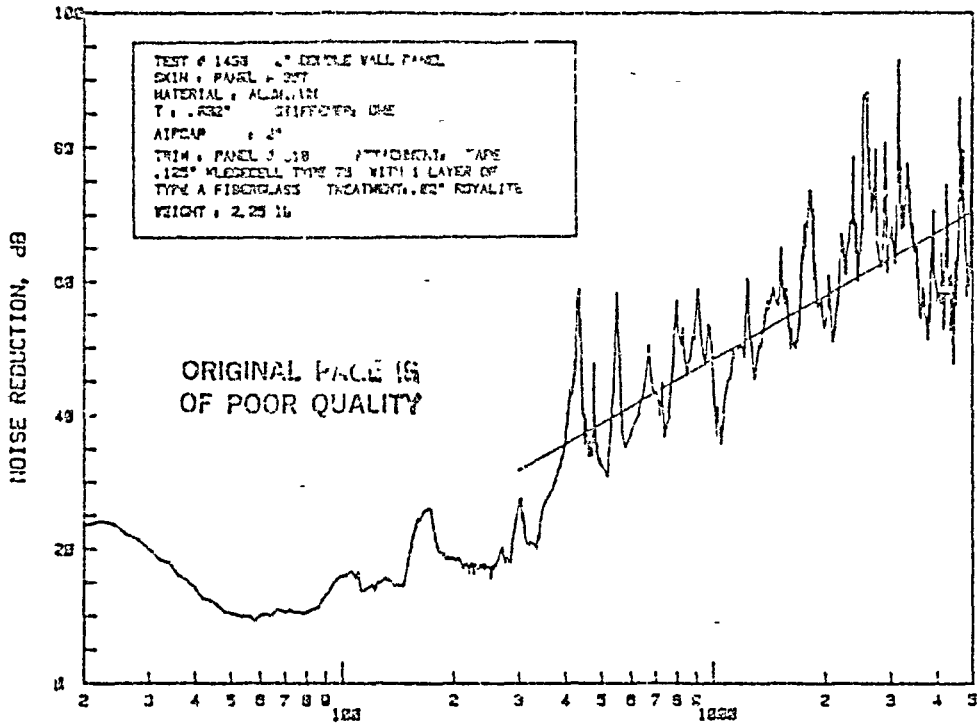

a. Airgap

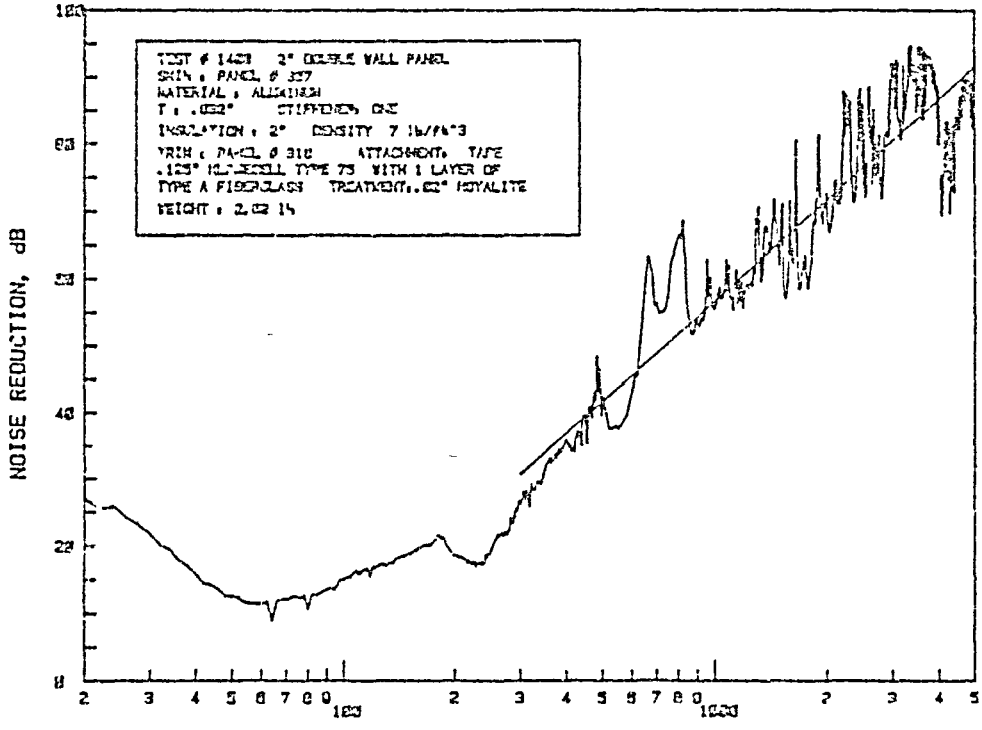

b. Fiberglass Insulation

Figure B.63: Noise Reduction Characteristics of Double-Wall Panel Made of Aluminum Skin Panel 357 and "Floating" Trim Panel 318, Panel Depth 2"

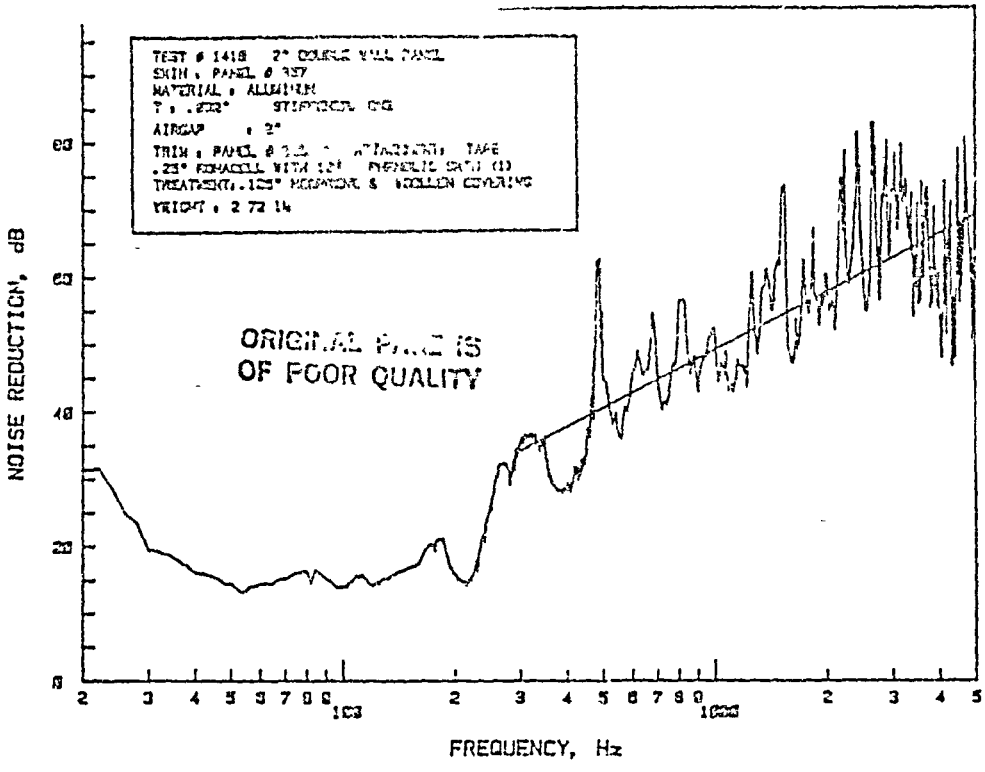

a. Airgap

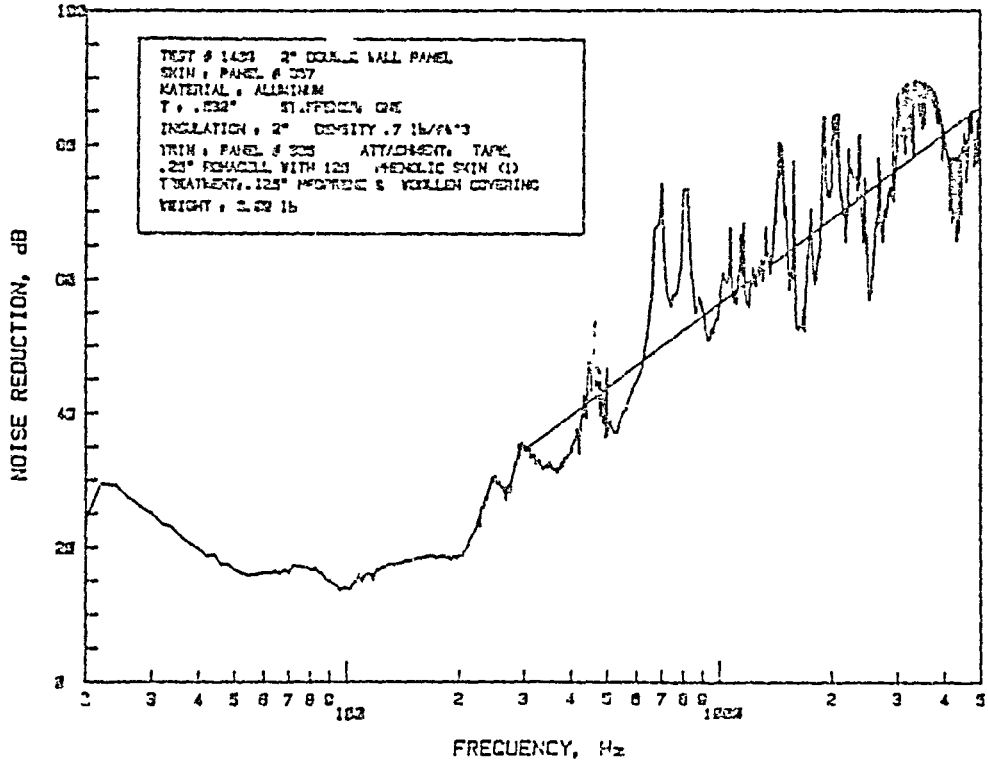

b. Fiberglass Insulation

Figure B.64: Noise Reduction Characteristics of Double-Wall Panel Made of Aluminum Skin Panel 357 and "Floating" Trim Panel 325; Panel Depth 2"

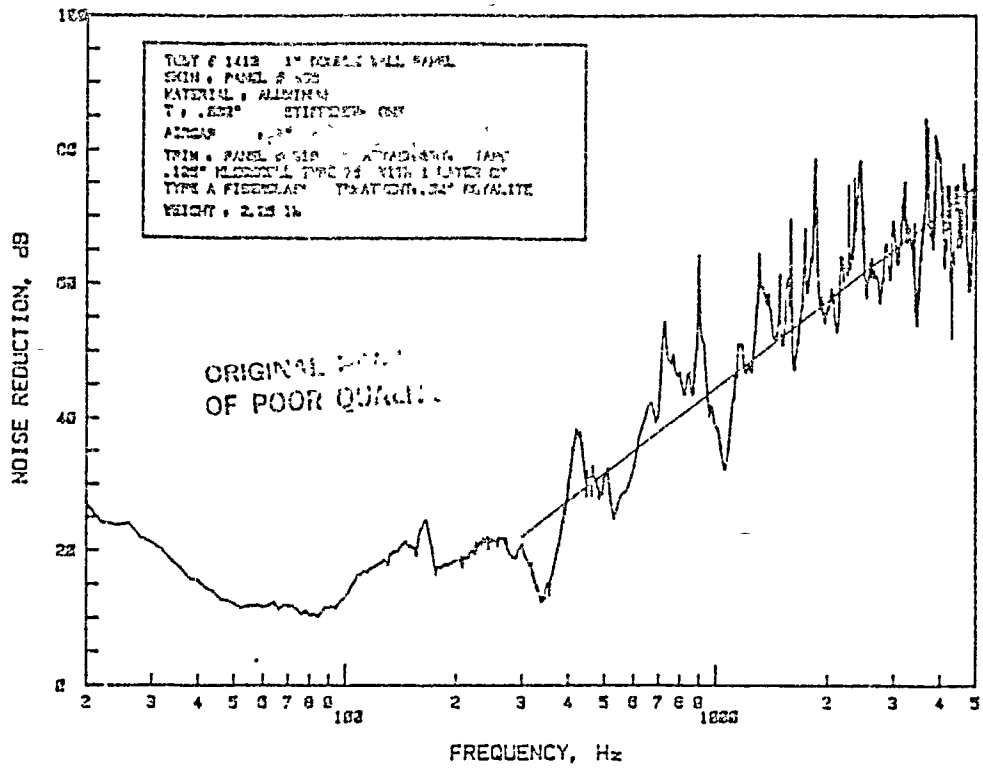

a. Airgap

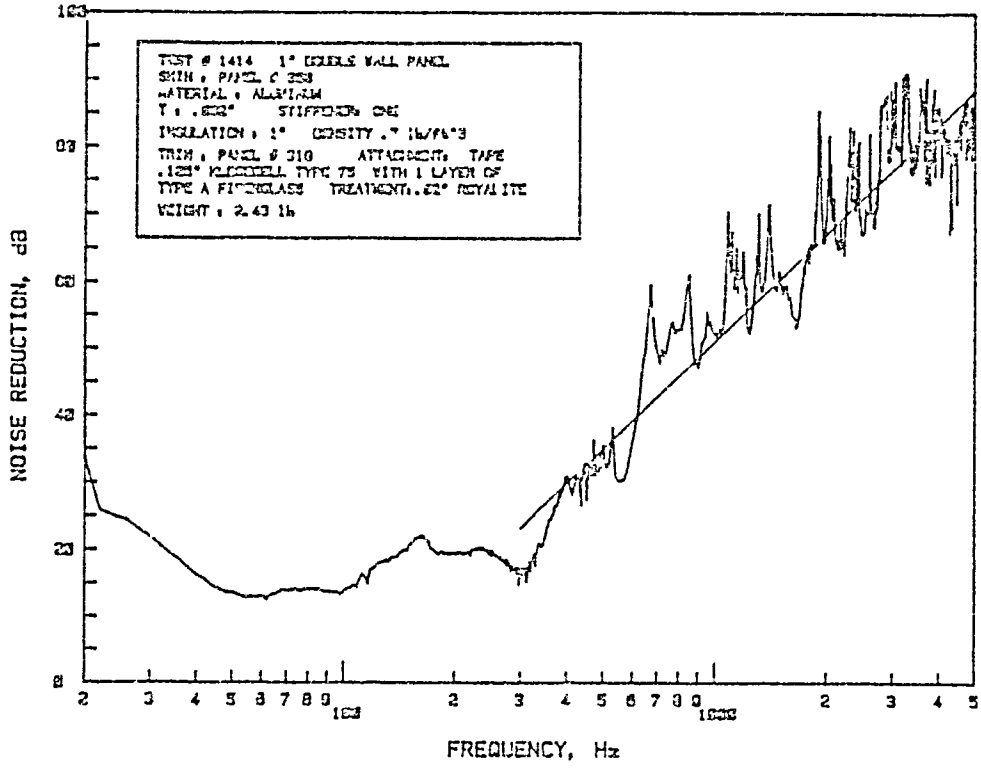

b. Fiberglass Insulation

Figure B.65: Noise Reduction Characteristics of Double-Wall Panel Made of Aluminum Skin Panel 358 and "Floating" Trim Panel 313; Panel Depth 1"

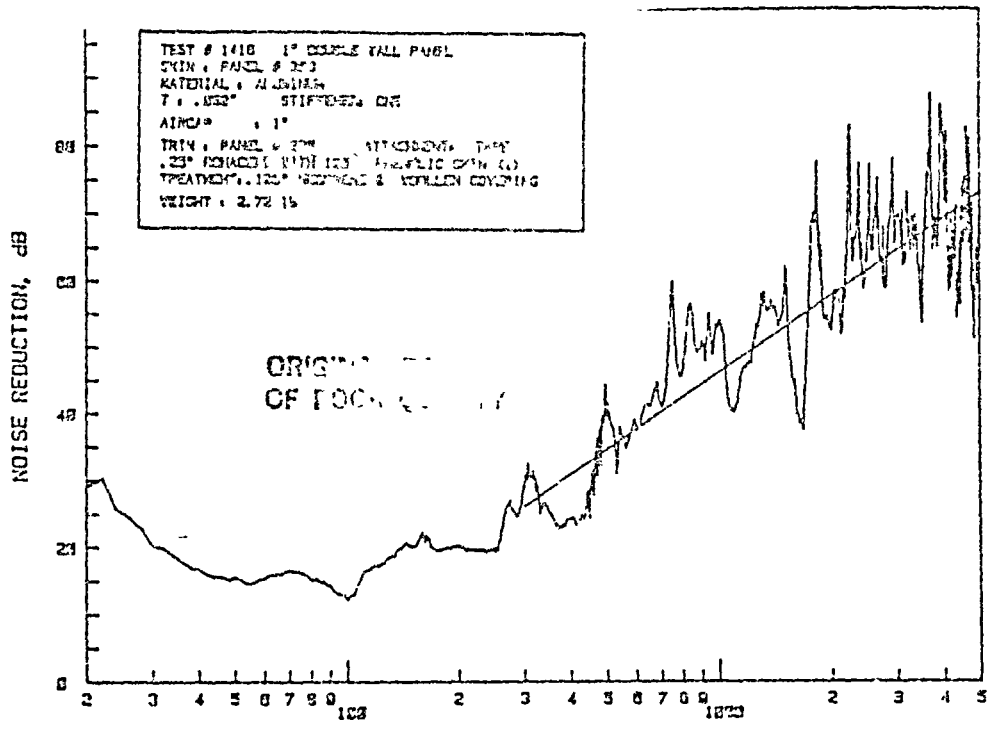

a. Airgap

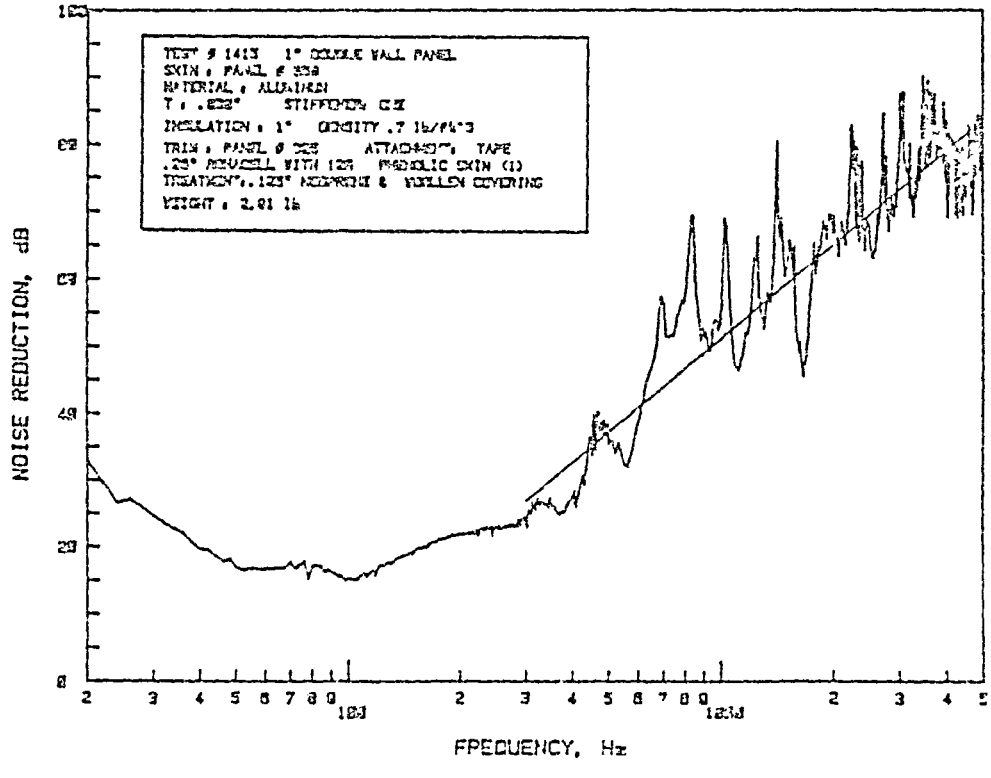

b. Fiberglass Insulation

Figure B.66: Noise Reduction Characteristics of Double-Wall Panel Made of Aluminum Skin Panel 358 and "Floating" Trim Panel 325; Panel Depth 1"

End of Document